ЖУРНАЛ
ПРИКЛАДНОЙ ХИМИИ

*Volume 32, No. 3*

*March, 1959*

# JOURNAL OF
# APPLIED CHEMISTRY
## OF THE USSR

(ZHURNAL PRIKLADNOI KHIMII)

**IN ENGLISH TRANSLATION**

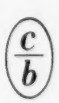

*CONSULTANTS BUREAU, INC.*

*Two volumes sponsored by*

# The Geochemical Society

*and translated from Russian*

## PHYSICOCHEMICAL BASIS OF THE ANALYSIS OF THE PARAGENESIS OF MINERALS

*by* **D.S. Korzhinskii**

*Member, Academy of Sciences, USSR*

THIS ENTIRE WORK, based on the author's twenty years of investigative experience, has been written with a twofold purpose: a) *To provide a complete text on the subject, heretofore unavailable;* b) *To supplement the comparatively sketchy training of most geologists in physical chemistry.*

The main part of Academician Korzhinskii's volume is devoted to the presentation of different methods of analysis of dependence of mineralogical composition on: *chemical composition, temperature, pressure and chemical potentials of the completely mobile components under conditions of chemical equilibrium*—with emphasis laid on the use of projective geometry, so important for representing these relationships. To assure complete coverage of the subject, the author—in cooperation with the Geochemical Society—has personally edited and *amplified* this translation of his work. (Case-bound, 180 pp., illustrated, $7.50)

ABRIDGED CONTENTS

**General conditions of equilibrium • Reversible (equilibrium) processes • Derivation of thermodynamic potentials for systems of different types • Representation of two-component compounds and projective transformation of a set of points • Three-component diagrams of composition and their projective transformations • Representation of multicomponent systems • Application of the phase rule to paragenetic analysis of minerals • Examples of paragenetic diagrams of minerals in multicomponent systems • Relation between composition and the magnitude of the chemical potentials of a component • Method of equipotential lines on the composition-paragenesis diagrams • Chemical potential surface in the three-component systems and its projection • Algebraic calculations of reactions in multicomponent systems by means of determinants • Systems with a negative number of degrees of freedom and general properties of multi-bundle diagrams**

ABRIDGED CONTENTS

**Methods of determination of rare and dispersed elements in soils • General geochemical regularities in distribution of rare elements • Soil-forming rocks and soils of the East European Plain • Boron in soils • Fluorine, bromine and iodine in soils • Arsenic and selenium in soils • Lithium, rubidium and cesium in soils • Strontium and barium in soils • Rare earths and yttrium • Titanium and zirconium in soils • Vanadium, chromium, manganese, cobalt and nickel in soils • Copper, zinc and cadmium in soils • Lead and tin in soils • Molybdenum and tungsten • Radioactive elements in soils • Other dispersed elements in soils • Certain geochemical regularities in distribution of rare elements in soils**

## THE GEOCHEMISTRY OF RARE AND WIDELY SCATTERED CHEMICAL ELEMENTS IN SOILS

*2nd Edition, Revised and Enlarged*

*by* **A.P. Vinogradov**

IN THE LIGHT OF new data from the laboratories of the *V.I. Vernadskii Institute of Geochemistry and Analytical Chemistry, Academy of Sciences, USSR,* the author has brought his work completely up to date—particularly with respect to the *physicochemical properties* of the individual rare elements, and to their *occurrence and distribution* in soils and rocks, as well as their role in the lives of *plants, animals and humans.* (236 pp., illustrated, $9.50)

*C.B. translations by bilingual scientists include all diagrammatic, tabular and photographic material integral with the text.*

*C/b CONSULTANTS BUREAU, INC.*
*227 W. 17th St., NEW YORK 11, N.Y.*

*Volume 32, No. 3*

*March, 1959*

# JOURNAL OF
# APPLIED CHEMISTRY
## OF THE USSR

**(ZHURNAL PRIKLADNOI KHIMII)**

*A publication of the Academy of Sciences of the USSR*

**IN ENGLISH TRANSLATION**

*Year and issue of first translation:*
*Vol. 23, No. 1 January 1950*

| | *U. S. and Canada* | *Foreign* |
|---|---|---|
| *Annual subscription* | *$60.00* | *$65.00* |
| *Annual subscription for libraries of non-profit academic institutions* | *20.00* | *25.00* |
| *Single issue* | *7.50* | *7.50* |

Copyright 1960
CONSULTANTS BUREAU ENTERPRISES, INC.
227 West 17th Street, New York, N. Y.

Editorial Board
(ZHURNAL PRIKLADNOI KHIMII)

P. P. Budnikov, S. I. Vol'fkovich, A. F. Dobrianskii,
O. E. Zviagintsev, N. I. Nikitin (Editor in Chief),
G. V. Pigulevskii, M. E. Pozin, L. K. Simonova
(Secretary), V. V. Skorchelletti, N. P. Fedot'ev

---

*Note: The sale of photostatic copies of any portion of this copyright translation is expressly prohibited by the copyright owners.*

*Printed in the United States of America*

JOURNAL OF APPLIED CHEMISTRY OF THE USSR

Volume 32, Number 3 March 1959

# CONTENTS


| | PAGE | RUSS. PAGE |
|---|---|---|
| Reduction of Sodium Sulfate by Hydrogen in a Fluidized Bed. Ya. Tsiborovskii and S. Vronskii | 501 | 473 |
| Dissolution of Monocrystalline Germanium in Hydrogen Peroxide. G. S. Supin | 506 | 478 |
| Study of the Reaction of Stannous Sulfide with Sulfur Dioxide . D. N. Klushin and O. V. Nadinskaya | 510 | 482 |
| Effect of Thermal Aging on the Pore Structure and Catalytic Activity of Synthetic Aluminosilicates. D. P. Dobychin and T. F. Tsellinskaya | 514 | 486 |
| Alteration of the Structure of an Anode Surface in the Course of Destruction. B. M. Bulygin | 521 | 494 |
| Mineral Composition of the Roasted Mass in Dichromate Production. O. I. Pudovkina, M. V. Kireeva, and E. M. Morgunova | 528 | 499 |
| The Hardening of Magnesium Oxychloride (Sorel) Cements. A. G. Bergman and I. P. Vyrodov | 534 | 504 |
| The Rate of Decomposition of Apatite by Phosphoric Acid. M. E. Pozin, B. A. Kopylev, and D. F. Zhil'tsova | 539 | 509 |
| The Rate of Burning of Flotation Pyrite in the Suspended State. A. I. Fefelov and E. M. Lyapustina | 544 | 515 |
| Kinetics of the Reduction of Manganese Oxides by Solid Carbon. V. A. Kozlov and V. G. Vlasov | 551 | 523 |
| Separation of Carbon and Oxygen Isotopes by Rectification of CO in a 12-Meter Column. M. V. Tikhomirov and N. N. Tunitskii | 559 | 531 |
| Stirring Rates of Solutions and Purity of the Crystals Formed. L. N. Matusevich | 565 | 536 |
| Calculation of Batch Distillation Units with Supplementary Feeding. Tszyui-Fu-Fu | 571 | 543 |
| Method for Construction of Phase Diagrams for Multicomponent Systems. L. N. Lambin and N. N. Ermolenko | 577 | 548 |
| Some Questions of the Theory and Practice of the Furnace Refining of Tin. N. N. Murach | 584 | 556 |
| Dissolution of Aluminum in Acids and Alkalies in an Ultrasonic Field. A. M. Ginberg | 591 | 563 |
| Investigation of Nickel Plating without Application of Current, with Ammonium Fluoride Buffer. N. A. Solov'ev | 594 | 566 |
| Electrolytic Nickel Deposits Formed in the Presence of Sulfonated Naphthalene. V. V. Ostroumov | 600 | 572 |

# CONTENTS (continued)


| | PAGE | RUSS. PAGE |
|---|---|---|
| Electrolytic Separation of Binary Alloys of Lead with Silver and Arsenic. E. B. Gitman and Yu. K. Delimarskii | 607 | 578 |
| Electrochemical Tinning of Iron from Halide Solutions Containing Fluorides of Alkali and Alkaline-Earth Metals. A. N. Kruglov and V. P. Kochergin | 611 | 582 |
| Electrodeposition of Chromium from a Tetrachromate Bath. A. Ya. Ryaboi and M. A. Shluger | 617 | 588 |
| Catalytic Reduction of Furfural to Sylvan. A. S. Sultanov and V. A. Maslennikova | 623 | 595 |
| Effect of the Geometrical Parameters of the Sorbent Layer on Sorptional Purification of Maize Sugar. N. I. Gel'perin and A. I. Altykis | 628 | 599 |
| A Study of the Separation of Butylene–Divinyl Mixtures by an Absorption Method. M. I. Bogdanov and E. P. Krushinskaya | 632 | 603 |
| The Benzenoid Structure of Hydrolytic Lignin. M. I. Chudakov, S. I. Sukhanovskii, and M. P. Akimova | 638 | 608 |
| Effect of Wood Pretreatment on the Yield and Properties of Dioxane Lignin. M. M. Chochieva and N. I. Nikitin | 643 | 613 |
| Accelerated Polymerization of Caprolactam. A. S. Shpital'nyi, M. A. Shpital'nyi, and N. S. Yablochnik | 647 | 617 |
| Effect of Average Molecular Weight of the Polymer on the Rate of Caprolactam Formation During Thermal Depolymerization of Unstabilized Polycaprolactam. N. D. Katorzhnov and A. A. Strepikheev | 655 | 625 |
| Dissolution of Coals in Oils Derived from Coal for Production of Coal–Oil Pitch. V. N. Novikov and B. S. Gurevich | 659 | 628 |
| Production of Quinaldinic Acid from Coal–Tar Bases. M. M. Potashnikov and B. E. Kogan | 667 | 636 |
| Liquid-Phase Oxidation of High-Molecular Petroleum Hydrocarbons. S. R. Sergienko, R. Ya. Semyachko, and P. N. Galich | 672 | 641 |
| The Use of Hydrocarbon Fuel in Cells with Solid Electrolytes. V. S. Daniel'-Bek, M. Z. Mints, V. V. Sysoeva, and M. V. Tikhonova | 679 | 649 |
| Effect of Thio Derivatives of Unsaturated Phosphonic Acids on the Antioxidant Properties of Mineral Oil. K. K. Papok, K. N. Anisimov, B. S. Zuseva, and N. E. Kolobova | 685 | 656 |
| The Possibility of Gas-Phase Catalytic Synthesis of Vinyl Acetate with the Reaction Components in Stoichiometric Proportions. R. M. Flid and A. V. Chirikova | 689 | 660 |
| Direct Disazo Dyes–Derivatives of Oxadiazole and Thiodiazole. N. S. Dokunikhin, B. M. Krasovitskii, R. M. Matskevich, V. A. Blinov, and Z. Ya. Vitokhina | 693 | 664 |
| Synthesis of Monoalkyl Maleates. S. N. Ushakov, A. F. Nikolaev, A. M. Toroptseva, and M. S. Trizno | 697 | 667 |
| Mechanism of Joint Polycondensation Processes. G. A. Shtraikhman | 702 | 673 |

# CONTENTS (continued)


| | PAGE | RUSS. PAGE |
|---|---|---|
| Dependence of the Polymerization Rate of Acrylonitrile on the Hydrodynamic Process Conditions. E. S. Roskin | 706 | 676 |
| Esterification of Weakly Hydroxyethylated Cellulose. N. I. Klenkova and O. M. Kulakova | 710 | 680 |
| Ozonation of Lignin. D. V. Tishchenko | 717 | 686 |
| Dulcitol from Larch Arabogalactan. A. F. Zaitseva, A. Z. Karpov, S. Z. Levin, and S. D. Antonovskii | 721 | 690 |
| **Book Reviews** | | |
| Data Book on Liquid—Vapor Equilibria. (V.B. Kogan and V.M. Fridman) A. V. Storonkin, A. G. Morachevskii and M. P. Susarev | 724 | 694 |
| Hydrogen Peroxide (W. Schumb, C. N. Satterfield and R. L. Wentworth) . . I. Ya. Volkind | 725 | 695 |
| Plastics and their Fire Hazards (V.V. Bokshitskii) . . . . I. G. Filatov . . . . . | 727 | 697 |

# REDUCTION OF SODIUM SULFATE BY HYDROGEN IN A FLUIDIZED BED

Ya. Tsiborovskii and S. Vronskii

Chair of Chemical Technology Processes and Equipment, the Warsaw Polytechnic Institute and Institute of General Chemistry

Characteristics of the process. In conection with improvements of sodium sulfide production, the recent scientific literature on the subject contains frequent references to the reduction of $Na_2SO_4$ by hydrogen in a fluidized bed [1,2]. In view of the advantages of this method, it might be expected that it could be used for the production of high-percentage $Na_2S$ by a single continuous process instead of the complex and costly batch process, with the use of simpler equipment operated at lower cost and more economically than the rotary or shaft furnaces used for reduction of sodium sulfate.

However, the properties of the $Na_2SO_4$–$Na_2S$ system are very unfavorable for treatment by means of gaseous reducing agents with the whole reduction mass at the same temperature, which is characteristic for fluidized-bed processes.

A eutectic of low melting point is formed; its reported composition and melting point vary within wide limits in different publications. According to Ley [3], the eutectic for technical sodium sulfate corresponds to 20 wt.% $Na_2S$ and m.p. 620°. Nyman and O'Brien [4] found that the pure components form a eutectic at 43 wt.% $Na_2S$, with m.p. 665° ± 10°; Courtois found 50 molar % and 703°; Kohlmeyer and Lohrke [5] 28 molar % $Na_2S$ and 740°.

The following gases are used as reducing agents in the production of $Na_2S$: hydrogen, carbon monoxide, natural gas, producer gas, and semiwater gas. The reactions are

$$Na_2SO_4 + 4H_2 = Na_2S + 4H_2O, \quad (1)$$

$$Na_2SO_4 + 4CO = Na_2S + 4CO_2, \quad (2)$$

$$Na_2S + CO_2 + H_2O = Na_2CO_3 + H_2S. \quad (3)$$

Reaction (1) commences at about 600° and proceeds at a rate adequate for practical purposes at 700°. The corresponding temperatures for Reaction (2) are 700° and 730-850°. If the reducing gas contains $H_2$ (or $H_2O$) and CO simultaneously, sodium carbonate is formed. Carbonate formation may be the purpose of the reduction [6,7], or carbonate may be an unwanted by-product, formed even in reduction by means of producer gas [1]. Sodium carbonate lowers the melting point of the whole system. The temperature of the process may be lowered by the use of catalysts; in presence of catalysts the reaction proceeds below the eutectic point at a rate satisfactory for production purposes. Nyman and O'Brien [4] studied catalytic reduction at 600 and 650°. If the process was conducted at 600°, the amount of sodium sulfide formed in 2 hours in presence of 0.4% of iron catalyst was from 26 to 54%, and in presence of 1.5% catalyst, from 54 to 80%, according to grain size (fraction from 2 to 0.074 mm).

Increase of the temperature to 650° raised the degree of reduction from 26 to 46% for the 2-0.84 mm fraction in presence of 0.4% catalyst. The authors studied a number of metal catalysts and the gases: $H_2$, $CH_4$, $NH_3$, $H_2S$, and concluded that the most active reducing agent up to 700° is hydrogen in presence of iron catalyst. Takeyoshi Haga [8] reduced $Na_2SO_4$ by hydrogen in presence of 1.5% $Fe_2O_3$ and 1.5% C, and obtained 97% $Na_2S$ in 2 hours.

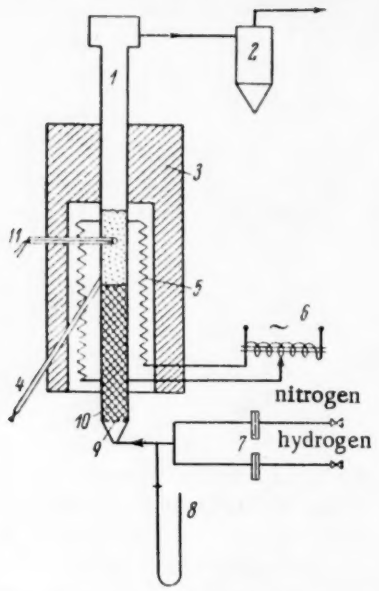


Fig. 1. Diagram of experimental unit: 1) column; 2) cyclone; 3) heat indulation; 4) discharge tube; 5)electric heater; 6) autotransformer; 7) diaphragms; 8) manometer; 9)porous plate; 10) quartz packing; 11) thermocouple.

Wintersberger and Koudela [9] investigated and patented sodium salts of aliphatic acids as catalysts. In presence of 5% sodium oxalate they obtained in 3-4 hours a product containing 95-97% $Na_2S$. A very important feature in this case is the absence of color, such as is found with the use of iron catalyst, in the reaction products.

Catalytic reduction has long been used industrially. The process is conducted in shaft or rotary furnaces at temperatures from 600 to 850°. The catalyst is iron (from 0.1 to 0.3%), usually present as an impurity in technical sodium sulfate. The product contains 95-97% $Na_2S$. The high productivity of the reduction process in presence of a small amount of catalyst is due to the use of a countercurrent process with continuous increase of temperature as the starting material is consumed, to the end of the process at 850°. Thus the entire process is carried out below the melting point of the mixture. The hydrogen conversion is 10%. The material remains for up to 24 hours in the shaft furnaces. This is because the material is used in the form of fairly large grains or briquets. In a fluidized bed the material must be very fine, and the reduction rate can therefore be raised considerably. There are two possibilities for conducting the process in a fluidized bed, with the necessary temperature conditions taken into account.

1. The process could be conducted at a temperature below the eutectic point, i.e., up to 650°. It is known from the literature that at such temperatures the duration of catalytic reduction, even for a fine fraction (grains smaller than 1 mm), is so great that the production cost would increase with the use of a reactor with a fluidized bed for the process.

2. The fluidized-bed principle is most suitable if the rate of the chemical reaction is fairly high. Therefore only the reduction process taking place at a high temperature is considered. The rate of the reduction reaction at 700° in presence of catalysts is considerable. Vigorous agitation and the presence of a considerable amount of sulfide would prevent aggregation, despite the possible formation of a liquid phase on the grain surfaces.

This solution of the problem is proposed in the patents of Koudela and Wintersberger [10]. The catalytic reduction should be performed at 675-750° in a reaction furnace fitted with three shelves, with heat recovery; the amount of added sulfate did not exceed 5% by weight of the total furnace charge.

However, the experimental data available in the literature on reduction of sodium sulfate in a fluidized bed are still inadequate. The purpose of the present investigation was to study the process in a large-scale laboratory unit.

Apparatus and method of investigation. The experiments were performed in a unit shown schematically in Fig. 1.

The main component of the experimental unit was a column made of heat-resisting steel of 50 mm inside diameter, equipped with an electric heater. A porous plate was fitted in the bottom of the column, with a thermocouple and a discharge tube above. The material was fluidized above a layer of quartz packing which filled the furnace up to the discharge tube.

It was essential to separate the reaction zone from the junction of the column with its bottom, as at the high temperatures used it is very difficult to avoid losses of hydrogen through leaks.

Hydrogen and nitrogen were fed in through tubes with diaphragms. Nitrogen served as an inert gas. The temperature was measured by means of the thermocouple.

Pure sodium sulfate was investigated. Iron salts were used as catalysts, the total amount of iron being 1%

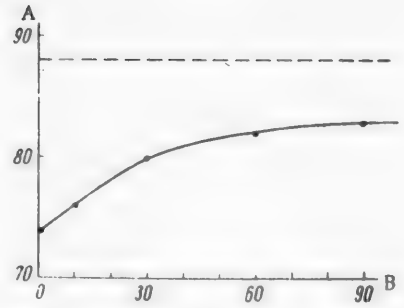


Fig. 2. Reduction of $Na_2SO_4$ added in 20% amount to a bed containing 88% $Na_2S$ at 640°:
A) average amount of $Na_2S$ in bed (%)
B) time (minutes).

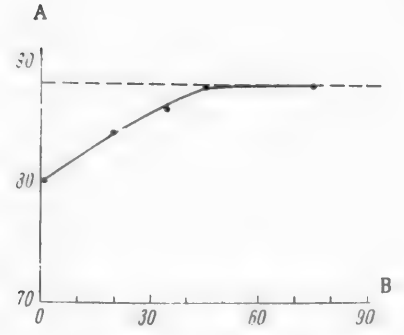


Fig. 3. Reduction of $Na_2SO_4$ added in 10% amount to a bed containing 88% $Na_2S$ at 680°:
A) average amount of $Na_2S$ is bed (%),
B) time (minutes).

of the weight of the original dry substance. The material was granulated and dried for several hours at 150-200°, and then sifted. The amount of sodium sulfide in the product was determined iodometrically.

The influence of the amount of catalyst on the reaction kinetics was not considered in the experiments, as the purpose of this work was to study the reduction of sodium sulfate at fairly high rates. It is known from the literature that the requisite reaction rate is reached in presence of 1% catalyst.

The experiments were performed batchwise. The material was introduced into the furnace from above; it was first preheated by means of nitrogen, and the nitrogen supply was then discontinued and hydrogen was let in. Samples of the material were taken during the process by means of a special probe through the top of the furnace directly from the fluidized bed. At the end of the experiment the material was discharged through the discharge tube; the packing was then removed, as it was necessary to find whether fusion products are formed on the packing and on the tube walls.

As a check, additional analyses were performed on average samples taken from the whole mass of material and on separate samples of fine fractions, and on coarse fractions consisting of agglomerates.

Two series of experiments were carried out: 1) batch reduction of $Na_2SO_4$ for production of high-percentage $Na_2S$; 2) batch reduction of $Na_2SO_4$ mixed with high-percentage $Na_2S$; i.e., under conditions close to a continuous production process.

Reduction of homogeneous $Na_2SO_4$. The reduction was performed in several stages, at temperatures of 620, 640, 680, and 720-760° during 3-4 hours. The product contained 88-97% $Na_2S$. Despite the great care taken in raising the temperature, local overheating took place, the grains of the material often stuck together, and material was retained on the furnace walls. Cohesion of the grains generally did not lead to formation of large agglomerates, so that the bed returned to the fluidized state when the temperature was lowered again.

The numerous experiments in this series reveal certain general relationships for the process. It was found that sodium sulfate with added catalyst is difficult to bring into the fluidized state at high temperatures.

Fractions of the material with particle diameters of 0.6-0.45, 0.45-0.3, 0.3-0.15 mm were reduced. Because of partial agglomeration of the grains during the reduction process, it was not possible to determine the relationship between reduction time and grain diameter for the fine fractions. To maintain the bed continuously in the fluidized state and to prevent agglomeration it was necessary to pass hydrogen at several times the critical rate. The gas rate was not observed to have an influence on the rate of reduction in the range of rates studied (from 15 to 40 liters/minute). This confirms the hypothesis that the reduction reaction is controlled by kinetics and not diffusion, and therefore increase of the agitation rate and improvement of diffusion conditions do not influence the reaction rate. Since the properties of the material are such that very high gas rates must be used, the degree of hydrogen conversion is very low. The reduction reaction slows down near the end of the process. At 680-700° a product containing 88-92% $Na_2S$ was formed in 3-4 hours. The reaction did not proceed further. To obtain an almost pure product (96-97.5% $Na_2S$) it was necessary to stop the reduction process at 740-760°.

Reduction of $Na_2SO_4$ in a fluidized bed with $Na_2S$. A definite amount of $Na_2SO_4$ was introduced into fluidized $Na_2S$ in a stream of hydrogen (so that the sulfate concentration in the fluidized bed corresponded to the calculated value). Trial experiments showed that the sulfate grains become distributed rapidly and uniformly

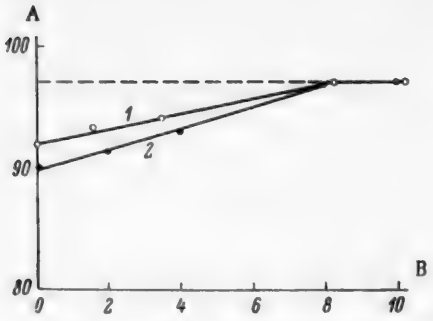


Fig. 4. Reduction of $Na_2SO_4$ in a bed of 97% $Na_2S$ concentration at 740°: A) average amount of $Na_2S$ in bed (%), B) time (minutes); $Na_2SO_4$ contents (%): 1) 5, 2) 7.5.

in the fluidized layer of sulfide grains. Trials of the use of nitrogen as an inert gas to agitate the bed before hydrogen was passed through were not successful because of the additional difficulties arising in removal of oxygen from large volumes of nitrogen (gas rates of the order of tens of liters per minute were used). The grains of material were oxidized by even small amounts of oxygen, and the bed became agglomerated, so that 600° was the practical limit of the use of nitrogen as inert gas.

The initial mass of the bed was 200 g; in the stationary state it occupied 15 cm of the column height. The sulfide layer consisted of 0.6-0.15 mm grain fractions, and the added sulfate, of 0.3-0.15 mm grains. The hydrogen rate was 20 liters/minute, which is equivalent to 17 cm/second (at 20°).

In this series the results of the previous experiments were used to study the influence of tempeature on the reduction process. In experiments conducted at low temperatures the original bed contained 88% sulfide, and at temperatures above 700°, 97% sulfide.

The results of the experiments are plotted in Figs. 2-4. The permissible sulfate content of the original bed increased with decrease of temperature. The curves represent the increase of the sulfide content of the bed with time.

The dash line represents the composition of the sulfide layer without added sulfate.

Fig. 2 shows the results obtained when 20% of $Na_2SO_4$ was added to an original bed containing 88% $Na_2S$ (the average $Na_2S$ concentration in the initial mixture was 74%). At 640° the reduction process was almost complete after 90 minutes.

Fig. 3. represents reduction of a mixture with 10% $Na_2SO_4$ (initial average composition 80% $Na_2S$) at 680°. It is seen that after about 45 minutes the reduction process ceases.

Fig. 4 shows the results of reduction of $Na_2SO_4$ mixed with a product containing 97% $Na_2S$, at 740°. The results for a mixture containing 5% $Na_2SO_4$ are represented by Curve 1, and for a mixture with 7.5% $Na_2SO_4$, by Curve 2. The results were in good agreement. All the added sulfate was reduced within 8 minutes.

Linearity in this case is not a significant characteristic of the process, as there must be inevitable deviations form the initial composition in sampling from a fluidized bed, with an excessively high $Na_2S$ concentration in the initial bed. The duration of the reduction process may be considered as the determining factor in the kinetics of the process, which is in reality complicated by the formation of a liquid phase. The hydrogen conversion is 5% under the most favorable process conditions. However, the degree of hydrogen conversion may be increased by increasing the height of the bed, without change in the gas rate, which is associated with the properties of the fluidized system.

Additional studies of the process kinetics and selection of suitable catalyst are very important.

The costs of the process should be studied in detail from the economic standpoint on the pilot-plant scale.

## SUMMARY

It is shown that $Na_2SO_4$ may be reduced in a fluidized bed at temperatures above the eutectic point, with low concentrations of $Na_2SO_4$ in the bed and high hydrogen rates. The time required for reduction is 8 minutes with 5 and 7.5% sodium sulfate in the mixture, with grains 0.3-0.15 mm in diameter, in presence of 1% of iron catalyst. The grain diameter was found to increase as the result of agglomeration. The experimental results suggest that despite the large amount of catalyst the reaction proceeds in the kinetic region.

## LITERATURE CITED

[1] K. I. Makarov, Trans. Moscow Eng. Econ. Inst., Chem. and Chem. Ind., 1 (Moscow, Soviet Science Press, 1954) p. 83 [in Russian].

[2] F. Kozmal, Papir a celulosa 9, 210 (1954).

[3] P. Ley, Chem. Ztg. 58, 859 (1934).

[4] C. I. Nyman and T. O. O'Brien, Ind. Eng. Ch., 39, 1019 (1947).

[5] F. Kohlmeyer, and G. Lohrke, Z. anorg. allg. Ch., 281, 54 (1955).

[6] A. I. Gorbanev and V. Ya. Nikolina, Sodium Sulfate [in Russian] (State Political Press, Moscow, 1954).

[7] A. I. Gorbanev, J. Appl. Chem. 27, 805, 921, 1033 (1954), [USSR].

[8] Takeyoshi Haga, Chem. Abs., 48, 2335d (1954).

[9] K. Wintersberger and G. Koudela, U.S. Patent 2690958, (1954); Chem. Abs., 49, 3489c (1955).

[10] G. Koudela and K. Winterberger, British Patent 700132 (1953), U.S. Patent 2719076 (1955).

Received June 17, 1958.

# DISSOLUTION OF MONOCRYSTALLINE GERMANIUM IN HYDROGEN PEROXIDE

G. S. Supin

In the production of germanium semiconductor components, very close attention is devoted to the surface quality of the germanium crystals which, after the technological cycle, are converted into various semiconductor components. After being cut by mechanical saws, the crystals have damaged surface layers; these layers must be removed to expose the single-crystal surface. The crystal surface attains the required quality as the result of chemical "etching," i.e., dissolution of part of the germanium from the surface in an etching agent. One of the substances used for this purpose is hydrogen peroxide.

This paper deals with some aspects of the solution rate of germanium in hydrogen peroxide solutions of different hydrogen-ion concentrations.

This investigation may be of practical value for laboratories and factories producing semiconductor equipment. The results may be used for selection of the medium and etching conditions in accordance with requirements. It has been found by experience that surfaces etched by hydrogen peroxide solutions differing in their hydrogen-ion concentrations do not show any significant differences and behave similarly during the subsequent stages in the technological production of semiconductor equipment.

## EXPERIMENTAL

The germanium specimens used in the experiments were in the form of rectangular parallelepipeds cut from single-crystal blocks grown by Chokhral'skii's method. The specimens were in the form of plates, the average dimensions of which were 10 × 5 × 1 mm. After being cut, the plates used for the experiments were polished with fine emery paper and etched to make sure that the results obtained related to the etching of single-crystal surfaces. The specimens tested differed in specific ohmic resistance (from 1 to 10-12 ohm · cm). It was found that differences in resistance did not influence the etching rate of germanium, within the limits of experimental error. Germanium of the n type was used in all cases.

The hydrogen peroxide used was of "medical" grade (GOST 177-55), and had an initial concentration of 28-32%; the required concentrations were obtained by dilution with distilled water. The concentrations were determined areometrically.

The original hydrogen peroxide had pH = 2-4; caustic soda was added to give the required alkalinity. The hydrogen-ion concentration was estimated by the colorimetric method with the aid of a universal indicator consisting of 0.1 g phenolphthalein, 0.3 g methyl yellow, 0.2 g methyl red, 0.4 g bromothymol blue, and 0.5 g thymol blue, dissolved in 500 ml of ethyl alcohol, with the use of standard solutions. This method was used because it was impossible to determine the hydrogen-ion concentration directly with the quinhydrone electrode (oxidizing medium), and also because determinations of the pH of hydrogen peroxide solutions by means of the glass electrode are known to give low results [1].

In view of the fact that the determinations were performed only in media of pH = 4-5 and pH = 7-8, this rough method of pH determination was quite admissible.

Before the experiments the apparent geometrical dimensions of the plates were measured to an accuracy of 0.01 mm, and the plates were weighed on an analytical balance to within 0.0001 g. A measured quantity of

hydrogen peroxide, brought to the required concentration and pH, was warmed until the start of the decomposition reaction (100-103°), and the germanium plates were then put into the reaction vessel. After the required time the plates were taken out of the solution, thoroughly washed and dried, and their geometrical dimensions and weights were again determined.

The contents of the reaction vessel were agitated vigorously during the etching. Agitation influences the etching rate only up to a certain limit; further increase of the agitation rate has no effect on the solution rate of germanium; this limit corresponds to about 1-2 shakings per minute. In the experiments described the agitation rate was about 30-40 shakings per minute.

To ensure greater reliability of the results, several specimens with different geometrical proportions were etched simultaneously. The final result was calculated as the mean for several plates. The discrepancies between the etching rates of different specimens did not exceed the experimental error. The specimens were etched for 10 minutes; it was assumed that the etching rate and hydrogen peroxide concentration varied little during this time. This assumption proved to be justified: the same etching rate was found in control experiments in which etching was continued for 20 minutes. The heating rate was as low as possible in all cases in order to avoid considerable changes of hydrogen peroxide concentration during the reaction.

Method of calculation. The apparent surface area was calculated from the geometrical measurements of the plates before and after etching. The average of the two values was taken as the etched surface for the calculations. The volume of germanium dissolved was found from the difference in weights before and after etching, and the etched depth on one side of the material was then calculated.

$$l = \frac{G_1 - G_2}{d \cdot t \cdot \frac{S_1 + S_2}{2}} = \frac{2}{5.32} \cdot \frac{G_1 - G_2}{S_1 + S_2} \cdot \frac{1}{t} = \frac{1}{2.66} \cdot \frac{G_1 - G_2}{S_1 + S_2} \cdot \frac{1}{t},$$

where $G_1$ is the weight of the plate before etching (in g); $G_2$ is the weight of the plate after etching (in g); $S_1$ is the apparent surface before etching (in $cm^2$); $S_2$ is the apparent surface after etching (in $cm^2$); $d$ is the density of germanium (in g/cc) (the density of germanium taken as 5.32 g/cc); $t$ is the etching time (minutes); $l$ is the depth of the dissolved germanium (in cm/minute).

## RESULTS AND DISCUSSION

The results of the experiments are presented in the diagram.

The solution rate of germanium in hydrogen peroxide of hydrogen-ion concentration corresponding to pH = = 4-5 does not vary over a wide range of hydrogen peroxide concentrations (7-30%), and is 1.3 μ/minute. The solution rate of germanium in a more alkaline medium, at pH = 7-8, varies slightly (from 3.3 to 3.6 μ/minute) with variations of hydrogen peroxide concentration in the 10-30% range. It follows that change of pH has a strong influence on the solution rate of germanium in hydrogen peroxide.

The calculated hydrogen-ion concentrations for aqueous solutions of hydrogen peroxide correspond to pH values of 5.3 for 30% solution and 5.8 for 3% solution [2]. It follows from the graph that when germanium reacts with hydrogen peroxide of hydrogen-ion concentration close to the theoretical the solution rate of germanium is low and remains constant over a very wide range of concentrations.

Hydrogen peroxide containing a certain amount of free alkali (corresponding to pH = 7-8) dissolves germanium much more rapidly.

The following reaction mechanism is postulated to account for the observed effects:

$$H_2O_2 + Ge = GeO + H_2O \quad \text{or} \quad O_2'' + Ge = GeO + O'',$$

$$H_2O_2 + GeO = GeO_2 + H_2O \quad \text{or} \quad O_2'' + GeO = GeO_2 + O'',$$

i.e., the $-O-O-$ group in hydrogen peroxide changes into water oxygen ions.

The germanium dioxide formed dissolves in water (the solubility of $GeO_2$ in water is 4 g/liter), or goes into solution in the form of sodium germanate, $Na_2GeO_3$, if the solution contains alkali.

The intermediate formation of germanium peroxides, or their participation in the reaction, must be regarded as improbable becaus of their instability (germanium peroxides only exist below 0°).

Thus, the heterogeneous reaction of solution of germanium in hydrogen peroxide is considered to consist of three processes: oxidation of germanium to germanium oxide, oxidation of the oxide to the dioxide, and solution of the germanium dioxide.

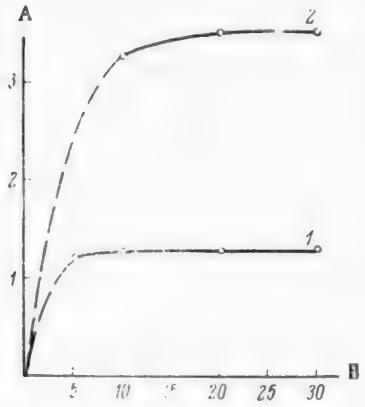


Variation of the solution rate of germanium with the hydrogen peroxide concentration:
A) solution rate (in $\mu$/minute), B)concentration (%); pH 1) 4-5, 2) 7-8.

Data on the oxidation rates of germanium to the oxide and of the oxide to the dioxide are not available, and therefore in this paper the two processes are considered jointly without separation of the solution of germanium in hydrogen peroxide as the first stage. The second stage in the dissolution of germanium is passage of $GeO_2$ into solution.

It is highly probable that the over-all rate of dissolution of germanium is determined by the rate of the second stage – solution of the germanium dioxide formed. This hypothesis is supported by the sharp increase in the solution rate of germanium in presence of free alkali. From this standpoint it is also easy to explain the observed fact that the solution rate of germanium depends little on the hydrogen peroxide concentration: variation of the hydrogen peroxide concentration can influence only the first stage of the process, oxidation of metallic germanium to germanium peroxide, without affecting the rate at which germanium peroxide goes into solution (if the very unlikely possibility of peroxide formation at 100-103° is excluded).

The hypothesis that addition of alkali increases the oxidizing power of hydrogen peroxide, which would account for the increased solution rate of germanium, meets with the objection that in that case it is difficult to explain why the solution rate of germanium remains constant in hydrogen peroxide solutions of different concentrations (at constant pH).

If hydrofluoric acid is present in the hydrogen peroxide solution, the solution of germanium is greatly accelerated, and takes place even at room temperature. One possible explanation of this fact is the hypothesis that hydrofluoric acid reacts with germanium dioxide to form hydrofluogermanic acid.

$$6HF + GeO_2 = H_2GeF_6 + 2H_2O,$$

i.e., in this case the accelerating factor in dissolution of germanium is again passage of germanium dioxide into solution.

Hydrogen fluoride is a stabilizer for hydrogen peroxide [2], and it is therefore difficult to attribute the observed effect to the influence of hydrofluoric acid on the oxidizing properties of hydrogen peroxide.

In the experiments described in this paper germanium plates were used with their horizontal surfaces oriented in the 111 direction. Several experiments were performed on the simultaneous etching of plates with different linear proportions; thus, different areas with other orientations were brought in contact with the solution. No differences were found in the etching rates. It may be assumed that such differences are not found if boiling hydrogen peroxide solution is used for the etching; it is also possible that the differences in this case lie beyond the accuracy limits of the experiments.

A series of experiments was performed in which the specimens were etched several times in succession under the same conditions; calculations showed that the etching rate remained the same. This leads to the conclusion that the surface structure is unchanged as the result of etching, otherwise it would influence the ratio between the apparent geometrical surface and the true surface of the specimen with a definite microstructure;

the calculated value of the etching rate would then be different. The fact that the calculated etching rate was independent of the amount of substance previously removed in hydrogen peroxide solution must be regarded as evidence that hydrogen peroxide does not alter the surface microstructure of germanium whether in alkaline or in acid media. The behavior of a specimen in hydrogen peroxide does not depend on the previous history of its surface treatment with hydrogen peroxide, in contrast to behavior in etching agents containing bromine or hydrofluoric and nitric acids, which change the surface microstructure of germanium.

The fact that the etching rate of germanium does not depend on the hydrogen peroxide concentration or etching time (this is especially pronounced at pH = 4.5) can be used in determinations of the surface areas of germanium specimens of irregular geometrical shape. If the weight loss in etching, the etching time, and the etching rate of germanium (determined graphically) are known, it is easy to calculate the average surface area of the etched specimen:

$$S_{av} = \frac{\Delta G}{d \cdot l \cdot t} .$$

Because of the low accuracy of the colorimetric method used for determinations of the pH of hydrogen peroxide solutions, these results are approximate. However, because of its simplicity and convenience, this method can be used as a control method under production conditions. It would be very desirable to continue these investigations in order to obtain more accurate data.

## SUMMARY

The dissolution rate of germanium in hydrogen peroxide was studied at pH = 4-5 and pH 7-8 (temperature 100-103°); it was found that the rate increases with increase of pH.

## LITERATURE CITED

[1] J. R. Kolczynski and E. S. Shanley, J. Am. Chem. Soc., 79, 531 (1957).

[2] M. E. Pozin (editor), Hydrogen Peroxide and Peroxide Compounds [in Russian] (Goskhimizdat, 1955).

Received September 2, 1957.

# STUDY OF THE REACTION OF STANNOUS SULFIDE WITH SULFUR DIOXIDE

D. N. Klushin and O. V. Nadinskaya

This paper reports on a continuation of earlier studies [1-3] of the technology of extraction of tin from lean materials, and deals with certain data, lacking in the literature, on the side reactions in oxidation of stannous sulfide by atmospheric oxygen.

## EXPERIMENTAL

The reaction of stannous sulfide with sulfur dioxide was studied by means of the apparatus shown in Fig. 1.

The experimental procedure was as follows. A weighed sample of stannous sulfide was placed in a sintered alumina crucible, previously heated to constant weight and weighed. The crucible with the sample was put in a quartz tube connected by a ground-glass joint to a series of absorption flasks containing 0.1 N iodine solution.

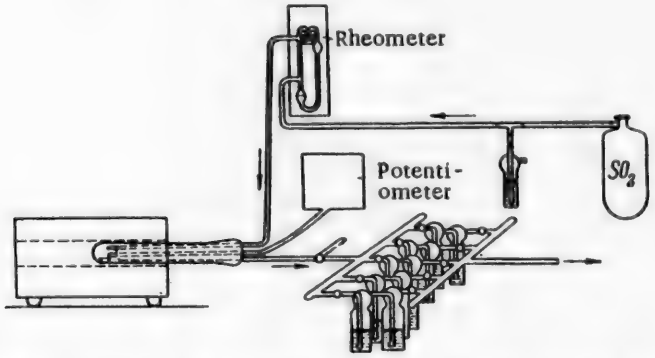


Fig. 1. Apparatus for investigation of the reaction between $SO_2$ and stannous sulfide.

The volume of the reaction space was reduced to a minimum; a quartz bung was inserted for this purpose in the reaction tube. The temperature was measured by means of a platinum-platinum/rhodium thermocouple connected to an electronic automatic regulating potentiometer which maintained the required conditions to within $\pm 5^{\circ}$. The hot junction of the thermocouple was above the crucible with the sample. The sulfur dioxide was fed into the reaction tube through a rheometer at a rate of 500 cc/minute. Before each experiment the completely assembled apparatus was rinsed through with sulfur dioxide.

When the furnace temperature reached 50° above the required value, the tubular furnace was moved onto the quartz reaction tube, the potentiometer regulator was set to the required temperature, and the instant when this was reached was taken as the start of the experiment. The required temperature was reached 3-5 minutes after the furnace was moved over. At the end of the experiment the furnace was moved away from the quartz tube and cooled to room temperature.

The cooled alumina crucible was weighed, and the cinder was separated off and analyzed chemically for tin and sulfur, and by mineralogical and x-ray methods for metallic tin, stannous sulfide, tin disulfide, stannous and stannic oxides, and stannous sulfate.

The experiments were performed with 3.0 g samples at the following temperatures: 550, 600, 650, 700, 750, 800, 850, 900, 950, 1000, 1050, 1100°; the duration was 30 minutes.

The experimental results are given in Tables 1-2 and Fig. 2.

TABLE 1

Weight Changes, Contents of Tin and Sulfate and Sulfide Sulfur in Cinders at Various Temperatures

| Temperature (°C) | Wt. of cinder after expt. (g) | Change in weight of cinder (%) | $Sn_{tot}$ | | $S_{sulfide}$ | | $S_{sulfate}$ | |
|---|---|---|---|---|---|---|---|---|
| | | | in % | in g | in % | in g | in % | in g |
| 550 | 3.147 | +5.8 | 73.7 | 2.34 | 16.3 | 0.517 | 4.3 | 0.136 |
| 600 | 3.230 | +7.7 | 72.4 | 2.34 | 14.2 | 0.459 | 6.0 | 0.195 |
| 650 | 3.250 | +8.3 | 71.7 | 2.33 | 11.2 | 0.364 | 8.9 | 0.290 |
| 700 | 3.254 | +8.5 | 71.9 | 2.34 | 10.9 | 0.355 | 6.9 | 0.224 |
| 750 | 3.161 | +5.4 | 74.0 | 2.34 | 15.1 | 0.477 | 1.4 | 0.045 |
| 800 | 3.124 | +4.1 | 75.5 | 2.36 | 20.6 | 0.650 | 0.1 | 0.03 |
| 850 | 3.117 | +3.9 | 75.1 | 2.34 | 19.8 | 0.62 | 0.1 | 0.03 |
| 900 | 3.116 | +3.8 | 75.1 | 2.34 | 19.0 | 0.60 | 0.01 | 0.003 |
| 950 | 3.108 | +3.6 | 75.3 | 2.39 | 19.3 | 0.60 | traces | traces |
| 1000 | 3.005 | +0.2 | 76.2 | 2.29 | 19.6 | 0.59 | traces | traces |
| 1050 | 2.804 | −6.6 | 77.4 | 2.17 | 18.0 | 0.50 | none | none |
| 1100 | 2.708 | −9.8 | 77.2 | 2.09 | 18.0 | 0.49 | none | none |

TABLE 2

Phase Composition of Cinders for Various Temperatures

| Temperature (°C) | Composition of cinder | | | | | | | | |
|---|---|---|---|---|---|---|---|---|---|
| | $Sn_{met}$ | | $SnSO_4$ | | $SnO_2$ | | $SnS$, $Sn_2S_3$, $SnS_2$ | | deviation from 100% |
| | in % | in g | in % | in g | in % | in g | in % | in g | |
| 550 | — | — | 28.7 | 0.91 | 20.2 | 0.64 | 54.2 | 1.72 | + 3.1 |
| 600 | — | — | 40.7 | 1.31 | 28.5 | 0.92 | 35.9 | 1.16 | + 4.9 |
| 650 | — | — | 59.7 | 1.94 | 43.1 | 1.36 | 8.3 | 0.27 | +11.1 |
| 700 | — | — | 46.1 | 1.5 | 32.6 | 1.06 | 27.6 | 0.87 | + 5.4 |
| 750 | — | — | 9.4 | 6.3 | 6.3 | 0.20 | 82.2 | 2.60 | − 7.9 |
| 800 | 0.4 | 0.013 | 6.4 | 0.2 | 22.7 | 0.71 | 74.6 | 2.33 | + 4.1 |
| 850 | 0.4 | 0.014 | 6.4 | 0.2 | 30.5 | 0.95 | 70.9 | 2.21 | + 8.1 |
| 900 | 0.5 | 0.016 | 0.6 | 0.02 | 19.2 | 0.62 | 77.9 | 2.43 | − 1.1 |
| 950 | 0.4 | 0.013 | traces | traces | 20.9 | 0.65 | 77.9 | 2.42 | − 0.8 |
| 1000 | 0.5 | 0.016 | traces | traces | 24.1 | 0.75 | 73.5 | 2.21 | − 1.9 |

Mineralogical and x-ray structural analysis of the cinders showed that they contain $Sn_{met}$, SnS, $Sn_2S_3$ ($SnS \cdot SnS_2$) $SnS_2$, $SnO_2$, $SnSO_4$.

Elemental sulfur was liberated during the experiments; it proved impossible to collect it completely.

Elemental sulfur could not be detected in the cinder either by x-ray or by mineralogical methods; this is easily accounted for by the high vapor pressure of sulfur at the experimental temperatures. The vapor pressure of sulfur already reaches 760 mm at 440°.

The compositions of the cinders are given in Table 2.

It follows from the data in Table 1 and Fig. 2 that the weight of the cinder changes in the temperature range from 550 to 1100°. The maximum weight increase occurs at 700°, and is 8.5%.

The maximum weight loss occurs at 1100°, and is 9.8%; the loss of tin is then 10.7% of the weight put in. This loss can probably be attributed to loss (volatilization) of tin as sulfide.

Fig. 2 shows that increase of the cinder weight corresponds to an increase of its stannous sulfate content. Hence it may be concluded that the increase in the weight of the cinder is due to stannous sulfate formation.

It follows from the data in Table 2 that in the 550-800° range the cinder consists of stannic oxide, sulfate and sulfides of tin, and metallic tin. At temperatures of 800° and over there is virtually no stannous sulfate in the cinder.

The data below give an indication of the nature of the reactions taking place in the 800-1000° range in oxidation of stannous sulfide by sulfur dioxide.

Amounts of Tin Reacted in Sulfide Form and Converted to Oxide at Various Temperatures

| | Temperature (°C) | | | | |
|---|---|---|---|---|---|
| | 800 | 850 | 900 | 950 | 1000 |
| Tin reacted as sulfide (g) | 0.67 | 0.76 | 0.53 | 0.53 | 0.74 |
| Tin converted to oxide | 0.56 | 0.75 | 0.49 | 0.51 | 0.59 |

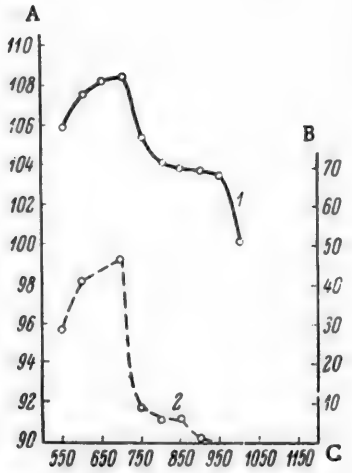


Fig. 2. Effect of temperature on the cinder weight (1) and $SnSO_4$ content (2) in the interaction of SnS with $SO_2$: A) weight change (% of original), B) $SnSO_4$ content of cinder (%), C) temperature (°C).

It is seen from the above data that in the cinder formed in the 800-1000° range the ratio between the tin reacted as sulfide and converted to oxide is close to unity; this indicates that stannous sulfide is oxidized at these temperatures mainly with formation of stannic oxide.

These data are supported by the results obtained by Milbaur and Tucek [4] who found in experiments on oxidation of the sulfides of zinc, copper, and other metals by sulfur dioxide that sulfur dioxide oxidizes metal sulfides with simultaneous reduction of sulfur. They also showed that sulfates are predominant in the oxidation products at lower temperatures, and oxides at higher temperatures.

It is seen in the micrograph (Fig. 3) of a polished section of the cinder formed at 600° that a grain of stannous sulfide is surrounded by metallic tin and $Sn_2S_3$ grains, which are in turn surrounded by $SnS_2$ grains, with stannic oxide grains at the edges of the $SnS_2$ grains. The micrograph (Fig. 3) does not show the stannous sulfate phase, as this is leached out during preparation of the specimen; but it is clearly revealed by x-ray structural analysis.

Microscopic examination of a section of cinder formed at low temperatures showed the presence of metallic tin at the edges of $Sn_2S_3$ and $SnS_2$ grains. However, attempts to photograph this were not successful.

Thus, it follows from the data presented in Table 2 and Fig. 3 that in the 550-750° range the interaction of stannous sulfide with sulfur dioxide proceeds mainly by the reactions,

$$3SnS = Sn_2S_3 + Sn$$

$$2Sn_2S_3 = 3SnS_2 + Sn$$

$$2SnS_2 + 3SO_2 = SnSO_4 + SnO_2 + 6S,$$

and above 800° by the reactions

$$3SnS = Sn_2S_3 + Sn$$
$$2Sn_2S_3 = 3SnS_2 + Sn$$
$$SnS_2 + SO_2 = SnO_2 + 3S.$$

The formation of stannous sulfate in the oxidation of stannic sulfide, established by x-ray structural and chemical analyses, rather than of stannic sulfate, is evidently due to the low stability of stannic sulfate at the temperature used

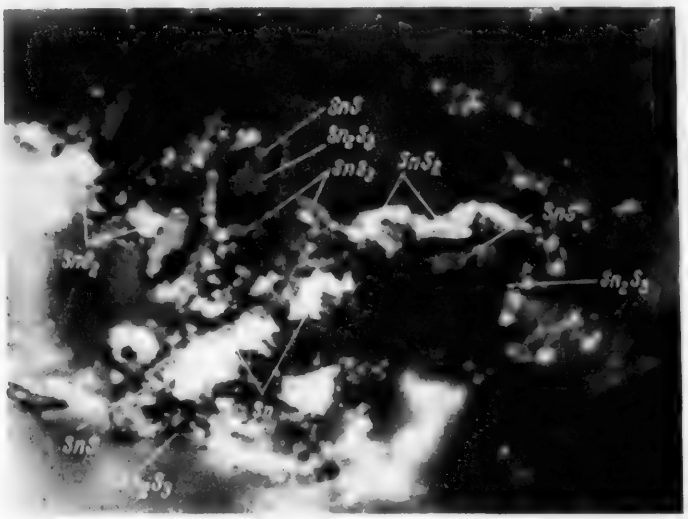


Fig. 3. Section of cinder formed at 600°.

## LITERATURE CITED

[1] D. N. Klushin and O. V. Nadinskaya, J. Appl. Chem. 29, No. 10, 1493 (1956).

[2] D. N. Klushin, O. V. Nadinskaya, and K. G. Bogatina, Coll. Sci. Trans. State Res. Inst. for Nonferrous Metals, 13 (Moscow, Metallurgy Press, 1957) p. 211.

[3] D. N. Klushin, O. V. Nadinskaya, and K. G. Bogatina, J. Appl. Chem. 32, No. 2, 273 (1959).

[4] Milbaur and Tucek, Chem. Z., 30, 32 (1926).

Received September 6, 1957.

# EFFECT OF THERMAL AGING ON THE PORE STRUCTURE AND CATALYTIC ACTIVITY OF SYNTHETIC ALUMINOSILICATES

D. P. Dobychin and T. F. Tsellinskaya

All-Union Scientific-Research Institute of Petrochemical Processes, Leningrad

Thermal aging of aluminosilicate cracking catalysts and associated changes in their structure and activity are of considerable practical and scientific interest.

This question is considered in the publications by Milliken, Mills, and Oblad [1] and Ries [2], which appeared in 1950-1952, and in a paper by Nikitin [3]. The most important fact noted in these papers is the disappearance of fine and also of coarse pores in aluminosilicates as the result of deep thermal aging. In this connection we consider it desirable to publish the results of our investigations, conducted in 1947-1949, of the stability of pore structure and catalytic activity of synthetic bead-type and tablet aluminosilicates.

Fine-pore and coarse-pore samples of bead-type aluminosilicates [4], consisting of 10% $Al_2O_3$ and 90% $SiO_2$ *, were calcined at 500, 800, 900, and 1000° for two hours, and also in steam at 750° for 6 hours. In addition, industrial samples of tableted aluminosilicate of similar composition, used for different periods, were studied.

The pore structure was studied by measurements of adsorption of benzene vapor at 16.5° in an apparatus of the static type. The specific surface was calculated by the BET method, and the pore radii from the Thomson formula. The catalytic activity was determined by the standard method [4] in a flow unit, by cracking of standard gas oil. As the bulk densities of different aluminosilicate samples varied in the range of 0.55-0.8, the volume raw-feed rates were varied in the different experiments so as to keep the degree of conversion as constant as possible. Therefore the gas-oil feed rate per unit weight of the charged catalyst $\left(\frac{\text{1.2 cc raw feed}}{\text{g of catalyst per hour}}\right)$ rather than per unit volume of the catalyst space V, which was 25 cc, was kept constant.

Table 1 contains the result of adsorption determinations which illustrate the influence of heat-treatment on aluminosilicate samples of different pore structures. The pore volume-radius distribution functions for these samples are plotted in Figs. 1-3. The specific surface, which decreases continuously with progressive sintering is highly sensitive to the influence of high temperatures (Fig. 4).

The most characteristic feature in the structural changes of aluminosilicates during thermal aging is the sharp decrease in the height of the maximum on the distribution curve, i.e., decrease of the volume of pores with small radii. The driving force in thermal sintering of highly disperse and porous bodies is their surface energy. Disappearance of small pores in a sintering disperse solid phase leads to increases of the average pore dimensions and particle size (thickness of pore walls). Coarsening of the pore structure can therefore be regarded as a manifestation of the growth of particles constituting the disperse solid phase. Particle-growth effects in highly disperse systems during sintering processes are diffusional in character [5,6]. The mechanism and kinetics of sintering processes in disperse systems have been considered in detail in the literature. The views of Frankel'[5] developed by Pines [6] on the concentration of "vacancies" on solid surfaces make it possible to regard thermal

*The authors thank E.M. Kaganova and B. L. Moldavskii for supplying these samples of bead-type catalysts.

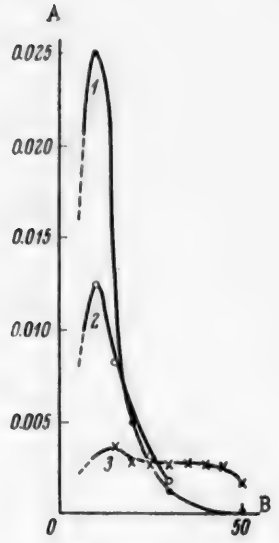


Fig. 1. Pore volume-radius distribution functions for samples of fine-pore bead-type catalyst: A) derivative of pore volume with respect to radius $\frac{dv}{dr} \cdot 10^8 (cm^2/g)$, B) pore radius (A). Aluminosilicate heated at (°C) 1) 550, 2) 800, 3) 750 (in steam).

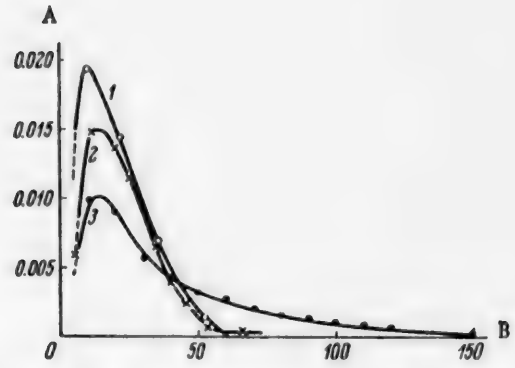


Fig. 2. Pore volume-radius distribution functions for coarse-pore bead-type catalyst: A) $\frac{dv}{dr} \cdot 10^8 (cm^2/g)$, B) pore radius (A); Catalyst heated at (°C): 1) 500, 2) 800, 3) 900.

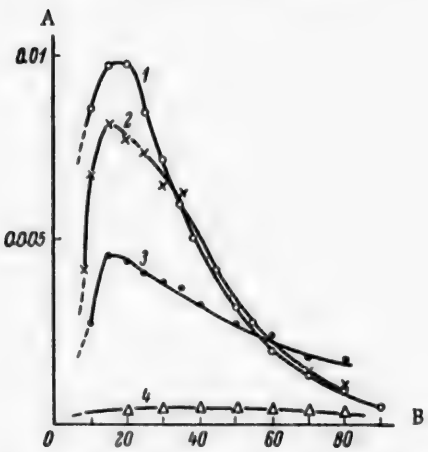


Fig. 3. Pore volume-radius distribution functions for tableted catalyst: A) $\frac{dv}{dr} \cdot 10^8 (cm^2/g)$, B) pore radius (A) Catalyst heated at (°C): 1) 500, 2) 800, 3) 900, 4) 1000.

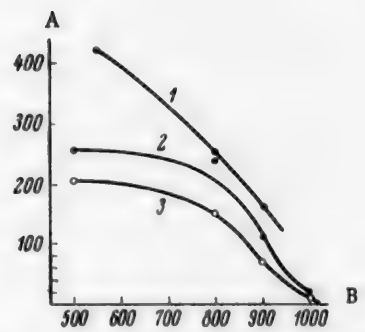


Fig. 4. Variations of specific surface of aluminosilicates with heating temperature: A) specific surface ($m^2/g$), B) temperature (°C); aluminosilicates: 1) fine-pore heads, 2) coarse-pore beads, 3) tableted

sintering of highly disperse bodies, not having high vapor pressures, as a recondensation process, which occurs, however, through a two-dimensional surface layer and not through the gas phase. A surface element in the lattice of a highly disperse body with excess free energy acquires mobility at high temperatures, which enables

it to migrate over the particle surface to regions of lower free energy. The thermodynamic analog of vapor pressure in a three-dimensional gas phase is in this case the plane pressure of the mobile elements of the lattice in a two-dimensional layer on the surface of the solid, determined by the sign and magnitude of the curvature of this surface. The close contact between particles in highly disperse bodies, and continuity of the pore walls in the particles of porous bodies, ensure the possibility of surface migration of these surface elements of the lattice from smaller to larger particles, and therefore from the walls of larger to the walls of smaller pores [6]. This concept is evidently just as valid as the concept of the diffusion of "vacant sites." In the light of the foregoing, an analogy may be drawn between our data and the results obtained by Todes [7] in his analysis of the kinetics of recondensation (overcondensation) processes, from which it follows that the effects studied by him should be accompanied by the changes in the form of the distribution function observed by us. Recondensation results in a continuous shift of the particle-size distribution function toward an increase of particle size, accompanied by a decrease in their number, and also a general broadening of the distribution function with a lowering of the maximum on the distribution curve. Sintering of aluminosilicates is accompanied by considerable volume shrinkage of the granules, and the pore volume decreases considerably. Thus, the change of pore structure in the sintering of the samples studied by us is represented by preferential disappearance of fine pores, as the result of coalescence of small particles and covering of fine pores. The volume increase of the larger pores, imperceptible at the initial stages of sintering, is revealed at later stages in the process (Figs. 1-3, Curves 3).

TABLE 1

Effect of Heating Temperature on the Pore Structure of Synthetic Aluminosilicates

| Heating temperating (°C) | Specific surface ($m^2/g$) | Pore volume (in cc/g) for diameters | | | Pore-volume distribution % for diameters | |
|---|---|---|---|---|---|---|
| | | to 30 Å | 30—150 Å | from 150 Å | to 30 Å | 30—150 Å |
| **Fine-pore beaded aluminosilicate gel (bulk density Δ = 0.8)** | | | | | | |
| 550 | 430 | 0.265 | 0.140 | 0.405 | 65.5 | 34.5 |
| 800 | 252 | 0.155 | 0.140 | 0.295 | 52.5 | 47.5 |
| 900 | 166 | 0.102 | 0.101 | 0.203 | 50.0 | 50.0 |
| 750 (in current of steam | 91 | 0.055 | 0.123 | 0.178 | 31.0 | 69.0 |
| **Coarse-pore beaded aluminosilicate gel (bulk density Δ = 0.6)** | | | | | | |
| 500 | 257 | 0.178 | 0.318 | 0.496 | 36.0 | 64.0 |
| 800 | 248 | 0.144 | 0.273 | 0.417 | 35.0 | 65.0 |
| 900 | 108 | 0.070 | 0.110 | 0.180 | 38.0 | 62.0 |
| 1000 | 28 | 0.012 | 0.026 | 0.038 | 31.0 | 69.0 |
| **Tableted aluminosilicate gel (bulk density Δ = 0.56)** | | | | | | |
| 500 | 206 | 0.106 | 0.288 | 0.394 | 27.0 | 73.0 |
| 800 | 147 | 0.086 | 0.249 | 0.355 | 24.0 | 76.0 |
| 900 | 68 | 0.044 | 0.172 | 0.216 | 20.5 | 79.5 |
| 1000 | 14 | 0.006 | 0.026 | 0.032 | 19.0 | 81.0 |

The higher the dispersity of the system, the greater is the surface energy and therefore the driving force of the thermal aging process. It follows that highly disperse (fine-pore) systems should be more susceptible to thermal aging, and growth processes in them should be more rapid and should begin at lower temperatures than in coarsely disperse (coarse-pore) systems. Indeed, as is clear from the data in Table 1 and Fig. 4, at temperatures up to 800° the coarse-pore structure is somewhat more stable thermally than the fine-pore structure. At higher temperatures this difference tends to vanish. Similar results were obtained by Boreskov, Kiselev, et al.[8], who found that fine-pore silica gel is less stable than coarse-pore silica gel.

It is known from the literature [4,9-11] that aluminosilicate catalysts are rapidly aged when heated in steam it is therefore possible to obtain high degrees of thermal aging and deactivation in model experiments. The data in Table 1 and Fig. 1 characterize the pore structure of fine-pore aluminosilicate gel deactivated by the action of heat in steam at 750°. The specific surface of such samples falls to 90 $m^2$, and the pore volume-radius distribution functions become very diffuse and are shifted in the direction of larger pore radii.

TABLE 2

Pore-Structure Characteristics of Used Industrial Tableted Aluminosilicates

| Duration of use (in months) | Specific surface ($m^2/g$) | Pore volume (cc/g) for diameters | | | Pore-volume distribution (%) for diameter | |
|---|---|---|---|---|---|---|
| | | to 30 Å | 30–150 Å | to 150 Å | to 30 Å | 30–150 Å |
| Fresh catalyst | 200 | 0.106 | 0.288 | 0.394 | 27.0 | 73.0 |
| 2,5* | 116 | 0.059 | 0.268 | 0.327 | 18.0 | 82.0 |
| 11 | 107 | 0.059 | 0.268 | 0.327 | 18.0 | 82.0 |
| 18a** | 108 | 0.059 | 0.216 | 0.275 | 21.5 | 78.5 |
| 18b** | 87 | 0.048 | 0.220 | 0.268 | 17.9 | 82.1 |
| 19 | 108 | 0.053 | 0.242 | 0.295 | 18.6 | 81.4 |
| Catalyst B*** | | | | | | |
| fresh | 191 | 0.091 | 0.258 | 0.344 | 23.0 | 77.0 |
| 11 | 126 | 0.063 | 0.267 | 0.330 | 19.0 | 81.0 |

*Heated to 800° in steam during use.

**Samples taken from the upper (a) and lower (b) zones of the reactor.

***B, first-stage ("treating") catalyst, was used in milder conditions.

Similar results were obtained in investigations of industrial tableted aluminosilicate catalysts (Table 2). Figs. 5 and 6 show the pore volume–radius distribution functions for these samples. The structural characteristics of samples which had aged extensively in use and had been treated with steam provide a vivid illustration of the effects of thermal aging described above–disappearance of fine pores and shift of the pore-volume distribution function in the direction of larger radii.

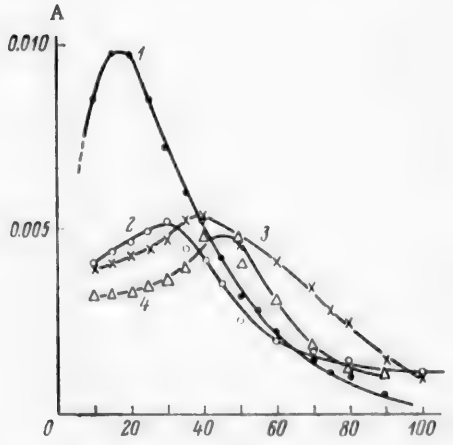


Fig. 5. Pore volume-radius distribution functions for samples of industrial tableted aluminosilicate catalyst:

A) $\frac{dv}{dr} \cdot 10^8$ ($cm^2/g$), B) pore radius (Å); service life of catalyst (months); 1) fresh catalyst, 2) 11, 3) 18 (upper zone of reactor), 4) 18 (lower zone of reactor).

To summarize the foregoing, we may state that the above experimental data on the sintering of aluminosilicates confirm the diffusion theory of thermal aging (sintering) of disperse solids and the associated hypothesis of possible two-dimensional surface recondensation.

Results of determinations of the catalytic activity of the aluminosilicate samples are given in Tables 3 and 4. The degree of cracking means the difference between the amount of converted material and the unconverted residue, taken as the fraction of the reaction products boiling at 200° and over expressed as a percentage of the raw feed. Because of the consecutive nature of the process, the yield of gasoline fraction changes little with variations of the cracking power of the catalyst, as the maximum yield depends on the ratio of the rate constants for the successive stages and not on their absolute values. Therefore, as Figs. 7 and 8 show, the fall in the cracking power of the samples has more influence on the degree of cracking than on the yield of gasoline fraction.

It must also be taken into account that, because the raw feed rate per unit weight of catalyst was standardized

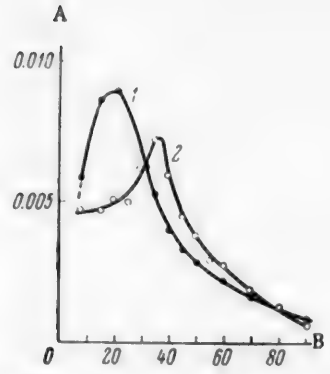


Fig. 6. Pore volume-radius distribution functions for samples of industrial tableted aluminosilicate catalyst: A) $\frac{dv}{dr} \cdot 10^8$ ($cm^3/g$). B) pore radius (A); aluminosilicate: 1) fresh, 2) after 11 months of service.

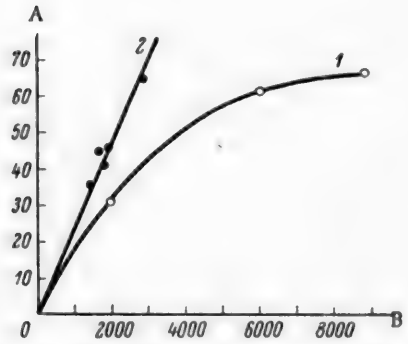


Fig. 7. Effect of total surface area of the catalyst in the reactor on the degree of cracking:
A) degree of cracking (%), B) total surface $S \cdot \Delta \cdot V$ ($m^3$); catalysts: 1) fine-pore beads, 2) tablets.

for comparison of the results obtained with bead samples, a correction is necessary for variations of contact time.

It has been shown [12, 13] that the rate of catalytic cracking of isopropylbenzene is proportional to the total surface area of the catalyst in the reactor; this shows that the cracking power per unit area of aluminosilicate is constant. It follows from the data in Table 4 and Figs. 7 and 8 that this is also valid for tableted samples, the surface of which is accessible to the molecules of gas-oil hydrocarbons, owing to the presence of intermediate and large pores. The degree of cracking and even the yield of gasoline fraction are proportional to the surface area of the tableted catalyst in the reactor. On the other hand, in fine-pore samples of aluminosilicate beads a considerable proportion of the surface is inaccessible to the relatively large gas-oil molecules, and the experimental points in Figs. 7 and 8 lie on flattening curves and not on straight lines. As the fine pores, inaccessible to the molecules of gas-oil hydrocarbons, are accessible to the hydrocarbon molecules of the gasoline and gas fractions, the yield of gas increases more rapidly than the yield of gasoline fraction with increase of surface in fine-pore catalysts (Figs. 8 and 9).

During the reactions the molecules of the gas-oil hydrocarbons may displace the lighter molecules of the reaction products (gasoline, gas) from the catalyst surface accessible to them, with a relative suppression of gas-formation reactions. Therefore in the case of fine-pore catalysts reactions of gas formation may proceed without hindrance on the surfaces of fine pores which are inaccessible to the large gas-oil molecules. This "catalytic ultraporosity" effect [12] becomes evident on comparison of the dependence of the yield of gaseous cracking products on the total surface area of the catalyst in the reactor ($S \cdot \Delta \cdot V$) for beaded and tableted catalysts (Fig. 9). Although the results show that the cracking power per unit accessible surface area of aluminosilicates of different pore structures and degrees of sintering is constant, this conclusion cannot be extended to the catalytic activity of aluminosilicate catalysts in general. Aluminosilicate catalysts, on the one hand, split heavy hydrocarbon molecules, and on the other they effect isomerization and hydrogenation reactions by redistribution of hydrogen, improving the qualities of the end products. The olefin content of the gasoline fraction depends on the extent of the hydrogen redistribution processes.

It follows from the data in Table 4 that the bromine numbers of gasoline fractions formed over used catalysts greatly increase with catalyst age. It follows that the catalytic properties per unit area of aluminosilicate cracking catalysts change significantly with catalyst age. Whereas the cracking power per unit accessible surface remains almost constant, such finer specific properties as the power to catalyze hydrogen redistribution deteriorate considerably as the result of aging and sintering. This leads to the conclusion, at variance with the results of Topchieva's work [14], that at least two types of active centers exist on the surface of aluminosilicate catalysts. One type is responsible for the actual cracking of hydrocarbon molecules, and their number per unit catalyst surface remains almost constant during aging. The centers of the other type catalyze processes of hydrogen redistribution (and possibly other processes), and their properties and number per unit catalyst surface vary considerably during aging.

TABLE 3

Cracking of Standard Gas Oil Over Fine-Pore Pelleted Aluminosilicates Heated at High Temperatures in Air and in Steam

| Heating Temperature (°C) | Yield (in wt.% on oil) | | Distillation results (in wt.% on oil) | | | Degree of cracking (%) | Bulk density Δ (g/cc) | Catalyst volume V (cc) | Specific surface S ($m^2/g$) | $S \cdot \Delta \cdot V$ ($m^2$) |
|---|---|---|---|---|---|---|---|---|---|---|
| | distillate | gas | to 200° | above 200° | debutanization gas | | | | | |
| 500 | 80 | 11.3 | 40.0 | 34.0 | 5.2 | 66 | 0.825 | 25 | 430 | 8860 |
| 800 | 83.8 | 8.25 | 38.3 | 35.1 | 3.8 | 61.7 | 0.952 | 25 | 452 | 5970 |
| 750 (in current of steam) | 95 | 3.3 | 22.1 | 68.6 | 4.0 | 31.4 | 0.967 | 22.4 | 91 | 1970 |

TABLE 4

Cracking of Standard Gas Oil Over Used Industrial Tableted Aluminosilicates Volume of catalyst in reactor (V) = 25 cc

| Operating state of sample | Bulk density (g/cc) | Yield of cracking products (wt. % on oil) | | | | | Degree of cracking (%) | Bromine number of fraction up to 200° | S ($m^2/g$) | $S \cdot \Delta \cdot V$($m^2$) |
|---|---|---|---|---|---|---|---|---|---|---|
| | | distillate | cracking gases | to 200° | above 200° | debutanization gas | | | | |
| Fresh | 0.56 | 85.8 | 9.05 | 38.0 | 38.5 | 4.3 | 64.5 | 18.5 | 200 | 2800 |
| Used for 2.5 months | 0.635 | 88.0 | 8.3 | 26.1 | 54.4 | 3.56 | 45.6 | 18.6 | 116 | 1850 |
| Used for 11 months | 0.624 | 87.75 | 9.2 | 26.2 | 54.6 | 2.3 | 45.4 | 17.5 | 107 | 1680 |
| Used for 18 months (top of reactor) | 0.633 | 90.4 | 6.6 | 25.0 | 58.3 | 3.6 | 41.7 | 28.0 | 108 | 1700 |
| Used for 18 months (bottom of reactor) | 0.658 | 91.86 | 7.3 | 21.4 | 64.4 | 2.3 | 35.6 | 34.0 | 87 | 1420 |
| Used for 19 months | 0.636 | 89.0 | 8.1 | 27.6 | 53.0 | 3.0 | 47.0 | 25.0 | 108 | 1730 |

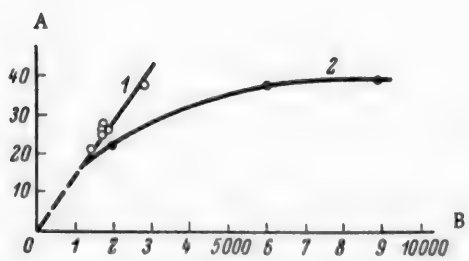


Fig. 8. Effect of total surface area of the catalyst in the reactor on the yield of gasoline fraction:
A) yield of fraction up to 200° (%), B) total surface $S \cdot \Delta \cdot V$ ($m^2$); catalysts: 1) tablets, 2) fine-pore beads.

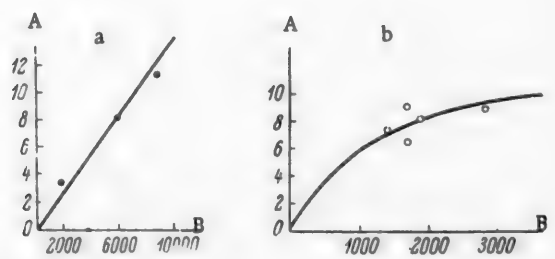


Fig. 9. Effect of total surface area of catalyst in the reactor on the gas yield:
A) gas yield (%), B) total surface $S \cdot \Delta \cdot V$ ($m^2$); catalysts: a) fine-pore beads, b) tableted.

These conclusions are consistent with the view that two forms of acid centers, protonic (Bronsted) and aprotic (Lewis), exist on aluminosilicate surfaces [15]. We consider that the centers which have cracking power are closer to the ionic (protonic) type of catalytically active centers, whereas the centers which reactions of hydrogen redistribution are closer to the electronic (semiconductor) type [16].

## SUMMARY

1. Thermal aging of aluminosilicate catalysts results in coarsening of their pore structure, accompanied by a shift of the pore volume-radius distribution function in the direction of larger pore radii.

2. It is suggested that processes of thermal aging in highly disperse and porous bodies can be regarded in the light of the diffusion theory of sintering as recondensation processes taking place through a two-dimensional surface phase.

3. Fine-pore structures are less thermally stable than coarse-pore structures, and the finer pores disappear before the larger.

4. Cracking of gas oil over fine-pore aluminosilicate catalysts is accompanied by the "catalytic ultraporosity" effect, which consists of inaccessibility of the surfaces of the fine pores to large molecules, and which influences the composition of the products.

5. The cracking power per unit surface area of aluminosilicate catalysts remains virtually constant during thermal aging, whereas the ability per unit surface area to catalyze reactions of hydrogen redistribution decreases; this shows that two types of catalytically active centers are present on the surface of aluminosilicate catalysts.

## LITERATURE CITED

[1] T. H. Milliken, G. A. Mills and A. G. Oblad, Trans. Far. Soc., 8, 270 (1950); Catalysis in Organic Chemistry [in Russian] (Moscow, 1953) p. 185.

[2] H. E. Ries. Advances in Catalysis, IV. N. Y. (1952).

[3] Yu. S. Nikitin, in the book: Surface Chemical Compounds and Their Role in Adsorption Phenomena [in Russian] (Moscow, 1957) p. 170.

[4] A. V. Agafonov, Aluminosilicate Catalysts [in Russian] (State Fuel Tech. Press, 1952).

[5] Ya. I. Frenkel', J. Exp. Theoret. Phys. 16, 29 (1946); Introduction to the Theory of Metals, 2nd edition [in Russian] (Moscow-Leningrad, State Tech. Press, 1950) p. 196.

[6] B. Ya. Pines, J. Exp. Theoret. Phys. 16, 737 (1946); Progr. Phys. Sci. 52, No. 4, 501 (1954). [USSR].

[7] O. M. Todes, Colloid J. 15, No. 5, 391 (1953); Problems of Kinetics and Catalysis 7, 137 (1949).

[8] G. I. Boreskov, M. S. Borisova, V. A. Dzis'ko, A. V. Kiselev, O. A. Likhacheva and T. N. Morokhovets, Proc. Acad. Sci. USSR 62, 649 (1948).

[9] S. K. Makarov and M. A. Kaliko, Petroleum Economy 2, 42 (1947).

[10] H. A. Schabaker. Houdry Pioneer, 3, 1 (1948).

[11] E. M. Rabinovich, in the book: Methods for Testing Petroleum and Petroleum and Petroleum Products (edited by L. A. Potolovskii) [in Russian] (Moscow, 1955).

[12] A. V. Agafonov and M. A. Kaliko, J. Gen. Chem. 19, 39 (1949), [USSR].

[13] D. P. Dobychin and T. F. Tsellinskaya, Proc. Acad. Sci. USSR 109, 351 (1956).

[14] K. V. Topchieva, Sci. Mem. MGU 174, 75 (1955).

[15] I. Trambouze, L. Mourgues, and M. Perrin, I. Chim. phys. et Phys.-chim.biol. 51, 11-12, 723 (1954).

[16] S. Z. Roginskii, Problems of Kinetics and Catalysis 6, 9 (1949) [in Russian].

Received July 11, 1958.

# ALTERATION OF THE STRUCTURE OF AN ANODE SURFACE IN THE COURSE OF DESTRUCTION*

B. M. Bulygin

The Ivanovo Institute of Chemical Technology

In the previous communications [1, 2] a distinction was established between the mechanisms of external and internal destruction of graphite anodes. In accordance with the electrolysis conditions, either external electrochemical destruction accompanied by mechanical disintegration or internal chemical oxidation by hypochlorous acid may prevail. The limit of external destruction is determined by the extent of electrolysis.

The structure of the corroding external layer should play an important role in the course of destruction, as it is interconnected with the extent of the true specific surface of the graphite and therefore with the true current density. Moreover, the start of mechanical crumbling should be related to a certain maximum porosity of this layer, when the cohesion between adjoining graphite region breaks down. The structural characteristics of the disintegrating anode surface vary in accordance with the electrolyte temperature and current density, and the relative proportions of chemical and mechanical losses may vary accordingly.

Studies of the course of wear and structural changes in disintegrating anode layers are few, and relate mainly to determinations of the limiting degree of electrolysis [3] and swelling effects in acids [4].

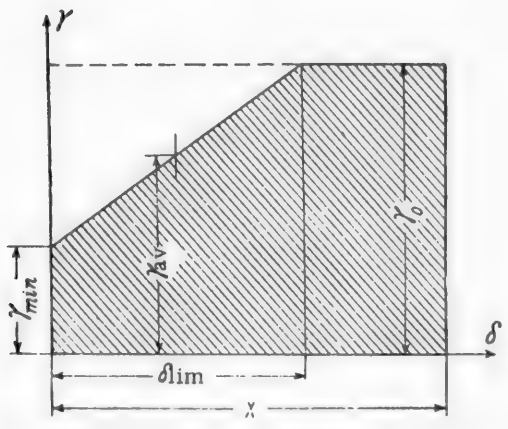


Fig. 1 Schematic density distribution in the disintegrating layer of a graphite anode.

We studied the distribution of destruction in the outer layer of a graphite anode with the aid of two methods: 1) determination of the apparent density of the graphite in various regions of this layer (this method was first used by Sirak [5]), and 2) by microphotography. Our aims were: to determine the limit of external destruction, to investigate the porosity variations in different layers during destruction, and to compare structural changes in the surface layers of impregnated and unimpregnated anodes.

## EXPERIMENTAL

Method of density determination. The apparent densities of porous bodies are usually determined by means of a pycnometer; the pycnometric liquid should have the highest possible interfacial tension so that it should not penetrate into the pores. The pores are sometimes previously blocked by a suitable fusible substance (such as paraffin wax). The larger the specimen, the less is the error in the determination.

*Communication III in the series on studies of certain relationships in the destruction of graphite anodes in aqueous electrolyte solutions.

TABLE 1

Destruction of the External Layer of an Unimpregnated Graphite Anode as a Function of the Electrolysis Time

| | Electrolysis time (hours) | | | | | |
|---|---|---|---|---|---|---|
| | 1 | 2 | 3 | 4 | 6 | 10 |
| Weight loss (g) | 0.0341 | 0.0684 | 0.0988 | 0.2230 | 0.3616 | 0.6617 |
| Thickness decrease (mm) | 0.01 | 0.03 | 0.05 | 0.28 | 0.42 | 0.83 |
| $\delta_{lim}$ (mm) . . . . . | 0.195 | 0.27 | 0.32 | 0.40 | 0.38 | 0.38 |
| $\gamma_{av}$ (g/cc) . . . . . | 1.279 | 1.286 | 1.191 | 0.169 | 1.061 | 1.075 |
| $\gamma_{min}$ (g/cc) . . . . . | 1.013 | 0.968 | 0.735 | 0.681 | 0.475 | 0.466 |
| Mechanical losses (%) . . | 9.95 | 12.8 | 11.0 | 25.6 | 17.2 | 18.2 |
| Chemical losses (%) . . . | 90.05 | 87.2 | 89.0 | 74.4 | 82.2 | 81.8 |

Note. $\delta_{lim}$ is the limiting thickness of the crumbling layer, $\gamma_{av}$ is the average density of the crumbling layer, $\gamma_{min}$ is the minimum density at the surface of the crumbling layer.

In our experiments it was necessary to use the thinnest possible specimens, for accurate determinations of density changes in the disintegrating layer, about 0.5 mm thick. The pycnometric method proved unsuitable, as it gave variations of up to 25% in the density values.

Satisfactory results were obtained by direct weighing of specimens of measured volume. The specimens were parallelepipeds, the linear dimensions of which were measured by means of a micrometer to an accuracy of 0.01 mm. They were weighed on an analytical balance to the nearest 0.2 mg. With the smallest specimens used (1.5 × 4 × 8 mm) the average error in this method for determination of $\gamma_{app}$ was 1.25%.

Density variations with depth are shown schematically in Fig. 1. At depth $\delta_{lim}$ electrolysis virtually ceases, and the apparent density reaches the value $\gamma_0$, beyond which it remains constant. The minimum density of the crumbling layer is $\gamma_{min}$. The value $\gamma_{av}$ is the average density of the crumbling layer. Taking a specimen, a part of which is known to be indestructible, and dividing its weight by its volume, we find $\gamma_1$, intermediate between $\gamma_{av}$ and $\gamma_0$. To find a series of values for $\gamma$ corresponding to different $\delta$ for one specimen, we gradually cut the specimen down from its front and back faces. Having cut off several successive layers from the front (working) face, we found a series of values of $\gamma$, between $\gamma_1$ and $\gamma_0$. Cutting of the specimen from the back face gave values of $\gamma$ intermediate between $\gamma_1$ and $\gamma_{av}$. The density found in each measurement refers to the middle of the full thickness of the specimen. Values of $\gamma_{av}$, $\gamma_{min}$ and $\delta_{lim}$ were found by simple calculations and the apparent densities were plotted against the distance from the working face.

Electrolysis conditions. The experiments were performed in a solution containing 5 g of hydrochloric acid per liter. This electrolyte is fairly corrosive, and destruction in it is similar in character to destruction in the industrial electrolyte (NaCl, 310 g/liter. Graphite anodes in the form of thin plates (1.5-2 mm) were used in electrolysis under the following conditions: a) electrolysis time: 1, 2, 3, 4, 6, and 10 hours at current density 4000 amp/$m^2$ and t = 60°; b) current densities 500, 2000, and 4000 amp/$m^2$ with electrolysis time 3 hours and t = 60°.

Unimpregnated specimens and specimens impregnated with linseed oil were tested separately. At the end of electrolysis the anodes were washed in cold water for 3-4 hours and dried at 120° to constant weight. Specimens of about 4 × 8 mm were then cut from them, and the densities were determined.

The results of the experiments are given in Tables 1-4 and Figs. 2-5.

TABLE 2

Destruction of the External Layer of an Impregnated Graphite Anode as a Function of the Electrolysis Time
$D_a$ = 4000 amp /$m^2$, t = 60°, electrolyte HCl (5 g/liter)

| Data | Electrolysis time (hours) | | | | |
|---|---|---|---|---|---|
| | 1 | 2 | 3 | 6 | 10 |
| Weight loss (g) | 0.0581 | 0.1240 | 0.1831 | 0.3585 | 0.6031 |
| Thickness decrease (mm) | 0.045 | 0.145 | 0.245 | 0.570 | 0.905 |
| $\delta_{lim}$ (mm) | 0.16 | 0.44 | 0.40 | 0.34 | 0.50 |
| $\gamma_{av}$ (g/cc) | 1.216 | 1.165 | 1.147 | 1.107 | 1.068 |
| $\gamma_{min}$ (g/cc) | 0.950 | 0.792 | 0.806 | 0.672 | 0.585 |
| Mechanical losses (%) | 12.4 | 14.9 | 18.6 | 18.0 | 15.0 |
| Chemical losses . (%) | 87.6 | 85.1 | 81.4 | 82.0 | 85.0 |

TABLE 3

Destruction of the External Layer of an Unimpregnated Graphite Anode as a Function of the Electrolysis Temperature

| Data | Temperature (°C) | | |
|---|---|---|---|
| | 40 | 60 | 80 |
| Weight loss (g) | 0.2933 | 0.0988 | 0.2813 |
| Thickness decrease (mm) | 0.355 | 0.05 | 0.36 |
| $\delta_{lim}$ (mm) | 0.29 | 0.32 | 0.35 |
| $\gamma_{av}$ (g/cc) | 1.105 | 1.192 | 1.116 |
| $\gamma_{min}$ (g/cc) | 0.548 | 0.730 | 0.596 |
| Mechanical losses (%) | 20.3 | 11.0 | 22.9 |
| Chemical losses (%) | 79.7 | 89.0 | 77.1 |

TABLE 4

Destruction of the External Layer of an Unimpregnated Graphite Anode as a Function of Current Density
(Electrolyte HCl, 5 g/liter, t = 60°)

| Data | Current density (amp/$m^2$) | | |
|---|---|---|---|
| | 500 | 2000 | 4000 |
| Weight loss (g) | 0.0190 | 0.0456 | 0.0988 |
| Thickness decrease (mm) | 0.025 | 0.045 | 0.050 |
| $\delta_{lim}$ (mm) | 0.26 | 0.37 | 0.32 |
| $\gamma_{av}$ (g/cc) | 1.894 | 1.241 | 1.118 |
| $\gamma_{min}$ (g/cc) | 1.070 | 0.894 | 0.735 |
| Mechanical losses (%) | 42.0 | 29.0 | 11.0 |
| Chemical losses (%) | 58.0 | 71.0 | 89.0 |

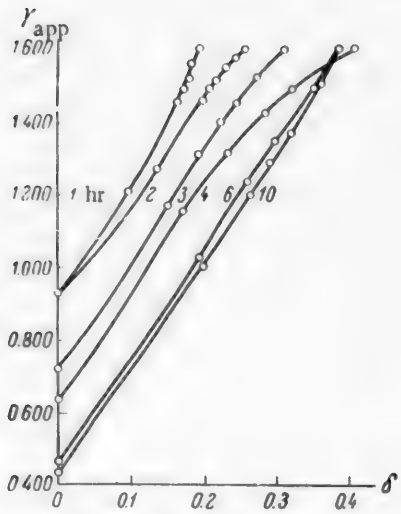


Fig. 2. Density distribution in the outer layer of an unimpregnated graphite anode: $D_a$ = 4000 amp/$m^2$, t = 60°, electrolyte HCl, 5 g/liter.

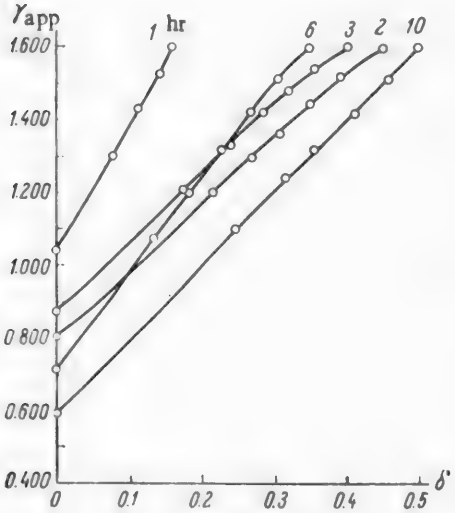


Fig. 3. Density distribution in the outer layer of an impregnated graphite anode: $D_a$ = 4000 amp/$m^2$, t = 60°, electrolyte HCl, 5 g/liter.

## DISCUSSION OF RESULTS

During the first three hours of electrolysis the total breakdown of an unimpregnated anode increases little, and mechanical crumbling is only about 10%. Therefore the thickness decrease of the specimen is measured in only hundredths of a millimeter. The surface relief shows almost no change in comparison with unused specimens (Fig. 4,a). The limiting depth of destruction gradually increases. However, after 4 hours of electrolysis the total losses increase sharply, especially as the result of mechanical crumbling, which reaches 25.6%. Microphotographs reveal considerable surface pitting. The density-distribution curves descend further, but the limiting depth of destruction is stabilized at 0.38-0.40 cm. Electrolysis for 6 and 10 hours results in few further changes in the structure of the surface layer, and the micrographs of the specimens in these experiments are similar. All this leads to the following conclusions concerning the destruction mechanism.

At first, losses arise only as the result of chemical oxidation of the surface and external pores. Widening of the pores facilitates electrolysis within the electrode, and therefore $\delta_{lim}$ gradually increases. Cohesion between the graphite grains deteriorates. Finally this leads (after 4 hours of electrolysis in the present instance) to abrupt crumbling of the initially firm external layer. This exposes a rough surface which favors considerable mechanical losses (17-18%), and which retains its structure during the entire subsequent electrolysis. From this instant there begins regular layer-by-layer chemical oxidation, accompanied by equally regular mechanical crumbling.

This form of destruction is characteristic only for electrolysis at a high current density (4000 amp/$m^2$) when ion discharge does not take place in all the external pores, but is concentrated only in the large pores. There are relatively few such pores on the surface, but it is these pores, with their deep branching, which result in abrupt crumbling of the surface layer. If the current density is lowered, electrolysis penetrates into the fine pores. As a result, the whole bulk of the surface layer begins to undergo corrosion. This, naturally, must accelerate surface mechanical breakdown. The external layer is eroded very uniformly and from beneath it appears a new, equally smooth layer with a high $\gamma_{min}$ and low $\delta_{lim}$. Abrupt crumbling of the external layer evidently does not occur in this case.

Let us compare the course of destruction in impregnated and unimpregnated graphite. It is known that impregnation has little influence on the intensity of electrochemical oxidation, but, by strengthening the graphite structure, it lowers mechanical losses and prevents surface disintegration. In this case after the first hour of electrolysis there is a much greater loss in weight, and especially in thickness, of the electrode. However, $\gamma_{min}$ remains at the same level, and $\delta_{lim}$ even decreases somewhat (0.16 mm as compared with 0.195 mm. Thus, more intensive but only surface destruction occurs in this case. Impregnation deactivates a certain part of the

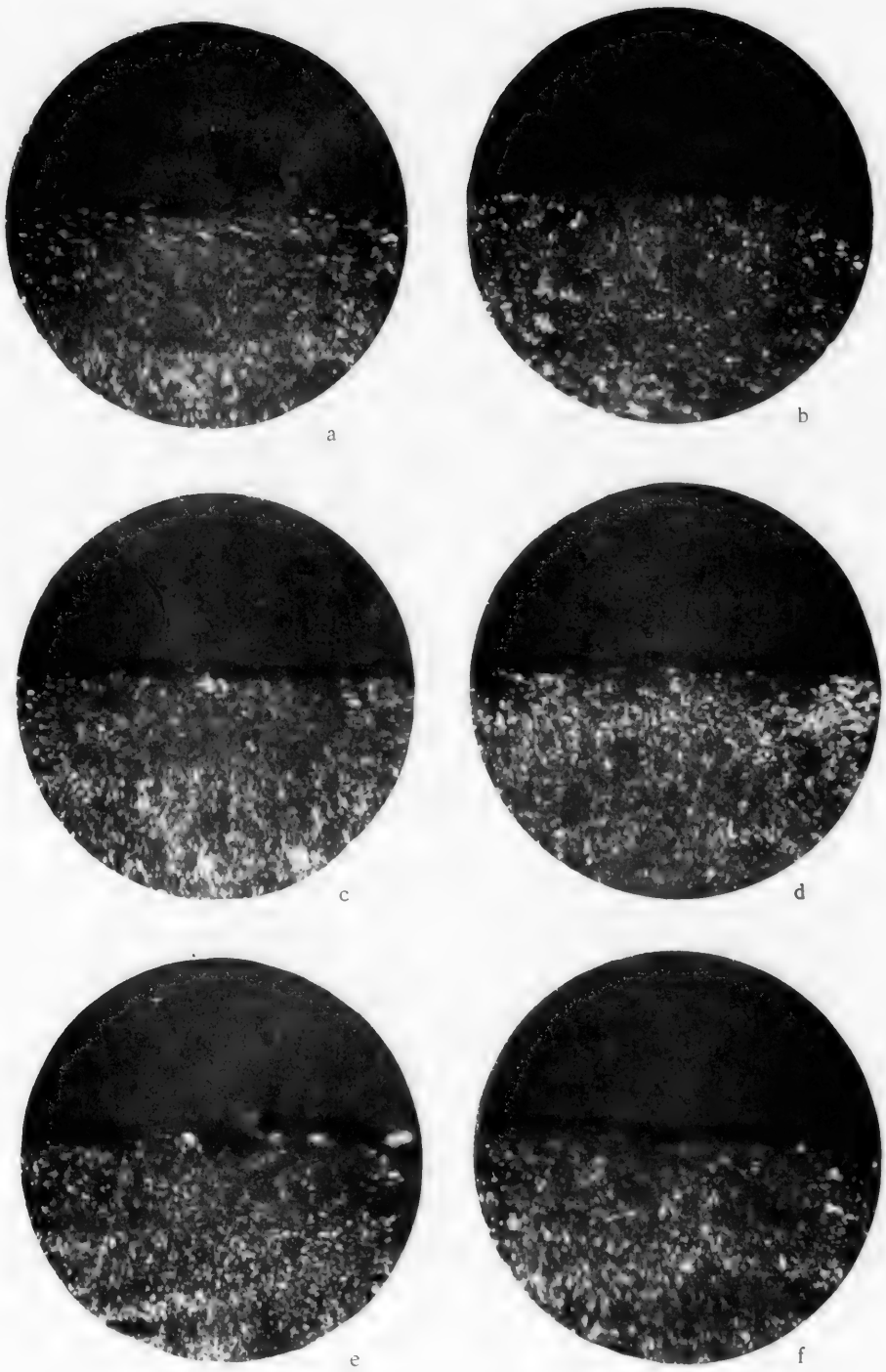


Fig. 4. Destruction of the external layer of an unimpregnated graphite anode: electrolysis time (hours): a) before electrolysis, b) 1, c) 2, d) 3, e) 4, f) 6 $D_a$ = 4000 amp/$m^2$, t = 60°.

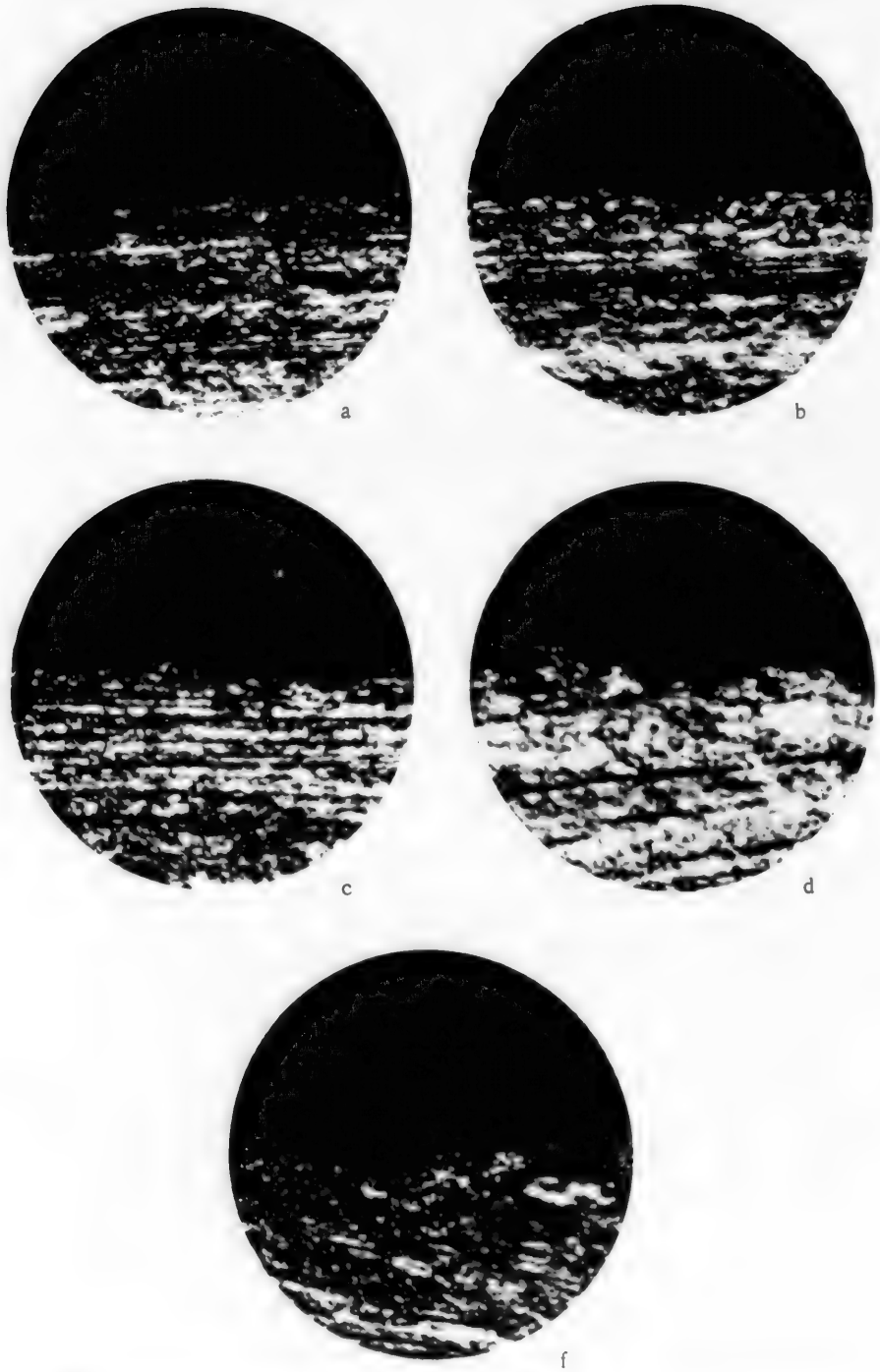


Fig. 5. Destruction of the external layer of an impregnated graphite anode: electrolysis time (hours) a) 1, b) 2, e) 3, d) 6, f) 10.
$D_a$ = 4000 amp/m$^2$, t = 60°.

surface, and electrolysis can spread inward only through a small number of the largest pores (Fig. 5, b). The strength of the main graphite mass is not reduced, and therefore on further electrolysis we do not observe abrupt crumbling accompanied by a sharp increase in the percentage of mechanical loss. On the contrary, in this instance further electrolysis leads after some time to fresh leveling of the surface. For example, in 3 and 6 hours of electrolysis $\delta_{lim}$ decreases, while the change of $\gamma_{min}$ is slight. The photographs (Fig. 5, d, e) show a decrease of surface roughness in these specimens. After some time the uniform erosion of the surface may again lead to the appearance of large pores on the surface, which were previously within the electrode. These pores begin to extend and deepen (in 10 hours of electrolysis $\gamma_{min}$ decreases again, and $\delta_{lim}$ increases). However, this does not affect $\Delta G_{total}$ and the percentage of mechanical losses, which, as before, are solely the results of uniform surface oxidation which has extended to the walls of the large pores.

## SUMMARY


1. It was shown in a study of the density distribution in the surface layer of a graphite electrode undergoing destruction that at high current densities the electrolysis process, occurring only in a small number of large pores, leads after some time to abrupt crumbling of the surface layer. This exposes a rough surface which subsequently retains its structure without change.

2. At low current densities the destruction is of a surface character because the electrolysis takes place in the finest pores of the graphite.

3. The limiting depth of electrolysis (and external destruction) varies in the range of 0.2-0.4 mm.

4. Impregnation of the anode strengthens the graphite structure, and therefore the destruction is of a surface character even at high current densities, and total losses diminish.


## LITERATURE CITED


[1] B. M. Bulygin, J. Appl. Chem. 31, No. 12, 1832 (1958).

[2] B. M. Bulygin, J. Appl. Chem. 32, No. 1, 121 (1959).

[3] O. S. Ksënzhek and V. V. Stender, Proc. Acad. Sci. USSR 107, 280 (1956).

[4] H. Thiele, Z. Elektroch., 55, 193 (1951).

[5] I. Ya. Sirak, J. Appl. Chem. 6, 808 (1933).



Received April 26, 1957.

# MINERAL COMPOSITION OF THE ROASTED MASS IN DICHROMATE PRODUCTION

O. I. Pudovkina, M. V. Kireeva, and E. M. Morgunova

The Urals Chemical Scientific-Research Institute

Earlier data [1] referred to sintered masses obtained under laboratory conditions in the roasting of a mixture of chromite with soda and dolomite until the chromium was completely oxidized.

In the present investigation different samples of the roasted mass from production kilns were studied.

Method of investigation. During the period when samples of the roasted mass were taken, the works kilns were charged with a mixture having the composition: $Cr_2O_3$ 15-19%, $Na_2CO_3$ 75-86% of the theoretical amount required to form $Na_2CrO_4$; CaO 90-206% of the theoretical amount required to form $C_2S$, $C_4AF$,* $C_5A_3$ and to make up for any deficiency of sodium carbonate.

In addition to ordinary chemical analysis, most of the samples of the roasted mass were treated with various solvents for selective extraction of individual minerals. The first aim was to dissolve out sodium chromate, which is the principal mineral phase of the mass and which cements all the other minerals during crystallization. After removal of sodium chromate it was usually easier to detect grains of the other minerals in the product. Methyl alcohol and, less often, hot water was used to remove sodium chromate. Calcium silicates were extracted in 5% boric acid solution [2]. Tricalcium aluminate and calcium silicates were dissolved in 1 N acetic acid solution [3]. The mass was treated with 5% solution of acetic acid in methyl alcohol to remove free magnesium oxide [1, 4]. Investigations of chromium-containing minerals of the mass which were soluble and insoluble in acids were of considerable interest. To establish their presence and composition, 5-20 g of the roasted mass was treated in one case with 5% boric acid solution and in another case with 10% sulfuric acid solution at the boil for 10-30 minutes. The solutions were analyzed chemically. The acid-insoluble minerals were isolated in pure form by consecutive treatment of 15-20 g of the mass with water, hydrochloric acid (1:1), sulfuric acid (1:4) at the boil for 30 minutes, and hydrofluoric acid; the residue was then calcined. The residues were weighed and analyzed.

The microscopic investigations were performed by means of transmitted light with the aid of a polarization microscope and immersion liquids with a range of refractive indices from 1.408 to 2.054. Minerals with higher refractive indices were determined with the aid of immersion melts.

A large number of samples were subjected to x-ray structural analysis in addition to the chemical and microscopical methods. RPK cameras of $R_{eff}$ = 28.35 cm were used, with BSV tubes with copper and iron anticathodes and filtered radiation.

## Investigation of the Mineral Phases

Sodium and calcium chromates. All the samples of roasted mass contained large yellow crystals with refractive indices $N_g$ = 1.775 and $N_p$ = 1.769, corresponding to pure sodium chromate [1].

The samples were also found to contain yellow grains with higher refractive indices, $N_g$ = 1.783-1.826, consisting of solid solutions of calcium chromate in sodium chromate [5, 1]. The formation of calcium chromate in the masses is due to the composition of the original charges, in which a considerable proportion of sodium carbonate was replaced by calcium oxide.

*$C_2S$ = dicalcium orthosilicate; $C_4AF$ = tetracalcium aluminoferrite.

Calcium silicates and chromite. Calcium silicates were clearly observed in all the sinters in the form of pale and dark green crystals. The pale green crystals of Ng = 1.730-1.737 and $N_p$ = 1.716-1.720 were analogous to the calcium silicates observed by us earlier in laboratory clinkers [1]. Crystals of a deeper green color, dark green, had higher refractive indices (Ng= 1.754-1.780). Both forms of green crystals occasionally exhibited polysynthetic twinning.

The green minerals were not soluble in hot water or methyl alcohol, but dissolved readily in 5% boric acid solution. Chemical analysis of the boric acid extracts showed presence of silica, hexavalent chromium, trivalent chromium, and calcium oxide. It was shown by calculations from the analytical data that up to 70% of the minerals dissolved in 5% boric acid solution belong to calcium silicates in which are dissolved about 6% calcium chromate and over 16% calcium chromite ( $CaO \cdot Cr_2O_3$). The pale green color in the crystals of calcium silicate comes from calcium chromate, and the dark green from calcium chromite.

The presence of calcium chromite as a nonequilibrium compound in the masses was also confirmed by the fact that after additional grinding and calcination of the factory roasted mass at 1150° for 2 hours the dark green crystals disappeared. Only pale green crystals with Ng = 1.730-1.740 and Np = 1.716-1.718 were detected. The degree of oxidation of the chromium increased by oxidation of $CaO \cdot Cr_2O_3$ to $CaCrO_4$. Laboratory clinkers [1] calcined to complete oxidation of the chromium did not contain dark green calcium silicate grains.

In the production kiln, calcium chromite is not oxidized completely to calcium chromate and partially dissolves in calcium silicates.

Chemical analysis of the boric acid extracts also showed that the industrial masses contain considerable amounts of $C_3S$* in addition to $\beta$-$C_2S$. Owing to the presence of chromium compounds as admixtures in the calcium silicates, separate determination of $C_2S$ and $C_3S$ under the microscope is very difficult.

TABLE 1

Investigations of Pellets of Clinker from Chromate Kiln

| Size (diameter) of pellet, mm | Part of pellet studied | Contents of $Cr^{VI}$ and $Cr^{III}$ in pellets (% of total chromium) | | | |
|---|---|---|---|---|---|
| | | $Cr^{VI}$ | | $Cr^{III}$ | |
| | | water soluble | acid soluble | | insoluble |
| 25 | External | 66.70 | 2.38 | 27.40 | 3.52 |
| | Internal | 42.30 | 1.39 | 49.50 | 6.81 |
| 15 × 18 | External | 70.50 | 0.72 | 23.60 | 5.18 |
| | Internal | 49.50 | 0.76 | 42.20 | 7.54 |
| 12 | External | 83.50 | 2.26 | 8.15 | 6.09 |
| | Internal | 75.50 | 2.67 | 15.60 | 6.23 |
| 20 × 35 | External | 80.60 | 0.87 | 12.80 | 6.33 |
| | Internal | 67.20 | 0.75 | 15.80 | 16.25 |
| 22 | External | 85.50 | 1.27 | 4.15 | 9.08 |
| | Internal | 66.20 | 1.93 | 18.50 | 13.37 |

Aluminates. In contrast to the laboratory clinkers, it was very difficult to detect calcium or sodium aluminates in the industrial samples. To detect $C_5A_3$ and $C_3A$* crystals under the microscope, the roasted mass was first treated with methyl alcohol, boric and acetic acid solutions, and stained with bright blue dye "3".

No $C_3A$ crystals were detected in any of the samples. Crystals of $C_5A_3$ in the form of very rare isotropic colorless grains of N = 1.610 were found only in samples in which the A : F ratio of the iron phase** very much exceeds 0.64.

*$C_3S$ = tricalcium silicate; $C_3A$ = tricalcium aluminate.

**Oxides present in nonequilibrium phases (sodium aluminate and chrome spinellides are excluded).

TABLE 2

Chemical Analysis of Works Clinkers (wt. %)

| Clinker No | Chromium as $Cr_2O_3$ | | | $SiO_2$ | $Al_2O_3$ | | Free alkalinity calculated as $Na_2CO_3$ | $Fe_2O_3$ | CaO | | MgO | | $CO_2$ |
|---|---|---|---|---|---|---|---|---|---|---|---|---|---|
| | $Cr^{VI}$ | | $Cr^{III}$ | | | | | | | | | | |
| | water-soluble | acid-soluble | chrome spinellides | | water-soluble | chrome spinellides | total | chrome spinellides | total | free | free | chrome spinellides | total | |
| 1 | 16.05 | 0.51 | 3.42 | 2.21 | 3.53 | 1.22 | 0.49 | 5.74 | 3.13 | 0.46 | 7.30 | 0.37 | 20.68 | 16.68 | 0.68 | 18.12 | 0.72 |
| 2 | 17.63 | 0.35 | 3.31 | 1.97 | 3.83 | 1.18 | 0.52 | 5.62 | 4.52 | 0.44 | 6.92 | 0.35 | 18.51 | 14.87 | 0.71 | 18.23 | 0.85 |
| 3 | 19.08 | 0.40 | 3.20 | 1.37 | 3.53 | 1.26 | 0.43 | 5.03 | 3.49 | 0.42 | 6.78 | 0.41 | 18.32 | 15.63 | 0.58 | 17.45 | 0.80 |
| 4 | 19.39 | 0.35 | 2.87 | 1.05 | 3.82 | 1.27 | 0.34 | 5.08 | 5.02 | 0.30 | 6.72 | 0.58 | 18.23 | 15.58 | 0.35 | 17.50 | 0.89 |
| 5 | 18.86 | 0.26 | 1.85 | 1.96 | 3.04 | 0.89 | 0.75 | 3.08 | 6.02 | 0.68 | 10.51 | 0.47 | 15.53 | 14.04 | 0.84 | 17.01 | 1.06 |
| 6 | 19.20 | 0.48 | 2.97 | 1.93 | 2.65 | 0.40 | 0.45 | 4.63 | 1.20 | 0.41 | 6.83 | 0.35 | 17.83 | — | 0.61 | 18.25 | 0.78 |
| 7 | 18.20 | 0.22 | 2.59 | 2.06 | 4.00 | 0.80 | 0.75 | 7.80 | 1.80 | 0.69 | 5.74 | none | 19.80 | — | 0.90 | 18.10 | 1.70 |
| 8 | 18.70 | 0.34 | 2.02 | 1.44 | 3.45 | 0.40 | 0.60 | 5.09 | 1.37 | 0.44 | 5.99 | 0.46 | 20.11 | — | 0.56 | 18.77 | 0.75 |
| 9 | 18.70 | 0.45 | 1.86 | 0.93 | 3.35 | 0.41 | 0.40 | 5.30 | 0.77 | 0.41 | 5.59 | 0.90 | 20.18 | — | 0.40 | 18.77 | 0.47 |

In a number of samples of the roasted mass rare colorless crystals of $N_g$ = 1.576 and $N_p$ = 1.570 were detected. These crystals were identified as sodium aluminate, $Na_2O \cdot Al_2O_3$.

The iron phase. All the samples studied contained $C_4AF$ crystals with $N_g$ = 2.038-2.08 and $N_p$ = = 1.874-1.99 in the form of pleochromatic plates. The presence of $C_4AF$ was also confirmed by x-ray analysis.

Samples in which the A : F ratio of the iron phase was less than 0.64 contained brown crystals of somewhat higher refractive index, $N_g$ = 1.995-1.98, belonging to solid solutions of $C_4AF$ in $C_2F$. Crimson grains of $C_2F$* with $N_g$ = 2.23 were also found.

Samples in which the A:F ratio of the iron phase was greater than 0.64 contained rare brown crystals with $N_g$ = 1.99 and $N_p$ = 1.85, belonging to solid solutions of $C_4AF$ with calcium aluminates.

Magnesium oxide. Magnesium oxide was found in large amounts in all samples, in the form of pale isotropic grains with refractive index N = 1.711-1.737. The crystals were completely soluble in 5% acetic acid solution in methyl alcohol, and insoluble in acetic and boric acid solutions. The observed decrease in the refractive indices of periclase may be attributed to the presence of impurities, the nature of which was not determined. The presence of free magnesium oxide in the industrial samples was also confirmed by x-ray analysis.

Chrome spinellides were observed in all the samples in the form of isotropic yellowish brown opaque crystals. In a thin layer the color of the crystals changed from yellow to brown-red. Similar crystals, but more clearly defined and darker, were observed in the original ores. Analysis of chrome spinellides isolated from various industrial clinkers and original ores showed that their composition does not undergo any significant changes during the roasting. The external appearance of the chrome spinellide crystals changes; they react with alkalies during the roasting, decrease in size, and become thin. The values of the highest refractive index of the chrome spinellides varied in the range of 2.048-2.054.

Clinkers made from charges containing 80-85% of the theoretical amount of soda and the theoretical amount of calcium oxide contained 2.0-4.5% of chrome spinellides. A considerable deficit of soda and lime in the charge leads to a sharp increase in the content of chrome spinellides and, conversely, increase in the amounts of soda and calcium oxide in the charge results in a considerable decrease of the chrome spinellide content.

*$C_2F$ = calcium fluoride.

TABLE 3

Calculated Phase Composition of Works Clinkers

| Mineral phases | Mineral composition of different works clinkers (% of total mass) | | | | | | | | |
|---|---|---|---|---|---|---|---|---|---|
| | № 1 | № 2 | № 3 | № 4 | № 5 | № 6 | № 7 | № 8 | № 9 |
| $Na_2CrO_4$ | 34.21 | 37.57 | 40.67 | 41.32 | 40.20 | 40.80 | 38.80 | 39.80 | 39.80 |
| $CaCrO_4$ (solid solution in $Na_2CrO_4$) | 1.05 | 0.72 | 0.82 | 0.72 | 0.53 | 0.99 | 0.45 | 0.70 | 0.92 |
| $CaO \cdot Cr_2O_3$ | 4.46 | 4.58 | 4.11 | 4.16 | 2.54 | 4.06 | 3.55 | 2.79 | 2.54 |
| Chrome spinellides | 3.84 | 3.64 | 2.85 | 2.04 | 4.22 | 3.40 | 4.40 | 3.04 | 2.14 |
| $Na_2O \cdot Al_2O_3$ | 1.96 | 1.90 | 2.03 | 2.04 | 1.73 | 0.64 | 1.29 | 0.64 | 0.66 |
| $C_2S$ and $C_3S$ | 12.11 | 11.01 | 10.95 | 11.00 | 8.75 | 9.03 | 11.50 | 12.78 | 12.65 |
| $C_4AF$ | 19.20 | 17.45 | 15.69 | 16.00 | 6.96 | 18.07 | 15.40 | 16.88 | 15.78 |
| $C_2F$ (solid solution in $C_4AF$) | 0.90 | 0.85 | 2.04 | 1.40 | 8.34 | 0.80 | None | None | None |
| $C_5A_3$ (solid solution in $C_4AF$) | None | None | None | None | None | 3.87 | 1.08 | 2.29 | 0.86 |
| MgO (solid solution in $C_4AF$) | 0.75 | 2.64 | 1.25 | 1.57 | 2.13 | 2.13 | 1.79 | 2.25 | 2.40 |
| MgO | 16.68 | 14.87 | 15.63 | 15.58 | 14.04 | 15.51 | 15.41 | 15.97 | 15.97 |
| $CaCO_3$ | 1.64 | 1.93 | 1.82 | 2.02 | 2.41 | 1.77 | 3.86 | 1.71 | 1.07 |
| CaO | 0.37 | 0.35 | 0.41 | 0.58 | 0.47 | 0.35 | None | 0.49 | 0.90 |
| Glass phase | 1.09 | 2.40 | 1.27 | 2.61 | 5.62 | 0.70 | 2.04 | None | None |

Other minerals. In addition to the minerals described above, the masses contained small numbers of colorless isotropic grains with N = 1.624-1.648, and yellow isotropic grains with N= 1.775-1.85, which we classified as glasses. There were also rare crimson minerals of high refractive index, possibly ferrates. Some samples contained isotropic grains of calcium oxide and rare crystals of calcium carbonate.

## Investigation of Pellets

The roasted mass leaving the kiln consists mainly of small and large pellets (round grains) and pellet aggregates.

Analysis showed that the smaller pellets contain more chromates and less calcium chromite and chrome spinellides than the larger. In the densest surface layers of the pellets most of the crystals are chromates. Very occasionally green silicate grains are found. The iron phase and periclase are present in small amounts. The interior of the pellets differs sharply from the outside layers. It contains numerous green grains of calcium silicates with an admixture of calcium chromate and crystals of the iron phase with inclusions of yellow-brown chrome spinellide grains.

Microscopical observations are in agreement with the results of chemical analysis. The external parts of the pellets contain much hexavalent chromium, while the amount of trivalent chromium is considerably lower (Table 1). It follows that calcium chromite and chrome spinellides are preserved within the pellets; the coating consisting of reaction products prevents access of alkalies and oxygen to them.

## Calculation of the Phase Composition of the Clinkers

The results of chemical analyses of different samples of the works-roasted mass are given in Table 2. We attempted, with some degree of arbitrariness, to calculate their phase composition from the combined results of microscopical and chemical investigations of the works clinkers.

Analysis of an aqueous extract of the clinker for calcium showed that the calcium chromate content of the solution is in the range of 2-4% of the total chromates. It was therefore justifiable to allot all the hexavalent chromium ($Cr^{VI}$) extracted by water from the clinker to sodium chromate. Acid-soluble $Cr^{VI}$ was calculated as calcium chromate, and acid-soluble $Cr^{III}$ as calcium chromite. The amounts and composition of chrome spinellides in the clinkers were determined by analysis.

It was found that after treatment of the clinker with boric acid solution a very small amount of silica remains in the sludge; over 90% of the silica present in the clinker is in the calcium silicates. To simplify the calculations, we calculated all the silica present in the clinkers as dicalcium silicate, since $C_3S$ and $C_2S$ were not always determined separately.

Water-soluble alumina was reckoned together with the corresponding amount of free alkali as sodium aluminate.

In clinkers in which the iron phase had A:F ratio above 0.64 all the iron less the amount present in chrome spinellides was taken as combined in tetracalcium aluminoferrite. The alumina remaining from $C_4AF$, less the amounts present in sodium aluminate and chrome spinellides, was reckoned with calcium oxide as $C_5A_3$.

In clinkers in which A:F of the iron phase was less than 0.64 all the $Al_2O_3$ less the amount in sodium aluminate was first reckoned as $C_4AF$, and the remaining iron, less the amount in chrome spinellides, as included with $C_2F$.

Free calcium oxide in the clinkers was determined by analysis.

Free magnesium oxide in the clinkers was also determined by analysis or taken as 85% of the total MgO in the clinker (average value found by analysis for a number of clinkers). The magnesium oxide representing the difference between total bound MgO and the amount in the chrome spinellides was reckoned as solid solution with $C_4AF$. This also included calcium aluminates and ferrites.

The small amounts of bound calcium oxide not accounted for were included with calcium silicates, in view of the presence of $C_3S$ in the clinkers.

The free alkali remaining from sodium aluminate was included with the glasses, which also included silica not extracted by 5% boric acid solution, i.e., not combined in calcium silicates. The small amounts of iron and aluminum oxides not accounted for were also included in the glass phase.

The $CO_2$ present in the clinkers was calculated as $CaCO_3$, as it is unlikely that the clinkers contained undecomposed soda, since in the fused state it is the most active alkaline reagent (of those present in the clinker) with respect to the acidic oxides.

The results of these calculations, representing the approximate contents of individual minerals in works clinkers made from soda-dolomite charges, are given in Table 3.

Because of the soda deficiency in the charge and the specific roasting conditions, the reaction of chromate formation does not go to the end in the works kiln. In contrast to "equilibrium" clinkers made in the laboratory [1], a considerable amount of the chromium in the roasted mass remains included in other minerals, such as calcium chromate and chromite and chrome spinellides, which cause losses of chromium in the process.

In conclusion, we must offer our sincere thanks to Professor V. V. Lapin for consultation on methods during this work.

## SUMMARY

1. Qualitative and quantitative characteristics of the composition of the works-roasted mass are given, and minerals responsible for losses of chromium in the production processes were found.

2. Formation of pellets of the roasted mass in the industrial kiln is one cause of a lower percentage of oxidation of chromium.

## LITERATURE CITED

[1] O. I. Pudovkina and M. V. Kireeva, J. Appl. Chem. 29, No. 6, 628 (1956) [USSR]

[2] Control of Cement Production, 2 [in Russian] (Industrial Construction Press, Moscow, 1952).

[3] S. M. Royak et al., Trans. Sci. Res. Inst. Cement 5 (1952).

[4] N. A. Toropov and N. D. Katsenelenbogen, Cement 7 (1938) [USSR].

[5] Ya. E. Vil'nyanskii and O. I. Pudovkina, J. Gen. Chem. 6 (1948) [USSR].

Received November 26, 1957.

# THE HARDENING OF MAGNESIUM OXYCHLORIDE (SOREL)CEMENTS•

A. G. Bergman and I. P. Vyrodov

Investigations of the composition of Sorel cements carried out by the methods of x-ray structural analysis during hardening, and determinations of the composition and properties of Sorel cements by tensimetric and thermographic analysis, are not in agreement with the theory of hardening of Sorel cements which still persists in our literature, and which postulates hydration of magnesium oxide and formation of magnesium hydroxide, $Mg(OH)_2$, in the final product [1-4]

The experimental results obtained in a series of analyses and presented in this paper not only confirm our views, but also open up possibilities for a new approach to the kinetics of hardening of Sorel cements.

## EXPERIMENTAL

To avoid ambiguous conclusions and errors which might result from the use of impure substances, we used very pure starting materials: magnesium chloride hexahydrate (chemically pure), and magnesium oxide (analytical grade). The cements used in the study conformed to the general formula

$$[K\%\ H_2O + (100 - K)\%\ MgCl_2] + n\%\ MgO,$$

where K varied from 60 to 80%, and n from 5 to 105.

It follows from the x-ray patterns of cements (Table 1)containing from 5 to 85 %MgO•• that as the magnesium oxide content of the cement increases the positions of the lines change sharply in the transition from samples containing less than 50% magnesium oxide to samples containing over 50% (K here was taken as 65%; the suitability of the choice of this solution is shown later in this paper). The change consists not only on alterations in the position of the lines (appearance of a new crystalline structure) but also of changes in the form of these lines (dispersity of the cyrstalline phase) [5].

A common feature of the x-ray patterns of these cements is absence of lines with large Wulff-Bragg angles, This is due, on the one hand, to the finely disperse structure of the phases constituting the cement [6], the crystals of which are up to 100 $m\mu$ in size (which influences the exposures) and on the other, to relatively large lattice imperfections in the phases constituting the cement. Lattice imperfections in the phases arise both as the result of layer displacement owing to the weak bonding between them, and as the result of mechanical stresses arising arising during hardening of the cements (these stresses are released by annealing at 100-120°).

From the data of Table 1 and the earlier results [5] it is possible to distinguish three varieties of oxychlorides in the cement (Table 2).

As the MgO content increases from 20 to 45%, oxychloride I is present in the cement. When the MgO: :$MgCl_2$ ratio is somewhat higher than 3:1, the cement does not contain oxychloride I. The principal component is the oxychloride II (50-60% MgO). When the component ratio is close to 5:1, oxychloride III appears in the cements.

---

•Communication II.

••The x-ray patterns are given in the first communication [5].

TABLE 1

Interplanar Spacings of Cement Samples Cu Radiation, Camera Diameter D = 57.3 mm

| $\frac{d}{n}$ (kX) | Positions of lines in cement x-ray patterns | | | | | | | | | |
|---|---|---|---|---|---|---|---|---|---|---|
| | | contents of MgO lines in cement (%) | | | | | | $Mg(OH)_2 \cdot MgCl_2 \cdot 10H_2O$ | $Mg(OH)_2$ | MgO |
| | Oxychloride* | 5 | 25 | 40 | 50 | 60 | 75 | 85 | | | |
| 11.5 | | | | | | | | | | | |
| 8.0 | | | | | m | | | | | | |
| 7.7 | | | | | | w | | s | s | | |
| 6.8 | | | | | | | | | vw | | |
| 6.0 | | | | | w | | | | vw | | |
| 5.75 | | | | | | | | | vw | | |
| 4.75 | | | | | | | | | | | |
| 4.15 | | | | | | s | s | s | | | |
| 4.00 | vs | vs | vs | vs | s | | | | s | | |
| 3.85 | | | | | s | | | | | | |
| 3.80 | vs | vs | vs | vs | | m | m | m | s | | |
| 3.56 | s | | | | w | | | | | | |
| 3.48 | m | w | w | w | | | | | vw | | |
| 3.30 | w | vw | vw | vw | vw | | | | | | |
| 3.26 | | | | | | w | w | vw | | | |
| 3.00 | m | s | s | s | s | | | | m | | |
| 2.94 | | | | | | w | m | m | | | |
| 2.84 | s | | | | | | | | | | |
| 2.79 | | | | | | | | | vw | | |
| 2.70 | s | s | | s | s | | | | | | |
| 2.65 | | | | | | s | s | s | | | |
| 2.60 | | s | m | m | w | w | w | w | w | | |
| 2.49 | | | | | | | | | w | | |
| 2.425 | vs | vs | vs | vs | vs | | | | | | |
| 2.390 | | | | | | vs | vs | vs | | | |
| 2.360 | | | | | | | | | | | |
| 2.290 | w | | | | | | | | | vs | |
| 2.210 | w | m | vw | vw | | | | | | | |
| 1.170 | | w | | | | | | | | | |
| 2.140 | vw | | vw | | | | | | | | |
| 2.092 | vw | vw | vw | vw | vw | vw | | | | | |
| 1.992 | vw | s | s | s | m | | vw | vw | vw | | vs |
| 1.951 | | | | | | s | s | s | | | |
| 1.920 | | | | | | | w | m | | | |
| 1.848 | w | | | | w | | | | vw | | |
| 1.820 | | m | m | m | | vw | | vw | | | |
| 1.780 | v.w. | | | | vw | | w | | | | |
| 1.740 | | w | | | | | | m | | w | |
| 1.725 | vw | | | | | | | | | | |
| 1.710 | | vw | vs | vw | | | | | | | |
| 1.690 | | w | | | vw | vw | vw | vw | | | |
| 1.637 | w | | | | vw | vw | w | vs | | | |
| 1.630 | | vs | vs | vw | | | | | | | |
| 1.610 | | | | | | | | m | | | |
| 1.565 | | | | | | | | | | vs | |
| 1.560 | | | | | w | vw | vw | | | | |
| 1.555 | | vs | w | vw | | | | | | | |
| 1.535 | | | | | | m | | | | | |
| 1.520 | | vw | | | | | | | | | |
| 1.515 | | | | | | | vw | | | | |
| 1.485 | vw | vw | vw | vw | w | vw | vw | | | vw | s |

*This oxychloride was prepared by mixing of MgO in excess $MgCl_2$, with subsequent brief washing of the powdered sample with cold water. Drying temperature of the sample 120°.

TABLE 1 (Cont'd.

| $\frac{d}{n}$ (kX) | Positions of lines in cement x-ray patterns | | | | | | | | | | |
|---|---|---|---|---|---|---|---|---|---|---|---|
| | | contents of MgO lines in cement (%) | | | | | | | | | |
| | oxy-chloride • | 5 | 25 | 40 | 50 | 60 | 75 | 85 | $MgOH_2 : MgCl_2 : 10H_2O$ | $Mg(OH)_2$ | MgO |
| 1.480 | | | w | | | | | m | | | |
| 1.450 | | | | | | w | vw | vw | | | |
| 1.417 | | | | vw | vw | | | | | | |
| 1.405 | | vw | vw | | | | | | | | |
| 1.390 | vw | | | | | | | | | | |
| 1.359 | vw | | | vw | vw | vw | vw | vw | | | |
| 1.339 | | w | vw | | | | | | | | |
| 1.305 | | | | | | | vw | | | | |
| 1.215 | | ; | | | | | | w | | | vw |
| 1.050 | | | | | | | | w | | | |

Note- Lines: s) strong, w) weak, m) moderate, vs) very strong, vw) very weak.

TABLE 2

Interplanar Spacings of Oxychloride

| Oxychloride I | | Oxychloride II | | Oxychloride III | | Oxychloride I | | Oxychloride II | | Oxychloride III | |
|---|---|---|---|---|---|---|---|---|---|---|---|
| $\frac{d}{n}$ (kX) | I | $\frac{d}{n}$ (kX) | I | $\frac{d}{n}$ (kX) | I | $\frac{d}{n}$ (kX) | I | $\frac{d}{n}$ (kX) | I | $\frac{d}{n}$ (kX) | I |
| 4.00 | vs | 4.0 | s | 4.15 | s | 2.210 | vw | 1.992 | m | 1.820 | w |
| 3.80 | vs | 3.85 | s | 3.85 | m | 2.092 | vw | 1.820 | vw | 1.690 | vw |
| 3.48 | w | 3.52 | w | 3.26 | w | 1.992 | s | 1.690 | vw | 1.637 | vw |
| 3.30 | vw | 3.30 | vw | 2.94 | m | 1.820 | m | 1.640 | w | 1.560 | vw |
| 3.00 | s | 3.00 | s | 2.65 | s | 1.710 | vw | 1.560 | w | 1.485 | vw |
| 2.70 | s | 2.70 | s | 2.60 | w | 1.630 | vw | 1.360 | vw | 1.450 | w |
| 2.60 | w | 2.70 | w | 2.390 | vs | 1.550 | vw | — | | 1.360 | vw |
| 2.425 | vw | 2.425 | vs | 1.951 | s | 1.485 | vw | | | | |

It is quite reasonable to suppose that the water content of the oxychlorides decreases with increase of the percentage of MgO in the cement. This supposition is consistent with the results of tensimetric analysis. The vapor pressure isotherm for the cements, as Fig. 1 shows, descends with increase of the percentage of magnesium oxide. It should be noted that the form of the $P_{H_2O} = P(n)$ isotherm, like the general appearance of the x-ray pattern, changes as we pass from cements with MgO : $MgCl_2$, ratio of 3:1 to cements with ratio 5:1. After the break in the $P_{H_2O} = P(n)$ graph at the point n = 45% considerable dehydration of the oxychlorides is observed up to the point when the ratio of MgO to $MgCl_2$ is close to 5:1.

It is also of interest to note that the plot of the maximum temperature rise in the reaction of cement formation ($T_{max}$) against the percentage MgO content (n) (the function $T_{max} = T(n)$ shows characteristic peaks at MgO:$MgCl_2$ ratios of 3:1 and 5:1 and 5:1 (Fig. 2).

Keeping the ratios of MgO to $MgCl_2$ constant (3:1, 5:1, and 7:1), but varying the $MgCl_2$ concentration from 40 to 20%, we plotted (Fig. 3) $T_{max} = T(q)$, curves for the samples, where q is the $MgCl_2$ concentration (wt.%). These curves have sharp peaks for samples made with 35% $MgCl_2$ solution .

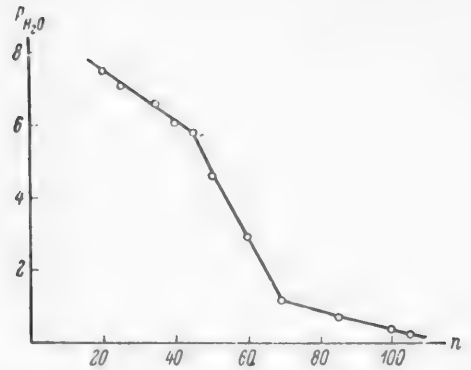


Fig. 1. Isotherm of vapor pressure ($P_{H_2O}$ in mm Hg) as a function of the magnesium oxide content (n).

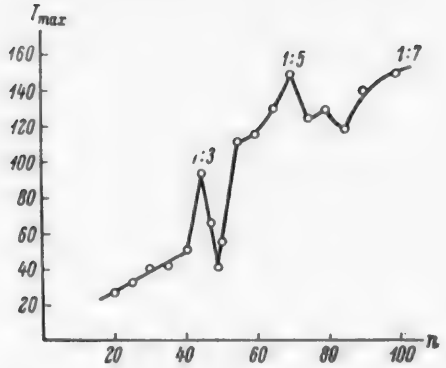


Fig. 2. Maximum reaction temperature ($T_{max}$) as a function of the magnesium oxide content (n).

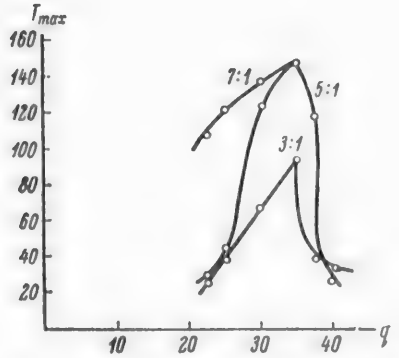


Fig. 3. Maximum temperature of the reaction of cement formation ($T_{max}$) as a function of the concentration of $MgCl_2$ solution (q) for three ratios of MgO to $MgCl_2$: 7:1 ,5:1,3:1.

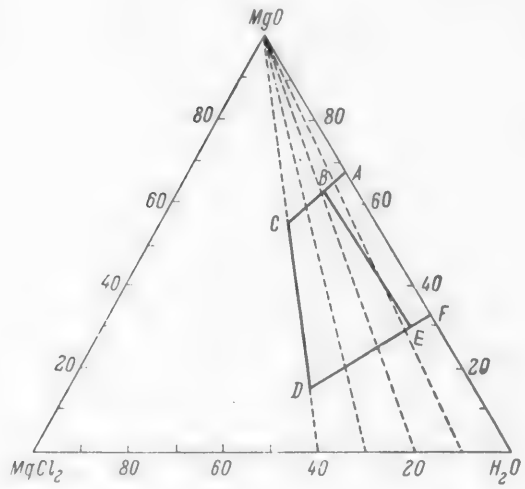


Fig. 4. Diagram for the system: magnesium oxide-chloride-water.

The $P_{H_2O} = P(q)$ isotherms also have extremals (minima) at points corresponding to q = 35%.

It follows from these experimental data that individual phases are formed in Sorel cement made with 35% $MgCl_2$ solutions at 3:1 and 5:1 ratios of MgO to $MgCl_2$.

Investigation of the system $MgO-MgCl_2-H_2O$ revealed the formation boundaries of Sorel cements (sides of the quadrangle ACDF, Fig. 4) for which the time of temperature rise in the reaction does not exceed 6-8 hours.

None of the samples enclosed within the region BCDE was found to contain $Mg(OH)_2$.

Magnesium oxychloride made by mixing of the largest amount of magnesium oxide with which stirring was possible with 35% $MgCl_2$ solution was kept for 2-3 months and the powdered product was mixed with 35% $MgCl_2$ solution; it formed a completely homogeneous mass of very high mechanical strength. This is undoubted evidence of the formation of oxychlorides of variable composition.

Moreover, magnesium hydroxide mixed with 35% magnesium chloride solution in the ratio $Mg(OH)_2$ : $:MgCl_2 \cdot 10\ H_2O$ also reacts completely, forming a hard mass of relatively high strength [5]. It follows that 35% magnesium chloride solution effectively dissolves $Mg(OH)_2$ and reacts with it. This accounts for the absence

*Original Russian pagination. See C. B. translation.

of $Mg(OH)_2$ in Sorel cements. It is reasonable to suppose that the solubility of $Mg(OH)_2$ decreases with decrease in the concentration of magnesium chloride solution. For compositions lying outside the quadrangle BCDE, to the right of the side BE, in Fig. 4 the x-ray patterns show the presence of magnesium hydroxide together with oxychlorides.

Certain conclusions concerning the dispersity of the cement structure can be drawn from our x-ray patterns.

Comparison of x-ray patterns for samples containing less than 45% MgO and for samples containing more than 45% MgO (MgO: $MgCl_2$ greater than 3:1) shows that the lines in the latter are somewhat wider. On one hand, widening of the lines is attributable to lattice deformations of the phases constituting the cements, and on the other, as already noted, widening of the interference lines is caused by layer displacement. This is found for lines with the interplanar spacings

$$\frac{d}{n} = 2.65\text{kX}, \quad \frac{d}{n} = 2.40\text{kX}.$$

This layer displacement breaks down the three-dimensional periodicity of the structure and leads to appearance of irregular lines in the x-ray patterns.

Finally, continuity of the lines in x-ray patterns for samples in which the ratio of MgO to $MgCl_2$ is 3:1 and higher is due to the more finely disperse structure of these cements as compared with cements in which this ratio is less than 3:1.

This is understandable; excess of water in such cements favors crystal growth.

## SUMMARY

1. It is shown that oxychlorides are formed during hardening of the cements. The presence of oxychlorides accounts for the high mechanical strength of the cements.

2. At 3:1 and 5:1 ratios of the components MgO and $MgCl_2$ the cements have maximum mechanical strength, and consist of oxychlorides I and III.

3. The presence of water, forming hydrates with different vapor pressures, in cement samples was demonstrated by x-ray and tensimetric analysis.

4. As the result of this investigation the authors reject the theory of Sorel cement hardening generally accepted in our literature, according to which hardening depends on hydration of magnesium oxide.

## LITERATURE CITED

[1] A. A. Baikov, Collected Works, 5 [in Russian] (Izd. AN SSSR, 1948).

[2] V. V. Shellyagin, Sorel Cement [in Russian] (State Press, 1933).

[3] V. F. Zhuravlev, Chemistry of Cements [in Russian] (Goskhimizdat, 1952).

[4] A. M. Kuznetsov, Production of Caustic Magnesite [in Russian] Industrial Construction Press, 1948).

[5] A. G. Bergman and I. P. Vyrodov, J. Appl. Chem. 31, 19 (1958).*

[6] A. I. Kitaigorodskii, X-Ray Structure Analysis of Microcrystalline and Amorphous Substances [in Russian] (State Press, 1954).

Received May 3, 1957.

*Original Russian pagination. See C. B. translation.

# THE RATE OF DECOMPOSITION OF APATITE BY PHOSPHORIC ACID

M. E. Pozin, B. A. Kopylev, and D. F. Zhil'tsova

The Lensoviet Technological Institute, Leningrad

Double superphosphate is a concentrated phosphate fertilizer the production of which is due for extensive development. The material and operational costs in the production of double superphosphate are lower than in the production of precipitated phosphate by neutralization of phosphoric acid by limestone or milk of lime, and are little higher than the production costs of ordinary superphosphate. However, the production of double superphosphate is characterized by a low degree of conversion of the raw material and the need for prolonged aging. This is due to the low rate of reaction between phosphoric acid and the phosphate, the rate decreasing still further as the acid solution becomes saturated with monocalcium phosphate and the latter crystallizes, especially at the final stages of the process.

Conversion Coefficients of Apatite (from the Data of Voskresenskii et al. [5])

| Concentration and amount of phosphoric acid | | Mixing temperature of the reagents (°C) | Decomposition of apatite (%) |
|---|---|---|---|
| $P_2O_5$ content (wt.%) | amount of acid (% of stoichiometric) | | |
| 55.9 | 100 | 65 – 75 | 65.9 |
| 55.9 | 105 | 35 | 64.8 |
| 49.6 | 100 | 35 | 58.0 |
| 49.6 | 105 | 35 | 59.2 |
| 54.0 | 100 | 65 – 75 | 56.0 |

Of interest in this connection is a cyclic form of the process, with incomplete decomposition of apatite by phosphoric acid (in the range of relatively high reaction rates), and recycling of the unconverted apatite. The decomposition product may be separated from the unconverted residue by leaching of the mass with water. The solution obtained by the leaching can be converted into precipitated phosphate at a cost roughly the same as in the production of triple or ordinary superphosphate.

Operation of such a process would satisfy a part of the demand for concentrated phosphate fertilizers, for example for acid soils, sierozems, etc., by a supply of precipitated phosphate which would be considerably cheaper than the product obtained by neutralization of wet-process phosphoric acid. The conversion of apatite by means of phosphoric acid is thereby simplified and intensified.

It might also be possible under certain conditions to produce precipitated phosphate for fodder in this process.

For development of a cyclic process for conversion of apatite by the action of phosphoric acid, it is necessary to determine the optimum conditions for decomposition of apatite (amount and concentration of acid,

decomposition time, temperature, etc.) and the conditions for leaching the incompletely decomposed product, and to study the hydrolysis of monocalcium phosphate in acid media.

The attempts described in the literature [1] at partial recovery of phosphoric acid by hydrolysis of monocalcium phosphate differ substantially from the process under consideration.

Most investigations of the influence of various factors on the rate of decomposition of apatite by phosphoric acid [2] relate to the final stage of the process (aging), which is the slowest. There have been relatively few investigations of the rate of the process in its initial period, but under conditions differing considerably from those used in practice; for example, at low S: L ratios.

Chepelevetskii [3] showed that the decomposition rate of apatite in a large excess of phosphoric acid containing 20% $P_2O_5$ (at S : L = 1:30) is proportional to the hydrogen-ion concentration and the surface area of the apatite grains, and increases with the temperature. The conversion coefficient of apatite concentrate under these conditions at 60° is 64% in 0.5 hour, 77% in 1 hour, and 81% in 1.5 hours. At 80° the conversion reaches 77, 88, and 91% respectively.

Krasnov [4], in his study of the solution rate of apatite in saturated solutions of monocalcium phosphate monohydrate, also used a large excess of liquid phase (S:L = 1:30) The percentage dissolution of apatite under these conditions at 75° in 1 hour is 8% in saturated solutions containing 40.18% $P_2O_5$, 11.5% with 42.7% $P_2O_5$, and 30.7% with 47.72% $P_2O_5$.

According to the data of Voskresenskii, Milovanova, and Remen [5], the conversion coefficients of freshly made double superphosphate are as given in the table.

According to different authors, the optimum acid concentration for decomposition of apatite is in the range of 51-52% $P_2O_5$ [3], 50-54% $P_2O_5$ [5], 54-55% $P_2O_5$ [6].

Thus, the published data do not provide a basis for selection of the optimum conditions and the conversion coefficient of apatite for a cyclic process.

Below are presented the results of experiments on determination of the decomposition rate of apatite during the first stage, i.e., when it is mixed with phosphoric acid, and also during formation of the den product.

## EXPERIMENTAL

The starting materials were apatite concentrate containing 39.45% $P_2O_5$, and phosphoric acid of "chemically pure" grade. The ratio of phosphoric acid per 100 wt. parts of apatite, R, was calculated from the equation [3]:

$$H = \frac{a \cdot 2.33\,[P_2O_5]_{ap}}{[P_2O_5]_{fa}}, \qquad (1)$$

where a is the fraction of the theoretical amount of acid, $[P_2O_5]_{ap}$ is the $P_2O_5$ content of the apatite concentrate (%), and $[P_2O_5]_{fa}$ is the content of free $P_2O_5$ in the phosphoric acid (%).

Apatite was added, with stirring, to acid contained in a porcelain beaker in a thermostat. The stirring was continued until the slurry thickened to the consistency of dough. Samples were taken into beakers containing water. The conversion coefficient was determined by titration with caustic soda solution.

Titration is less accurate than the gravimetric method, and therefore at the end of each experiment analyses were performed by the standard gravimetric method. The values for the conversion coefficient found by the two methods were in satisfactory agreement (the difference did not exceed 2-5% absolute).

Fig. 1 shows variations of the conversion coefficient of apatite by phosphoric acid of different concentrations (from 13.6 to 64.8% $P_2O_5$) at 20°, with the stoichiometric amount of acid.

For acid containing 13.6% $P_2O_5$ the conversion coefficient K reaches 20.5% during the first hour from the start of the reaction; during the subsequent two hours the hourly increases of K are 2 and 1.5%. For acid containing 53.6% $P_2O_5$, during the first hour 54.5% of the apatite is decomposed, and subequently K increases by 8.5% during the 2nd hour, and by 2% during the 3rd. With acid containing 64.8% $P_2O_5$, K is 30% after 1 hour, 37% after 2 hours, and 41% after 3 hours.

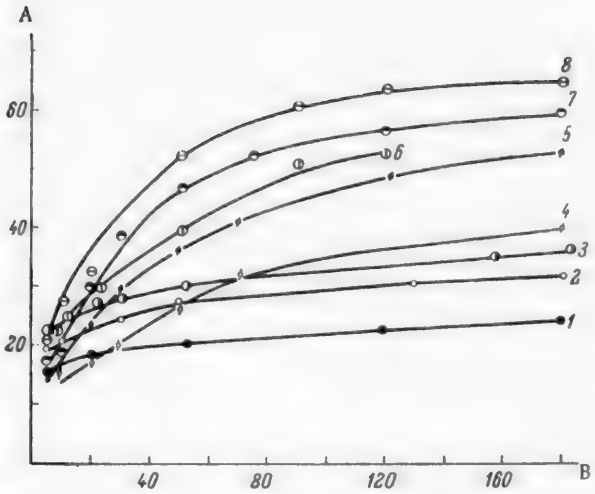


Fig. 1. Coefficients of conversion of apatite by phosphoric acid at 20° with the theoretical acid ratio: A) conversion coefficient (%), B) time (minutes); acid concentration (% $P_2O_5$): 1) 13.6, 2) 21.0, 3) 36.4, 4) 64.8, 5) 45.6, 6) 55.8, 7) 51.5, 8) 53.6.

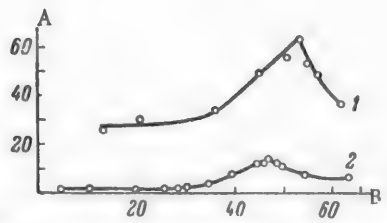


Fig. 2. Isotherm-isochrone for decomposition of apatite by phosphoric acid: A) conversion coefficients (%), B)acid concentration (% $P_2O_5$); 1) two-hour isotherm-isochrone for the conversion coefficient of apatite as a function of the original phosphoric acid concentration at 20° and 100% acid ratio; 2) two-hour isotherm-isochrone for the conversion coefficient of apatite in concentrated $CaO - P_2O_5 - H_2O$ solutions as a function of the $P_2O_5$ concentration in solution at 40°.

The rate of decomposition of apatite by phosphoric acid at 20°, and, accordingly, the conversion coefficient reached after different time intervals, therefore depends on the concentration of the acid used.

Decomposition of apatite by dilute (13.6-36.1% $P_2O_5$), and concentrated (over 53.6% $P_2O_5$) acid solutions proceeds relatively slowly. The conversion of apatite by dilute acids during 20-30 minutes is low, and increases slowly with time. With more concentrated acids the conversion of apatite in 20-30 minutes is considerably higher, and increases somewhat more rapidly with time than with the dilute acids.

Fig. 2 shows the 2-hour isotherm-isochrone for the conversion coefficient of apatite as a function of the original phosphoric acid concentration at 20° and S:L = 1:2-6; the maximum conversion is reached when the acid concentration is ~54% $P_2O_5$. Curve 2 refers to dissolution of apatite in saturated solutions of monocalcium phosphate monohydrate at 40°, S : L = 1:30; it is characterized by a maximum corresponding to 48% $P_2O_5$ in a saturated solution of the ternary system (Curve 2 is plotted from Krasnov's data [4]).

It is seen that the conversion coefficient of apatite in saturated solutions of monocalcium phosphate, even at initial S:L = 1:30, is much lower than in phosphoric acid at S:L = 1:1.35-6.

The influence of the initial S:L ratio on the rate of decomposition of apatite by phosphoric acid is very important in relation to estimation of crystallization of $Ca(H_2PO_4)_2 \cdot H_2O$ from solution, and requires further study.

Fig. 3 shows variations of the conversion coefficient of apatite with time at different ratios of phosphoric acid containing 53.0% $P_2O_5$ at 20°. During the first 10-20 minutes from the start of the reaction the conversion coefficient depends little on the acid ratio. The explanation is that, at first, only the surface layers of the apatite grains react, so that the acid is present in large excess at all ratios. The time before the rate of the process falls to very low values depends on the initial acid ratio, and different conversion coefficients are contained accordingly.

Thus, at 50 and 75% ratio the process virtually stops after 40-50 minutes. By this time the conversion coefficient reaches 35 and 45%, respectively. If the acid ratio is increased to 90-130%, the process can be continued at an appreciable rate for a longer time. Under these conditions the rate did not decrease as sharply as at 50 and 75% ratios during the same time (40-50 minutes).

The time variations of the conversion coefficient of apatite by phosphoric acid containing 53.6% $P_2O_5$

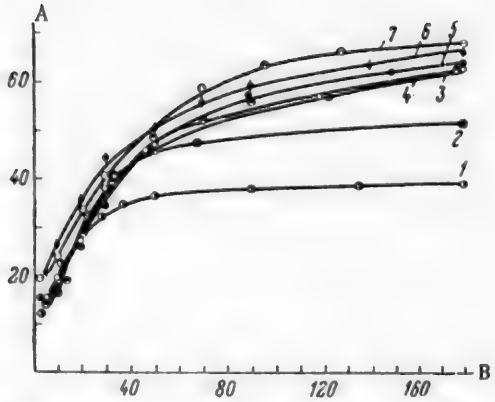


Fig. 3. Conversion coefficients of apatite by phosphoric acid at 20° and different acid ratios: A) conversion coefficient (%), B) time (minutes); amount of acid (% of theoretical): 1) 50, 2) 75, 3) 90, 4) 100, 5) 100, 6) 120, 7) 130.

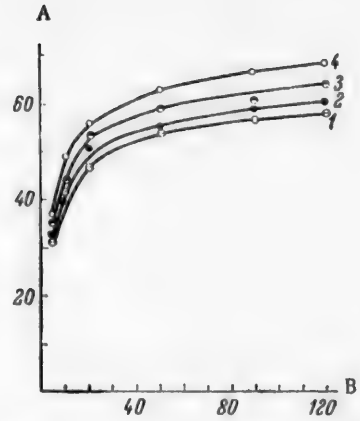


Fig. 4. Conversion coefficients of apatite by phosphoric acid at 40° and different acid ratios: A) conversion coefficient (%), B) time (minutes); amount of acid (% of theoretical): 1) 80, 2) 85, 3) 90, 4) 100.

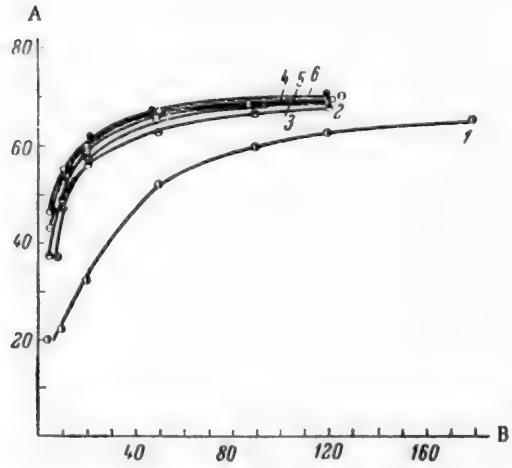


Fig. 5. Conversion coefficients of apatite by phosphoric acid containing 53.6% $P_2O_5$, at the stoichiometric acid ratio and various temperatures: A) conversion coefficient (%), B) time (minutes); temperature of acid (%): 1) 20, 2) 40, 3) 50, 4) 60, 5) 80, 6) 70.

at 40° at various acid ratios below the stoichiometric are plotted in Fig. 4. Deficiency of acid has a small influence on the conversion at higher temperatures.

Fig. 5 shows variations of the conversion coefficient of apatite with time for different temperatures of the original acid, at 100% acid ratio, containing 53.6% $P_2O_5$. The conversion coefficient increases considerably when the temperature is changed from 20 to 40°. Further rise of temperature to 80° increases the conversion coefficient by 3-5%

The relatively small influence of the temperature of the original acid, in the 40-90° range, on the conversion coefficient of apatite found in these experiments is in good agreement with the results of other workers [5-7].

The results can be used for selection of the optimum conditions for decomposition of apatite by phosphoric acid in a cyclic process.

Thus, if apatite is decomposed by phosphoric acid containing 54% $P_2O_5$ at 60° and acid ratio 95%, the conversion coefficient in 2 hours is ~ 70%.* If the process is conducted in two steps, the apatite not converted in the first step being recycled, a conversion coefficient of $(100+30) \cdot 0.7 = 91\%$ may be reached.

The acid consumption is then $130 \cdot 0.95 = 124\%$ of the stoichiometric.

The stoichiometric consumption (100% $P_2O_5$) per ton of $P_2O_5$ in the apatite is 2.33 tons. In the cyclic process the acid consumption (100% $P_2O_5$) per ton of available $P_2O_5$ obtained from the apatite is

$$\frac{2.33 \cdot 1.24}{0.91} = 3.17 \text{ tons.}$$

*Under less favorable decomposition conditions this coefficient can be reached by a certain increase of the aging time.

This is approximately equal to the acid consumption in the production of double superphosphate. Thus, in the production of double superphosphate at 110% acid ratio the conversion coefficient after 15 days of storage is 81% [5]. Therefore the acid consumption in tons of $P_2O_5$ per ton of $P_2O_5$ extracted from the apatite is

$$\frac{2.33 \cdot 1.1}{0.81} = 3.17 \text{ tons.}$$

The following scheme for a cyclic process of treatment of apatite with phosphoric acid can be recommended on the basis of these results:

1. Production of double superphosphate by the den process, with some increase of the aging time (to 1.5-2 hours), to give 65-70% conversion of apatite.

2. Leaching of the den superphosphate with water and separation of the slurry.

3. Conversion of the solution into precipitated phosphate.

The unconverted apatite residue is recycled for further decomposition.

## SUMMARY

1. The rate of decomposition of apatite by phosphoric acid falls sharply even at the den stage. Thus, with phosphoric acid containing 53.6% $P_2O_5$ the conversion coefficient reaches 70% in 2 hours at 60° at 100% acid ratio. During the first hour of this, the conversion is 66%, and during the second hour it increases by only 4%.

It is therefore appropriate to treat apatite in a cyclic process, with incomplete decomposition of the apatite by phosphoric acid and at a relatively high reaction rate, with recycling of the unchanged apatite to further decomposition.

2. The optimum conditions for the decomposition of apatite in the cyclic process are: acid concentration 54% $P_2O_5$, temperature 40-60°, acid ratio 95-100% of the stoichiometric. The conversion coefficient then reaches ~70 % in 2 hours.

3. The consumption of phosphoric acid per ton of available $P_2O_5$ in the product by the cyclic process is equal to the consumption in the production of double superphosphate.

## LITERA TURE CITED

[1] G. L. Bridger, T. I. Horzello and K. H. Lin, Agr. Food Chem. 4,4,331 (1956).

[2] E. B. Brutskus and D. L. Tsyrlin, J. Chem. Ind. 7, 394 (1956). [USSR]

[3] M. L. Chepelevetskii, Trans. Sci. Res. Inst. Fertilizers and Insectofungicides (ONTI, 1937) p. 137.

[4] K. S. Krasnov, J. Appl. Chem. 28, No. 12, 1275 (1955). [USSR] *

[5] S. K. Voskresenskii, S. K. Milovanova, and R. E. Remen, Trans. Sci. Res. Inst. Fertilizers and Insectofungicides (Goskhimizdat, 1940) p. 153.

[6] K. S. Krasnov, J. Appl. Chem. 30, No. 1, 25 (1957) [USSR]. *

[7] H. Marshall, L. Rader and K. Jacob, Ind. Eng. Ch., 25, 11, 1253 (1933).

Received April 10. 1958.

*Original Russian pagination. See C. B. Translation.

# THE RATE OF BURNING OF FLOTATION PYRITE IN THE SUSPENDED STATE

A. I. Fefelov and E. M. Lyapustina

Burning of flotation pyrite in the suspended state, which is now widely used in the sulfuric acid industry, has not yet been studied sufficiently from the theoretical aspect. In particular, there is no clear idea about the most important factor which determines the time during which the material remains in the reaction zone – the rate of the burning process, a knowledge of which must form the basis of rational equipment design and optimum operating conditions.

The rate of the process in a fixed layer (in a boat) for both lump and flotation pyrite as a function of temperature was studied by Mel'nikov et al. [1] and by Malin [2,3]. In both cases a linear relationship was found between the logarithm of the apparent reaction rate constant (K) and the reciprocal absolute temperature $\left(\frac{1}{T}\right)$. This led to the conclusion that the burning of pyrite conforms to an exponential law, i.e.

$$v = v_{\text{chem}} = Ae^{-E/RT}.$$

The burning of flotation pyrite in the suspended state was studied by Postnikov and Kunin [4], Kunin [5], Andreev [6,7] and Shurygin [6].

Kunin and Postnikov, who studied the burning process in the 600-1000° range, concluded that the log of $(K-1/T)$ relationship is linear, i.e., that, as in the case of burning in a fixed layer, the reaction rate as a function of temperature is represented by the Arrhenius equation. The same conclusion was reached by Andreev in a study of the process in the 800-1000° range. According to Andreev's data, further increase of temperature to 1200° leads to a sharp fall in the reaction rate, which he attributes to surface fusion of the cinder particles at these temperature, with consequent possible cessation or retardation of the reaction.

The decrease in the burning rate observed by Andreev is not confirmed by the data obtained by Shurygin in a study of the process in the 1100-1300° range. This discrepancy prompted us to carry out a study of the process over the 500-1250° range.

The results of this investigation are presented in this paper.

Whereas in burning in a fixed bed the time the material is in the reaction zone can be chosen arbitrarily and recorded quite accurately, in burning in the suspended state it depends on the height of the reaction space, the burning temperature and gas composition, particle size and shape, density of the material, and a number of other factors.

The reliability and reproducibility of the experimental results primarily depends on the homogeneity of the pyrite fractions with respect to particle size.

The pyrite was fractionated by repeated elutriation and sedimentation. The characteristics of the isolated pyrite fractions are given in the table.

The residence time of the pyrite particles in the reaction zone (under the experimental conditions) was calculated from Oseen's formula with a correction factor to allow for deviation of the pyrite particles from a spherical shape. The correction factor was derived by comparison of the particle sedimentation velocities determined in a special apparatus [9] with values calculated from the Oseen formula.

Characteristics of Pyrite Fractions

| Fraction code number | Average particle size (in $\mu$ *) | Deviation from average size (%) | Sulfur content (%) | Specific gravity |
|---|---|---|---|---|
| 180 | 181 | ± 19.6 | 50.13 | 4.8931 |
| 140 | 141 | ± 13.8 | 50.87 | 4.9042 |
| 120 | 119 | ± 13.9 | 51.57 | 4.9219 |
| 95 | 95 | ± 14.2 | 51.57 | 4.9185 |

*Particle sizes were determined under the microscope.

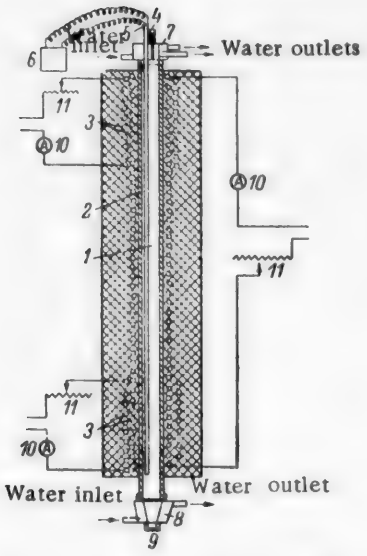


Fig. 1. Diagram of unit for burning of pyrite in the suspended state: 1) furnace chamber, 2) main heating element, 3) supplementary heating elements, 4) feed funnel, 5)thermocouple, 6) galvanometer, 7)furnace head, 8) furnace hopper, 9) detachable bottom of hopper, 10) ammeters, 11) rheostats.

Experiments on the burning of flotation pyrite in the suspended state were performed in a vertical tubular furnace 1.5 m high and 72 mm internal diameter. The furnace is shown schematically in Fig. 1.

The furnace was heated by means of Nichrome heating elements. To equalize the temperature along the height of the furnace, heaters were installed at its ends; this gave a fairly uniform temperature distribution over a height of 120 cm, which was taken as the height of the reaction zone. The temperature of the reaction zone was measured at intervals of 10 cm by means of a thermocouple. The average temperature was found from the results of these measurements.

The pyrite was burned in a stationary medium. The weight of sample taken for each experiment was determined by the amount of air present in the furnace at the experimental temperature. The experiments were performed in the following sequence: the furnace was heated to the required temperature and held at this (constant) temperature for 20-30 minutes; after the temperature distribution along the tube had been determined, the prepared pyrite sample was put into the feed funnel. The time required to pour the pyrite into the furnace was not less than 50-60 seconds. At the end of the experiments the gas in the furnace was withdrawn by means of a vacuum pump.

The cinders formed as the result of burning of the pyrite were analyzed for sulfur content and investigated under the microscope.

The results were used to calculate the apparent rate constants for the burning process in the suspended state, by means of the equation used for the corresponding calculations relating to the burning of coal dust [10].

$$\frac{dC}{C} = -K d\tau \quad \text{or} \quad K = \frac{2.3 \lg \frac{S_i}{S_f}}{\tau},$$

where K is the reaction rate constant, $S_i$ is the initial sulfur content of the pyrite, $S_f$ is the final sulfur content in the cinders, $\tau$ is the reaction time (seconds).

Since heterogeneous reactions develop at the surface of contact between interacting phases, the foregoing equations, used by earlier workers [4-7] and ourselves, is not an accurate reflection of the kinetics of the process in question. However, it is the most appropriate to the conditions of burning in the suspended state, because, in view of the small size of the particles, ti may be assumed with some degree of approximation that the whole volume of a particle takes part in the reaction simultaneously and at roughly the same rate.

In the development of a method for studying the burning of flotation pyrite in the suspended state, in order to obtain comparative data we also studied the burning of pyrite in a boat (fixed layer); the results confirmed the rate-temperature relationship established by Mel'nik and Malin.

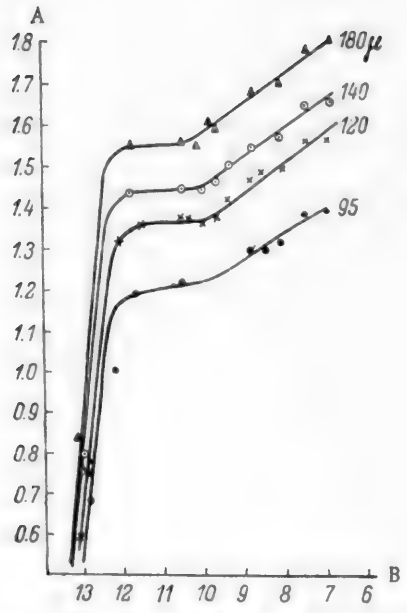


Fig. 2. Variation of the logarithm of the apparent reaction rate constant with the reciprocal absolute temperature: A) log K·10, B) $1/T \cdot 10^4$.

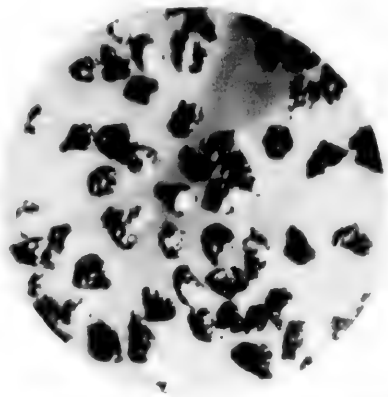

Fig. 3. Photomicrograph of pyrite fraction of 120 μ particle size.

The results of experiments on the burning of 180, 140, 120, and 95 μ fractions of flotation pyrite in the suspended state with a reaction zone 1.2 m high, in the 485-1155° range, are given in Fig. 2 in the form of a plot of the relationship $\log\left(K - \frac{1}{T}\right)$.

Microscopical examination of the cinders showed that up to 500° there are no appreciable changes in the form and surface of the particles, and the particles retain the characteristic pyrite luster. When the temperature is raised to 540°, bright iridescence colors appear on the particle surfaces, while the particle shape remains unchanged.

For comparison of the changes which take place during roasting with further increase of temperature, Fig. 3 shows a photomicrograph of pyrite consisting of particles 120 μ in size. •

When the burning temperature is 560° (Fig. 4), the microscopic picture already shows cracked particles, particles fused on the surface, especially at corners ("hedgehogs"), and very small surface-fused spheres. On further increase of temperature the number of fused particles increases, and at 1000° nearly all the particles are in the form of spheres and droplets, while at 1250° all the particles are completely spherical with smooth shining surfaces. This shows that the particles had passed through a liquid phase.

The external appearance of cinders formed by the burning of 120 μ pyrite fraction at 800, 1000, and 1250° respectively is shown in Figs. 5, 6, and 7.

The relationship between the apparent rate constant of the reaction and the temperature, plotted in Fig. 2, is represented by a broken line from which three temperature regions of the burning process can be identified. In the first region (485-580°) the burning rate rises rapidly with the temperature. In the second region (580-780°) the $\log\left(K - \frac{1}{T}\right)$ relationship is represented by a straight line almost parallel to the abscissa axis (for the 180, 140, and 120 μ fractions) and the apparent rate constant remains relatively constant and almost independent of the temperature. Finally, in the third region (780-1155°) the apparent rate constant again increases with temperature and the relationship is represented by a straight line, but of a smaller slope than in the first region.

The results of examination of the cinders under the microscope lead to the conclusion that the relative constancy of the apparent rate constant in the 580-780° range is due to the surface fusion of the particles which occurs in this temperature range. The viscous layer which forms apparently has a retarding effect on the reaction. Another possible explanation for the lack of any appreciable influence of increase of temperature of the particle itself, which remains constant during its fusion. After most of the particles have passed through the initial fusion stage, i.e., beyond 780-800°, further increase of temperature raises the reaction rate constant.

The apparent energy of activation calculated from the apparent rate constants for the reaction in the different regions, has the following values: first region (485-580° range), 52300 cal/mole; second region (580-780°), 620 cal/mole; third region (780-1155°), 3400 cal/mole.

• This and all the subsequent photomicrographs were taken under magnification of 60.

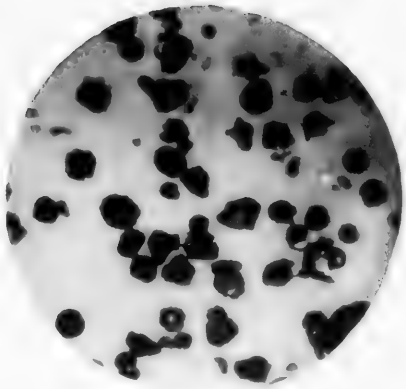

Fig. 4. Cinder formed by burning of 120 μ pyrite fraction at 560°.

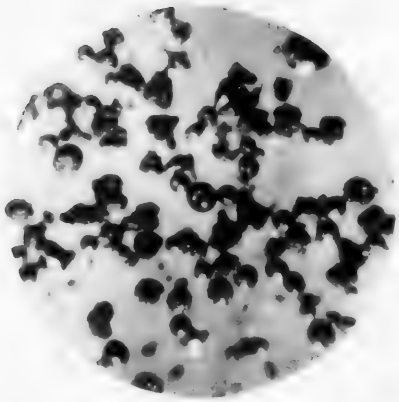

Fig. 5. Cinder formed by burning of 120 μ pyrite fraction at 800°.

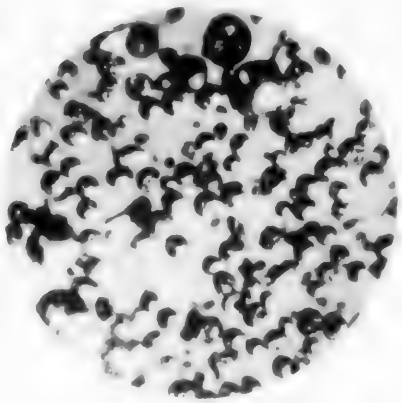

Fig. 6. Cinder formed by burning of 120 μ pyrite fraction at 1000°.

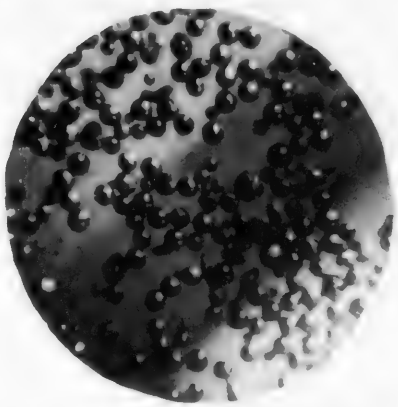

Fig. 7. Cinder formed by burning of 120 μ pyrite fraction at 1250°.

The value of the apparent activation energy for the first stage of pyrite burning (52300 cal/mole) is higher than than that given by Malin [11] for the dissociation of iron disulfide (30400 cal/mole). This is because this stage of the process involves not only dissociation of $FeS_2$ but also combustion of the second sulfur atom, i.e., combustion of sulfur from FeS. Thus, when the burning temperature is 500° the cinder contains 43.8% sulfur (for an initial sulfur content of 50-51% in the original pyrite), whereas at 560° the cinder contains only 4.09% sulfur.

The value of the apparent activation energy in the third region is close to that given by Malin for the combustion of iron monosulfide (3160 cal/mole).

For determination of the kinetic relationships of the burning of pyrite in the suspended state, experiments were performed with the same pyrite fractions and with the reaction zone 0.8 and 0.4 m high. •

The results of experiments on burning of pyrite with different heights of the reaction zone are shown graphically in Fig. 8, in the form of a plot of the percentage of sulfur removed as a function of temperature. Examination of the curves in Fig. 8 shows that decrease of the height of the reaction zone from 1.2 to 0.8 m has no influence on the degree of sulfur removal (the points all fit on the same curve) in the particle-size range studied. Decrease of the reaction zone to 0.4 m lowers the degree of sulfur removal.

• The furnace shown in Fig. 1 was used for the experiments. the height of the reaction zone was varied by installation of special cooler in the furnace.

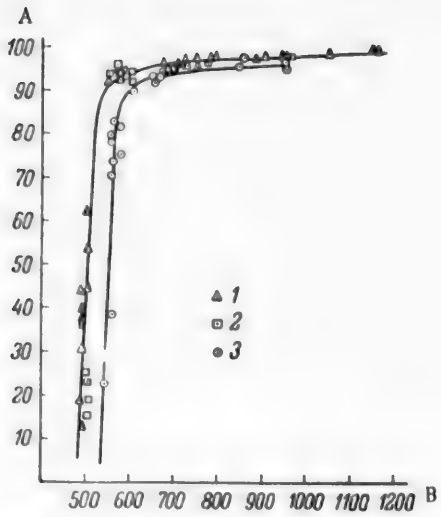


Fig. 8. Variation of the degree of sulfur removal with temperature for 95, 120, 140, and 180 μ pyrite fractions:
A) degree of sulfur removal (%), B) temperature (°C); height of reaction zone (m): 1) 1.2, 2) 0.8, 3) 0.4.

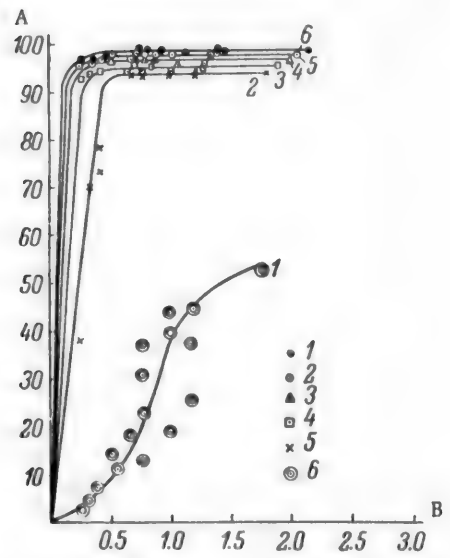


Fig. 9. Burning rate of flotation pyrite in the suspended state in a stationary medium:
A) degree of sulfur removal, B) time (minutes); temperature (deg): 1) 500, 2) 600, 3) 700, 4) 800, 5) 900, 6) 1000.

Curves representing the burning rate of pyrite in the suspended state in a stationary medium are plotted in Fig. 9.

Analysis of data on burning rates shows that the burning of pyrite in the suspended state is very rapid: even at low temperatures (700-750°) about 95% of the total sulfide sulfur is removed in 0.5 second. At 1000° the amount of sulfur removed in 0.5 second reaches 98.5%. Further increase of the residence time of the particles in the reaction zone has little influence on the degree of sulfur removal. Thus, increase of residence time of pyrite in the reaction zone from 0.5 to 2 seconds at 1000° increases the degree of sulfur removal by only 0.5%.

Our results show quite clearly that the main way to ensure fuller utilization of pyrite sulfur during burning of pyrite in the suspended state is by increase of the burning temperature, whereas various measures directed toward increasing the residence time of the particles in the reaction zone, such as increase of the furnace height, tangential motion of the particles, etc., do not lead to the desired goal.

In all the burning experiments described above pyrite fractions containing 50-51.5% sulfur were used, i.e., almost pure pyrite, whereas the flotation pyrite burned in industrial burners has a lower sulfur content owing to the presence of impurities such as $SiO_2$, CaO, etc. To test the influence of certain impurities, including $SiO_2$, on the burning process we carried out experiments on the burning of three pyrite fractions obtained after elutriation and sedimentation, with particle sizes of 95, 120, and 140 μ, containing 44.83, 36.88, and 33.30% sulfur respectively. The lower sulfur contents of these fractions are due almost entirely to the presence of quartz in the form of individual particles mixed with the pyrite particles, and in the form of quartz particles containing embedded pyrite.

Comparison of the degree of sulfur removal in experiments on burning of pyrite with a low sulfur content with the results for 51% pyrite showed that the degree of sulfur removal from pyrite containing 45% sulfur is almost the same as for pyrite containing 51% sulfur. There is a slight difference (a decrease) for pyrite containing 37% sulfur; this difference becomes greater with further decrease of the sulfur content (down to 33.30%). The degree of sulfur removal at 800° is 96% for 33.3% pyrite, and 98% for 51% pyrite. The decrease of the degree of sulfur removal from pyrite may be attributed, on the one hand, to a decrease of the reacting surface (presence of porphyritic formations) and on the other, to the retarding influence of possible reactions of silicate formation in presence of pyrite and quartz surfaces in close contact, even at relatively low temperatures (600-800°). Therefore our data on the burning of pyrite in the suspended state may be used for practical purposes, since the sulfur content of pyrites used for burning in industrial furnaces lies in the 38-45% range.

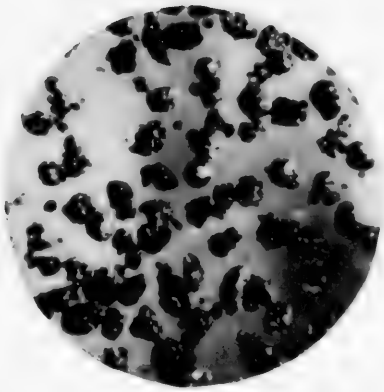

Fig. 10. 90 $\mu$ cinder fraction from the fourth crown of the rotary furnace of the Voskresenskii Chemical Combine; temperature 900°.

Fig. 11. 90 $\mu$ cinder fraction from the flash burner of the Kirovograd Chemical Plant.

In tests of the agreement of laboratory data on burning in a fixed layer (in a boat) and in the suspended state with the results obtained in industrial furnaces (rotary shelf burners and flash burners), the cinders formed under laboratory conditions and in industrial furnaces were examined under the microscope.

In burning in a fixed layer (in a boat) surface fusion of the particles (mainly at sharp corners) is so slight that it can hardly be detected when the particles are examined under the microscope. Since the main factor retarding the reaction – surface fusion – is absent, in this case the $\log\left(K - \frac{1}{T}\right)$ relationship is represented by a sloping straight line. In other words, increase of temperature anywhere between 500 and 1000° (the limits of the investigation) should increase the apparent rate constant of the burning reaction.

The photomicrograph in Fig. 10, which represents the cinder from the rotary burner of the Voskresenskii Chemical Combine, shows that the cinder particles have a fused surface, and the cinder structure is much nearer to that of the cinder formed by burning in the suspended state in the laboratory furnace (Fig. 5) and in the burner of the Kirovograd Chemical Plant (Fig. 11).

Surface fusion of the pyrite particles during burning in rotary tray burners indicates that in this case also the process is retarded, probably in the same temperature range (600-800°) as in burning in the suspended state. For flash burners operating at higher temperatures retardation of the process in this temperature range is of no practical importance, whereas in the case of rotary tray burners it must be taken into account in determination of the optimum operating temperatures.

## SUMMARY


1. The burning of flotation pyrite in the suspended state was investigated and three temperature regions of the burning process were established; in the first (485-580°) the apparent rate constant for the process increases sharply with the temperature, in the second (580-780°) it is virtually independent of the temperature, and in the third (780-1155°) it again increases with temperature, but less than in the first region.

2. The average values of the apparent energy of activation in the 1st, 2nd, and 3rd regions are 52300, 620, and 3400 cal/mole respectively.

3. Burning proceeds very rapidly in the suspended state – at 750 and 1000° 95 and 98.5% sulfur respectively is removed in 0.5 second.

4. The main way of ensuring the most complete utilization of pyrite sulfur (98.5-99%), i.e., of obtaining cinders containing less than 1% sulfur in existing flash roasting burners is to increase the temperature to 900-1000°, with a residence time of the particles in this temperature zone of not less than 2 seconds.

5. The $\log\left(K - \frac{1}{T}\right)$ relationship derived earlier [1-3] for burning in boats in the 500-1000° temperature range is not applicable to burning in rotary burners. Our investigations showed that surface fusion of the particles involves retardation of the burning of pyrite in the suspended state over a definite temperature range, and as surface fusion also occurs in rotary burners it is most probable that the burning rate decreases in them also.

6. The data obtained on the burning of pyrite in the suspended state may be applied for practical purposes.

## LITERATURE CITED


[1] B. D. Mel'nik et al., J. Chem. Ind. 2 (1938).

[2] K. M. Malin, J. Chem. Ind. 5 (1939).

[3] K. M. Malin, J. Chem. Ind. 5 (1948).

[4] V. F. Postnikov and T. I. Kunin, J. Chem. Ind. 3 (1938).

[5] T. I. Kunin et al., J. Chem. Ind. 1 (1949).

[6] A. F. Andreev, J. Chem. Ind. 8 (1947).

[7] A. F. Andreev, Candidate's Dissertation [in Russian] (Sverdlovsk, 1947).

[8] A. P. Shurygin, Author's Summary of Candidate's Dissertation [in Russian] (Moscow Power Inst. 1955).

[9] A. I. Fefelov and L. A. Kostromitin, Industrial Lab. 11 (1957).

[10] S. T. Rostovtsev, Theory of Metallurgical Processes [in Russian] Section 3 (Metallurgy Press, 1945)

[11] K. M. Malin et al., Sulfuric Acids Technology [in Russian] (Goskhimizdat, 1950) p. 116.



Received September 18, 1957.

# KINETICS OF THE REDUCTION OF MANGANESE OXIDES BY SOLID CARBON

V. A. Kozlov and V. G. Vlasov

The S. M. Kirov Polytechnic Institute of the Urals

In the course of research on thermal reduction by carbon various interpretations of the mechanism of this process were advanced [1-4]; these are now regarded as erroneous.

The most widely accepted viewpoint was that formulated by Baikov [5,6], Sokolov [7], and Pavlov [8] and developed further in subsequent investigations. According to this view, the reaction of a metal oxide with carbon consists of two coupled reactions: reduction of the oxide by carbon monoxide, and regeneration of the latter by the reaction $CO_2 + C \longrightarrow 2CO$.

It is now necessary to obtain deeper insight into the mechanism of interaction of oxides with carbon, and to accumulate experimental data on the reduction of different oxides by various kinds of carbon.

The purpose of the present investigation was to study the kinetics of reduction of higher manganese oxides by carbon at relatively low temperatures.

## EXPERIMENTAL

Starting materials and methods of investigation. The starting materials were artificially prepared manganese oxides: $MnO_2$, $Mn_2O_3$, and $Mn_3O_4$. Manganese dioxide was prepared by thermal decomposition of manganese nitrate, $Mn(NO_3)_2 \cdot 6H_2O$. The salt was dried on the water bath and heated in air at 200° to complete removal of nitrogen oxides. The product was ground in an agate mortar and again heated at 200° to constant weight. $Mn_2O_3$ and $Mn_3O_4$ were made by calcination of manganese dioxide in air at 500 and 940° respectively. The manganese oxides prepared by these methods were all $\beta$-modifications, in Rode's terminology [9].

The reducing agent was wood charcoal, previously degasified under vacuum at 1100° for 12 hours. The charcoal was used in 3-fold excess over the amount needed for complete reduction. The reagent mixtures were prepared by mixing and grinding of the oxide and charcoal in an agate mortar. Each series of experiments was performed with one mixture, as it was found that the reduction rate is influenced by differences in grinding.

Investigations of the reduction kinetics were performed in a high-vacuum unit fitted with a device for continuous determination of weight loss (Fig. 1).

Weighing was performed with the aid of a molybdenum spring with a sensistivity of 0.1 mg per scale division of the measuring microscope. The average weight of a mixture sample was 500 mg.

The experiments were performed as follows: a sample of the reagent mixture, weighed on an analytical balance, was placed in the reaction space of the system. Air was pumped out of the system. The evacuation was first performed at room temperature, and the sample was then warmed. The warming temperature was kept 50° below the temperature at which the components begin to react. After the weight became constant and a vacuum of the order of $10^{-4}$ mm had been produced, the furnace which had been previously heated to the required temperature was moved onto the sample. The time readings and determinations of the weight were commenced at the instant when the experimental temperature became established in the reaction tube. The gases formed by reduction were removed from the reaction zone, and carbon dioxide was frozen out in a trap cooled by liquid air.

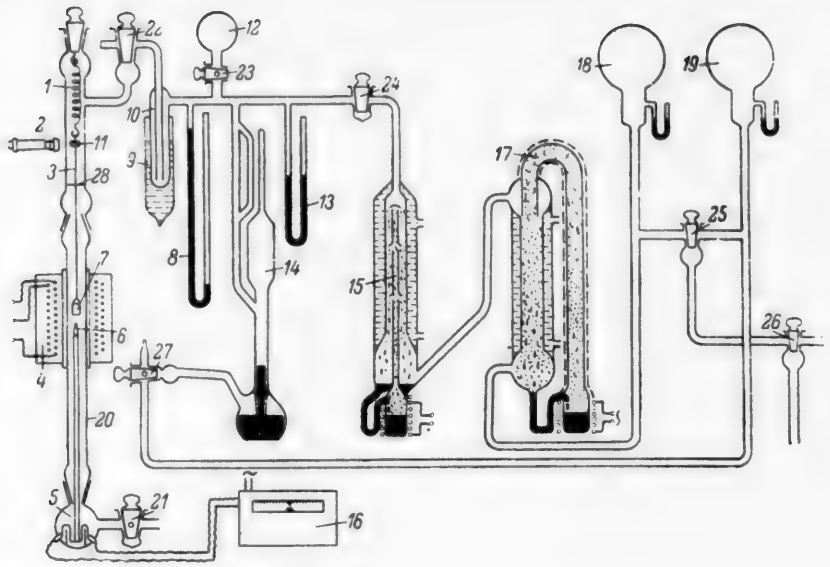

Fig. 1. Diagram of experimental unit:
1) molybdenum spring, 2) measuring microscope, 3) molybdenum suspension wire, 4) electric heating furnace, 5) head with sealed-in thermocouple, 6) Chromel-Alumel thermocouple, 7) quartz crucible, 8) open manometer, 9) Dewar flask, 10) trap, 11) balance indicator, 12) measuring flask, 13) closed manometer, 14) McLeod gage, 15) three-stage mercury condensation pump, 16) ERM-47 electronic thermoregulator, 17) single-stage mercury condensation pump, 18) and 19) exhaust bulbs, 20) quartz tube, 21-27) vacuum stopcocks, 28) mica shield.

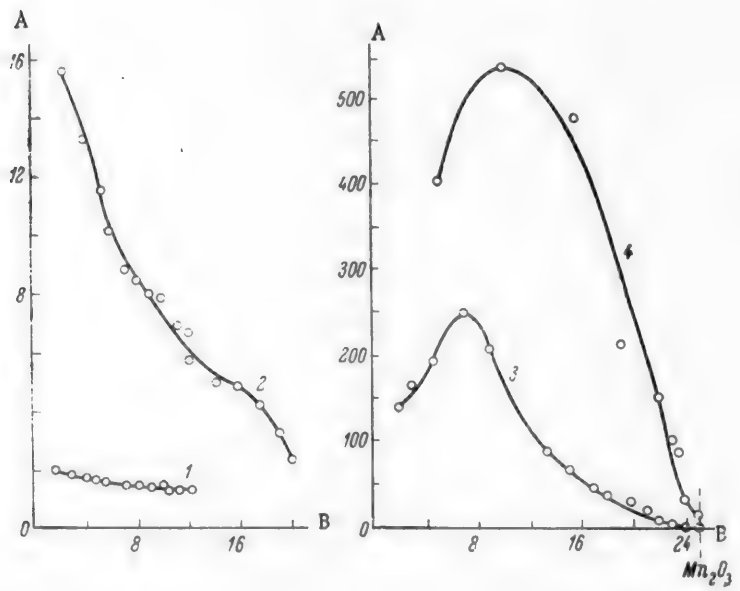

Fig. 2. Dependence of the rate of reduction of $MnO_2$ on the degree of oxygen removal:
A) reduction rate [in mg $O_2 \cdot 10^4$/mg $O_2$(init)/min]; B), degree of oxygen removal (%); temperature (°C) 1) 400, 2) 450, 3) 500, 4) 550.

In some experiments the gaseous products were allowed to accumulate in the reaction zone during the reduction.

The true rate of the reduction process was determined from the slope of the tangent to the curve for the degree of oxygen removal as a function of time. The apparent energy of activation was determined from the Arrhenius equation.

Results of the investigation. The results of experiments on the reduction of $MnO_2$ by wood charcoal under vacuum in the 400-500° range are plotted in Fig. 2. It is seen that in this temperature range manganese dioxide is in practice reduced only to $Mn_2O_3$. At 500 and 550° the reduction of $MnO_2$ is autocatalytic.

TABLE 1

$CO_2$ Contents of the Gas Phase in Reduction of Manganese Oxides by Wood Charcoal

| Temperature (°C) | $CO_2$ content (%) | Temperature (°C) | $CO_2$ content (%) | Temperature (°C) | $CO_2$ content (%) |
|---|---|---|---|---|---|
| 400 | 95 – 100 | 600 | 90 – 100 | 700 | 100 |
| 450 | 80 – 85 | 650 | | 750 | 97.0 |
| 500 | 55 – 60 | 700 | | 800 | 95.5 |
| 550 | 45 – 50 | 750 | | 850 | 85.0 |

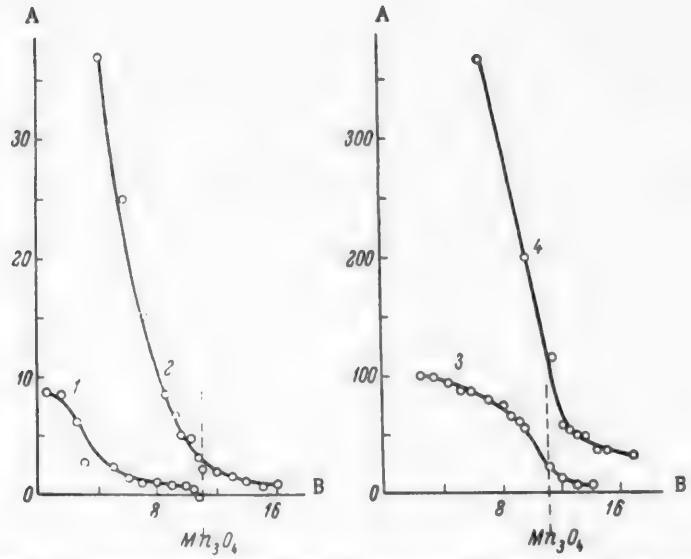


Fig. 3. Dependence of the rate of reduction of $Mn_2O_3$ on the degree of oxygen removal:
A) and B) as in Figure 2; temperature (°C): 1) 600, 2) 650, 3) 700, 4) 750.

The carbon dioxide content of the gas phase in the reduction of $MnO_2$ under vacuum decreases steadily with increase of temperature (Table 1). It was found that the gas phase contains oxygen in addition to carbon dioxide. This had been previously observed by Baukloh [10] and also by Chufarov and Tatievskaya [11].

The results obtained in studies of the reduction kinetics of $Mn_2O_3$ and $Mn_3O_4$ under vacuum are plotted in Figs. 3 and 4. In the temperature ranges studied $Mn_2O_3$ and $Mn_3O_4$ are reduced to manganous oxide. In the reduction of $Mn_2O_3$ there are inflections on the kinetic curves at 11% reduction, corresponding to conversion into $Mn_3O_4$. The reduction rates of $Mn_2O_3$ and $Mn_3O_4$ decrease with increased degree of oxygen removal.

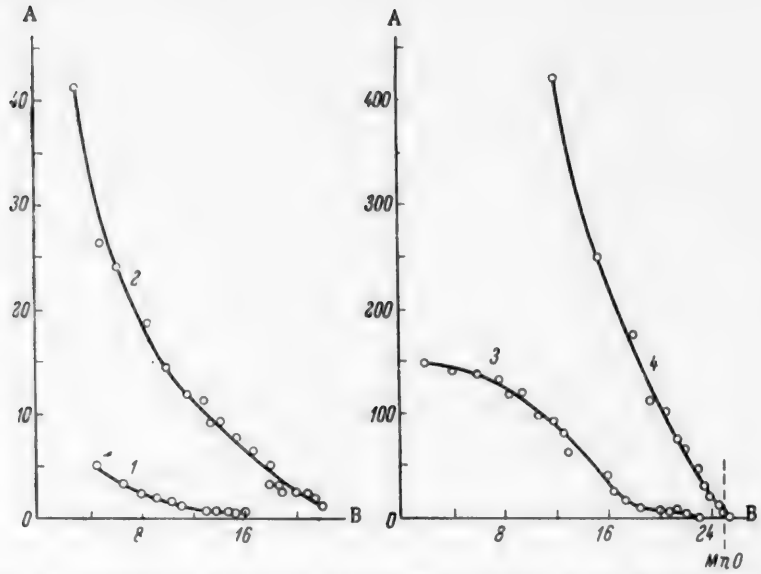


Fig. 4. Dependence of the rate of reduction of $Mn_3O_4$ on the degree of oxygen removal:
A) and B) as in Figure 2; temperature (°C): 1) 700, 2) 750, 3) 800 , 4) 850.

TABLE 2

Values of the Constants K and K' in the Kinetic Equations

| $MnO_2$ | | | $Mn_2O_3$ | | | $Mn_3O_4$ | | |
|---|---|---|---|---|---|---|---|---|
| Temperature (°C) | K | K' | Temperature (°C) | K | K' | Temperature (°C) | K | K' |
| 400 | 0.36 | — | 600 | 0.27 | $3.0 \cdot 10^{-3}$ | 700 | 0.37 | $0.72 \cdot 10^{-3}$ |
| 450 | 1.77 | — | 650 | — | $3.4 \cdot 10^{-2}$ | 750 | 3.36 | $0.48 \cdot 10^{-2}$ |
| 500 | 36.0 | $4.3 \cdot 10^{-2}$ | 700 | — | $2.3 \cdot 10^{-1}$ | 800 | 27.00 | $1.95 \cdot 10^{-2}$ |
| 550 | 225.0 | 0.44 | 750 | -- | 8.00 | 850 | — | 0.25 |

The carbon dioxide contents of the gas phase in the reduction of $Mn_2O_3$ and $Mn_3O_4$ under vacuum are given in Table 1. In the reduction of $Mn_2O_3$ the composition of the gas phase varies little with the temperature. In this case, as in the reduction of $MnO_2$, the gas phase contains oxygen.

The gas phase in the reduction of $Mn_3O_4$ consists of carbon dioxide and monoxide, and the $CO_2$ content decreases steadily with increase of temperature.

To determine the influence of the gas phase on the reduction rate of manganese oxides, experiments with accumulation of the gaseous products in the reaction zone were carried out in addition to the vacuum experiments.

The carbon dioxide content in the final gas phase formed in reduction of $MnO_2$ with accumulation of the gaseous reaction products varied as follows: with the temperature :

| | | | |
|---|---|---|---|
| Temperature (°C) . . . . . | 450 | 500 | 550 |
| $CO_2$ content (%) . . . . . | 100 | 85 | 80 |

In the reduction of $Mn_2O_3$ with accumulation of the gaseous products, the gas phase consists almost entirely of carbon dioxide.

In the reduction of $Mn_3O_4$ under these conditions, the $CO_2$ content of the gas phase decreases considerably. Whereas in reduction under vacuum at 750° the gas phase contains 97% $CO_2$, in reduction with accumulation of the gaseous products it contains only 60%.

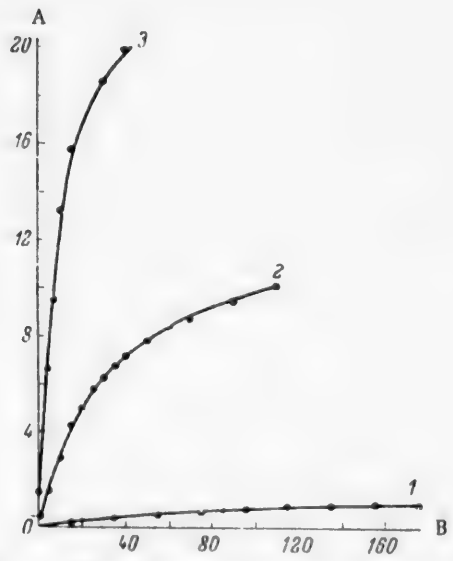


Fig. 5. Effect of contact between the reactants on the reduction of $Mn_3O_4$ at 800°: A) degree of oxygen removal (%), B) time minutes; 1) reactants in two layers, 2) reactants mixed, 3) reactants mixed and ground together.

Accumulation of gaseous products in the reaction zone leads to an increase in the reduction rate of manganese oxides. The rate increase is most pronounced in reduction of manganese dioxide, and is weaker in reduction of $Mn_2O_3$ and $Mn_3O_4$.

A series of experiments was carried out at 800° in order to determine the influence of contact between the reactants on the reduction rate of $Mn_3O_4$ under vacuum.

Reduction of this oxide was studied with three samples of the reagent mixture: in the first sample the oxide and carbon were in two layers, the oxide above and the carbon below; in the second sample the reactants were mixed in the same proportions, but not ground together; in the third sample they were mixed and thoroughly ground in a mortar.

The results of these experiments are shown in Fig. 5. It is seen that the reduction rate rises sharply with increased contact between the reactants. Mathemathical analysis of curves plotted in coordinates: degree of oxygen removal-time showed that the reduction under vacuum of each of the manganese oxides studied may be represented by two equations:

$$g^2 = K \cdot \tau, \quad \ln \frac{a}{a-g} = K' \cdot \tau,$$

where g is the degree of oxygen removal (%); $\tau$ is the time from the start of the experiment (minutes); K and K' are constants; $\underline{a}$ is the amount of oxygen (in %) which must be removed from the oxide in order to convert it completely into the next lower oxide (the numerical values of $\underline{a}$ are : for reduction of $MnO_2$, 25; for $Mn_2O_3$, 11.1; for $Mn_3O_4$, 25).

Equation (1) describes the reduction of manganese dioxide to approximately 18-19% reduction, of $Mn_2O_3$ to 6%, and of $Mn_3O_4$ to 14%; at higher degrees of oxygen removal Equation (2) becomes valid.

The values of the constants K and K' in the kinetic equations are given in Table 2.

The transition from Equation (1) to Equation (2), which is observed at a definite degree of oxygen removal for each oxide, represents a change in the character of the reduction process.

The observed transitions coincide with the boundary of α-kurnikite, β-hausmannite, and manganosite solid solutions which exist, according to Rode [9], in the composition ranges $MnO_{1.61}$ – $MnO_{1.5}$, $MnO_{1.40}$ – $MnO_{1.33}$, $MnO_{1.15}$ – $MnO$, which corresponds to 18.5-25.0% reduction of $MnO_2$, 6-11% reduction of $Mn_2O_3$, and 13.5-25% reduction of $Mn_3O_4$.

The values of the activation energy at different degrees of oxygen removal are given in Table 3.

It follows from Table 3 that the activation energy increases in the transition from the highest to the lowest oxide; the degree of oxygen removal also influences the activation energy.

TABLE 3

Effect of the Degree of Oxygen Removal on the Activation Energy of Reduction of Manganese Oxides

| $MnO_2$ | | $Mn_2O_3$ | | $Mn_3O_4$ | |
|---|---|---|---|---|---|
| Degree of oxygen removal | Activation energy (cal/mole) | Degree of oxygen removal | Activation energy (cal/mole) | Degree of oxygen removal | Activation energy (cal/mole) |
| 2 | 44200 | 3 | 55500 | 2 | 61400 |
| 8 | 44000 | 7 | 56400 | 4 | 66600 |
| 11 | 44000 | 8 | 56500 | 8 | 79200 |
| 18 | 48500 | 10 | 64000 | 12 | 85000 |
| 21 | 52000 | | | 16 | 88000 |
| | | | | 20 | 86000 |
| | | | | 22 | 89000 |

In the reduction of $MnO_2$ and $Mn_3O_4$ sharp changes in the value of the activation energy are observed at degrees of oxygen removal which are close to the boundary of the solid solution region.

## DISCUSSION OF RESULTS

Two independent processes take place during the interaction of higher manganese oxides with wood charcoal: dissociation and reduction. The increase in the rate of reaction of $MnO_2$ and $Mn_3O_4$ with wood charcoal relative to their dissociation is explained by the occurrence of an independent reduction process, which proceeds at a higher rate than dissociation [14].

The increase of the rate of interaction of higher manganese oxides with carbon on accumulation of gaseous products in the reaction zone shows that the gas phase plays a significant role in the reduction process.

There are indications in the literature that different mineral admixtures have different effects on the reaction $CO_2 + C \rightarrow 2CO$; in particular, the oxides of alkali and alkaline-earth metals, and oxides of iron, manganese, copper, nickel, and other metals accelerate the reduction of carbon dioxide by carbon. Moreover, the rate of the reaction $CO_2 + C \rightarrow 2CO$ also depends on the nature of the carbon [11].

The manganese oxides used in our experiments had virtually the same impurity contents, and only wood charcoal was used as the reducing agent, and therefore such experimental facts as differences between the reduction rates of the oxides and the pronounced stepwise nature of the reactions can be attributed only to the individual effects of the oxides on the reduction process, and in particular on the reaction $CO_2 + C \rightarrow 2CO$.

In the reduction of higher manganese oxides by wood charcoal reduction is accompanied by partial dissociation of the oxides; in this case oxygen atoms may be incorporated in the interbasal planes of the graphite lattice; this weakens the bonding of the carbon dioxide. This is confirmed by the work of Chukhanov [12], who showed that the reaction of carbon with oxygen at low temperatures (400-700°) occurs within the whole bulk of the carbon with oxygen at low temperatures (400-700°) occurs within the whole bulk of the carbon particle. According to Meyer [13] the first stage in the reaction of oxygen with carbon is rapid solution of oxygen in the graphite lattice, which facilitates the subsequent interaction.

It seems that carbon is activated by oxygen to a lesser extent in the reduction of $Mn_2O_3$, and not at all in the reduction of $Mn_3O_4$, where temperature has the predominant influence.

In addition to this factor, the course of the reaction $CO_2 + C \rightarrow 2CO$ at low temperatures is favorably influenced by the exothermic effect of the reactions between higher manganese oxides and carbon [1].

Contact between the reactants influences reduction because it favors formation of the gas phase which is necessary for further development of the process. Appearance of the gas phase is ensured by interaction of surface carbon complexes with the surface oxygen atoms of the oxide, and also by direct reaction of carbon with the

oxide at the very start of the process. Good contact between the reactants facilitates exchange of CO and $CO_2$ molecules between the oxide and carbon in the cyclic process of direct reduction, leading to an increase in the reduction rate. Moreover, close contact between the oxide and carbon increases the number of points at which they touch, so that the reaction of indirect reduction and the reaction of carbon gasificiation originate and develop at a considerably greater number of centers.

Our experimental data confirm the mechanism of direct reduction according to which the process is composed of two principal reactions:

$$Me_xO_y + CO \longrightarrow Me_xO_{y-1} + CO_2, \quad (I)$$

$$CO_2 + C \longrightarrow 2CO. \quad (II)$$

In this case the reduction is really in the gas phase. The reaction $CO_2 + C \rightarrow 2CO$ fulfills two important functions: 1) it supplies the reducing agent for the indirect reduction, and 2) it assists rapid removal of the gaseous product of Reaction (I), which is an important factor in the reduction of such oxides as MnO.

It is known that the rate of reaction between oxides and carbon is influenced both by the nature of the oxide and the nature of the reducing agent. As a result, difficulties arise in establishing which is the determining step in the direct reduction process.

Since Reactions (I) and (II) are interconnected, their rates must be equal in the steady process, and the reaction with the lower rate constant would be the determining step in the interaction process.

The following facts were established by our investigation: a) reduction of manganese oxide proceeds stepwise and in a single zone; b) the process is diffusional in character, as is shown by the fact that it conforms to the equation $g^2 = K\tau$; c) the reaction is autocatalytic in the reduction of $MnO_2$; d) the character of the process changes in the region of transitions in solid solutions; e) the activation energy increases regularly in the sequence from the highest to the lowest oxide.

Similar facts were established in our studies of the dissociation kinetics of $MnO_2$ and $Mn_2O_3$ [14].

All this leads to the conclusion that the kinetic picture of the interaction of oxides with carbon is determined by the reaction of indirect reduction, i.e., changes taking place in the oxide constitute the limiting stage of the reduction process. The experimental results show that these changes are diffusional in character.

Diffusion of gases into the cracks and pores of the oxide may be disregarded, as the activation energies found in our experiments were relatively high and a vacuum technique was used in the investigation. Diffusion of CO and $CO_2$ molecules through the oxide crystal lattice is not possible [15]. Therefore interaction between carbon monoxide and oxygen can occur only on the oxide surface, and the diffusional nature of the reduction shows that the stage determining the rate of reaction between the oxides and carbon consists of diffusion processes which ensure the presence of oxygen on the oxide surface.

The influence of the nature of the reducing agent (in particular, variations of the rate of the reaction $CO_2 + C \rightarrow 2CO$) on the rate of the reduction process depends on the fact that the rate of oxygen removal from the oxide surface varies, i.e., the ultimate effect is a change in the oxygen-concentration gradient across the oxide grain.

The difference between the kinetic characteristics of direct reduction of manganese oxides and the isolated reactions of indirect reduction is attributable to the different conditions under which these reactions occur (different pressures, different supply rates of the reducing agent).

## SUMMARY

1. The reduction of manganese oxides by wood charcoal under vacuum in the temperature ranges of 400-550° for $MnO_2$, 600-750° for $Mn_2O_3$, and 700-850° for $Mn_3O_4$ may be represented by the diffusion equation $g^2 = K \cdot \tau$; this shows that diffusion has the determining influence in the direct reduction process.

2. On transition into the region in which solid solutions exist, the character of interaction between the oxides and carbon changes, and the reduction process is represented by the equation

$$\ln \frac{a}{a-g} = K' \cdot \tau.$$

3. The apparent activation energies of the reduction process increase both in the sequence from the highest to the lowest oxide and with increased degree of oxygen removal from the oxide.

## LITERATURE CITED


[1] G. Tammann, and A. Sworykin, Z. allg. anorg. Ch., 170, 62 (1928).

[2] W. Baukloh, and R. Durrer, Archiv fur das Eisenhüttenwesen, 4, 455 (1930/31).

[3] W. Baukloh and G. Zimmermann, Stahl u. Eisen, 5, 172 (1933).

[4] W. Baukloh, and F. Springrum, Z. allg. anorg. Ch., 230, 315 (1937).

[5] A. A. Baikov, Metallurgist 3, 5 (1926).

[6] A. A. Baikov and A. S. Tumarev, Bull. Acad. Sci. USSR, OTN 1, 25 (1937).

[7] I. A. Sokolov, The Blast Furnace Process [in Russian] (GONTI, 1938).

[8] M. A. Pavlov, The Metallurgy of Pig Iron [in Russian] II (GONTI, 1945).

[9] E. Ya. Rode, Oxygen Compounds of Manganese [in Russian] (Izd. AN SSSR, 1952).

[10] W. Baukloh and Zibell, Z. all. anogr. Ch., 233, 424 (1937).

[11] G. I. Chufarov and E. I. Tatievskaya, Physicochemical Principles of Pig Iron Production [in Russian] (Metallurgy Press, Sverdlovsk, 1956) p. 21.

[12] Z. F. Chukhanov et al., The Process of Coal Combustion [in Russian] (GONTI, 1938).

[13] L. Meyer, Z. phys. Ch., 17, 385 (1932).

[14] V. A. Kozlov, Dissertation [in Russian] (S. M. Kirov Polytechnic Institute of the Urals, Sverdlovsk, 1956).

[15] V. I. Arkharov et al., J. Phys. Chem. 29, 272 (1955) [USSR].


Received October 19, 1957.

# SEPARATION OF CARBON AND OXYGEN ISOTOPES BY RECTIFICATION OF CO IN A 12-METER COLUMN

M. V. Tikhomirov and N. N. Tunitskii

At the present time there is a great demand for the stable carbon isotope $C^{13}$ in a number of fields: for investigation of the dissociation mechanism of molecules tagged with $C^{13}$, in studies of reaction mechanisms, for interpretation of optical and radiofrequency spectra, etc. The extensive use of the stable oxygen isotope $O^{18}$ in chemical research is well known. Economical methods for the production of these isotopes are therefore necessary.

Of the existing methods for production of $C^{13}$ the most effective are chemical exchange [1,2] and distillation [3,4]. The most promising and productive method for preparation of $C^{13}$ is probably low-temperature rectification of methane and carbon monoxide. The rectification of CO results, in addition to enrichment of CO with $C^{13}$, in its enrichment with the stable oxygen isotope $O^{18}$, i.e., in principle this method offers a solution to the problem of simultaneous production of two most important isotopes of light elements, $C^{13}$ and $O^{18}$.

The theoretical principles of separation of carbon and oxygen isotopes by low-temperature rectification of CO were considered by Devyatykh [3]. To verify the theoretical principles, we constructed a 12-meter column and studied the enrichment process with it.

Description of the column. The column is shown schematically in Fig. 1. It consists of the following parts: a) packed rectifying column and condenser, b) vacuum jacket, c) a system for feeding and collecting carbon monoxide and regulating the operating conditions of the column (Fig. 2).

The rectifying column consists of the column 6 itself, 12 meters long, a condenser 4, the middle and lower boilers 8 and 11, a feed device for carbon monoxide 7, and a system of tubes 1, 3, 18, 20, connected to the feed and collection systems, which can be used for changing the carbon monoxide in the upper reservoir, collecting the product at the bottom of the column, and regulating the pressure drop over different sections of the rectifying column. The column itself consists of two sections: the upper stripping section (2 meters long, 25 mm in diameter) and the lower enrichment section (total length 10 meters). The enrichment section is in cascade form: its lower part is 5 meters long and 17 mm in inside diameter, and the upper is 5 meters long and 25 mm in diameter. All the column sections are made from stainless steel tubes.

The packing consisted of three-sided spirals [5] 1.5 × 2 mm in size, made from stainless steel wire 0.2 mm in diameter. To avoid sharp pressure drops at regions where the packing was interrupted and at the ends of the column, these spaces were filled with Dixon packing of various sizes, made from stainless steel gauze (40 mesh). The packing was held in place by means of 7 × 7 mm gauzes mounted in rings; the latter were welded in the body of the column.

In the middle part of the enrichment section 8 and at the bottom of the column 11 boilers of 50 w each were installed, fed from a 100 w ferroresonant stabilizer. To improve heat transfer and to ensure uniform evaporation conditions for carbon monoxide, the boiler body 8 at the cascade point is made from a copper block with four openings 8 mm in diameter cut in it. The total area of these openings is approximately equal to the cross section of the lower part of the column, and therefore no additional resistance is created at this point. The Nichrome wire used as the heat source is wound on the copper block body. Mica is used for insulation

The lower heater 11, consisting of a Nichrome spiral, is placed directly in the bottom still of the column. Carbon monoxide is fed into the column through the socket 7, situated 2 meters below the condenser. For this purpose there are 8 openings 1.5 mm in diameter in the lower part of the stripping section of the column, enclosed in the socket. The socket, welded onto the column, provides additional cooling of the carbon monoxide entering the column; the preliminary cooling is effected in the tube 18 which is in contact with the condenser. The upper part of the column terminates in the condenser 4 which ensures a condensation rate of carbon monoxide to correspond with the heating rate (~1.5 kg per hour). It consists of a copper condenser and a steel reservoir for liquid nitrogen, 10 liters in capacity. At the lower part of the condenser there is a reservoir, 800 cc in capacity, for carbon monoxide; this is to provide a certain reserve of $C^{13}$ necessary for operation with periodic feeding and collection of carbon monoxide. Liquid nitrogen is fed into the condenser from 15-liter metallic Dewar vessels through the tube 2 by means of a blower. The copper tube 1 is connected to the feed and collection system, and serves for withdrawal of CO from the column and measurement of the pressure in the condenser. The tube 19 is used for periodic withdrawal of nitrogen, in which liquid oxygen accumulated, from below the condenser. •

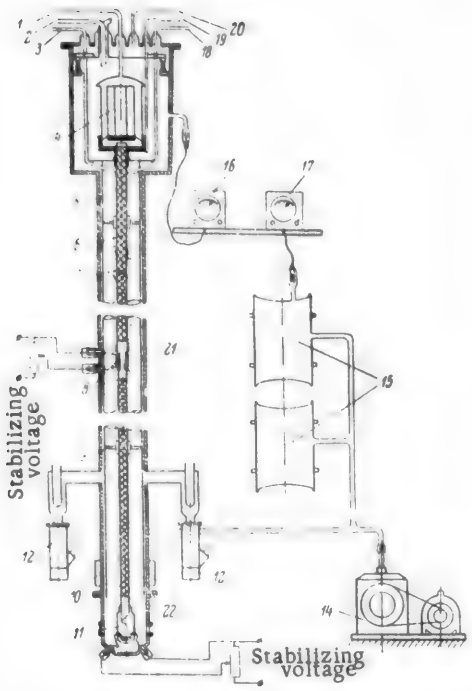


Fig. 1. Diagram of column (explanation in text).

The column is suspended in the body of the vacuum jacket by means of the arrangement shown schematically in the upper part of Fig. 1. Plates with cups are welded to the body of the vacuum jacket at three points at an angle of 120°. In these are inserted Teflon rods 25 mm in diameter and 80 mm high; they are good heat insulators and retain their mechanical properties at low temperatures. The lid of the nitrogen reservoir carries three plates symmetrically welded to it, with similar cups and regulating screws at the ends (the screws are not shown in Fig. 1). By means of these screws the column may be adjusted in a strictly vertical position. Teflon supports 9, holding the column in the center of the vacuum jacket, are fixed for the same purpose at three points in the column (feed point and the middle and lower boiler).

Vacuum jacket. To eliminate the influence of heat conductance of the medium, the column and condenser are enclosed in a vacuum jacket, consisting of the vacuum jacket 21 itself, a system of exhaust and diffusion pumps 14, 12, vacuum vessels 500 liters in capacity 15, and vacuum gages of the ionization and thermocouple type 16, 17. The vacuum jacket is made from 150 x 130 mm steel tube, and consists of four parts joined by flanges. Aluminum gaskets are used for sealing. In the lower section at the still level there are two sight glasses for observation of the level of liquid carbon monoxide in the bottom still. The leads for feeding the heater of the bottom boiler are fitted in the bottom of this section. To the second section of the jacket from the bottom are welded traps of the diffusion pumps, and leads for heating the middle boiler pass through by means of kovar-glass-molybdenum joints. To diminish heat radiation to the column the outer surface of the column was polished and a screen 5 made from polished tin plate was placed between the inner wall of the vacuum jacket and the column.

The jacket is evacuated continuously during operation by means of two N-5 oil diffusion pumps 12, and at intervals by three VN-461 mechanical pumps 14. The residual pressure was $1\text{-}2 \cdot 10^{-6}$ mm in the jacket, and $1.10^{-2}$ mm in the vacuum vessels.

Feed and collection system for carbon monoxide. The feed and collection system for carbon monoxide is shown in Fig. 2. Carbon monoxide prepared by the interaction of sulfuric and formic acids was used for isotope separation. For the preparation 2 liters of concentrated sulfuric acid was put in a 6-liter flask 2, placed in a

•Increase of the oxygen content in the liquid nitrogen results in a gradual increase of total pressure in the column and disturbs the operating conditions.

water bath at 100°. 270 cc of 85% formic acid was put in a graduated funnel 1, 0.5 liter in capacity. It was found in preliminary experiments that this amount of HCOOH yields 200 cc of liquid carbon monoxide. After evacuation of the whole system and of the flask containing $H_2SO_4$ the trap 3 was cooled in liquid oxygen and formic acid was added dropwise into the flask 2. The reaction was continued to 50% dilution of the $H_2SO_4$.

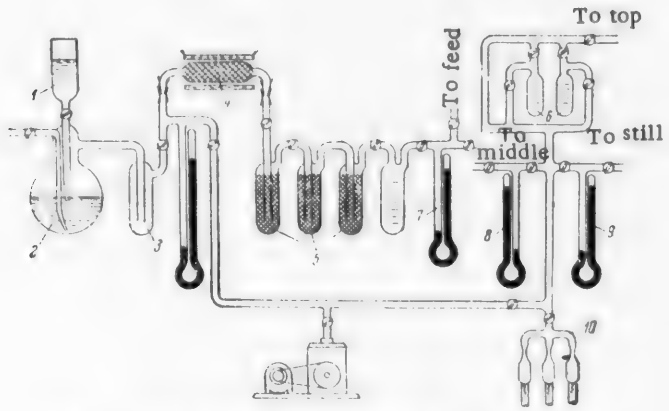


Fig. 2. Feed and collection system for CO:
1) graduated funnel; 2) flask; 3) trap; 4) quartz tube; 5) traps; 6) pair of graduated traps; 7, 8, 9) mercury manometers; 10) sampling tubes.

The carbon monoxide formed contained a small amount of air which had been dissolved in the HCOOH. Oxygen removal was effected in the quartz tube 4, heated to 450-500°. The carbon dioxide formed was retained in the system of packed traps 5, cooled in liquid oxygen. The purified carbon monoxide was fed into the column through the tube marked "to feed" in Fig. 2. A small amount of nitrogen and traces of argon entered the column together with CO; nitrogen was concentrated in the condenser and collected together with CO, while argon accumulated in the bottom still and was collected with the enriched product.

To wet the packing, excess CO was fed into the column before it was brought into operation, and the column was operated under flooding conditions for several hours. Under the usual conditions CO was collected from the condenser at the same time as it was fed into the column. The collection was effected by means of two graduated traps 6, each 300 cc in capacity, cooled in liquid nitrogen. The feeding and collection of CO were regulated in accordance with the amount of HCOOH consumed and the amount of liquid carbon monoxide collected. Small discrepancies (~15-20 cc) between the amounts fed and collected in replacement of CO had no practical effects on the operating conditions. However, it is necessary to ensure that the total amounts of carbon monoxide fed in and collected balance exactly. Constancy of the entrapment of carbon monoxide by the packing was checked from the pressure drop at different regions of the column by means of the mercury manometers 7,8, and 9. The sampling tubes 10 were used to collect samples from different parts of the column for mass spectrometry.

Separation of carbon and oxygen isotopes in a 12-meter column. The purpose of the investigation was to study the accumulation kinetics and to determine the transfer of $C^{13}$ and $O^{18}$ isotopes. In the transfer determinations carbon monoxide was not replaced in the column, as the determinations were based on impoverishment of the upper reservoir in $C^{13}$.

The column holdup in this experiment was 500 cc of liquid carbon monoxide; the upper reservoir contained 800 cc CO. At intervals 400-600 cc of CO 20-40% impoverished in $C^{13}$ was withdrawn from the upper reservoir, and an equal amount with the normal isotope composition was introduced. The total pressure drop at the normal power of the lower boiler (30 w) (the middle boiler was not in action) was about 90 mm. This power corresponded to evaporation of 500 g of carbon monoxide per hour. The liquid nitrogen consumption was 60-70 liters/day.

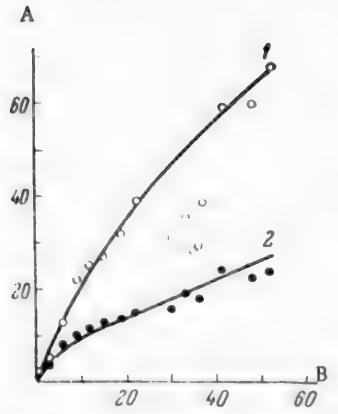


Fig. 3. Kinetics of enrichment of CO with the $C^{13}$ and $O^{18}$ isotopes: A) separation coefficient (F), B) time (days); 1) separation coefficient for carbon ($F_{sep}^{C}$), 2) separation coefficient for oxygen ($F_{sep}^{O}$).

Fig. 3 represents the kinetics of CO enrichment with the isotopes $C^{13}$ and $O^{18}$; here $F_{sep}^{C}$ is the separation coefficient for carbon, i.e., the ratio of the $C^{13}$ concentrations in the lower and upper parts of the column; $F_{sep}^{O}$ is the corresponding ratio for $O^{18}$. It follows from Fig. 3 that in 52 days of operation the separation coefficient for carbon reached 67.8, and for oxygen 23.6. The sharp drop in the separation coefficients at the points corresponding to 30 and 35 days is due to damage to the glass feed system and entry of air into the column. In the second case the column was connected to the atmosphere for two hours. However, even this did not influence significantly the subsequent operation of the column. After several days, despite the collection of 20 cc of liquid CO containing 30% $C^{13}$, the column began to operate normally. The nitrogen which entered the column was concentrated at the top of the column and was collected g together with CO poor in $C^{13}$. Oxygen partly reacted with CO at the hot wire of the lower boiler, forming $CO_2$, and apparently entered into isotope exchange with CO, lowering the separation coefficient for $O^{18}$.

The initial transfer of $C^{13}$ through the column was estimated from the course of impoverishment of the upper reservoir in $C^{13}$ at the start of the experiment in which the column was operated without replacement of CO. Two determinations were performed. In the first case during 5.5 hours of operation the $C^{13}$ concentration in the upper reservoir fell from 0.940 to 0.908%, i.e., by 0.032% (atomic); in the second case it fell by 0.038% in 8.5 hours. Calculations were performed by means of the formula

$$V\frac{dC}{dt} = -Hc, \qquad (1)$$

where V is the volume of the upper reservoir, 800 cc; $\frac{dC}{dt}$ is the change in the concentration of the rare isotope in unit time, and Hc is the transfer of $C_{13}$.

The transfer of $C_{13}$ through the column in these experiments, calculated from Formula (1), was found to be 7.6 $\frac{mg\ C^{13}}{cm^2 \cdot hour}$ and 5.86 $\frac{mg\ C^{13}}{cm^2 \cdot hour}$, respectively.

After these separation coefficients had been reached, the column was operated for 36 days with periodic collection, when the enrichment remained approximately constant. During this period not less than 82 g of CO was obtained, containing from 30 to 37% $C^{13}$ and 3.5 to 4.2% $O^{18}$. If the average $C^{13}$ concentration is taken as 33%, and the $O^{18}$ concentration as 3.8%, the transfer can be estimated from these results also. It was found to be approximately $\frac{6\ mg\ C^{13}}{cm^2 \cdot hour}$ for $C^{13}$, and 0.9 $\frac{mg\ O^{18}}{cm^2 \cdot hour}$ for $O^{18}$.

Johns, Kronberger, and London [4] found that the transfer of $C^{13}$ and $O^{18}$ along the column under steady conditions was 5.87 $\frac{mg\ C^{13}}{cm^2 \cdot hour}$ and 0.67 $\frac{mg\ O^{18}}{cm^2 \cdot hour}$, respectively. It follows that the productivity of our column is at least not inferior to that cited [4].

No conclusions can be drawn from Fig. 3 concerning the limiting enrichment of the column, as the values of $F_{sep}^{C}$ and $F_{sep}^{O}$ for 40 and 52 days of column operation were obtained with collection of the product from below. The fact that the initial transfer coincides with the transfer at collection is a qualitative indication that the column was still far from the steady state.

For determination of the height equivalent to one theoretical plate (HETP) in distillation of CO with the column packing used, we first carried out experiments with a similar column 3.7 meters long (17 mm in diameter). The column holdup was 150 cc CO; the upper reservoir contained 250 cc CO, and the boiler power was 23 w. The column was operated without replacement of CO. The time required to reach steady operation was 50 hours.

The equilibrium separation coefficient for $C^{13}$ obtained with this column was $F^{C}_{sep} = 3.67$. If $F^{C}_{sep}$ and the vapor pressure ratio $\alpha = 1.01$ [3,4] are known, the Fenske equation

$$F^{C}_{sep} = \alpha^{n} \qquad (2)$$

can be used to find $\underline{n}$, the number of theoretical plates, and HETP. In this experiment HETP was 2.82 cm. In other experiments similar values of HETP were obtained, in accordance with the column throughput.

Comparison of different data for the values of $\alpha$ for methane [6, 7] suggests that $\alpha$ depends on the isotope composition of methane ($\alpha$ decreases with increasing $C^{13}$ content). This decrease may be unfavorable for production of highly concentrated isotopes. In order to investigate the influence of concentration on the separation coefficient, experiments were performed on the separation of carbon and oxygen isotopes in CO previously enriched with the rare isotopes. The experiments were performed with a column 3.7 meters long. Carbon monoxide containing 5.9% $C^{13}$ was used. The separation coefficient for $C^{13}$ in this column was found to be 3.3 (column holdup 190 cc CO), which is in satisfactory agreement with the results of experiments with materials of natural isotope composition. This shows that a decrease of $\alpha$ at high concentrations of the rare isotopes is unlikely. This is in agreement with earlier data [4] and, as will be shown below, with our results for a 12-meter column.

Experiments with short columns suggest that the equilibrium separation coefficient for $C^{13}$ calculated from Equation (2) should be approximately 69.0. The maximum value found under conditions far from equilibrium was 67.8. A similar result was obtained for separation coefficients for $O^{18}$.

Thus, comparison of the separation coefficients found experimentally and calculated from Equation (2) with the minimum value of HETP (2.82 cm) found for the 3.7-meter column shows that the HETP for the 12-meter column is somewhat less. An approximate estimate of HETP by means of the Babkov and Zhavoronkov equation [8] gives 2.2 cm.

It was already noted earlier that the 12 meter column gave CO enriched 34.5-fold with $C^{13}$ and 21-fold with $O^{18}$ as compared with the natural compound. Therefore the column described can be used not only for production of carbon highly enriched with $C^{13}$, but also of $O^{18}$, if the starting materials contain 1% or more $O^{18}$. However, it is then necessary to provide a longer stripping section, so that the $O^{18}$ content of the collected CO should be equal to or less than the natural value (0.2%).

## SUMMARY

1. High separation coefficients for $C^{13}$ (67.8) and $O^{18}$ (23.6) were obtained, although maximum enrichment had not yet been reached.

2. During the work not less than 82 g of CO was obtained, containing from 30 to 37% $C^{13}$ and 3.5 to 4.2% $O^{18}$, and a considerable amount of CO containing from 10 to 20% $C^{13}$.

In conclusion, we offer our sincere thanks to N. I. Nikolaev, L. P. Lipikhin, A. K. Tsapuk and Yu. A. Shavarin for help in this investigation.

## LITERATURE CITED

[1] A Hutchison, D. W. Stewart and H. G. Urey, J. Chem. Phys., 8, 532 (1940).

[2] A. F. Reid and H. G. Urey, J. Chem. Phys. 11, 403 (1943).

[3] G. G. Devyatykh, Doctorate Dissertation [in Russian] (Moscow, 1954).

[4] T. F. John, H. Kronenberger and H. London, in Mass Spectrometry (Dist. Petroleum, London, 1954) p. 191.

[5] A. I. Levin, Petroleum Economy 10,40 (1949).

[6] W. Groth, H. Ihle and A. Murrenholf, Z. Naturforschung. 9A, 805 (1954).

[7] K. Glusius and H. H. Buller, Z. Naturforschung, 9A, 775 (1954).

[8] S. I Babkov and N. M. Zhavoronkov, Proc. Acad. Sci. USSR No. 5, 877 (1956).

Received November 10, 1957.

# STIRRING RATES OF SOLUTIONS AND PURITY OF THE CRYSTALS FORMED

L. N. Matusevich

The S. M. Kirov Polytechnic Institute of the Urals

In modern chemical industry stationary crystallizers with crystallization at rest have been displaced almost completely by mechanical crystallizers with agitation of the liquors. However, despite many years of operating experience with mechanical crystallizers, many problems relating to their operating conditions remain unsolved. Among these is the question of the influence of motion of the liquid on the chemical purity of the product under mass-crystallization conditions.

Industrial experience has shown that crystallization in mechanical crystallizers with agitation of the liquors does not yield products of lower purity than those obtained by crystallization at rest in stationary crystallizers. We consider, however, that the introduction of a new factor – agitation under crystallization conditions – should have some influence on the internal purity of the crystals formed.

Contamination of crystals with an impurity, if it is not isomorphous with the main component, occurs mainly as the result of mechanical trapping of the mother liquor in crystal cracks and pores, at junctions between individual crystals, etc. The amount of mother liquor entering the crystals in this way in its turn depends on the internal perfection of the growing crystals. The latter must evidently depend to a large extent on the hydraulic conditions of crystallization: whether it takes place at rest or in a moving medium, with agitation of the liquor. It is to be expected that the chemical purity of the crystals should be higher in crystallization with agitation of the liquor than in crystallization at rest. This view is confirmed by the following considerations.

Agitation of the liquor prevents deposition of crystals on the bottom and walls of the equipment and thereby prevents combined growth in druses, when there is always the probability of entrapment of the mother liquor by faces of adjacent crystals and in concretion regions. Moreover, the internal homogeneity of individual crystals is also increased by agitation. Observations of the growth of seed crystals have shown that concentration currents which arise near a growing crystal in a stationary solution cause both distortion of the perfect crystal form and internal heterogeneity by inclusion of mother liquor [1,2]. Ansheles and his associates [3] showed in a careful investigation that rotation in the liquor of individual seed crystals attached to a stirrer eliminates concentration currents near them, ensures uniform flow of the crystallizing substance to their faces, and leads to the formation not only of well-formed regular crystals but also of purer and internally homogeneous crystals without inclusions of mother liquor.

The results of these investigations suggest that in conditions of mass crystallization, which is characteristic for all industrial crystallizers, agitation of the liquor should also favor growth of crystals with greater internal homogeneity.

Internal purity of the crystals depends not only on whether crystallization takes place with agitation or at rest, but evidently also on the stirring rate. It was found in our previous investigations [4,5] that the aggregation of the product systematically diminishes with increase of the rate at which crystallizing solutions are stirred, and stirring at high rates leads to the formation of crystals of regular monolithic form only. We have already offered theoretical explanation [4] of these experimental facts. It is natural to assume that elimination of aggregated crystal growth, in which trapping of the mother liquor at the regions of coalescence between individual crystals is always possible, should give crystals of higher chemical purity.

The purpose of the present investigation was to study the effect of the stirring rate in crystallizing solutions on the chemical purity of the crystals formed, in presence of an ordinary (nonisomorphous) impurity in the solutions. The example chosen for the investigation was isohydric crystallization of potassium nitrate and potassium ferrocyanide in presence of potassium chloride as the impurity.

## EXPERIMENTAL

The same aqueous solutions of potassium nitrate and potassium ferrocyanide we used in our earlier work [4,5] were used in these experiments. These salts differ sharply in their physicochemical and crystallographic properties: $KNO_3$ crystallizes in the form of elongated prismatic needles in the rhombic system, and $K_4[Fe(CN)_6] \cdot 3H_2O$ crystallizes as square plates in the monoclinic parallelepiped system; one of the salts crystallizes as the hydrate. The added impurity in solutions of both salts was potassium chloride, which is a usual (nonisomorphous ) impurity in both salts, as it crystallizes in the cubic system. Salts of analytical reagent grade were used for preparation of the solutions.

The potassium nitrate solutions contained 448 g $KNO_3$ per liter (which corresponds to a saturation temperature of 30°), with additions of 6.30 and 60 g of KCl per liter. The ferrocyanide solutions contained 404 g $K_4[Fe(CN)_6] \cdot 3H_2O$ per liter (saturation temperature 41°), and additions of 21 and 42 g of KCl per liter.

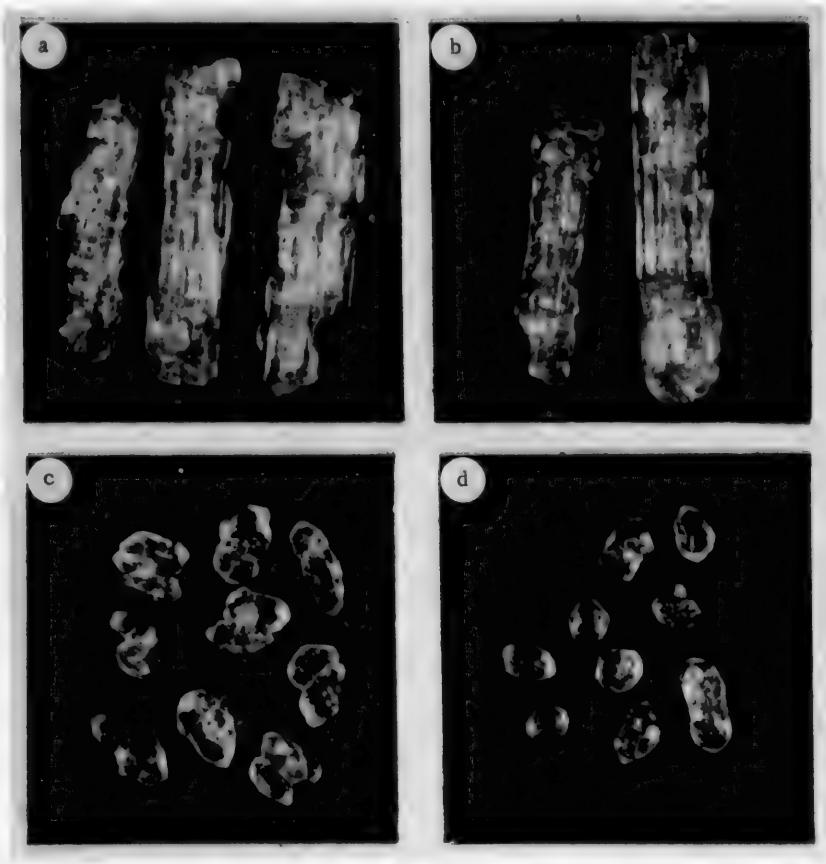


Fig. 1. Appearance of $KNO_3$ crystals formed at different stirrer speeds: stirrer speed (in rpm ): a) 0.6, b) 6, c) 60, d) 180.

Crystallization of the agitated solutions was effected in a laboratory crystallizer, which consisted of a horizontal cylinder of 90 mm internal diameter and 130 mm long, about 0.9 liter in capacity. Before the

experiments the crystallizer was hermetically closed by means of a lid screwed onto its end. The stirrer passed into the crystallizer through a gland fixed on the opposite end wall of the apparatus. It was in the form of a crankshaft with a horizontally extended blade which moved peripherally within the cylinder in direct proximity to the wall. The crystallizer and stirrer were made of stainless steel.

The peripheral velocity of the stirrer rotating on the horizontal shaft could be varied over a wide range. The following rotation speeds were chosen for the systematic experiments: 0.6, 6, 60, 110, and 180 rpm.

The experiments were performed in the following sequence. The test solution, containing a definite amount of potassium chloride impurity, was poured into the crystallizer at a temperature 20° above the saturation temperature. Not less than 40-45 minutes elapsed between the time when the solution was put in and the stirrer started and the time when the solution reached the saturation temperature; this eliminated possible local crystallization on the cold parts of the equipment when the solution was put in. The crystallizing solutions were cooled by loss of heat to the surrounding medium – air. With this type of cooling, changes in the stirring rate did not influence the cooling rate, because the over-all heat transfer coefficient was determined by external heat transfer to the air in this case. The solution was cooled to the final temperature of 22° with continuous stirring at a definite rate, fixed for each given experiment; the stirrer was then stopped and the experiment was terminated. The total cooling time was 4.5-5 hours, which is near to the average time in industrial conditions.

The crystals were transferred to a Buchner funnel and the mother liquor was filtered off. A portion of the crystals was removed from the funnel, dried to constant weight, and used for sieve analysis in order to determine the granulometric composition of the product and its degree of aggregation; the rest of the crystals were washed once on the Büchner funnel with distilled water, 1 cc of water being taken per 2 g of crystals. The washed crystals were also dried to constant weight, and the $Cl'$ ion impurity in them was determined.

The granulometric composition of the product was determined by means of sieve analysis with the 026 instrument; the following procedure was used for determining the degree of aggregation. Several parallel samples were taken from each fraction obtained by sieve analysis, and the crystals in them were examined under the microscope at 25-50 magnification. The numbers of aggregated and nonaggregated crystals were counted. The ratio of these numbers in the same sample was taken to be the weight ratio of the two types of crystals in it. The average of such determinations for samples of a given fraction, and then for all the fractions, gave the final value – the degree of aggregation of the crystals formed in the given experiment.

The $Cl'$ content in $KNO_3$ crystals was determined by Mohr's method – by titration of potassium nitrate solutions with silver nitrate solution in presence of potassium chromate.

Chemical analysis of $K_4[Fe(CN)_6] \cdot 3H_2O$ crystals for $Cl'$ was also performed by titration (by Mohr's method) of solutions of potassium ferrocyanide in presence of potassium chromate with silver nitrate solution, after removal of $[Fe(CN)_6]''''$ ions by precipitation by zinc sulfate.

In each experiment performed in the stirred laboratory crystallizer a 100 cc sample was taken from the hot test solution and put in a glass crystallizer to crystallize by natural cooling, but without stirring, i.e., at rest. After these samples had cooled to room temperature the crystals were filtered off on a Büchner funnel, washed with distilled water in the same proportions as before (1 cc of water per 2 g of crystals) and dried to constant weight; the $Cl'$ content was then determined.

It was found in these experiments that whereas large crystals (up to 8-12 mm) grown firmly into a continuous druse are formed during crystallization at rest, the crystals formed during crystallization with stirring are much smaller (down to 1-0.5 mm).

It was found, in full agreement with our earlier results [4], that the crystalline precipitate becomes more monodisperse and the average crystal size decreases somewhat with increase of stirring rate. For example, whereas at n = 0.6 rpm the average grain size is 0.5-0.7 mm, at n = 180 rpm it is 0.2-0.3 mm. At the same time the aggregation of the crystalline product decreases with increase of the stirrer speed from 80-90% at n = 0.6 rpm to 0% at n = 180 rpm.

The results of sieve analyses of crystalline precipitates formed at different stirrer speeds are not given here, as they are similar to our earlier data [4].

Tables 1 and 2 merely give data on the degree of aggregation of the precipitate and the purity of the crystals formed as functions of the stirrer speed.

TABLE 1

Purity of $KNO_3$ Crystals as a Function of Stirrer Speed

| Stirrer revolutions per minute | Degree of crystal aggregation (%) | Cl' contents of crystals (wt. %) at KCl concentration in solution (g/liter) | | |
|---|---|---|---|---|
| | | 6 | 30 | 60 |
| 0 • | 100 | 0.03 | 0.10 | 0.19 |
| 0.6 | 91 | 0.03 | 0.06 | 0.06 |
| 6 | 80 | 0.02 | 0.04 | 0.06 |
| 60 | 20 | 0.02 | 0.03 | 0.05 |
| 110 | 5 | 0.01 | 0.02 | 0.04 |
| 180 | 0 | 0.01 | 0.02 | 0.03 |

•Crystallization in glass crystallizer without stirring.

TABLE 2

Purity of $K_4[Fe(CN)_6] \cdot 3H_2O$ Crystals as a Function of Stirrer Speed

| Stirrer revolutions per minute | Degree of crystal aggregation (%) | Cl' contents of crystals (wt. %) at KCl concentration in solution (g/liter) | |
|---|---|---|---|
| | | 21 | 42 |
| 0 • | 100 | 0.27 | 0.31 |
| 0.6 | 85 | 0.23 | 0.27 |
| 6 | 63 | 0.17 | 0.24 |
| 60 | 6 | 0.13 | 0.23 |
| 100 | 2 | 0.09 | 0.19 |
| 180 | 1 | 0.06 | 0.16 |

•Crystallization in glass crystallizer without stirring.

The experimental results in Tables 1 and 2 show that transition from crystallization at rest (n = 0 rpm) to crystallization with stirring of the solution decreases the amount of Cl' impurity in the crystals both of potassium nitrate and of potassium ferrocyanide. Increase of the stirring rate also results in a systematic lowering of the impurity content of the crystalline product. For example, in $KNO_3$ crystals formed from solutions containing 30 g KCl per liter the Cl' content decreases from 0.10% (in crystallization at rest) to 0.06% (at n = 0.6 rpm) and 0.02% (at n = 180 rpm), i.e., it decreases by 65 and 80%, respectively, as compared with crystallization at rest. Similar results are obtained in the crystallization of $K_4[Fe(CN)_6]$. Thus, when the solution contained 21 g of KCl per liter the Cl' content of the product was 0.27, 0.23, and 0.06%, respectively, in crystallization at rest, at n = 0.6 rpm, and at n = 180 rpm. Thus, in this case the impurity content of the crystals decreases by 15% (at n = 0.6 rpm) and by 78% (at n = 180 rpm).

If the impurity content of the solution is low ($KNO_3$ solutions containing 6 g KCl per liter), the same relationship holds, but is less pronounced. This may be due to some inaccuracy in determinations of small amounts of Cl'.

These results are fully consistent with the considerations advanced earlier.

The increase in the purity of the crystals with increase of stirring rate is explained as follows. As already stated, in crystallization with stirring the product consists both of regularly formed single crystals and of firm concretions of crystals. Examination of these distorted crystals under the microscope showed that they are not of the branched dendritic form which is the consequence of preferential growth of crystal tips and edges, and which is characteristic of distorted growth in single crystals [6]. On the contrary, these crystals are characterized

by distortion of their faces and the presence of large and small "lateral" outgrowths, not at the edges or vertices but predominantly in the middle regions of the faces. These outgrowths are mutually oriented merely in the general direction of the crystal growth: prismatic $KNO_3$ needles are parallel in their principal longitudinal direction, and $K_4[Fe(CN)_6] \cdot 3H_2O$ plates lie in parallel planes (Figs. 1 and 2).

As was already noted previously [4], it may be concluded from the above description of the aggregated crystals that they are formed as the result of intergrowth of crystals or overgrowth of smaller on larger crystals. It is clear that in the formation and subsequent growth of such aggregated crystals mother liquor can always be trapped (with all the impurities present in it) between individual adjacent overgrowths during their subsequent growth.

Fig. 2. Appearance of $K_4[Fe(CN)_6] \cdot 3H_2O$ crystals formed at different stirrer speeds: stirrer speed (in rpm ): a) 0.6, b) 6, c) 60, d) 180.

It follows from this and earlier [4, 5] investigations that the degree of aggregation of the product decreases systematically with increase of stirring rate. Moreover, the aggregates which still remain become of simpler form: the crystals composing them become increasingly distinct but less numerous (Figs. 1 and 2). Evidently entrapment of the mother liquor by the growing crystals also decreases, and the chemical purity of the crystals therefore increases.

Therefore, as the rate of stirring of crystallizing solutions increases the crystals become progressively purer owing to a decrease in the amount of mother liquor included in them; in evaluation of the results of the present investigation it must also be taken into account that as the stirrer speed increases the average crystal size diminishes; i.e., the specific surface of the crystals increases and therefore the total area in contact with the mother liquor becomes greater. This increase of surface was not taken into account when the crystals were washed, as the amount of wash water was always calculated per unit weight; it is therefore evident that the internal purity of the crystals increases with stirrer speed to a somewhat greater extent than is indicated by the data in Tables 1 and 2.

## SUMMARY

1. The effect of motion of the solution on the chemical purity of crystals formed in presence of a usual (nonisomorphous) impurity has been studied, and it was found that the chemical purity is considerably higher in crystallization with stirring than in crystallization at rest.

2. Increase of the rate stirring of a crystallizing solution leads to a systematic decrease of the amounts of impurities present in the forming crystals; a theoretical explanation is offered for the experimental facts.

3. The results of this investigation lead to the conclusion, important from the technical standpoint, that in some cases, when a pure product is required, repeated recrystallization may be replaced by a single crystallization under appropriate hydrodynamic conditions.



The author thanks Professor K. N. Shabalin for valuable advice in the course of the present investigation.


## LITERATURE CITED


[1] G. V. Wulff, Nature 9, 1091 (1915).

[2] P. S. Vadilo, J. Exp. Theoret. Phys. 8, No. 10-11, 1218 (1938) [USSR].

[3] O. M. Ansheles, V. B. Tatarskii, and A. A. Shternberg, Rapid Growing of Homogeneous Crystals from Solutions [in Russian] (Leningrad State Press, 1945).

[4] L. N. Matusevich and K. N. Shabalin, J. Appl. Chem. 25, No. 11, 1157 (1952)[USSR].

[5] L. N. Matusevich, J. Appl. Chem. 27, No. 2, 148 (1954) [USSR].*

[4] D. D. Saratovkin, Dendritic Growth of Crystals [in Russian] (Metallurgy Press, Moscow, 1950).



Received July 12, 1957.


*Original Russian pagination. See C. B. translation.

# CALCULATION OF BATCH DISTILLATION UNITS WITH SUPPLEMENTARY FEEDING

Tszyui-Fu Fu

Supplementary feeding is often used in industrial batch distillation. For example, in rectification of crude benzene in order to obtain pure products the collection of benzene is continued until its content in the still is almost exhausted. Since crude benzene contains over 50 % of pure benzene, collection of benzene is stopped when half the still charge has gone. If fresh crude mixture is pumped continuously into the still as the benzene boils out, the amount of benzene is continuously restored and the amount of high-boiling components. Supplementary feeding is then stopped and the process is continued as in an ordinary batch unit. According to Kolyandr [1], the amount of crude benzene treated in this way in a single operation is about 135 tons,if crude benzene of 70% purity is fed into a still 50 tons in effective capacity, and the degree of extraction of benzene is 90%.

It is clear from the foregoing that by this procedure the productivity of the equipment is increased, while the time required for charging, discharging, and preparatory operations is reduced. The present paper contains a method for calculation of a number of operational characteristics of batch distillation units.

There are two variants of batch distillation units with supplementary feeding: 1) simple distillation, 2) rectification.

Both methods are considered below.

## Simple Distillation with Supplementary Feeding.

Relationship between the amount of distillate, its concentration, and concentration of the mixture in the still. It is shown in Fig. 1 that in order to obtain P kg-moles of distillate per unit time it is necessary to feed P kg-moles of fresh mixture into the still in order to maintain a constant amount W kg-moles of mixture in the still.

The following notation is used: dp is the instantaneous, infinitesimal quantity of distillate (in kg-moles) $\underline{x}$ is the instantaneous value of the concentration of the mixture in the still (molar %); $x_p$ is the concentration of the instantaneous quantity of distillate (dp) (molar %); $(x_p)_{av}$ is the average concentration of the distillate (molar %); y is equilibrium vapor concentration above the mixture in the still of concentration $\underline{x}$ (in this instance $y = x_p$ ); $k_f$ is the concentration of the original mixture (molar %); $x_w$ is the concentration of the residue in the still (molar %); $\underline{dx}$ is the differential change of the mixture concentration in the still on removal of the instantaneous quantity dp of the distillate.

From the material balance for the volatile component of a binary mixture we have

$$Wx + x_f dp = (x - dx)W + y dp$$

or

$$W dx = y dp - x_f dp,$$

then

$$\frac{dx}{y - x_f} = \frac{dp}{W}.$$

Since W remains constant, we have

$$\int_0^P \frac{dp}{W} = \frac{P}{W} = \int_{x_f}^{x_w} \frac{dx}{y - x_f} . \tag{1}$$

Equation (1) is similar to the Rayleigh equation with $x$ replaced by $x_f$ and $\ln \frac{F}{W}$, replaced by $\frac{P}{W}$, where $F$ is the amount of original mixture in the still (in kg-moles) and W is the amount of residue in the still (in kg-moles.

If the phase-equilibrium function $y = f(x)$ is known, this equation may be integrated by the graphical method to find the value of P corresponding to the concentration $x_w$.

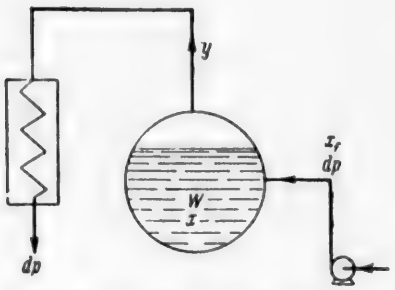


Fig. 1. Scheme of simple distillation with supplementary feeding.

The material balance equation

$$(W + P)\, x_f = W x_w + P\, (x_p)_a$$

is then used to find the average concentration of the distillate

$$(x_p)_{av} = \frac{(W + P)\, x_f - W x_w}{P} . \tag{2}$$

However, in the next two cases algebraic integration is also possible.

1. The case when in a definite concentration range the equilibrium line can be represented by the expression $y = Kx + C$ (where K and C are constants). Then Equation (1) can be integrated:

$$\frac{1}{K} \ln \frac{K x_w - x_f + C}{K x_f - x_f + C} = \frac{P}{W} . \tag{3}$$

Although this formula is derived for a binary mixture, it may be noted in analysis of the derivation that the value of $x$ in the material balance equation used for derivation of Equation (1) can also be the concentration of any component of a multicomponent mixture.

If the so-called phase-equilibrium constants K are used, then the functional relationship of the phase equilibrium for component $i$ can be represented by the formula $y_i = K_i x_i$. The following formula can be used for the calculation:

$$\frac{1}{K_i} \ln \frac{K_i x_{iw} - x_{if}}{K_i x_{if} - x_{if}} = \frac{P}{W} . \tag{4}$$

Since the phase-equilibrium constants depend on the temperature of the mixture, an average temperature convenient for calculation should be chosen on variation of the composition of the mixture in the still. The validity of the chosen temperature is determined by the expression $\Sigma x_{iw} = 1$ for a definite value of P.

2. For an ideal binary mixture the phase equilibrium is represented by the expression

$$y = \frac{\alpha x}{1 + (\alpha - 1)\, x} ,$$

where $\alpha$ is the relative volatility of the binary mixture. Equation (1) is then integrated as follows:

$$\frac{P}{W} = \frac{1}{\alpha - x_f (\alpha - 1)} \left\{ (\alpha - 1)(x_w - x_f) + \frac{(\alpha - 1) x_f}{\alpha - (\alpha - 1) x_f} \ln \frac{x_w [\alpha - x_f (\alpha - 1)] - x_f}{x_f [\alpha - x_f (\alpha - 1)] - x_f} + \right.$$
$$\left. + \ln \frac{x_w [\alpha - x_f (\alpha - 1)] - x_f}{x_f [\alpha - x_f (\alpha - 1)] - x_f} \right\} = \frac{1}{\alpha - x_f (\alpha - 1)} \left\{ (\alpha - 1)(x_w - x_f) + \right.$$
$$\left. + \left[ 1 + \frac{(\alpha - 1) x_f}{\alpha - (\alpha - 1) x_f} \right] \ln \frac{x_w [\alpha - x_f (\alpha - 1)] - x_f}{x_f [\alpha - x_f (\alpha - 1)] - x_f} \right\} . \tag{5}$$

Distillation time. Let V be the number of kg-moles of vapor evaporating in unit time (one hour). Then the distillation time (t) is

$$t = \frac{P}{V}. \tag{6}$$

## Rectification with Supplementary Feeding

Rectification with supplementary feeding is illustrated schematically in Fig. 2.

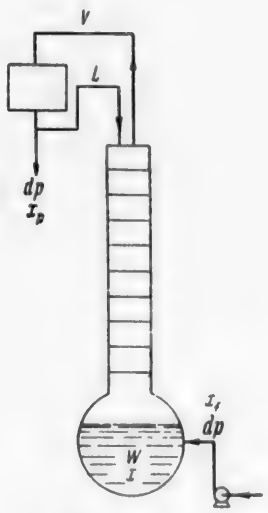


Fig. 2. Rectification scheme with supplementary feeding.

The difference between the schemes shown in Figs. 1 and 2 lies in the fact that the second scheme incorporates a rectification column of n theoretical plates, and therefore the distillate concentration $x_p$ is not equal to the vapor concentration y over the mixture in the still. As was noted in the preceding paper [2], $x_p$ is a function of many variables (n, R, $x_f$).

The following assumptions are made for the subsequent discussion: 1) the influence of column holdup may be disregarded, 2) the amount of vapor ascending the column is constant across any section of the column, 3) the number of theoretical plates is known.

### Relationship Between the Amount of Distillate and the Average Concentration of the Mixture in the Still.

1st variant. The rectification is performed at constant distillate concentration $x_p$.

From the material balance we have

$$Px_p = (W + P)x_f - Wx_w,$$
$$P = \frac{W(x_f - x_w)}{x_p - x_f}. \tag{7}$$

2nd variant. The rectification is performed at constant reflux ratio R.

In this case the main calculation formula is analogous to Equation (1), but with $x_p$ in place of y.

$$\frac{P}{W} = \int_{x_f}^{x_w} \frac{dx}{x_p - x_f}. \tag{8}$$

In the general case this equation may be integrated graphically, but algebraic integration is also possible if the equilibrium line can be represented by the formula y = Kx + C over a definite concentration range [2]. Thormann's formula [3] can then be written

$$x_p = Sx + D, \tag{9}$$

where

$$S = \frac{K - \frac{R}{R+1}}{\left[\frac{R}{K(R+1)}\right]^{n-1}\left(K - \frac{K+R}{R+1}\right) + \frac{1}{R+1}},$$

$$D = \frac{C\left\{1 - \frac{R}{R+1}\left[\frac{R}{K(R+1)}\right]^{n-1}\right\}}{\left[\frac{R}{K(R+1)}\right]^{n-1}\left(K - \frac{K+R}{R+1}\right) + \frac{1}{R+1}}.$$

Then after integration of Equation (8) we have

$$\frac{P}{W}=\frac{1}{S}\ln\frac{Sx_w+D-x_f}{Sx_f+D-x_f}. \tag{10}$$

If phase equilibrium for a multicomponent mixture can be represented by the equation $y_i = K_i x_i$ then, analogously to Equation (5), the following formula can be used for calculation:

$$\frac{P}{W}=\frac{1}{S}\ln\frac{Sx_{iw}-x_{if}}{Sx_{if}-x_{if}}. \tag{11}$$

For the reason stated earlier an average temperature suitable for this calculation should again be chosen. The validity of the chosen temperature is determined by the expression $\sum x_{iw} = 1$ for a definite value of P.

## Average Reflux Ratio $R_{av}$

No calculation is necessary for rectification at constant reflux ratio. If the rectification is performed at constant distillate concentration the basic calculation formula for the average reflux ratio is of the form [2]

$$R_{av}=\frac{\int_{R_f}^{R_w} Rdp}{P}, \tag{12}$$

where $R_f$ and $R_w$ are the initial and final reflux ratios corresponding to mixture concentrations $x_f$ and $x_w$.

From the material balance equation for an infinitesimal time period

$$xW+x_f dp=(x-dx)W+x_p dp$$

we have

$$dp=\frac{Wdx}{x_p-x_f}. \tag{13}$$

When the rectification process has gone so far that the concentration of the mixture in the still is $x_w$, the material balance equation

$$Px_p=(W+P)x_f-Wx_w$$

gives

$$P=\frac{W(x_f-x_w)}{x_p-x_f}. \tag{14}$$

Substitution of Equations (13) and (14) into (12) gives

$$R_{av}=\int_{x_f}^{x_w}\frac{Rdx}{x_f-x_w}. \tag{15}$$

In the general case this equation may be integrated graphically. Algebraic integration is possible with the following two assumptions: 1) the equilibrium line may be represented by the expression $y = Kx$, and $K > 1$, 2) the number of plates in the column is large enough. Then Equation (9) can be written in the form $x_p = Sx$.

Since $\left[\frac{R}{K(R+1)}\right]^{n-1}$ is very small, we may write approximately

$$S=K(R+1)-R.$$

Hence

$$x_p=(KR+K-R)x$$

or

$$R=\frac{x_p-Kx}{(K-1)x}. \tag{16}$$

Then after integration of Equation (15) we have

$$R_{av}=\frac{1}{(K-1)(x_f-x_w)}\left[x_p \ln\frac{x_w}{x_f}-K(x_w-x_f)\right]. \tag{17}$$

Distillation time t. For rectification at constant reflux ratio the distillation time may be calculated from the following equation:

$$t=\frac{P(R+1)}{V}. \tag{18}$$

If the process is carried out at constant distillate concentration and at maximum productivity of the column the amount of vapor (V) in kg-moles ascending the column in unit time remains unchanged. However, because of the gradual increase of the reflux ratio the amount of distillate collected per unit time (in kg-moles)gradually decreases.

Differentiation of Equation (14) with respect to time t gives

$$\frac{dp}{dt}=\frac{W}{x_p-x_f}\cdot\frac{dx}{dt}. \tag{19}$$

But

$$\frac{dp}{dt}=V-L=\left(1-\frac{L}{V}\right)V=\left(1-\frac{R}{R+1}\right)V=\frac{V}{R+1}, \tag{20}$$

where V is the amount of vapor rising in the column (in kg-moles/hour), and L is the amount of reflux flowing down the column (in kg-moles/hour).

Substitution of Equation (20) into (19) gives

$$\frac{V}{R+1}=-\frac{W}{x_p-x_f}\cdot\frac{dx}{dt}.$$

Since V is constant, we have

$$t=\int_0^t dt=-\frac{W}{V(x_p-x_f)}\int_{x_f}^{x_w}(R+1)\,dx. \tag{21}$$

In the general case Equation (21) can be integrated graphically. If the equilibrium line can be represented by the expression $y = Kx$ with $K > 1$, and the number of plates in the column is large enough, algebraic integration is possible. Then we have

$$t=\frac{-W}{V(x_p-x_f)(K-1)}\left[x_p \ln\frac{x_w}{x_f}-(x_w-x_f)\right]. \tag{22}$$

## SUMMARY

Basic equations are given for calculation of a number of operating characteristics of batch distillation units with supplementary feeding. These equations are not only of theoretical interest but have a practical value. In the general case all the equations may be integrated graphically and then used for calculations. In certain instances calculation may be simplied by algebraic integration (in particular, for calculations relating to multicomponent mixtures).

## LITERATURE CITED

[1] L. Ya. Kolyandr. Collection and Conversion of Chemical Products from Coking [in Russian] (metallurgy Press, 1953).

[2] Tszyui-Fu Fu, J. Appl. Chem. 30, No. 6, 862 (1957).

[3] K. Thormann, Destillieren und Rektifizieren, Leipzig (1929).

Received April 5, 1958.

# METHOD FOR CONSTRUCTION OF PHASE DIAGRAMS FOR MULTICOMPONENT SYSTEMS

L. N. Lambin and N. N. Ermolenko

Studies of phase diagrams for simple and multicomponent systems formed from various substances: oxides, chemical compounds, and individual chemical elements, are very important in many branches of chemical technology, and in particular in glass technology.

Without studies of phase diagrams for the oxide systems which constitute glass it is not possible to interpret the great variety of complex physicochemical processes which take place during the making and slow cooling of glass.

Graphical representation of the results obtained in studies of such systems makes it possible to determine new glass compositions and to predict the conditions and combinations of oxides which would give rise to particular physicochemical properties.

Methods for construction of diagrams for two- and three-component systems are well known, and are not considered here for that reason. A quaternary system may be represented in the form of a tetrahedron [1] with the pure components A, B, C, and D at the vertices (Fig. 1). The six edges (AB, AC, AD, BD, BC, and CD) of the tetrahedron represent six binary systems, and the four faces (ABD, ABC, BCD, ACD) represent four ternary systems. Any point within the tetrahedron corresponds to a definite quaternary composition, and every composition is represented by one point only. The content of each component of the quaternary system is determined by the distance from this point to the face opposite to the vertex corresponding to the particular component.

It is easy to see that if the tetrahedron is cut by planes parallel to one of the faces, all the points in any section correspond to compositions with equal contents of the component occurring at the vertex opposite to that face. A quaternary system may be investigated by studies of such individual sections, so that any region of the diagram can be investigated in any desired direction.

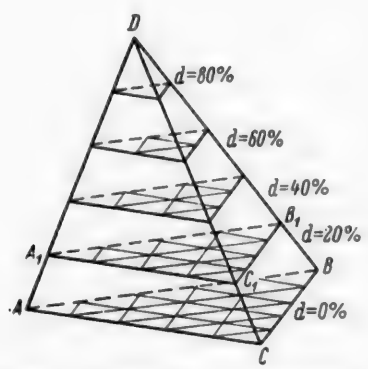


Fig. 1. Diagram of a quaternary system.

Let a series of sections corresponding to constant compositions of component D (Fig. 1) be drawn in a tetrahedron representing a system in question. In this instance the section is drawn through 20% composition. The tetrahedron is now projected so that each section is in the form of an equilateral triangle and does not overlap with its neighbors. The possibility of such projection follows from the fundamental theorem of axonometry. This gives a diagram of a quaternary system (Fig. 2) in which the content of component D is determined by the section containing the point corresponding to it, while the contents of components A, B, and C are determined by the position of this point within the section.

Different authors use different methods for graphical representation of five- and six-component systems.

In the method proposed by Schoute and applied by Böke for representation of five-component systems, each composition of five components A, B, C, D, and E is represented by four points or a tetrad

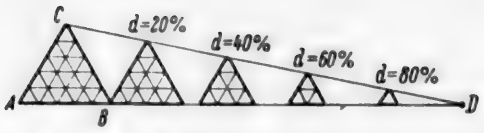


Fig. 2. Sections through a diagram of a quaternary system.

[2]. Along the four axes x, y, z, and t (Fig. 3), the respective contents of A, B, C, and D are marked off, and the projections of p', p", p, and p, points in a four-dimensional space, are obtained on the four coordinate planes xy, yz, zt, and xt. The content of the fifth component E is not shown in the diagram; it can be found as the difference between 100 % and the sum of the other four components. The components are represented by capitals and their percentage contents by the corresponding small letters in the subsequent diagrams and text.

This method is used by Academician N. S. Kurnakov's school for representation of aqueous multicomponent systems, but its application to problems of chemical technology encounters difficulties for the following reasons: every composition is represented by at least two projections which require either tie lines or symbolic representation, and projections of different compositions may coincide; to plot any particular property in the diagram it is necessary either to construct an additional projection, or to give a numerical indication of the value of the property for the projection of each composition. All this complicates the diagram, which loses its clarity if a large number of compositions is represented.

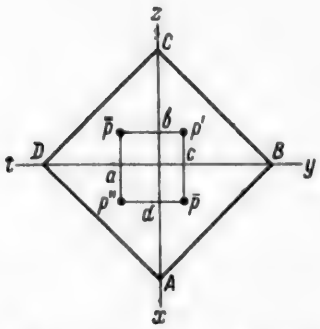


Fig. 3. Representation of a five-component system by the Schoute-Bőke method [2].

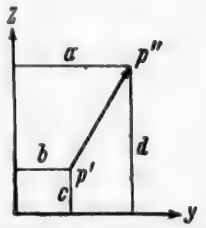


Fig. 4. Representation of a point of a four-dimensional space by the Fedorov method [3].

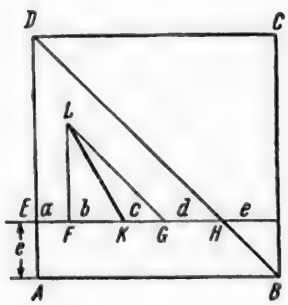


Fig. 5. Representation of five-component compositions by Lodochnikov's method [ 4 ].

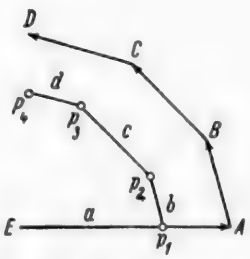


Fig. 6. Representation of multicomponent mixtures by Anosov's method [5-7].

By Fedorov's method [3] a point in a four-dimensional space is represented in the diagram by the vector p'p" (Fig. 4). In representation of a composition of five components A, B, C, D, E the origin of the vector is the point p' with coordinates y and z equal respectively to the contents of components B and C, and its terminus is the point p" with coordinates equal to the contents of components A and D. As in the Bőke method, the content of the fifth component is not shown in the diagram.

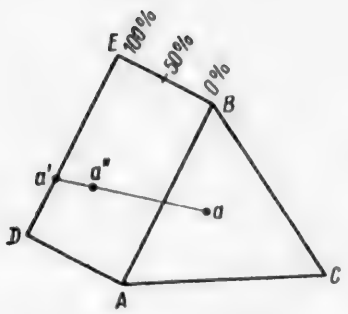


Fig. 7. Representation of five-component compositions by Bochvar's method [13].

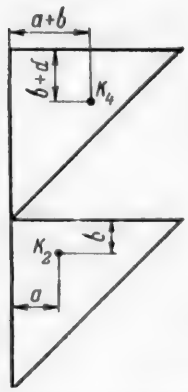


Fig. 8. Representation of multicomponent systems by Noskov's method [14].

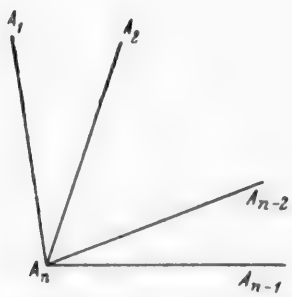


Fig. 9. Method for construction of diagrams for multicomponent systems.

Lodochnikov [4] proposed a method, based on Fedorov's theory of nonparallel vectors, for representation of five-component systems. Five-component systems are represented by intercepts contained in one half of the square ABCD (Fig. 5). The content of component B in the composition represented by the intercept LK is denoted by the rectangular projection KF of this intercept onto the straight line EH, parallel to the side AB. KG, the projection of the intercept LK onto the same straight line in a direction parallel to the diagonal BD of the square, represents the content of substance C. The height of the lower end of the intercept above the straight line AB gives the content of component E, while the contents of components A and D are represented by the intercepts EF and GH. Like Fedorov's method, Lodochnikov's method is convenient for representation of a relatively small number of compositions, as with a large number the diagram becomes so complicated that it becomes impossible to identify the multitude of vectors which intersect or coincide in direction.

Anosov proposed a method for representation of multicomponent mixtures which he termed the "method of spiral coordinates" [5-7]. In this method an axonometric diagram is drawn in which each point is represented by its broken coordinate line. From the point E (Fig. 6) intercepts representing the contents of components A, B, C, and D are drawn in directions parallel to intercepts EA, AB, BC, and CD (in the case of a four-component system) chosen arbitrarily in the plane. Because of the dense network of tie lines, which often intersect, this method is suitable only for representing small numbers of compositions The same is true of Fedorov's second method [8] and of the "method of sixty-degree coordinates" proposed by Nikolaev [9], which are very similar to the method of spiral coordinates.

Radishchev [10-12] represented multicomponent compositions by points of a regular multidimensional simplex, and projected this simplex onto several projection planes, the number of which is determined by the number of components. Because of the complex graphical operations involved in construction of the projections, this method is inconvenient for the needs of chemical technology.

In the method proposed by Bochvar [13] each composition of a five-component system is represented by three points a, a' and a", lying on the same straight line (Fig. 7). The position of point a determines the proportions of the components A, B, and C; point a' gives the quantitative ratio of D and E; point a" gives the ratio of the sums a+b+c and d+e. The contents of the components are not shown directly on the diagram. Since for any position of point a, point a" may be almost anywhere in the rectangle ABDE, and point a' can be anywhere in the line DE, the projections are bound to coincide if a large number of compositions is represented, so that each point must be individually marked. This makes this type of diagram unsuitable for extensive investigations.

Noskov [14] proposed a method based on axonometric representation of a multidimensional simplex. The composition of a five-component system is represented by two points, and of a six-component system by three. In representation of the composition of a five-component system ABCDE one point $K_3$ has the coordinates x and y, equal to a and b respectively, and the coordinates of the other point $K_4$ are a + c and b + d (Fig. 8). To represent a property of this composition another point is plotted, projectionally connected with the point $K_4$.

Since in the methods described here (and also in others) each composition is represented by at least two points or a geometrical figure, these methods can only be used to represent a relatively small number of compositions, and certain constructions are necessary to show each composition in the diagram. Therefore they have not been adopted in chemical technology, including silicate technology. Syntheses of new complex glasses with more than four components are based mainly on the somewhat obsolete "addition" and "substitution" methods developed by M. V. Lomonosov.

In the addition method a definite component, the effect of which it is desired to determine, is added to a certain batch. By this method it is possible to determine how the glass properties alter if a certain new component is added to the original batch.

The substitution method is based on replacement of one component A in the original composition by a new component B; it is then possible to determine how the glass properties alter on replacement of A by B [15].

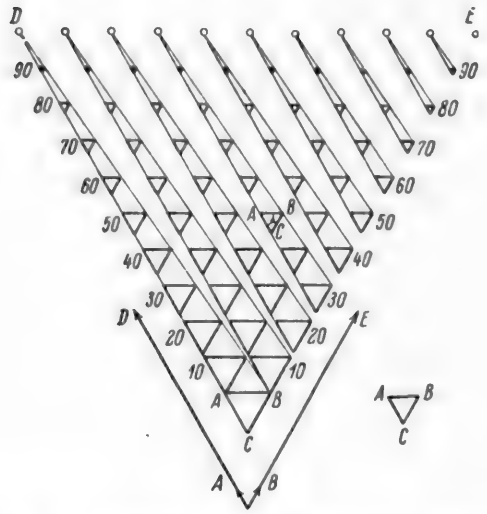


Fig. 10. Diagram of a five-component system.

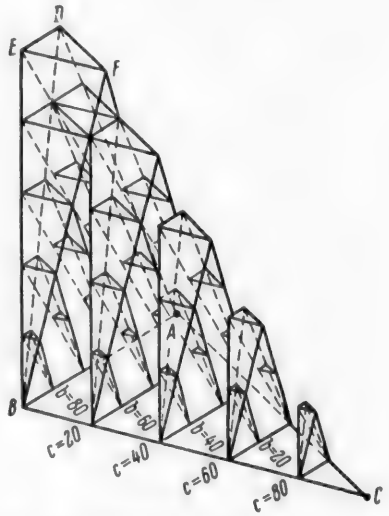


Fig. 11. Axonometric representation of a diagram of a six-component system.

These methods cannot be used for systematic syntheses of glasses with given properties, as the latter depend, in addition to technological factors, on the quantitative proportions of all the components in the glass.

Our proposed method for construction of diagrams for multicomponent systems is based on graphical representation of sections of multidimensional simplexes, the points of which represent the compositions of the systems.

Consider a system consisting of n components $A_1, A_2, \ldots A_{n-1}, A_n$. Since the sum of the percentage contents of all the components is constant, each mixture is determined by the percentage contents of (n-1) substances; i.e., it can be considered as a point in a space of (n-1) dimensions.

A space of n dimensions is denoted by $\Pi^n$. Elements of this space are points, straight lines, planes, and spaces of three, four, and more dimensions. A space of dimensions one unit less than the space under consideration is termed a hyperplane. Analytically, a hyperplane is represented by one linear equation. The simplest n-dimensional figure is termed the S(n+1) simplex; the n-dimensional simplex S (n+1) has n+1 vertices and is bounded by n+1 "hyperfaces" each of which is a hyperplane.

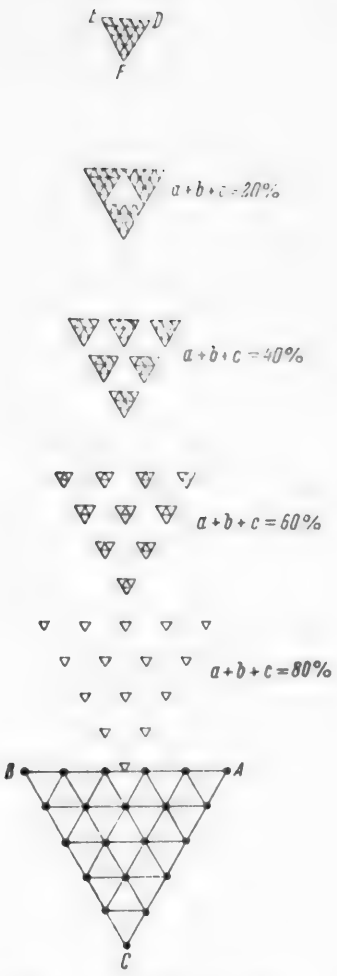


Fig. 12. Diagram of a six-component system.

Through the point $A_n$ in the (n-1)-dimensional space $\Pi^{n-1}$ we draw (n − 1) coordinate axes $A_nA_1$, $A_nA_2$, . . . $A_nA_{n-1}$, which do not lie in one space of (n −2) dimensions (Fig. 9). Along these axes we take the percentage contents $a_1, a_2, \ldots a_{n-2}, a_{n-1}$ of the components $A_1, A_2, \ldots A_{n-2}, A_{n-1}$. The pure components are represented by the points $A_1, A_2, \ldots A_{n-2}, A_{n-1}$. The coordinate origin represents the pure component $A_n$.

It is easy to show that the figurative points belong to the (n−1)-dimensional simplex S(n). The vertices of the simplex represent the pure components [16].

If there are two components (n = 2), the figurative points form the simplex S(2), which is an intercept; when n = 3 they form a two-dimensional simplex (triangle); when n = 4 the figurative points form the simplex S(4) of a three-dimensional space, or a tetrahedron; when n = 5, we have a simplex S(6) of a five-dimensional space.

We shall prove that the section of the S(n) simplex of an (n−1)-dimensional space $\Pi^{n-1}$ by a hyperplane $\Pi^{n-2}$ parallel to one of the faces of the simplex S(n) is the simplex S(n−1).

We denote the vertices of the simplex S(n) by $A_1, A_2, \ldots A_n$. The vertex $A_n$ and the edges $A_nA_1$, $A_nA_2$, . . . $A_nA_{n-1}$ are taken as the origin and the coordinate axes along which $a_1, a_2, \ldots a_{n-1}$, respectively, are taken. We now draw the hyperplane ($a_1 = a'$) corresponding to constant composition a' of component $A_1$. This divides the space into two parts; in the first $a_1 > a'$, and in the second $a_1 < a'$. Since $0 < a' < 100\%$, the vertex $A_1$ will be in the first part and all the other vertices in the second. Therefore the straight lines joining the vertex $A_1$ to all the other vertices of the simplex cut the hyperplane $a_1 = a'$. We must now show that the points of intersection $a'_2, a'_3, \ldots a'_n$ do not lie in one (n −3)-dimensional space $\Pi^{n-3}$. Suppose that the reverse is true. Then these intersection points together with the point $A_1$ determine a space of (n− 2) dimensions. Yet these points lie on the straight lines $A_1A_2$, $A_1A_3$, . . . $A_1A_n$, which are in a (n − 1)-dimensional space and therefore together with the point $A_1$ they determine a space of (n − 1) dimensions. This absurdity proves the proposition.

A system of five components A, B, C, D, E is represented by a four-dimensional simplex S(5) or pentatope. Let it be cut by a series of hyperplanes $\Pi^3$ corresponding to constant contents of component E ($e_1 = 10\%$, $e_2 = 20\%$, $e_3 = 30\%$ etc. ). Each such section is a simplex S(4) or tetrahedron. The tetrahedrons become smaller with increasing contents of component E. Let each tetrahedron be cut by a series of planes $d_1 = 10\%$ $d_2 = 20\%$ etc. Each of these sections is S(3), or a triangle. We now draw an axonometric diagram of the pentatope. It follows from the fundamental theorem of multidimensional axometry that the directions of the axonometric axes and their scales (distortion coefficients) may be chosen arbitrarily [16]. We chose them in such a way that the sections are not superposed and the triangles are projected in the form of equilateral triangles (Fig. 10).

The diagram which is thus obtained for a five-component system consists of a diminishing series of tetrahedrons, sections of the pentatope by hyperplanes corresponding to constant values of one of the components D or E. The percentage contents of components A, B, and C are determined by the composition of the figurative point in the triangle, and the contents of the other two components are determined by the position of the triangle in the diagram. For example, the point representing the composition a = 10%, b = 20%, c = 20%, d = 20% and e = 30% must lie in a triangle which is contained simultaneously in the tetrahedron corresponding to d = 20% and in the tetrahedron corresponding to e = 30% This triangle lies in the horizontal series of triangles which correspond to the constant value of the sum d + e = 50% The distance from the figurative point to the horizontal side of the triangle determines the content of component C; a and b are determined by the distance of the figurative point from the right and left sides of the triangle respectively.

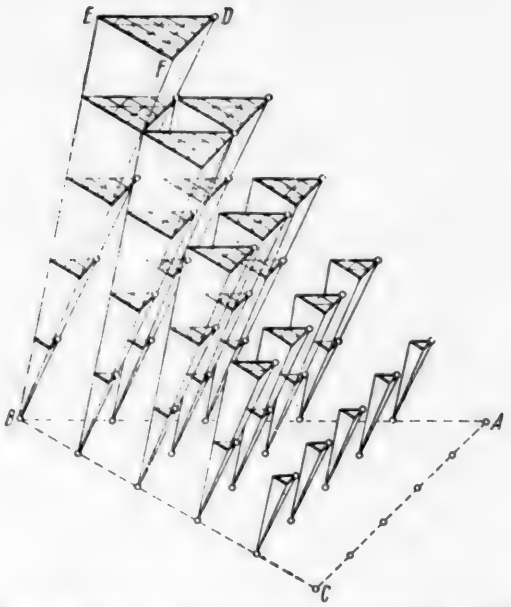


Fig. 13. Spatial representation of sections of a six-component system.

A similar construction of a five-component diagram was published by Berger [17]. However, he did not give the theory of this representation and the description of the method used for obtaining the required sections is not sufficiently clear.

In just the same way we can construct a diagram for a six-component system, which is an axonometric representation of a five-dimensional simplex. In the simplex S(6) representing the six-component system A–B–C–D–E–F, we make a number of sections by the hyperplanes $\Pi^4$ corresponding to definite contents of one of the components; for example, c = 20%, c = = 40% etc. In each of these sections, which are pentatopes, we make sections by three-dimensional spaces $\Pi^3$, corresponding to constant contents of another component; for example, b = 20, b = 40% etc. (Fig. 11). These secondary sections are tetrahedrons in which we make plane sections corresponding to contents of A equal to 20, 40, 60%, etc. We can now project all the triangles so obtained onto the plane of the drawing in the form of equilateral triangles which do not overlap, and so obtain a plane diagram for a six-component system (Fig. 12).

Our diagrams of five-and six-component systems can also be explained without the use of the concepts of multidimensional geometry. Consider a system of five components A, B, C, D, and E, and regard the sum of A, B, and C as one component M. The position of the figurative point for this reduced "ternary" system, which may be represented as an equilateral triangle DEM, merely represent the proportions of the components D, E, and M, but does not determine the composition of the mixture, as it does not give the percentage compositions of the components A, B, and C. This means that at any point of the reduced system we can construct a triangle, the side of which is proportional to m = a + b + c, and the percentage contents of the components A, B, and C is determined by the position of the point within the triangle (Fig. 10). The contents of the components D and E in the diagram so obtained is determined by the position of the triangle itself in the reduced system.

The same procedure can be used for constructing a diagram of a six-component system A–B–C–D–E–F. If b + d + e + f is denoted by M, then at each point of the reduced system we can construct a tetrahedron, the edge of which is proportional to m, and the percentage contents of components B, D, E, and F can be found from the position of the point within the tetrahedron (Fig. 13). The bases of the tetrahedrons should be parallel, and similar to the triangle representing the reduced system. In this way we obtain a three-dimensional model or three-dimensional projection of the six-component system. We cut this model by a series of planes corresponding to definite values of the sum of the percentage contents of A, B, and C; for example, 20%, 40%, etc.,; assuming that the reduced system is represented by an equilateral triangle, we project the model onto the plane of its base in such a way that the sections do not overlap. The plane diagram so obtained is also an axonometric representation of the simplex S(6) (Fig. 12).

Diagrams for systems of more than six components may be constructed analogously.

This method for graphical construction of diagrams of five- and six-component system can be used in extensive investigations of the dependence of properties of materials on their chemical composition.

## LITERATURE CITED

[1] V. Ya. Anosov, Application of Descriptive Geometry to Chemical Diagrams for Ternary and Quaternary Systems [in Russian] (Izd. AN SSSR, Moscow-Leningrad, 1949).

[2] P. H. Schoute. Mehrdimensionale Geometrie. I. Teil. Die linearen Raume. Leipzig (1902).

[3] E. S. Fedorov, Mem. Mining Inst. 2, 3 (1909). [in Russian]

[4] V. N. Lodochnikov, Ann. Sector Phys.-Chem. Analysis 2,3,255 (1924); 3, 1, 42 (1926).

[5] V. Ya. Anosov, Ann. Sector Phys.-Chem. Analysis 9 (1936) [USSR].

[6] V. Ya. Anosov, Bull. Acad. Sci. USSR, Chem. Ser. 4, 855 (1938).

[7] V. Ya. Anosov, Progr. Chem. 5, 7-8, 987 (1936) [USSR].

[8] E. S. Fedorov, Bull. Russian Acad. Sci. 12, 7 (1918); Mem. Mining Inst. 2, 3 (1919).

[9] V. I. Nikolaev, A. G. Kogan, and G. F. Ogorodnikov, Bull. Acad. Sci. USSR, Chem. Ser. 1 (1936).

[10] N. S. Kurnakov, Introduction to Physicochemical Analysis [in Russian] (Izd. AN SSSR, Moscow-Leningrad, 1940).

[11] V. P. Radishchev, Ann. Sector Phys. - Chem. Analysis 13 (1940) [USSR].

[12] V. P. Radishchev, Ann. Sector Phys. - Chem. Analysis 14 (1941) [USSR].

[13] A. A. Bochvar, Bull. Acad. Sci. USSR, OTN, 12, 851 (1944).

[14] N. I. Noskov, Ann. Sector Phys. - Chem. Analysis 26, 14 (1955) [USSR]

[15] M. A. Bezborodov, Essays on the History of the Russian Glass Industry [in Russian] (Industrial Construction Press, Moscow, 1952) p. 48.

[16] E. A. Glazunov and N. F. Chetvertukhin, Axonometry [in Russian] (GITTL, Moscow, 1953).

[17] E. Berger, Glastech. Ber. 5, 569 (1928).

Received July 25, 1957.

# SOME QUESTIONS OF THE THEORY AND PRACTICE OF THE FURNACE REFINING OF TIN

N. N. Murach

During the past 2-3 decades there has been a pronounced tendency to increase the purity standards of all smelted nonferrous and rare metals, owing to increased service demands made on them and to the development of new fields of application.

This is quite true in the case of tin used for coatings, alloys, etc. During recent years the standard specifications for different tin grades have been changing consitently in the direction of higher purity requirements, and the demand for the highest tin grades, 0-1, and 0-2, has increased at the same time. Tin refining is most closely associated with the composition of the original concentrates and the processes chosen for the preliminary treatment and reduction smelting of the concentrates. The more thorough the purification of the concentrate before smelting, the simpler, more effective, and better is the refining of the crude tin.

Because of the varied composition of the original tin ores, the concentrates contain a wide range of impurities: Fe, Mn, Cu, Zn, As, S, Pb, Sb, Bi, Ag, W, Ni, Co, Ta, Nb and gangue components: $Al_2O_3$, $SiO_2$, CaO, MgO etc.

Concentrates from several small tin mines are usually combined in large batches, so that their composition is leveled out somewhat.

The preliminary processes (roasting, sintering, magnetic and electrostatic separation, leaching, etc.) remove a considerable proportion of these impurities before the smelting, but a certain amount inevitably remains in the concentrate and enters the metal during the reduction smelting. Among these impurities are those specified in the GOST: Fe, Cu, As, Pb, Sb, Bi, S, and Al, and also Ni, Co, Cd, Ag, and Zn, which are not specified in the GOST, and partial removal of which from crude tin is briefly considered here.

Of the two essentially different processes of tin refining: a) by electrolysis, and b) the furnace process, the first has not been adequately developed, although it is operated on a large scale by certain plants in the United States. We shall not consider this promising method because of the lack of industrial data.

The numerous methods proposed for furnace refining of tin can be divided into three groups: 1) purely physical methods, based on phase separation (solid-liquid and liquid-gas), such as filtration, liquation, segregation, fractional crystallization, vacuum distillation, etc.; 2) physicochemical methods based on preliminary formation of intermetallic compounds of the impurities or compounds of the impurities with oxygen, chlorine, sulfur, or arsenic, and their subsequent separation from the refined tin; 3) chemical methods, based on metathetical reactions in metallic and salt systems (such as $SnCl_2 + Pb \rightleftharpoons Sn + PbCl_2$), whereby the impurities can be isolated from the tin.

In selection of methods for removal of impurities from crude tin the following factors must be taken into consideration:

1) the high affinity of tin for oxygen, chlorine, and sulfur;

2) the tendency of tin to form intermetallic compounds; 3) the chemical inertness of tin oxide; 4) the low vapor pressure of tin and the high vapor pressure of the compounds SnS, SnO; 5) inevitable loss of the metallic tin in skimmings, scale, salts, etc.

Because of the high cost of tin, special attention must be paid to this last factor, Data were presented earlier [1] on the amounts of tin lost with ferruginous dross in refining by liquation or segregation. The amounts of dross are just as great in removal of copper by means of sulfur as of arsenic by means of aluminum.

The conversion of ferruginous, sulfur, aluminum, and other dross has become a difficult independent problem in tin metallurgy, and much effort has been expended in its solution.

It is not surprising that in recent years the attention of research scientists and works metallurgists has been directed toward searches for new and improved methods of tin refining.

The following trends may be considered briefly in the light of available data.

Removal of impurities from tin by formation of intermetallic and other compounds*. Some of the impurities present in crude tin are capable of forming stable compounds with tin and with each other, with physical properties greatly different from those of tin. These compounds include $FeSn_2$, $Cu_3As$, $Cu_3Sb$, $Cu_3Sn$, $SnSb_2$, $Sb_2As_3$, NiSb, SnAs, FeAs, AlAs, PbS, SnS etc.

The existence of ternary and more complex intermetallic compounds is considered little in the literature, and is not discussed here [2].

In absence of basic thermodynamic data on most intermetallic compounds, generally their formation in the melted tin mass is to a certain degree determined by their heats of formation and melting points, which are quoted from a number of literature sources [3-5] in Table 1.

TABLE 1

Some Properties of Intermetallic Compounds

| Compounds | Heat of formation | Melting point (°C) | Compounds | Heat of formation | Melting point (°C) |
|---|---|---|---|---|---|
| $Cu_3As$ | 25.6 ± 5 | 830 | NiAs | 11* | 968 |
| $Cu_3Sb$ | 2.5 ± 1 | 681 | SnAs | 20 | 605 |
| $Cu_3Sn$ | 7.2 ± 0.5 | 675 | FeSi | 19.2 ± 1.5 | 1410 |
| $Cu_2Al$ | 16 ± 1.5 | 1011 | $FeAl_3$ | 26.8 ± 2 | 1170 |
| $FeSb_2$ | 3.6 ± 0.4 | 722 | $FeSn_2$ | 20 | 1110 |
| SbAl | 23 ± 2.5 | 1050 | $Ni_3Sn$ | 22.8 ± 1.5 | 1174 |
| NiSb | 15.8 ± 1 | 1160 | NiSn | 14 | 1200 |
| $Sn_3Sb_2$ | 3.6 | 500 | NiAl | 34 ± 2.5 | 1640 |
| $Ca_3Sb_2$ | 174 ± 9 | 1350 | AlCo | 26.4 | 1628 |
| $Ca_3Bi_2$ | 126 ± 7.5 | 928 | $CaSn_3$ | 43.0 ± 4 | 627 |
| AlAs | 40* | 1600 | $Ca_2Pb$ | 51.5 ± 2.5 | 1110 |
| FeAs | 30* | 1030 | | | |

*Approximate data.

Melted crude tin contains a relatively small number of intermetallic compounds stable enough to be separated by physical methods (filtration, centrifugation); the most important is the compound $FeSn_2$ which, together with FeAs, binds nearly all the iron in crude tin into high-melting crystals of lower density.

To form stable intermetallic compounds which differ in their properties from metallic tin it is necessary to introduce the elements Si, Ca, Na, Mg, and Al, which give rise to compounds of this type. If it is assumed that liquid tin contains only ternary systems – tin + impurity + added element – then the principal impurities must give rise to over 40 ternary systems, of which only seven have been partially studied [2]. This shows the difficulty in making theoretical predictions relating to refining of multicomponent crude tin if the contents of individual impurities after refining must be restricted to hundredths of one per cent.

*E. V. Kiseleva carried out the experimental work.

Because of this, in studies of the refining processes of tin it becomes necessary to establish empirical relationships for the introduction of refining additives and subsequent removal of the intermetallic phases or chemical compounds formed.

Removal of iron and arsenic from tin by filtration under vacuum. As an example, we describe experiments on the refining of crude tin by vacuum filtration through porous filters.

Two grades of crude tin were investigated:

| | Fe | As | Cu | Pb | Al | Bi |
|---|---|---|---|---|---|---|
| I (%): | 0.96-1.14 | 0.49-0.52 | 0.11-0.12 | 0.01-0.05 | 0.015 | 0.004 |
| II (%): | 2.87-3.17 | 0.71-0.74 | 0.55-0.68 | 0.41-0.47 | 0.025 | 0.012 |

Analytical data for different parts of the ingots, presented below, showed great variability of composition (Fig. 1).

| Part of ingot | Contents (%) | |
|---|---|---|
| | Fe | As |
| A | 0.14 | 0.12 |
| B | 1.28 | 0.83 |
| C | 1.28 | 0.79 |

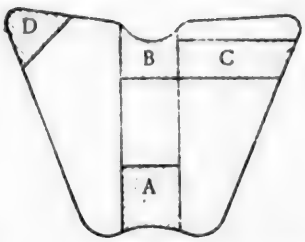


Fig. 1. Samples across an ingot section.

To prepare average samples for the experiments, the ingots were cut into a series of plates and the cuttings were mixed thoroughly.

The average size of the inclusions was 0.020-0.040 mm in the purer crude tin, and up to 0.40 mm in the more contaminated material.

The intermetallic compounds $FeSn_2$ and FeAs were determined by their color and microhardness: $FeSn_2$ crystals have microhardness of the order of 55 kg/mm$^2$ (tin has 15 kg/mm$^2$) and are of a light silvery color; FeAs crystals are gray-blue (after etching with a mixture of glycerol, glacial acetic, and nitric acids.

Photomicrographs of tin batches I and II are shown in Fig. 2.

Since the crystal size of the impurities greatly depends on the filtration temperature and the conditions of crystal growth, average tin samples were melted, overheated, and quenched at the experimental filtration temperature, or cooled slowly (over 3-8 hours) down to the filtration temperature.

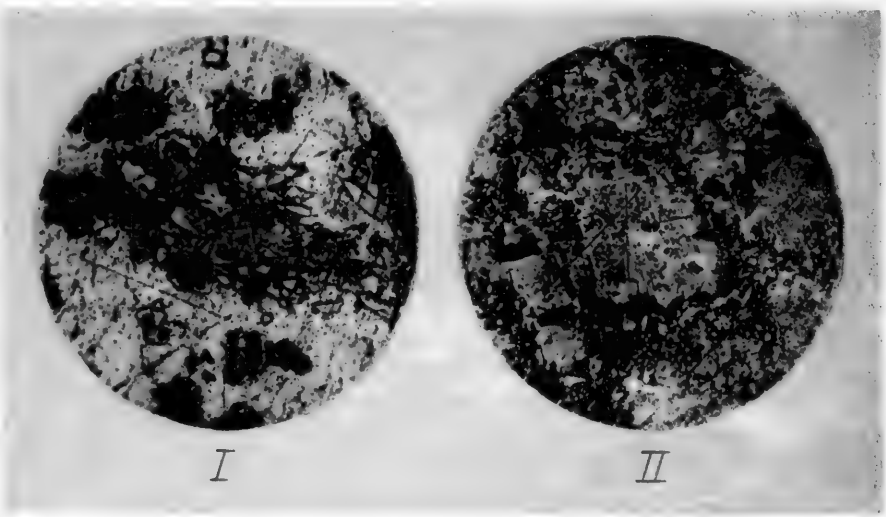


Fig. 2. Photomicrographs of tin batches I and II.

TABLE 2

Properties of Filtering Materials

| Material | Porosity (%) | Bulk density (g/cc) | Thickness (mm) |
|---|---|---|---|
| Electrode graphite | 29.5 | 1.58 | 3 – 5• |
| Special dense graphite | 19.4 | 1.66 | 5 |
| Schott plates | 26.4 | 1.84 | 4 – 6 |
| Porous fireclay | 40 | 1.65 | 30 – 50 |

•30 mm in a larger unit.

TABLE 3

Removal of Impurities from Tin by Filtration

| Tin batch | Original metal | | Filtrate | | Filtrate skimmings | |
|---|---|---|---|---|---|---|
| | Cu | Al | Cu | Al | Cu | Al |
| I | 0.11 | 0.015 | 0.086 | 0.009 | 0.054 | 0.20 |
| II | 0.68 | 0.024 | 0.60 | 0.01 | 0.40 | 0.22 |

With rapid cooling the crystals were of the order of a few hundredths of a millimeter in size; on slow cooling, the impurity crystals grew to 1 mm and larger.

The substances used as filtering materials are listed in Table 2.

Filtration was studied in the 250-500° temperature range. The most suitable material proved to be electrode graphite, through which tin filtered well at an initial rate of the order of 60 tons/$m^2$/hour. The amount of tin retained by the graphite filter was very small; with porous fireclay it exceeded the weight of the filter.

The first portions of the filtered tin had a higher impurity content because of breakthrough of fine crystals through the filter pores; this can be detected in small-scale experiments.

After a layer of impurities had been formed on the filter, it acted as a filter itself, and pure metal was obtained.

Fig. 3. Photomicrograph of tin after filtration.

As was to be expected, filtered tin of the best composition was obtained at lower temperatures: 0.007-0.04 Fe and 0.07-0.09% As at 250-300°, and up to 0.2% Fe and As at 400-500°. In filtration some of the impurity particles became coagulated into larger aggregates (Fig. 3).

Of the other impurities, aluminum is removed most effectively, while copper is retained in the tin, as is clear from Table 3.

The yield of filtered tin from crude tin of batch I was about 90% with 9.5% in the skimmings; batch II gave about 75% with 24% in the skimmings.

The same experiments showed that: 1) loss of tin in dross is considerably less in vacuum filtration than in liquation or segregation; 2) the amount of filtered tin obtained does not depend on the filter material, but

depends only on the composition of the crude tin; 3) the iron and arsenic contents of the filtered tin depend most on the temperature of the metal being filtered; 4) the iron contents of the dross vary from 8 to 18%, and the arsenic contents from 2.5 to 8.5%; 5) the degree of vacuum influences only the filtration rate and not the composition of the filtered metal.

Two types of units can be used for filtration of tin under works conditions: 1) a filter unit heated by resistance heaters, in which vacuum is created by means of a vacuum pump (Fig. 4); 2) a filter unit in which vacuum is created by a column of liquid tin in a tube (Fig. 5).

Each of these has its merits and defects; the best designs can be worked out after studies of their performance.

Separation of tin from iron by means of silicon. In the usual processes for smelting and refining of tin considerable amounts of iron-containing dross are formed; this is often converted by being added to the charge in the smelting of concentrates. The iron in the skimmings then serves as a reducing agent for the cassiterite, and enters the slag in the form of FeO.

This procedure is only partially possible in smelting in reverberatory furnaces: in electric furnaces the atmosphere is strongly reducing and the iron in the skimmings passes completely into the crude tin and is therefore not removed from the cycle.

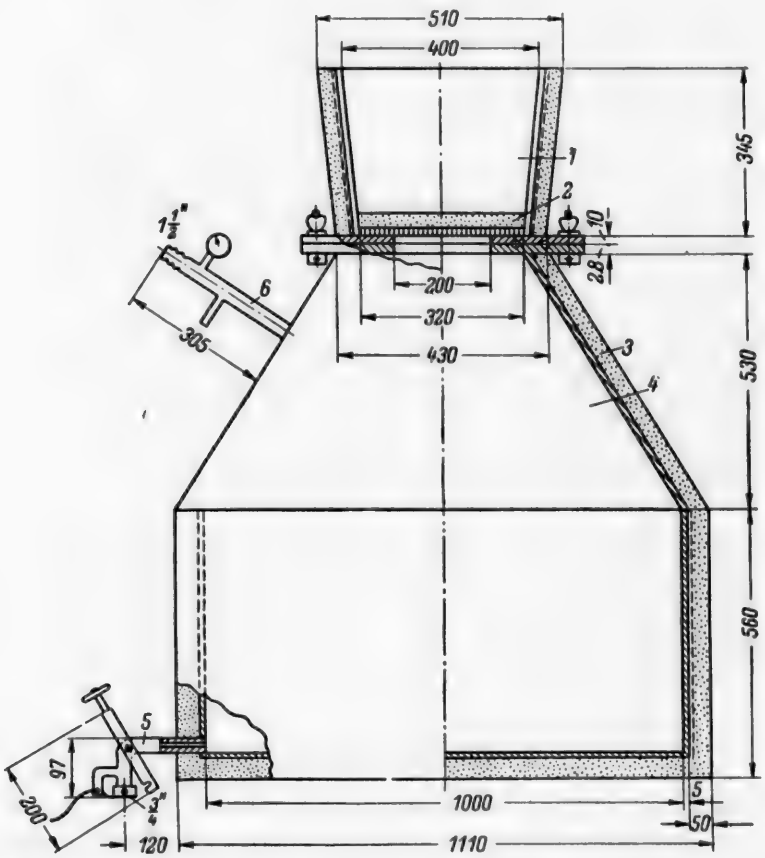


Fig. 4. Filtration unit:
1) receiver for crude tin to be refined, 2) filter plate, 3) heat insulation, 4) receiver for pure tin, 5) discharge device, 6) tube to vacuum pump.

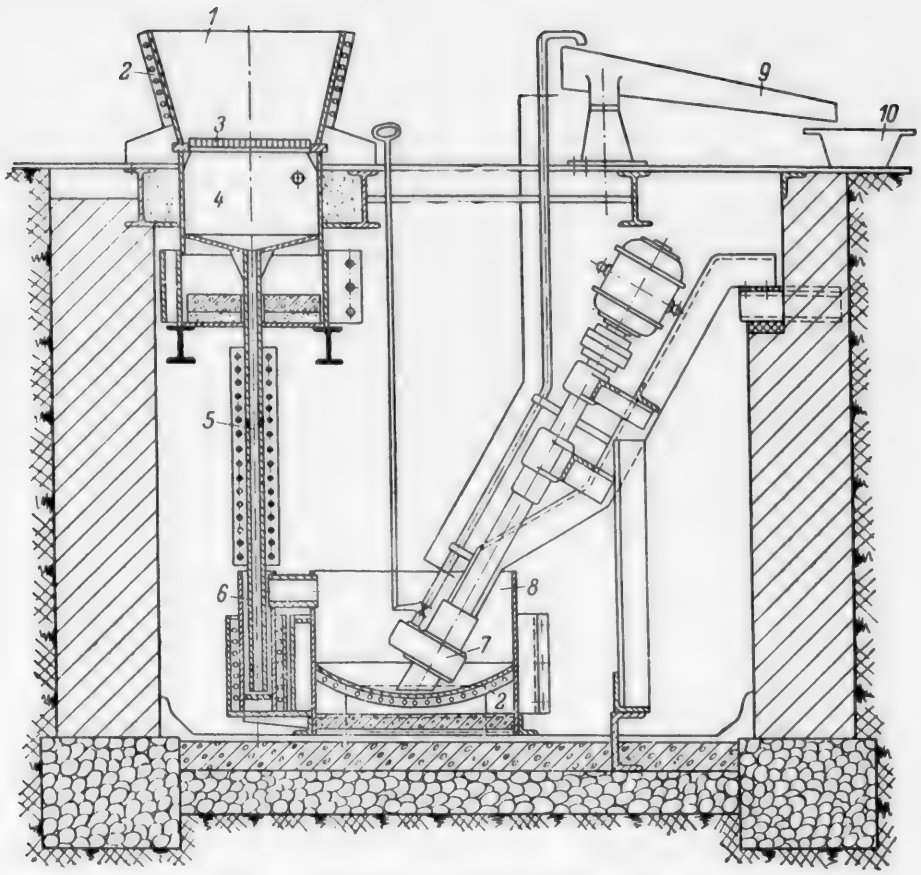


Fig. 5. Vacuum filter with receiving vessel and pump for tin casting:
1) heated funnel for crude tin, 2) resistance heaters, 3) graphite filter, 4) receiving funnel, 5) hydraulic column of tin, 6) container, 7) pump, 8) receiving vessel, 9) conduit, 10) mold for pure tin.

For this reason other and better methods are needed for conversion of iron-containing dross. We have developed a method for separation of tin and iron through formation of a stable intermetallic compound.

Methods have been developed and adopted for removal of arsenic from tin by addition of aluminum (with formation of the compound AlAs of m.p. about 1600°), and for removal of antimony and bismuth by addition of alkali or alkaline-earth metals (with formation of refractory NaSb, $CaBi_3$, etc.).

Investigations of the demixing regions of a number of ternary systems, carried out by N. N. Murach and Z. P. Likhnitskaya [1], demonstrated the undoubted advantages of the system Sn – Fe – Si; when silicon is added to tin containing iron the very stable intermetallic compound FeSi is formed, while tin remains free. The specific gravity of the ferrosilicon compound is about 4.0, which is considerably less than that of tin, and the two almost immiscible liquids separate very easily.

Certain difficulties arise on addition of infusible silicon (m.p. 1430°) to fusible tin, but they are easily resolved if silicon is added to strongly overheated crude tin or dross while they are in the furnace. The reaction of FeSi formation is exothermic, with much evolution of heat, and occurs at 1250° [4].

When the tin cools it separates completely from the ferrosilicon, apart from entrapment of 0.5-2% of tin in the form of beads. A small amount of FeSi is also trapped in the tin, but it is easily removed by a repeated melting at a moderate temperature.

## SUMMARY

1. Vacuum filtration of crude tin is a highly productive process, yields pure metal, and is worthy of serious attention on the part of industry.

2. Removal of iron from tin in skimmings by means of silicon with formation of the compound FeSi and subsequent separation of the liquid phases tin-iron silicide on cooling has been studied theoretically, and can be easily effected in practice.

3. In conjunction with progressive methods for vacuum removal of lead, bismuth, arsenic, and antimony from crude tin [6], the proposed refining methods can radically simplify and improve the general procedure of tin refining.

## LITERATURE CITED

[1] N. N. Murach, Metallurgy of Tin [in Russian] (Metallurgy Press, 1947) pp. 221, 226.

[2] R. Vogel. Die Heterogenen Gleichgewichte. Akad. Verlag, Leipzig (1937).

[3] N. N. Murach, Metallurgist's Handbook of Nonferrous Metals, II, Section "Tin" [in Russian] (Metallurgical Press, 1947).

[4] F. Weibke u. O. Kubaschewski. Thermochemie der Legierungen Springer Verlag, Berlin (1943).

[5] O. Kubaschewski and E. Evans, Metallurgical Thermochemistry (Moscow, 1954) [Russian translation].

[6] N. N. Murach and L. G. Povedskaya, Collection of Papers, Ministry of Nonferrous Metals and Gold, 25 [in Russian] (Metallurgy Press, 1955).

Received July 11, 1957.

# DISSOLUTION OF ALUMINUM IN ACIDS AND ALKALIES IN AN ULTRASONIC FIELD

A. M. Ginberg

Mandrels of aluminum and its alloys are used in electroforming practice for production of complex hollow articles from various metals (usually of copper).

At the end of the electrodeposition the layer of deposited metal is removed from the ends of the mandrel which is then dissolved in NaOH or HCl solution to release the molded object.

The time required for production of hollow objects by electroforming is mainly determined by two factors: the rate of deposition of the metal on the mandrel, and the rate of solution of the latter.

Our earlier investigations [1] established the optimum concentrations and temperatures of acid and alkali solutions for dissolving aluminum and its alloys. However, even under the optimum conditions the solution process is very lengthy, and it greatly increases the time required for production of hollow objects. Electrochemical dissolution of aluminum mandrel with application of external current proved unsuitable, as it had an adverse effect on the surface quality of hollow copper objects. Moreover, because of the considerable edge effect the dissolution rate was not greatly increased with hollow objects of complex configuration.

We studied the possibility of accelerating the dissolution of aluminum mandrels in acids and alkalies by application of an ultrasonic field. Some justification for this was provided by the known influence of ultrasound on the kinetics of electrode processes in electrochemical dissolution and its accelerating effect on most chemical reactions.

## EXPERIMENTAL

The specimens were rod aluminum of AD1 grade, of the following chemical composition (%): Fe 0.21, Si 0.37, Cu 0.01, Al 99.41. Each specimen was 30 mm long and 4 mm in diameter. The specimens were coated with a layer of copper 0.4 mm thick. After the electrodeposition the copper was removed from the ends of the specimens by milling until the aluminum surface was exposed. The specimens prepared in this manner were dissolved in 7.5 N NaOH or 8.4 N HCl solutions. Glass beakers 1 liter in capacity, fixed over an oscillator in a vessel containing water, were used for the purpose (Fig. 1). The ultrasonic generator was an instrument of the "Bar" type giving frequencies from 7 to 100 kilocycles/second, with an output power of 800 w. The oscillator was of the magnetostriction type. The temperature was kept constant by a current of water passing through the vessel 1. The dissolution was performed at different frequencies and field intensities. The solution rate was determined from the weight changes of the specimens.

The results obtained in dissolution of aluminum in NaOH and HCl solutions are shown in Figs. 2 and 3, respectively.

## DISCUSSION OF RESULTS

The results show that application of ultrasound of various frequencies and intensities accelerates the dissolution of aluminum in alkali in all cases.

The highest solution rate in NaOH at 60° is found at a frequency of 16 kilocycles/second and intensity of

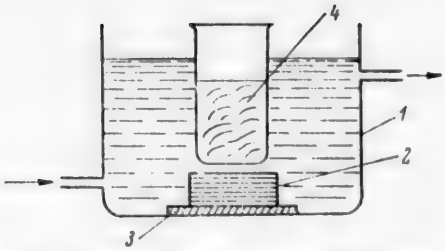


Fig. 1. Apparatus for dissolution of aluminum with application of ultrasound:
1) vessel with water, 2) oscillator 3) rubber lining, 4) beaker with solvent.

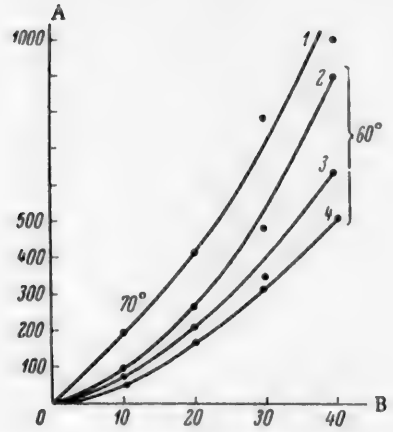


Fig. 2. Dissolution of copper-plated Al in 7.5 N NaOH solution:
A) amount of aluminum dissolved (in mg), B) dissolution time (minutes); dissolution with application of ultrasound of frequency (kilocycles/second) and intensity (w/cm$^2$), respectively; 1) 70, 1; 2) 16, 1.3; 3) 35, 0.44; 4) without applied ultrasound.

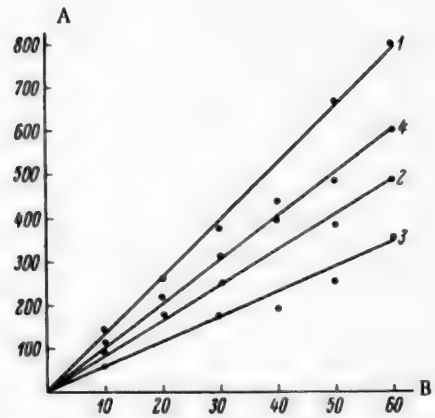


Fig. 3. Dissolution of copper-plated Al in 30% HCl solution (8.3 N) at 24°:
A) amount of aluminum dissolved (in mg), B) dissolution time (minutes); dissolution with application of ultrasound of frequency (kilocycles/second) and intensity (w/cm$^2$), respectively: 1) 16, 1.3; 2) 26, 0.35; 3) 36, 0.44; 4) without applied ultrasound.

1 w/cm$^2$. The solution rate of aluminum in HCl decreases on application of ultrasound, and only at a frequency of 16 kilocycles/second) and intensity of 1.3 w/cm$^2$ is there some acceleration of the process.

The dissolution of aluminum in contact with copper may be regarded as an electrochemical process with a difference effect. A positive difference effect is observed in dissolution in alkalies.

The reaction at the anode in electrochemical dissolution may be represented as follows:

$$Al \longrightarrow Al^{3+} \quad 3\ominus$$

$$Al^{3+} + 3OH^- \longrightarrow Al(OH)_3.$$

Aluminum hydroxide formed at the anode dissolves to form aluminate according to the equation

$$Al(OH)_3 + NaOH \longrightarrow NaAlO_2 + H_2O.$$

The aluminate formed diffuses into the solution. The reaction of aluminate formation is considerably slower than ionic reactions, and the aluminum hydroxide forms films on the aluminum which hinder diffusion of alkali to the metal and hinder or prevent the action of galvanic couples. Thus the process of aluminate formation, being the slowest, determines the dissolution rate as a whole.

When an ultrasonic field is applied, as the result of the cavitation produced the hydroxide film is readily removed from the metal surface and the considerable agitating effect of the ultrasound accelerates formation of aluminate and its diffusion into the solution, so that the dissolution rate increases. Thus the influence of ultrasound on the dissolution of aluminum in alkalies reduces mainly to acceleration of the chemical process of aluminate formation, which leads to accelerated dissolution. It seems likely that an ultrasonic field would also influence the kinetics of the electrode processes, but this cannot have a considerable influence on the dissolution

rate of aluminum as this process is ultimately determined by the rate of aluminate formation and the rate of aluminate diffusion into the solution.

When aluminum dissolves in HCl, the anode reaction may be represented as follows:

$$Al \longrightarrow Al^{3+} + 3\ominus,$$

$$Al^{3+} + 3Cl^{-} \longrightarrow AlCl_3.$$

Readily-soluble aluminum chloride is formed. It can be seen that the role of the ultrasonic field in the dissolution of aluminum in hydrochloric acid reduces mainly to its influence on the kinetics of the electrode processes.

It is known from the available literature data that ultrasound has a depolarizing effect on electrode processes in most cases. In a number of cases the depolarizing action is so great that in acid and alkaline media hydrogen is liberated at cathodic regions at potentials below the reversible equilibrium potential. A similar effect is observed in the anodic liberation of oxygen and chlorine.

However, according to a number of authors ultrasound may also have a polarizing effect. Thus, according to Schmidt and Ehret [2] and Bergmann [3] at low intensities ultrasound has a weak polarizing effect, and at high intensities a strong depolarizing one.

The retardation on acceleration of the dissolution of aluminum in hydrochloric acid solutions produced by applied ultrasonic fields of different frequencies and intensities can therefore be accounted for as follows: at frequencies of 26 and 36 kilocycles/second and corresponding intensities of 0.35 and 0.44 w/cm$^2$ the ultrasonic field had a polarizing effect, and the anodic process of aluminum dissolution was retarded; at 16 kilocycles/second and 1.3 w/cm$^2$ it had a depolarizing effect, and the dissolution rate increased accordingly.

## SUMMARY

1. It is shown that the rate of solution of aluminum in contact with copper in alkalies can be increased considerably by application of ultrasound, and the influence of frequency and intensity of the ultrasonic field was determined.

2. It was found that the dissolution of aluminum in contact with copper in hydrochloric acid solution may be influenced in different ways by an ultrasonic field; it may be retarded or accelerated in accordance with the frequency and intensity of the field.

## LITERATURE CITED

[1] A. M. Ginberg, Electroforming of Complex Hollow Objects [in Russian] (Shipbuilding Industry State Press, 1948).

[2] G. Schmidt, and L. Ehret, Z. Electroch., 43, 597 (1937).

[3] L. Bergmann, Ultrasonics and their Scientific and Technical Applications (IL, 1956) [Russian translation].

Received May 12, 1958

# INVESTIGATION OF NICKEL PLATING WITHOUT APPLICATION OF CURRENT, WITH AMMONIUM FLUORIDE BUFFER

N. A. Solov'ev

In contrast to the well-known and widely used process of galvanic nickel plating, which has been studied by Kudryavtsev, Lainer [1,2] and others, nickel plating without an applied current known as chemical nickel plating, is a relatively new process. According to Gostin [3], this process was first operated industrially in 1950.

The history of the chemical nickel-plating process and the reactions of reduction of nickel to the metal from solutions have been described by Gorbunova and Nikiforova [4], Belyaev, Zil'berfarb, and Garetovskaya [5], Gutzeit and Mapp [6], and others.

Belyaev, Zil'berfarb, and Garetovskaya [5] reported that the porosity of their nickel deposits, with layers from 9 to 122 $\mu$ thick, formed without application of current was as high as in nickel deposited electrolytically. The number of pores per 1 $dm^2$ surface area runs into thousands. They concluded that the porosity of the nickel layer can be diminished somewhat only upon repeated coating of the same specimen. Their value for the microhardness of the nickel deposits was 480-530 kg $mm^2$. On additional heat treatment of the nickel-coated articles the microhardness of the coatings increases only to 530-590 $kg/mm^2$.

Gorbunova and Nikiforova [2] found for layers of equal thickness that the deposits formed by nickel plating without current had only one half the number of pores found in deposits formed with the use of current.

They correlated the corrosion resistance of nickel layers formed without current with the number of pores in these layers. They concluded from their experimental data that the corrosion resistance of nickel layers of equal thickness is a quantitative function of porosity. With the use of sodium glycolate buffer they obtained a fairly stable potential for the deposited nickel, from $-0.34$ to 0.35 v under different coating conditions

The porosity of nickel deposited by the Kanigen• and Brenner porcesses, determined by the autoradiographic method, was lowest for the Kanigen process [7].

According to Gutzeit and Mapp [6], nickel layers formed by the Kanigen process are free from pores. The microhardness of deposits formed by this process reaches 500 $kg/mm^2$ after the deposition, and increases 1.5-2 fold and more after heat treatment. According to the literature, in the Kanigen process the growth of the layer begins at catalytic centers in the surface of the base metal. From these points the nickel layer grows at an equal rate in all directions [8].

In order to reduce the cost of the coatings, Starr [9] deposited dull or semidull nickel layers. In his opinion the surface appearance has no influence on the quality of the layer. To produce bright nickel coatings he recommends the addition of the same brighteners to the plating solution as are used in electroplating.

It is clear from the above literature survey that there are discrepancies in estimates of the porosity of the layers formed by chemical nickel coating, in the hardness values, in the influence of the external appearance of the layer on its resitance, and other characteristics.

The purpose of the present investigation was to study the influence of solution composition and operating conditions on the rate of growth of the layer, hardness, porosity, and electrode potential of the layer, and the physicochemical state of the solution.

•Kanigen is the trade mark of the chemical nickel plating process used by the General American Transportation Corporation.

## EXPERIMENTAL

The experimental specimens were made from polished KP-10 steel strip 0.5 mm thick. The specimens were all of equal size, 0.15 $dm^2$ in surface area. Before the tests all the specimens were marked with serial numbers. The layer thickness was determined by weighing of the specimens before and after coating on the AD-200 analytical balance to the nearest 0.1 mg. Microhardness was determined by the indentation method by means of the PMT-3 microhardness meter [10]. The solution pH was determined immediately before the plating by means of the P-5 pH-meter with an antimony electrode. The surface of the working part of the electrode was polished daily before the experiments with fine emery paper and powdered antimony. The cleaned electrode was washed and kept for 1 hour in distilled water. The electrode potentials of the nickel deposits were measured by the usual compensation method in 1 N nickel sulfate solution. The electrolyte was renewed for each determination with a new specimen. A saturated calomel electrode was used as the reference electrode. Porosity of the layers was determined by application of filter paper moistened with a solution of 40 g $K_3Fe(CN)_6$ and 15 g NaCl per liter [4]. The chemical resistance of the nickel layers was determined by the streaming method (GOST 3003-50). The nickel-plating solutions were prepared from the chemically pure salts in distilled water. A new solution was prepared for each coating, to give consistent results for all the experiments.

In the nickel-plating process without current, the specimens were: 1) rubbed with chalk, 2) degreased by means of slaked lime, 3) washed in running water, 4) pickled in 25% hydrochloric acid solution, 5) washed in running water, 6) nickel plated, 7) washed in running water, 8) washed in hot water, 9) dried by filter paper.

In comparative experiments the specimens were coated simultaneously in 0.1 liter glass beakers on the same water bath.

In tests of the coating process with the usual buffer addition of sodium acetate, at initial solution pH 5.0-5.5 and solution temperature 90-92°, we obtained deposits of considerable porosity. The microhardness of the surface nickel layer was 450-500 $kg/cm^2$, and the electrode potentials were negative (approximately − 0.3 v); i.e., we obtained the same results as other workers.

In subsequent experiments we studied the influence of ammonium fluoride as a buffer addition.

In preliminary experiments with ammonium fluoride buffer it was found that the porosity of the layers decreases appreciably at solution temperatures above 70° and at layer thicknesses above 10 $\mu$. For example, with a solution of the same composition containing ammonium fluoride buffer at 50-55° the layer deposited in 3 hours was 12.5 $\mu$, and the deposit was completely porous. At 70-75° in 1 hour a nickel layer 12.4 $\mu$ thick was formed, and the porosity was relatively low: 19 pores in an area of 7.5 $cm^2$.

The deposits formed at 90-92° with ammonium fluoride buffer contained small numbers of individual pores which could be easily counted, whereas the specimens coated in presence of sodium acetate buffer had very numerous pores which could not be counted; this is shown in Table 1.

TABLE 1

Effect of Buffer Additions on the Porosity of Nickel Layers

| Thickness of nickel layer ($\mu$) | Buffer addition | Appearance of coated surface | Number of pores per 7.5 $cm^2$ |
|---|---|---|---|
| 10.6<br>12.1 | Sodium acetate | Bright | Continuous porosity |
| 16.0 | Ammonium fluoride | Dull | 9 small pores |
| 12.3 | | Bright | 18 small pores |

Tests showed that with the use of ammonium fluoride buffer the appearance of the surface nickel layer did not have any significant influence on its porosity. The surface appearance has an exceptionally strong influence on the chemical resistance of the nickel layer.

TABLE 2

Chemical Resistance of Nickel Layers in Tests by the GOST 3003-50 Streaming Method

| Specimen Number | Thickness of nickel layer ($\mu$) from weight | Buffer addition | Thickness of electrodeposited nickel layer which should be destroyed in the tests ($\mu$) | Ratio of the resistance of the layer to that of an electrodeposited layer* | Destruction of nickel layer during test |
|---|---|---|---|---|---|
| 15 | 3.5 | | 160 | 45.8 | |
| 16 | 3.5 | Sodium acetate | 26 | 7.4 | Destroyed |
| 20 | 2.8 | | 38 | 13.5 | |
| 28 | 4.0 | Ammonium | 1015 | 258.7 | Not destroyed |
| 48 | 6.25 | fluoride | 1900 | 300.0 | |

*The equivalent thickness of the nickel layer relative to an electrodeposited coating was calculated from the layer thickness found by weight and the amount of reagent used for its destruction by the accepted standards for destruction of galvanic coatings. The amounts of reagent used to destroy the layers on specimens Nos. 28 and 48 were such as would be required to destroy galvanic nickel coatings 1015 and 1900 $\mu$ thick respectively, but the layers were not destroyed, and were even unchanged in appearance.

In tests, by the streaming method, of specimens coated with the use of ammonium fluoride buffer the following was found: 1) coatings with a dull surface were destroyed as quickly as galvanic deposits; 2) brighter nickel deposits were attacked less; 3) bright nickel deposits were almost unattacked, as is seen in Table 2. These tests were performed by the GOST 3003-50 streaming method. All the specimens has a bright surface before the tests. The external appearance of the nickel layers in specimens Nos. 28 and 48, formed in presence of ammonium fluoride buffer, was unchanged after the tests.

It follows from the data in Table 2 that specimens plated in presence of sodium acetate buffer were considerably more resistant than galvanic coatings, but the layers were nevertheless destroyed.

The influence of ammonium fluoride concentration on the growth rate of the layer, and on the physicochemical state of the nickel layers and plating solutions, can be seen in Table 3. The solution pH increases with increase of ammonium fluoride concentration. The highest growth rate of the nickel layer, 33.6 $\mu$ per hour, was obtained with an ammonium fluoride concentration of 15 g/liter. The lowest microhardness of the layer (417 kg/mm$^2$) was obtained with the lowest concentration of ammonium fluoride (5 g/liter), when the solution pH had the lowest value. At higher ammonium fluoride concentrations the microhardness of the layer remains fairly constant at 604 kg/mm$^2$. The lowest electrode potential of the layer is $-0.225$ v at 5 g of ammonium fluoride per liter, while at 10 g/liter the highest potential (+ 0.07 v) is found. The electrode potentials decrease on further increase of the ammonium fluoride concentration. Bright nickel deposits are formed at ammonium fluoride concentrations from 5 to 20 g/liter.

The hardness of the nickel layer is greatly influenced by the sodium hypophosphite concentration (Table 4) With 5 g of sodium hypophosphite per liter the microhardness of the nickel layer is 286 kg/mm$^2$, and reaches 604 kg/mm$^2$ only with 15 g/liter. On further increase of the sodium hypophosphite concentration the microhardness of the coatings varies from 635 to 707 kg/mm$^2$. Bright nickel deposits are formed at sodium hypophosphite concentrations from 25 to 35 g/liter, and the highest growth rate of the layer is obtained at 30-35 g/liter.

Variations of the nickel sulfate concentration from 20 to 50 g/liter have less effect on the growth rate of the layer and on the physicochemical state of the surface, as is clear from Table 5. With increase of the nickel sulfate concentration the color of the solution after the experiment became deeper green, and the amount of powderlike precipitate increased. The highest electrode potential, $-0.012$ v, was obtained with 25 g of nickel sulfate per liter, and the highest growth rate of the layer (38.7 $\mu$ per hour) was found at 35 g/liter. The microhardness of the layer was 604 kg/mm$^2$ for all the specimens. Bright nickel deposits were formed at nickel sulfate concentrations from 20 to 45 g/liter.

TABLE 3

Effect of Ammonium Fluoride Concentration on the Growth Rate and Quality of the Layer and the Physicochemical State of the Solution•

| Amount of $NH_4F$ (g/liter) | Solution pH | | Layer thickness ($\mu$) after exposure time | | Microhardness of coating (kg/mm$^2$) | Potential of layer (v) | External appearance of coating | Appearance of solution after experiment |
|---|---|---|---|---|---|---|---|---|
| | before expt. | after expt. | 20 minutes | 60 minutes (average) | | | | |
| 5 | 6.01 | 6.0 | 6.7<br>7.0 | 20.5 | 417 | —0.225 | Bright | Green |
| 10 | 6.62 | 6.35 | 9.7<br>9.7 | 29.1 | 604 | +0.07 | » | Pale green, slight precipitate |
| 15 | 6.85 | 6.85 | 11.2<br>11.4 | 33.6 | 604 | —0.01 | » | The same |
| 20 | 6.98 | 6.72 | 10.0<br>10.0 | 30.0 | 604 | —0.02 | » | » |
| 25 | 7.02 | 7.08 | 7.7<br>7.9 | 23.4 | 604 | —0.05 | Milk-white | Colorless, with precipitate and dendrites |
| 30 | 7.08 | 7.02 | 7.0<br>7.0 | 21.0 | 604 | —0.102 | Rough | The same |
| 35 | 7.13 | 7.35 | 6.6<br>6.5 | 19.5 | 604 | —0.116 | The same | » |

•The solution composition (in g/liter) was: nickel sulfate 25, sodium hypophosphite 30. Before addition of ammonium fluoride the solution pH was 5. The initial and final solution temperatures were 86 and 90°, respectively. The charge was 0.3 dm$^2$/liter. The solution was not stirred. The pH was determined a second time on the following day.

## DISCUSSION OF RESULTS

It was established experimentally that with the use of ammonium fluoride buffer the formation of bright deposits depends on the composition of the solution, temperature, and especially on the area immersed. Bright deposits are obtained with charges of not less than 2.5-3.0 dm$^2$ per liter of solution, and the greater the charge the brighter is the nickel deposit. Stirring of the solution also favors brightening of the layer. The probable explanation is that the greater the surface area per unit volume of solution, the more hydrogen is liberated and the greater is the agitation intensity of the solution, especially near the coated surface. This suggests that hydrogen, on becoming detached from the specimens, favors transport of nickel ions and reducing agent to the coated surface. The more hydrogen is liberated, the more intensive is the agitation and leveling of the solution concentration near the coated surface, and therefore the concentrations of the solution components near the surface do not decrease and bright deposits are formed.

We consider that the high chemical resistance of bright nickel layers deposited under definite conditions in presence of ammonium fluoride buffer (on the basis of the work of Vagramyan and Solov'eva [11]) may be attributed to uniformity of the deposits and close packing of the crystals. Evidently the corrosive reagent cannot penetrate between the crystals and break down their cohesion in bright deposits, but penetrates freely into the layer in dull coatings, where the distances between the crystals are greater.

Starr [9] considers that the appearance of nickel-coated surfaces does not affect the layer quality. With the use of ammonium fluoride buffer there are no great differences between bright and dull surfaces with regard

TABLE 4

Effect of Sodium Hypophosphite Concentration on the Growth Rate and Quality of the Layer•

| Amount of $NaH_2PO_4 \cdot H_2O$ (g/liter) | Layer thickness ($\mu$) after exposure time | | Microhardness of coating (kg/mm²) | Potential of nickel layer (v) | External appearance of coating | Appearance of solution after experiment |
|---|---|---|---|---|---|---|
| | 30 min. | 60 min. (average) | | | | |
| 5 | 3<br>3 | 6 | 286 | —0.18 | Milk-white | Green |
| 10 | 6.3<br>6.5 | 12.8 | 385 | —0.016 | | |
| 15 | 10.9<br>10.3 | 21.2 | 604 | —0.071 | Dark with stripes | Pale green |
| 20 | 13.5<br>12.9 | 26.4 | 707 | —0.116 | Dark with stripes and pitting | Colorless, powder-like precipitate |
| 25 | 16.0<br>16.1 | 32.1 | 707 | —0.094 | Bright | |
| 30 | 17.3<br>17.2 | 34.5 | 635 | —0.102 | » | » |
| 35 | 17.1<br>17.4 | 34.5 | 707 | —0.142 | » | » |
| 40 | 16.5<br>17.1 | 33.6 | 635 | —0.15 | Milk-white with stripes | » |

•The solution composition (in g/liter) was: nickel sulfate 25, ammonium fluoride 20. Solution temperature: initial 83°, final 88°. Charge 0.3 $dm^2$/0.1 liter. Solution not stirred.

TABLE 5

Effect of Nickel Sulfate Concentration on the Growth Rate and Quality of the Layer and the Physicochemical State of the Solution•

| Amount of $NiSO_4 \cdot 7H_2O$ (g/liter) | Solution pH | | Layer thickness ($\mu$) after exposure time | | Microhardness of coating (kg/mm²) | Potential of layer (v) | External appearance of coating | Appearance of solution after experiment |
|---|---|---|---|---|---|---|---|---|
| | before expt. | after expt. | 20 min. | 60 min. average | | | | |
| 20 | 6.92 | 7.07 | 10.3<br>10.0 | 30.45 | 604 | —0.162 | Bright | Colorless |
| 25 | 6.86 | 6.8 | 12.1<br>11.2 | 34.95 | 604 | —0.012 | The same | Greenish |
| 30 | 6.8 | 6.72 | 12.1<br>12.2 | 36.45 | 604 | —0.05 | » | Green, powder-like precipitate |
| 35 | 6.78 | 6.68 | 13.0<br>12.8 | 38.7 | 604 | —0.071 | » | The same |
| 40 | 6.78 | 6.55 | 12.6<br>12.9 | 38.25 | 604 | —0.086 | » | » |
| 45 | 6.73 | 6.5 | 12.2<br>12.7 | 37.8 | 604 | —0.096 | » | » |
| 50 | 6.73 | 6.55 | 12.1<br>12.7 | 37.2 | 604 | —0.137 | Milk-white with stripes | » |

•The solution composition (in g/liter) was: sodium hypophosphite 30, ammonium fluoride 15. Solution temperature: initial 84°, final 90°. Charge 0.3 $dm^2$/0.1 liter. Solution not stirred. The pH was determined a second time on the following day.

to hardness and porosity (for layers deposited under constant conditions) but there are considerable differences in their chemical resistance.

It is possible that under conditions of frictional wear with the use of lubricants a dull surface, having spaces between the crystals because of looser packing, would absorb more oil and would therefore suffer less wear, but, under conditions in which the layer must also be chemically resistant, dull surfaces apparently cannot compete with bright.

## SUMMARY

1. With the use of ammonium fluoride as a buffer addi tive nickel plating may be effected at solution pH of about 7, the deposition rate of nickel in a freshly prepared solution being up to 30-35$\mu$ per hour.

2. Bright nickel deposits formed with the use of ammonium fluoride buffer and under specified conditions have high chemical resistance when tested in accordance with GOST 3003-50.

3. Deposits of different physicochemical properties may be obtained by the use of solutions of different compositions.

4. With a solution containing 25-30 g sodium hypophosphite per liter and at high pH the hardness of the nickel layer reaches 600-700 kg/mm$^2$ after deposition, and increases considerably after heat treatment.

5. The nickel layers formed in presence of ammonium fluoride buffer have low porosity both in bright and in dull deposits if the solution temperature is above 70° and the layers are over 10$\mu$ thick.

6. The electrode potentials of nickel layers formed in presence of ammonium fluoride buffer vary by + 0.3 v (from − 0.225 to +0.07 v) in accordance with the solution concentration and operating conditions.

## LITERATURE CITED

[1] N. T. Kudryavtsev, Electroplating Technology [in Russian] (State Light Industry Press, 1940).

[2] V. I. Lainer and N. T. Kudryavtsev, Fundamentals of Electroplating, I [in Russian] (Metallurgy Press, 1953).

[3] E. Lamer Gostin, Iron Age, 171, 24, 115 (1953).

[4] K. M. Gorbunova and A. A. Nikiforova, J. Phys. Chem. 28, 883 (1954) [USSR].

[5] P. P. Belyaev, M. I. Zil'berfarb and M. P. Garetovskaya, Metallic Coatings in Chemical Equipment Construction, II [in Russian] (Sci. Res. Inst. for Chemical Machinery Construction, 1951) p. 144.

[6] G. Gutzett and E. T. Mapp, Corros. Technol., 3, 10, 331 (1956).

[7] Russell H. Wolff, Mary Ann Henderson, and Stanley L. Eisler, Plating, 5, 537 (1955).

[8] "New nonelectrolytic process," Precis Metal Mold, 14, 6, 66 (1956).

[9] J. Starr, Pacif. Factory, 83, 6, 30, 60 (1955).

[10] M. M. Khrushchev and E. S. Berkovich, Microhardness Determination by the Indentation Method [in Russian] (Izd. AN SSSR, 1943).

[11] A. T. Vagramyan and Z. A. Solov'eva, J. Phys. Chem. 26, 903 (1952), [USSR].

Received July 5, 1957.

# ELECTROLYTIC NICKEL DEPOSITS FORMED IN THE PRESENCE OF SULFONATED NAPHTHALENE

V. V. Ostroumov

The presence of sulfonated naphthalene in nickel electrolytes causes a number of changes in the course of electrolytic deposition of nickel and in the properties of the metal deposits formed. Certain observations characterizing these changes are detailed below.

## EXPERIMENTAL DATA AND DISCUSSION

Fig. 1 shows photographs of ordinary and bright nickel deposits with layers 100 $\mu$ thick. The deposits were formed on flat polished brass cathodes. No surface roughness can be detected on the bright nickel under the metallographic microscope. Individual grains cannot be resolved by the ordinary microscope in cross sections of bright nickel deposits; only a layer structure parallel to the cathode plane can be detected [1]. The view held by certain workers that bright nickel deposits have an extremely fine microcrystalline structure therefore seems probable. It is known that a sufficient condition for the formation of bright layers in some cases is that the grains constituting the deposits should be very small [2]. However, other workers found that the crystallites in bright and dull deposits are of the same order of magnitude [3], and that differences in properties are determined by the texture and the specific crystallization conditions. Thus, there is no complete agreement on this subject as yet.

Variations of surface relief of the nickel deposits are shown by profilograms obtained with the aid of Levin's profilograph, Model IZP-5 [4]. Nickel layers were deposited on flat polished cathode surfaces from electrolytes without additives (Fig. 2, a) and with addition of sulfonated naphthalene (Fig. 2, b). The thickness of the nickel layers was varied form 3 to 100 $\mu$ in both cases. The profilograms were obtained with 1000-fold enlargement in the horizontal direction, and 2000-fold in the vertical direction.

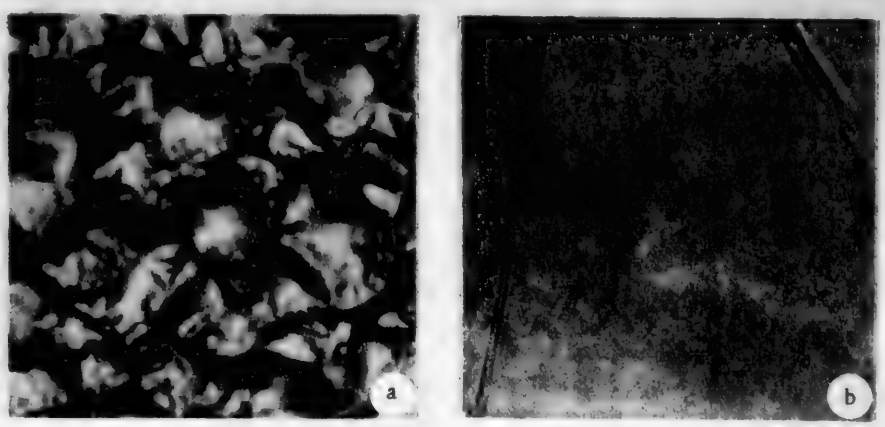


Fig. 1. Surfaces of electrolytic nickel deposits (not etched): nickel deposits: a) dull, b) bright; magnification 2600.

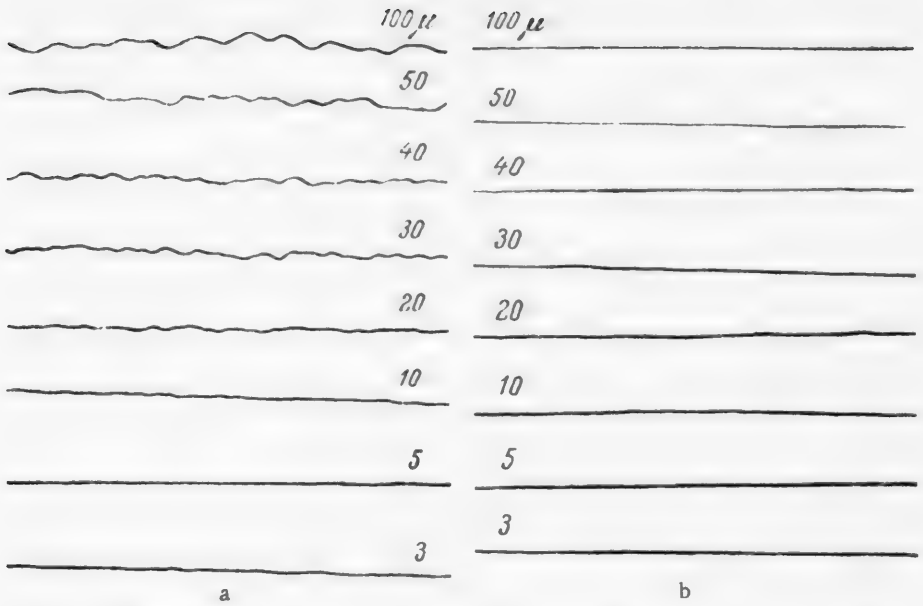


Fig. 2. Profilograms of dull (a) and bright (b) nickel deposits of different thickness: magnification: horizontal, 1000; vertical, 2000.

The profilograms show that the surface roughness of ordinary nickel deposits increases with increasing layer thickness. Measurements showed that in layers 100 $\mu$ thick the height of the surface projections exceeds 1 $\mu$. The surface of a bright nickel layer remains specular from the start of electrolysis up to a layer thickness of 100 $\mu$.

For evaluation of the "leveling power" of deposits, often discussed in the literature [5], the experimental conditions were modified somewhat. Three cuts each 4-5 $\mu$ deep were made on the surface of each polished bronze cathode by means of the diamond cutter of an indexing machine. The profilograms shown in Fig. 3 were taken in a direction at right angles to the cuts before and after deposition of nickel layers 5, 15, 30, and 50 $\mu$ thick. The diagram clearly shows progressive leveling of the cuts, which disappear completely at a sufficient layer thickness. Whereas the surface or ordinary nickel (Fig. 3, a) develops its own roughness, only leveling of the cuts made by the diamond cutter can be observed on the bright nickel surface (Fig. 3, b).

These experiments do not justify the assertion that leveling of irregularities on the cathode surface is characteristic of bright nickel deposits only. Leveling occurs with dull deposits also, as in clearly seen in the photograph of a cross section of a nickel deposit formed from an electrolyte without added sulfonated naphthalene (Fig. 4).

In this case the cathode surface was again cut, and nickel layers 5, 10, 15, and 27 $\mu$ (total nickel thickness 57 $\mu$) were deposited. To separate the nickel layers, thin layers of copper were deposited between them from a cyanide bath. The photograph shows clearly that the original surface irregularity of the cathode is leveled out during deposition of dull nickel.

Simple geometrical considerations suggest that almost any electrodeposited metal gradually levels out microirregularities on the cathode (certain details of the leveling process have been discussed in the literature [6]). In the deposition of dull layers (for example, of nickel) the leveling effect is obscured by the roughness due to the deposit itself.

The results of numerous observations have led to the conclusion that decrease of the grain size in the deposit increases hardness [7]. Recently the hardness of nickel deposited from electrolytes free from brighteners were determined by Fedot'ev and Vyacheslavov in relation to electrolysis conditions and electrolyte composition [8]. The existence of an inverse relationship between grain size and hardness of the deposit was confirmed

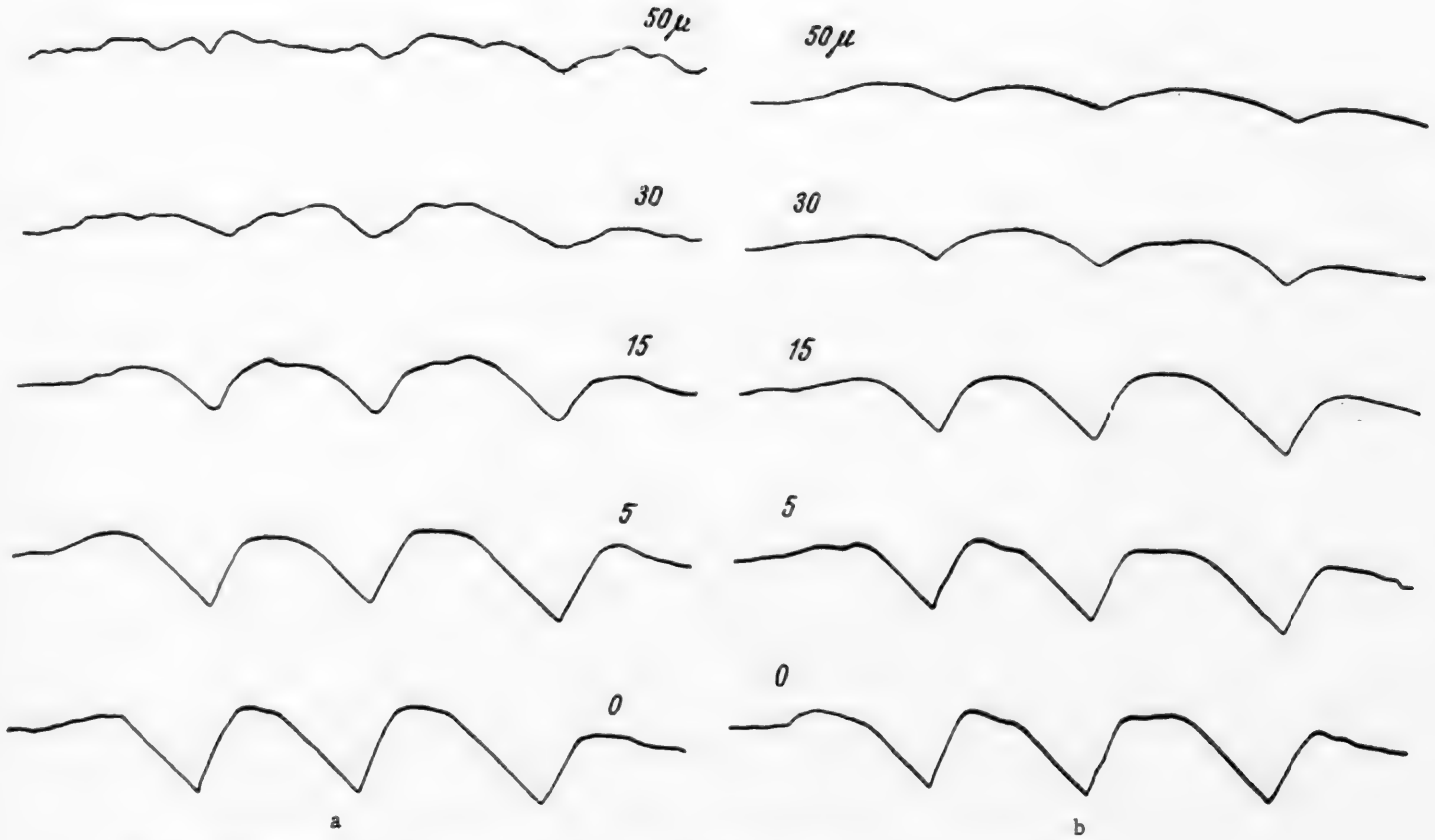


Fig. 3. Leveling of surface roughness of a cathode in deposition of a) dull and b) bright nickel; Deposit thickness ( $\mu$): 0, 5, 15, 30, 50. Magnification: horizontal, 1000 ; vertical, 2000.

by a number of examples. Since crystallite size influences the surface relief of the deposit, Fedot'ev and Vyacheslavov were even able to deduce a quantitative relationship between the surface roughness and the hardness of the nickel deposit.

Our measurements show that bright nickel deposits are harder than ordinary nickel (Fig. 5). This is an indirect indication that the metal crystallites formed in presence of sulfonated naphtalene are smaller.

The hardness determinations were carried out by means of the Hanemann microhardness tester (model D-30) [9].

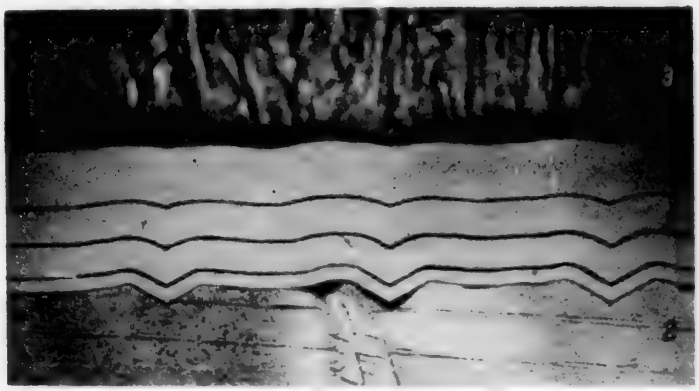

Fig. 4. Cross section of dull nickel deposits of thickness: 5, 10, 15, and 27 $\mu$ etched in hot solution of 1% KOH + 1% $K_2S_2O_8$: 1) nickel layers, 2) basis metal, 3) protective copper layer; magnification 610

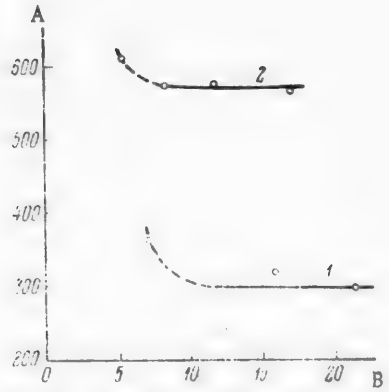


Fig. 5. Hardness of nickel deposits: A) hardness (kg / mm$^2$), B) length of diagonal of imprint ( $\mu$); curves: 1) dull nickel, 2) bright nickel.

In all cases nickel layers 20-40 $\mu$ thick were deposited in order to eliminate the influence of the properties of the basis metal on the results. Nickel deposits of equal thickness were made when it was necessary to compare their hardness. The metal was deposited from a solution of $NiSO_4 \cdot 7H_2O$, 170 g/liter, $H_3BO_3$, 30 g/liter, KCl, 5 g/liter, pH 6-6.3; temperature 40°; current density 30 ma/cm$^2$; the electrolyte contains 4.6 g of sulfonated naphthalene per liter.

Internal mechanical stresses in electrolytic nickel deposits can reach very high values [10]. Nickel deposits formed from electrolytes without brighteners have a tendency to contract. Introduction of sulfonated naphthalene into the electrolyte changes the nature of the stresses: the deposits show a tendency to expansion [11].

To illustrate this behavior, Fig. 7 shows the results of observations of the deflection of the free end of a flexible cathode, the other end of which was firmly fixed in a conducting clamp. The electrolyte was a solution of very low nickel sulfate content: $NiSO_4 \cdot 7H_2O$ 9.5 g/liter, $H_3BO_3$ 25 g/liter, NaCl 15 g/liter, pH = 4.6. This electrolyte composition was chosen in order to decrease the current efficiency for the metal and to cause appreciable evolution of hydrogen at the cathode.

The observation procedure did not differ from that described earlier for studies of mechanical stresses in palladium deposits [12].

After 30 minutes of electrolysis the current was switched off but the observations were continued. In the electrolyte without sulfonated naphthalene there was contraction of the deposit, which continued for some time after the current was switched off (Fig. 7, Curve 1). In presence of sulfonate naphthalene (3 g/liter) the deposit expanded during electrolysis – the flexible cathode deviated in the opposite direction (Fig. 7, Curve 2), but here also there was some contraction of the deposit after the current was switched off. In both cases contraction

after disconnection of the current was evidently caused by loss of dissolved hydrogen from the deposits and the consequent shortening of the distance between the lattice points in nickel. The degree of contraction after the end of electrolysis is small in comparison with the total effect indicated by deflection of the contractometer leaf.

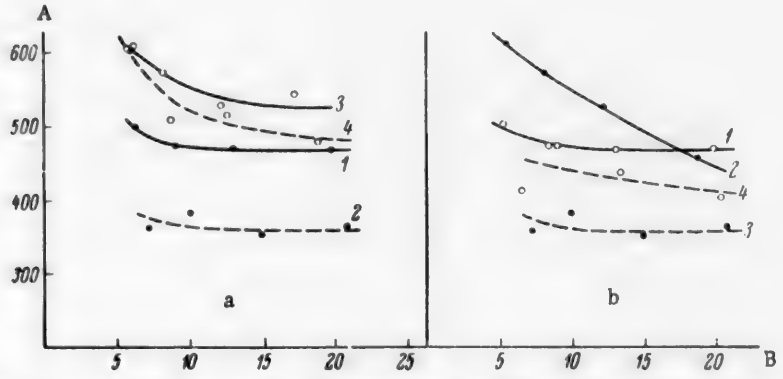


Fig. 6. Effects of electrolyte pH, temperature, and current density on the hardness of bright nickel deposits:
A) hardness (kg/mm$^2$), B) length of diagonal of imprint ($\mu$); a) current density 10 ma/cm$^2$ : pH and temperature (°C): 1) 4 and 20, 2) 4 and 40, 3) 6 and 20, 4) 6 and 40; b) pH = 4; temperature (° C) and current density (ma/cm$^2$): 1) 20 and 10, 2) 20 and 30, 3) 40 and 10, 4) 40 and 30.

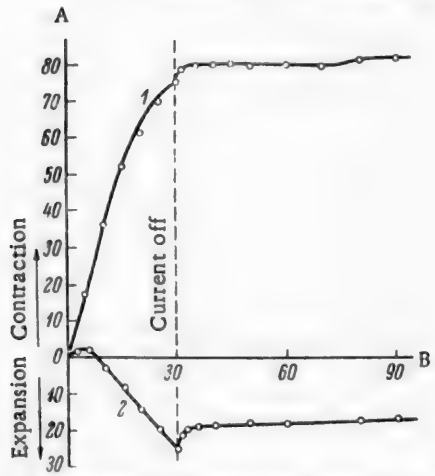


Fig. 7. Variations of mechanical stresses in nickel deposits during electrolysis and after cessation of electrolysis:
A) deflection of end of flexible cathode, B) time (minutes); electrolyte: 1) without additive, 2) with 3 g sulfonated naphthalene per liter.

To illustrate the influence of dissolving hydrogen on expansion of nickel deposits, Fig. 8 shows deflections of a flexible cathode (with a layer of electrolytic nickel on one side) during periodic polarization in a solution free from nickel salts. After the current was cut off the expansion of the deposit gradually vanished, and the contractometer leaf returned to its initial position, indicating loss of dissolved hydrogen from the nickel. The occurrence of volume changes in the nickel lattice, as indicated by x-ray data, has been repeatedly reported in the literature [13].

Whereas contraction of the nickel deposit (Fig. 7, Curve 1) during electrolysis may be attributed to simultaneous deposition of hydrogen, formation of an expanded metal lattice, and subsequent gradual loss of hydrogen to the surroundings, expansion of the deposit in presence of sulfonated naphthalene (Fig. 7, Curve 2) cannot be attributed to the action of hydrogen, if only because the expansion does not disappear after cessation of electrolysis.

It should be noted that the expansion of electrolytic metal deposits in the course of their formation is, in general, difficult to interpret in the light of the hypotheses advanced so far on this subject [2, 12]. Some investigators tend to ascribe an obviously exaggerated significance to intercrystallite layers in the deposit [11]. Apart from the fact that the nature of the presumed intercrystallite layers is not clear, another assumption is necessary – that in the substance of the intercrystalline layers changes take place which lead to increase in the volume of this substance and thereby to "expansion" of the whole electrolytic deposit.

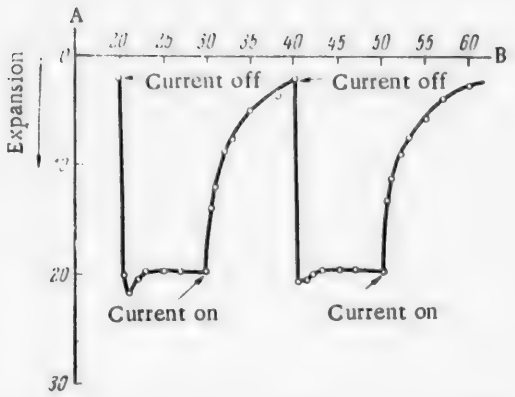


Fig. 8. Expansion of a nickel deposit in periodic cathodic hydrogenation in an electrolyte free from nickel salts (15 g $H_3BO_3$ and 5 g KCl per liter): A) deflection of end of flexible cathode, B) time (minutes).

We believe that the cause of expansion of the electrolytic deposit should rather be sought in characteristics of the growth of the crystallites of the metal itself, constituting the main bulk of the deposit. Expansion of the cathodic deposits is not a secondary effect, but is an effect associated with the main process — formation and growth of the metal crystallites.

Studies of the growth of single crystals of salts in aqueous saturated solutions have revealed the existence of pressure in the growth direction of the crystal face, i.e., at right angles to the plane of the face [14]. It is reasonable to postulate the existence of such pressure in the growth of crystallites constituting the multicrystalline metal deposit on the cathode. Each crystallite tends to increase in size and to be covered by the faces which are determined by the electrolysis conditions. However, this tendency is restricted because the space in lateral directions is limited by the presence of neighboring crystallites; this ultimately results in a tendency to expansion, acting along the cathode surface. If the cathode can bend, this tendency leads to a certain expansion of the deposit.

Secondary processes, foremost among which is dissolution of hydrogen in the metal, can disturb this normal tendency of the electrolytic deposit to expansion. In the case of palladium [12] and dull nickel the hydrogen dissolved in the metal has a strong influence on the natural course of stress formation; in consequence contraction rather than expansion may occur in the metal layers. Nickel deposits formed in presence of sulfonated naphthalene are composed of fine crystallites and therefore have an extensive network of interfaces. There is no doubt that growth of fine crystallites would result in a greater total expansion force than would be produced by large crystallites in a deposit of the same thickness. The tendency to expansion in a system of fine crystallites ultimately outweighs contraction of the deposit caused by secondary processes of hydrogen dissolution (Fig. 7, Curve 2).

## SUMMARY

1. It is shown that "leveling" of cathode roughness is caused by both bright and dull nickel deposits.

2. The hardness of bright nickel deposits was determined, and was found to be almost double the hardness of dull nickel deposits.

3. It is suggested that expansion of electrolytic deposits is a normal process which is disturbed by secondary processes such as liberation of hydrogen together with the metal.

## LITERATURE CITED

[1] E. Raub and M. Wittum, Z. Elektroch. 46, 2, 71 (1940).

[2] V. I. Lainer, Electrolytic Polishing and Etching of Metals [in Russian] (Moscow, 1947) p. 177; A. T. Vagramyan and Z. A. Solov'eva, Methods of Investigation of Processes of Metal Electrodeposition [in Russian] (Moscow, 1955) p. 122.

[3] K. M. Gorbunova, T. V. Ivanovskaya and N. A. Shishakov, Zh. Fiz. Khim. 25, No. 8, 981 (1951); G. L. Clark and S. H. Simonsen, J. Electroch. Soc., 98, 110 (1951).

[4] B. M. Levin, Contact Method for Measurement of Surface Microgeometry. Principles of the Method and Optical Profilographs [in Russian] (Moscow-Leningrad, 1950).

[5] A. Bregman, Met. Progr., 60, 1, 50 (1951).

[6] G. D. Foulke and O. Kardas, Techn. Proceed. 43-rd Ann. Convention Am. Electropl. Soc., June 17-21, 172 (1956); O. Kardas, ibid, p. 181.

[7] D. J. Mac Naughton, J. Iron and Steel Inst; 109, 409 (1936); D. J. Mac Naughton and A. W. Hothersall, Trans. Far. Soc., 24, 387 (1928); 31, 1168 (1935).

[8] N. P. Fedot'ev and P. M. Vyacheslavov, Inform. Tech. Leaflet No. 97 (785) (Sci.-Tech. Propaganda Office, Leningrad, 1955).

[9] E. O. Bernhardt, Zeiss Nachrichten, 3, 8, 280 (1940); Druckschrift, Mikro, 11-676-1 (554).

[10] V. S. Ioffe, Progr. Chem. 13, No. 1, 48 (1944) [USSR].

[11] A. G. Samartsev and Yu. V. Lyzlov, J. Phys. Chem. 29, No. 2, 374 (1955) [USSR].

[12] V. V. Ostroumov, J. Phys. Chem. 31, No. 8, 1812 (1957) [USSR].

[13] S. Ogawa, J. Tech. Phys. 8, 96 (1938); L. Jang, J. Electroch Soc., 97, 241 (1950).

[14] V. D. Kuznetsov, Crystals and Crystallization [in Russian] (Moscow, 1953) p. 110.

Received June 14, 1957.

# ELECTROLYTIC SEPARATION OF BINARY ALLOYS OF LEAD WITH SILVER AND ARSENIC

E. B. Gitman and Yu. K. Delimarskii

As is known, the crude lead which is the first product in the smelting of lead is purified by a complex metallurgical process which is followed by electrolytic refining from aqueous electrolytes.

Several investigations have recently been carried out on electrolytic refining of lead from fused salts. This method has a number of advantages, the most important of which is the possibility of intensifying the process by the use of high current densities; moreover, remelting of the metal for production of anodes is not necessary.

It has been shown by Alabyshev and Gel'man [1] and in our earlier investigations [2,3] that by treatment of lead alloys and crude lead by this method it is possible to reduce the bismuth content of the cathodic metal to 0.001-0.004%, and the antimony content to 0.02-0.06%. Gold does not enter the cathodic metal at all. If the zinc content of the alloy is low, zinc likewise does not enter the cathodic metal.

The question of the behavior of silver and arsenic was not elucidated in the series of investigations of the electrolytic refining of lead from fused salts. This question is also of interest because these metals are not extracted completely by furnace refining of lead. The behavior of lead alloys relatively rich in arsenic and silver has already been investigated [2,4], but the results were not very clear.

The aim of the present work was therefore to obtain more precise information on the behavior of these metals in electrolytic refining of lead from fused salts.

## EXPERIMENTAL

The salt melts and binary metallic alloys were prepared in the same way as in the previous investigations [2,3]. A porcelain beaker was used for electrolysis. After fusion of the electrolyte two test tubes were put into the beaker. One was filled with the binary metal alloy which acted as the anode, and the other served as the receiver for the cathodic metal. Each test tube had an orifice in its side 20 mm from the bottom. The leads all consisted of tungsten wire enclosed in thin porcelain tubes to insulate them from the electrolyte. The cathode and anode areas were chosen so as to give the lowest possible current density at the anode and fairly high current density at the cathode [5].

The silver and arsenic contents of the lead and electrolyte were determined by measurements of the radiation intensity of radioactive isotopes silver-110 and arsenic-76. Silver or arsenic tagged with the corresponding radioactive isotope was introduced for this purpose into melted lead during preparation of the original alloys. In addition, in some experiments arsenic was determined in the alloys by the chemical method in accordance with GOST 2076-48.

Analysis of three average one-gram samples of lead-silver alloys showed that the metallic impurity was distributed uniformly in the previously prepared original metallic alloy. The results indicate that the activities of different samples of solutions containing active silver differed little (2492, 2537, 2425 pulses per minute).

Electrolytic separation of lead-silver alloy. The electrolysis was performed at different current densities, with different silver contents in the original alloy, and with different degrees of extraction of lead from it.

It follows from the data in Table 1 that most of the silver remains in the anode alloy. With a silver content of the order of 0.25% in the original alloy its content in the cathodic metal is a few thousandths of one per cent. If the silver content of the anode alloy is increased to 2.5%, its content in the cathodic metal is approximately 1/20 of the original. It is noteworthy that at a very low silver content (about 0.0002%) in the original alloy (Experiment No. 4), at relatively high cathodic and anodic current densities, and with a fairly high percentage extraction of lead from the anode alloy the silver content of the cathodic lead decreases only slightly.

TABLE 1

Results of Experiments on Electrolytic Separation of Pb-Ag Alloys

| Experiment No. | Electrolysis conditions | | | | Total activity of solutions of cathodic and anodic metals and electrolyte (pulses/minute) | Activity of solution of original metal (pulses/minute) | Deviation (%) | Ag content of cathodic lead (%) | Ag content of electrolyte (%) |
|---|---|---|---|---|---|---|---|---|---|
| | Ag content of original alloy(%) | $D_a$ (amp/cm$^2$) | $D_c$ (amp/cm$^2$) | Extraction (%) | | | | | |
| 1 | 0.06 | 0.2 | 1.0 | 80 | 5492 | 5115 | 7.3 | 0.0001 | 0.0003 |
| 2 | 0.06 | 0.5 | 2.2 | 80 | 5206 | 5115 | 1.8 | 0.0001 | 0.0003 |
| 3 | 0.06 | 0.5 | 2.2 | 80 | 4920 | 5115 | 3.8 | 0.0002 | 0.0003 |
| 4* | 0.0002 | 0.5 | 2.2 | 80 | — | — | — | 0.00016 | — |
| 5 | 0.125 | 0.2 | 1.0 | 75 | — | — | — | 0.003 | 0.001 |
| 6 | 0.125 | 0.5 | 2.2 | 77 | — | — | — | 0.001 | — |
| 7 | 0.125 | 0.5 | 2.2 | 80 | 9326 | 10000 | 6.7 | 0.001 | 0.001 |
| 8** | 0.125 | 0.5 | 2.2 | 85 | 10682 | 10000 | 6.8 | 0.005 | 0.002 |
| 9 | 0.25 | 0.2 | 1.0 | 50 | 20529 | 21670 | 5.2 | 0.00002 | 0.001 |
| 10 | 0.25 | 0.2 | 1.0 | 75 | 21534 | 21850 | 1.4 | 0.0014 | 0.002 |
| 11 | 0.25 | 0.2 | 1.0 | 79 | 21196 | 21990 | 3.6 | 0.009 | 0.004 |
| 12 | 0.25 | 0.5 | 2.2 | 81 | 21112 | 20260 | 4.2 | 0.002 | 0.002 |
| 13 | 0.25 | 0.5 | 2.2 | 82 | 18819 | 22150 | 7.0 | 0.001 | 0.001 |
| 14 | 2.5 | 0.2 | 1.0 | 50 | 221326 | 238700 | 7.2 | 0.01 | — |
| 15 | 2.5 | 0.2 | 1.0 | 50 | 101273 | 101850 | 0.6 | 0.2 | 0.004 |
| 16 | 2.5 | 0.2 | 1.0 | 50 | 96024 | 109750 | 12.5 | 0.16 | 0.009 |

*Original alloy-cathodic metal of Experiment No. 3; electrolyte of Experiment No. 3.

**Electrolysis performed in cell with communicating cathode and anode compartments.

The second series of experiments was conducted under the same conditions as the first, but in a cell of different design. In this case the cathode and anode compartments of the cell were not test tubes with orifices but two porcelain crucibles under the electrolyte. The anodic crucible contained Pb-Ag alloy, and the cathodic, pure lead. Tungsten wire was used for the leads. The results show that in this case there was more silver in the cathodic metal and electrolyte than was found in the preceding experiments. This is probably because mixing can take place more easily in a cell of this type than in the cell described above.

These results lead to the conclusion that if crude lead contains a relatively large amount of silver (from 0.25 to 2.5%), by a second refining of the anode alloy the silver content can be reduced to about 0.00016%, i.e., lead of S-O grade with respect to silver can be obtained.

Electrolytic separation of lead-arsenic alloy. It was found in one of the earlier investigations [2] that there is virtually no codeposition of arsenic with lead, but the arsenic content of the anode alloy falls somewhat. These results suggested that the arsenic trichloride formed at the anode during electrolysis volatilizes at the temperature of the experiment. This suggestion was based on studies of the anodic behavior of alloys rich in arsenic, the content of which was determined by chemical analysis. By this method it was not possible to determine the arsenic balance over all the parts of the cell.

To determine the arsenic distribution in the electrolysis products we performed two experiments with

lead-arsenic anode alloy containing about 2% of arsenic tagged with radioactive arsenic-76. The electrolysis was carried out under the following conditions: anodic current density 0.2 amp/cm$^2$, cathodic current density 1.0 amp/cm$^2$; extraction of lead from the anode alloy reached 90%. Results of the experiments are given in Table 2.

TABLE 2

Results of Experiments on Electrolytic Separation of Pb-As Alloy

| Balance of pulses in 5 minutes for solutions of | | | | Pulses in 5 minutes for solutions of original alloy | Deviation (%) |
|---|---|---|---|---|---|
| cathode alloy | anode alloy | electrolyte | total | | |
| 100 | 95426 | Not detected | 95526 | 109100 | 12.4 |
| 526 | 220800 | Not detected | 221326 | 229152 | 3.4 |

TABLE 3

Results of Experiments on Removal of Arsenic from Lead

| Electrolysis conditions | | | Degree of extraction (%) | Arsenic content of metal (%) | |
|---|---|---|---|---|---|
| $D_a$ (amp/cm$^2$) | $D_c$ (amp/cm$^2$) | U(amp-hr) | | original | cathodic |
| 0.2 | 1.0 | 1 | 50 | 1.3 | Not detected |
| 0.2 | 1.0 | 1 | 70 | 1.3 | 0.0008 |
| 0.5 | 2.2 | 1 | 60 | 1.3 | 0.003 |
| 0.5 | 2.2 | 1 | 96 | 1.3 | 0.015 |
| 0.5 | 2.2 | 1 | 80 | 0.64 | 0.001 |

It follows from the data in Table 2 that deviations of the aggregate pulses in all the solutions after electrolysis from the value for the original solution is within the limits of experimental error. Hence, it may be concluded that almost all the arsenic is concentrated in the anode alloy, and if any is present in the electrolyte, the amounts are negligible. The somewhat higher percentage deviation in the first experiment can, in our opinion, be attributed to the lower specific activity of the $As^{76}$ preparation available to us.

The results of some experiments on the removal of arsenic from lead are given in Table 3.

With 1.3% arsenic in the original anode alloy, at $D_a$ = 0.2 amp/cm$^2$, and with 50% extraction of lead, arsenic is not found in the cathodic metal. At higher extractions (up to 80%) traces of arsenic are detected in the cathodic metal, measured in thousandths of one per cent. Only if the extraction of lead is increased to 96% does the arsenic content of the cathodic metal rise above 0.1%.

## SUMMARY

1. When lead-silver alloy is refined from fused media, with 0.25% silver in the original alloy and 80% extraction of lead from the anode alloy, the silver content of the cathodic lead is a few thousandths of one per cent; with 2.5% silver in the original alloy and 50% extraction of lead from the anode alloy the silver content of the cathodic lead is some tenths of one per cent.

The silver content of cathodic lead can be reduced to about 0.0002% by repeated refining.

2. When lead containing arsenic is electrolytically refined from fused media, the arsenic is concentrated in the anode alloy. With 50% extraction of lead from the anode alloy, no arsenic is detected in the cathodic lead, while with 80% extraction of lead, the arsenic content of the cathodic metal is some thousandths of one per cent.

## LITERATURE CITED

[1] A. F. Alabyshev and E. M. Gel'man, Nonferrous Metals 2, 37 (1946). [USSR].

[2] Yu. K. Delimarskii, P. P. Turov, and E. B. Gitman, Ukrain. Chem. J., 21, 687 (1955).

[3] E. B. Gitman and Yu. K. Delimarskii, Ukrain. Chem. J. 22, 731 (1956).

[4] A. A. Kolotii and Yu. K. Delimarskii, Ukrain. Chem. J. 22, 466 (1956).

[5] P. Drossbach, Z. Elektroch., 45, 534 (1939).

Received May 27, 1957

# ELECTROCHEMICAL TINNING OF IRON FROM HALIDE SOLUTIONS CONTAINING FLUORIDES OF ALKALI AND ALKALINE-EARTH METALS

A. N. Kruglov and V. P. Kochergin

Halide solutions are used in modern high-speed electrolytic tinning iron. Among the components of these solutions are the fluorides of ammonia or sodium which, as is noted in the literature [1,2] assist in the formation of complex compounds of the type $Me_2[SnCl_2F_2]$, $Me_2[SnF_4]$ etc. Their stability depends not only on the nature of the central atom and, in part, of the ligands, but especially on the nature of the cations in the outer sphere of the complex. The greater the radius and the lower the charge of these cations, the less is their polarizing force, with the possibility of decomposition of the complex compound into its components.

In our earlier studies of halide electrolytes [3,4] it was assumed that the cations in the outer sphere of the above-mentioned complex compounds are sodium or ammonium. It was also shown experimentally that in the electrodeposition of tin, cathodic polarization increases sharply, owing to presence of complex anions in the electrolyte, and compact cathodic deposits of tin are formed.

If we take into account the dependence of the stability of a complex compound on the nature of the cations in its outer sphere and, further, the regular change of cathodic polarization in the electrodeposition of tin with changes in the stability of the complex compound, it is of great interest to investigate the deposition of tin in presence of alkali and alkaline-earth fluorides in the halide solutions. The possibility is not excluded that in presence of these fluoride cations in the halide solutions complex anions differing in stability would be formed, which could lead to a considerable improvement in the quality of cathodic tin deposits formed in electrode deposition of tin, and hence in the quality of the tin plate.

## EXPERIMENTAL AND DISCUSSION OF RESULTS

The fluorides of lithium, potassium, magnesium, calcium, strontium, and barium were used in preparation of halide solutions for tin plating, in addition to fluorides of sodium and ammonia [3]. It is known [5,6] that the former fluorides (apart from KF) have low solubility in water. There is almost no information in the literature concerning their solubilities in other media [7].

The solubilities of these fluorides in a solution of the composition*: $SnCl_2$ 0.21 mole/liter, HCl (free) 3-4 g/liter, gelatin 1 g/liter, was determined at 20, 30, 40, and 50° by a known method [7]. The time of stirring was 12 hours. After the solutions had been allowed to settle, LiF was determined from the fluorine content [9], $SrF_2$ and $BaF_2$ gravimetrically [10], and $MgF_2$ and $CaF_2$ by means of Trilon [11] after removal of stannous chloride from solution by means of $H_2S$ in hydrochloric acid. The results of the determinations are given in Fig. 1; it is seen that the solubilities of the fluorides of lithium and alkaline-earth metals increase with temperature and with increasing atomic number of group II elements in the Mendeleev periodic system. An interesting fact is that this variation of fluoride solubility also holds for 0.5 N HCl solution (see table).

Comparison of the data in the table and Fig. 1 shows that the solubilities of lithium and alkaline-earth fluorides is very much higher in the electrolytic tinning bath than in 0.5 N HCl solution. This may be the consequence of complex formation between stannous chloride and the added fluorides. Because of the high solubility found for the fluorides of alkali and alkaline-earth metals, they can be used as electrolyte components.

*The solutions were prepared from analytical-grade $SnCl_2$ and HCl, the synthesized fluorides [8], and redistilled water.

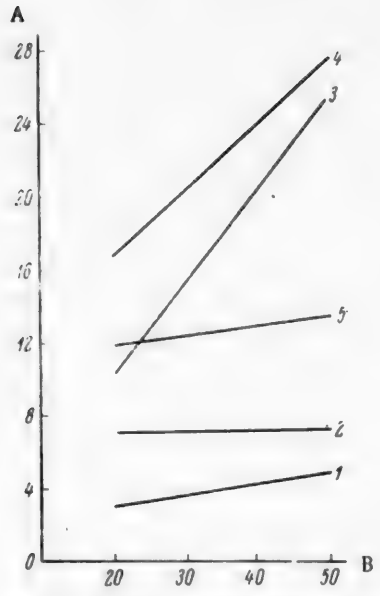


Fig. 1. Effect of temperature on the solubility of fluorides in a solution containing: $SnCl_2$ 0.21 mole/liter, $HCl_{free}$ 3-4 g/liter, gelatin 1 g/liter:
A) solubility (g/liter), B) temperature (deg); fluorides: 1) $MgF_2$, 2) $CaF_2$, 3) $SrF_2$, 4) $BaF_2$, 5) $LiF_2$.

If the assumption that these complex compounds are formed in the halide solutions is valid, these compounds may influence cathodic and anodic polarization [4, 12] in the electrodeposition of tin. To study this process, polarization curves were determined with the aid of a special electrolytic cell, and electronic potentiometer, and a universal 9-channel oscillograph. Before each experiment the platinum cathode and anode were coated with compact layers of tin (up to 100 $\mu$) from an alkaline stannate electrolyte [3]. The polarization current was measured by a milliammeter and varied by means of a rheostat, the slider of which was moved with the aid of a direct-current motor.

Halide solutions of the following composition were studied: $SnCl_2$ 0.2 /mole/liter, $HCl_{free}$ 3-4 g/liter, gelatin 1 g/liter, LiF 0.5, NaF (KF, $NH_4F$) 0.6 and 0.9 mole/liter, $MgF_2$ ($CaF_2$, $SrF_2$, $BaF_2$) 0.07 mole/liter.

The surface-active additives used were 0.05 mole/liter of phenol, Leukotron B, and Na cresolsulfonate. The results of determinations of anodic and cathodic polarization in electrodeposition of tin from halide solutions containing fluorides of alkali and alkaline-earth metals are combined in Fig. 2. It is seen that cathodic polarization in the electrodeposition of tin progressively increases in solutions containing $MgF_2 < CaF_2 < SrF_2 < BaF_2$, and also $LiF < NaF < KF < NH_4F$, while anodic polarization changes only slightly under these conditions.

This increase of cathodic polarization in electrocrystallization of tin from halide solutions by introduction of fluorides may be attributed to increasing stability of the tin-binding complex compounds forming in the solutions owing to decreasing polarizing action of the outer cations in the series $Li^{+1} > Na^{+1} > K^{+1}$ and $Mg^{+2} > Ca^{+2} > Sr^{+2} > Ba^{+2}$.

Solubilities of Fluorides in 0.5 N HCl Solution and in Water (20°) [6]

| Medium | Solubility (g/liter) | | | | | | |
|---|---|---|---|---|---|---|---|
| | LiF | NaF | KF | $MgF_2$ | $CaF_2$ | $SrF_2$ | $BaF_2$ |
| 0.5 N HCl . . . . . | 5.5 | 53.2 | – | 3.4 | 1.5 | 6.0 | 10 |
| $H_2O$ . . . . . | 2.6 | 41.7 | 949.3 | 0.075 | 0.0156 | 0.12 | 1.33 |

This relationship suggests that cathodic tin deposits formed from halide solutions containing KF or $BaF_2$ should be of better quality than deposits formed from solutions containing LiF or $MgF_2$.

The slight changes of anodic polarization in these experiments are most likely due to the low contents of complex compounds in the halide solutions [14].

The influence of surface-active substances such as phenol, Leukotron B, and Trilon B on cathodic and anodic polarization in electrodeposition of tin from halide solutions containing KF and $MgF_2$ is shown in Figs. 3 and 4. These graphs suggest that cationic organic additives (Leukotron B) have a considerable influence on cathodic polarization, while molecular additives (phenol) have less. This effectively confirms the views put forward by Antropov concerning the relationship between electrocapillary zero and the deposition potential of a metal. Since in the electrodeposition of tin its cathodic potential is shifted in the negative direction from the electrocapillary zero [16], cationic additives (such as Leukotron B) rather than molecular, and especially than anionic additives should influence the polarization and the structure of the cathodic deposit.

These investigations lead to another noteworthy result, namely, that surface-active additives have an

appreciable influence on cathodic polarization if unstable complex compounds are formed in solution, as in presence of $MgF_2$ (Fig. 4). In this case electrolytic reduction of the metal is hindered by adsorption of surface-active substances. Conversely, the latter do not have any appreciable effect on the cathode process in electrodeposition of the metal if complex anions which bind tin stably are formed in solution, as in the presence of KF.

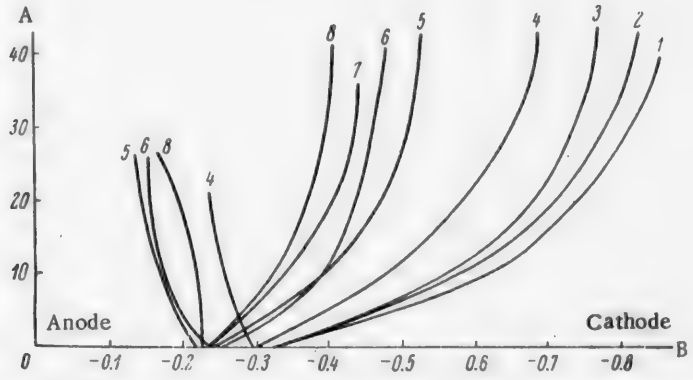


Fig. 2. Effects of alkali and alkaline-earth fluorides on cathodic and anodic polarization at 50° in a solution containing $SnCl_2$ 0.21 mole/liter, $HCl_{free}$ 3-4 g/liter, gelatin 1 g/liter:
A) current density (amp/dm$^2$), B) potential (v); Fluoride contents (moles/liter): 1) $NH_4F$ 0.9, 2) KF 0.9, 3) NaF 0.9, 4) LiF 0.5, 5) $BaF_2$ 0.07, 6) $SrF_2$ 0.9, 7) $CaF_2$ 0.07, 8) $MgF_2$ 0.07.

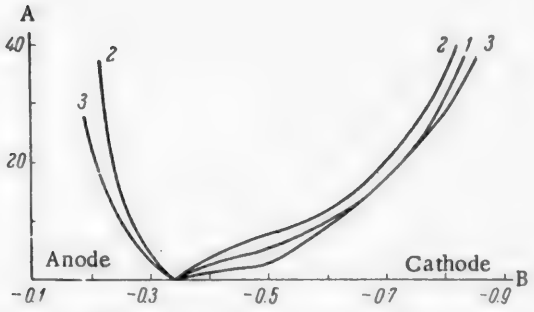


Fig. 3. Effects of surface-active additives on cathodic and anodic polarization at 50° in a solution containing $SnCl_2$ 0.21 mole/liter, $HCl_{free}$ 3-4 g/liter, gelatin 1 g/liter, KF 0.9 mole/liter:
A) current density (amp/dm$^2$), B) potential (v); additions (mole/liter): 1) no addition, 2) Trilon B 0.05, 3) phenol 0.05.

This result is of practical significance, as it gives rise to the possibility of a reduction in the concentration of organic additives, which in a number of cases decrease electrolyte stability.

To investigate the effect of the nature of organic compounds and their dissociation characteristics on their adsorbability, electrocapillary, curves on mercury were determined by the known method [17]. The results of the determinations are given in Fig. 5. As was to be expected, gelatin and Leukotron B are cationic while Na cresolsulfonate is anionic. In simultaneous presence of gelatin and phenol or gelatin and Leukotron B the surface tension of mercury decreases (as the result of increased adsorption) to a greater extent than in presence of gelatin alone. This is in agreement with the results of Loshkarev [17, 18] and also with results obtained in studies of cathodic polarization in electrodeposition of tin from halide solutions [3]. A different effect is observed when a technical dry-distilled coal-tar fraction (b.p. 150°) is added to the solution. In presence of this fraction and gelatin (Fig. 5) the surface tension of mercury (at the maximum of the electrocapillary curve) was greater than in presence of gelatin. This is most likely due to displacement • from the electric double layer of gelatin particles (amino compounds) by surface-active particles present in this coal-tar fraction. This accounts for the decrease of cathodic polarization in the electrodeposition of tin from a halide solution containing 1 g of gelatin and 10 g of the technical fraction per liter, as compared with cathodic polarization in a solution which contains only gelatin as the organic additive [4].

•This idea was put forward by Academician A. N. Frumkin at the Electrochemical Conference in Vilnius (1956). It has also been noted as the result of experimental investigations [19].

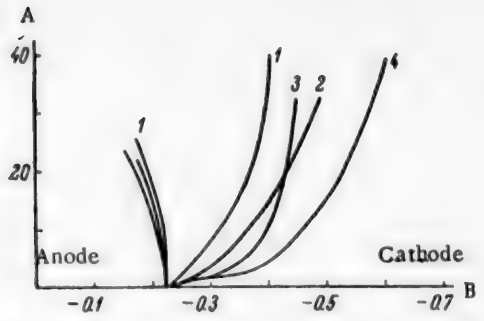


Fig. 4. Effects of surface-active substances on cathodic and anodic polarization at 50° in a solution containing: $SnCl_2$ 0.21 mole/liter, $HCl_{free}$ 3-4 g/liter, gelatin 1 g/liter, $MgF_2$ 0.07 mole/liter:
A) current density (amp/dm$^2$), B) potential (v); additions (mole/liter); 1) no addition, 2) phenol 0.05, 3) Trilon B 0.05, 4) Leukotron B 0.05.

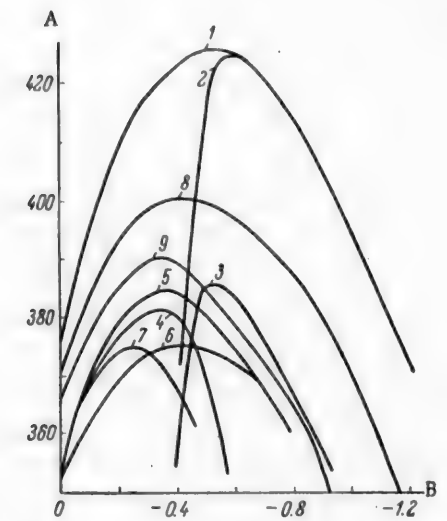


Fig. 5. Electrocapillary curves for solutions containing 11 g HCl per liter, 0.21 mole $SnCl_2$ per liter, and added surface-active substances: A) surface tension (ergs/cm$^2$), B) potential (v); additions: 1) no additive, 2) $SnCl_2$, 3) $SnCl_2$ + + gelatin 0.2 g/liter, 4) gelatin 1 g/liter, 5) gelatin 0.2 g/liter, 6) gelatin 0.2 g/liter + + phenol 0.05 mole/liter, 7) gelatin 0.2 g/liter + Leukotron B 0.05 mole/liter, 8) technical 150° fraction 5 g/liter, 9) technical 150° fraction 5 g/liter + gelatin 0.2 g/liter.

In Fig. 5 the anodic branch of the electrocapillary curve for a hydrochloric acid solution of $SnCl_2$ is almost vertical, and joins the cathodic branch at −0.62 v. This effect is due partially to formation of a dilute tin amalgam, and mainly to adsorption, at the low mercury potential, of complex anions (probably $[SnCl_4]^{-2}$ [20,21]) which at potentials above − 0.62 v are displaced from the electric double layer. These results qualitatively confirm the complex-forming power of stannous ions.

Introduction of sodium fluoride into halide solutions increased cathodic polarization and favored formation of compact cathodic tin deposits [3]. It was therefore of interest to study the quality of cathodic tin deposits formed from halide electrolytes in presence of fluorides of alkali and alkaline-earth metals. As before, tin was deposited from halide solutions on rotating specimens of cold-rolled sheet from the "Zaporozhstal'" works [3,4]. The halide solutions studied contained fluorides of alkali (0.6 or 0.9 mole/liter) and alkaline-earth (0.07 mole/liter) metals, phenol (0.05 mole/liter), stannous chloride (0.21 mole/liter), $HCl_{free}$ (3-4 g/liter), and gelatin (1 g/liter). The same organic surface-active additives were used as before. Tin was deposited on the specimens at current densities of 20, 30, 40, and 50 amp/dm$^2$ and 50°. The cathodic current density 20-40 amp/dm$^2$ was 85-95%. The tin deposits were surface-melted in presence of a flux at 600-700° [3,4].

Halide solutions containing magnesium or calcium fluoride and phenol or Leukotron B as the organic additive yielded microcrystalline tin deposits at $D_c$ = 20 and 30 amp/dm$^2$; at $D_c$ = 40-50 amp/dm$^2$ dendrites on a microgranular sublayer were deposited. Bright melting of these tin deposits gave a wavy surface. Good-quality tin deposits not more than 1 $\mu$ thick were formed at $D_c$ = 40-50 amp/dm$^2$ from solutions containing strontium or barium fluoride and the same organic additives. Tin deposits up to 1.5 $\mu$ thick were formed from halide solutions containing LiF and 0.05 mole/liter of phenol, Leukotron B, or Trilon B at $D_c$ = = 20-40 amp/dm$^2$. These deposits fused satisfactorily without droplet formation.

Halide solutions containing KF (0.3, 0.6, and 0.9 mole/liter) were studied in greater detail. At KF concentration of 0.3 mole/liter the tin deposits formed were similar to those formed from solutions containing $CaF_2$ or $MgF_2$ (0.07 mole/liter) at $D_c$ = 40-50 amp/dm$^2$; i.e, dendrites were formed. The probable reason was the small amount of complex tin compound present in solution. At KF concentration of 0.6 mole/liter compact gray tin deposits were formed which fused without droplet formation. Surface-active additives (phenol or Leukotron B, 0.05 mole/liter) favored the deposition of compact tin layers 2.0 $\mu$ thick, which had a specular surface after fusion. Tin deposits formed from solutions containing KF (0.9 mole/liter) and the above-named additives at $D_c$ = 40-50 amp/dm$^2$ were up to 3.5 $\mu$ thick, and were satisfactory in bright melting.

These investigations therefore confirmed that the electrodeposition of tin is influenced by the presence, in the halide solutions, of alkali and alkaline-earth fluorides, which form complex compounds with stannous ions. The stability of these compounds increases in the fluoride series: magnesium, calcium, strontium, barium, and lithium, sodium, potassium. Cathodic polarization in electrodeposition of tin increases in the same sequence, with improvement in the quality of the cathodic tin deposits, the thickness of which can be taken up to 3.5 $\mu$. Bright melting of these deposits is not accompanied by droplet formation. These results offer the possibility of a solution of the problem of the electrochemical production of tin plate with coatings over 2$\mu$ thick [22].

## SUMMARY

1. The solubility of alkali and alkaline-earth fluorides in 0.5 N HCl solution and in a solution containing $SnCl_2$ 0.21 mole/liter, HCl 3-4 g/liter, and gelatin 1 g/liter increases in the series of $Mg^{+2} - Ca^{+2} - Sr^{+2} - Ba^{+2}$, and $Li^{+1} - Na^{+1} - K^{+1}$ fluorides. Under the same conditions, the solubility of (for example) $BaF_2$ is 1.33 g/liter in water, 10 g/liter in 0.5 N HCl, and 16.61 g/liter in the tin-plating solution of the above composition.

2. Cathodic polarization is greater in the electrodeposition of tin from solutions containing the fluorides of lithium (0.5 mole/liter), sodium and potassium (0.9 mole/liter), and magnesium, calcium, strontium, and barium (0.07 mole/liter) in addition to $SnCl_2$, HCl, and gelatin. Cathodic polarization is lower in solutions containing alkaline-earth fluorides than in solutions containing alkali metal fluorides.

3. Cathodic tin deposits 1-1.5 $\mu$ thick, electrodeposited from halide solutions in presence of alkaline earth fluorides and organic additives (gelatin, phenol) at current densities not over 35 amp/dm$^2$ and 50° give specular surfaces by bright melting; compact tin deposits up to 3.5 $\mu$ thick are deposited from halide solutions in presence of KF and organic additives (phenol and Leukotron B) at $D_c$ = 40-50 amp/dm$^2$ (with a current efficiency of 85-95%); these give good bright melting.

## LITERATURE CITED


[1] J. W. Cuthbertson et al., J. Electrochem. Soc. 100, No. 3, 107 (1953).

[2] A. E. Davies and R. M. Angles, Metal Ind. 5, 463 (1953).

[3] V. P. Kochergin, T. A. Nimvitskaya, and M. Ya. V'yunova, J. Appl. Chem. 30, No. 1 97 (1957)[USSR].*

[4] V. P. Kochergin, T. A. Nimvitskaya and A. N. Kruglov, Proc. Conference on the Influence of Surface-Active Substances on Electrodeposition of Metals [in Russian] (Acad. Sci. Lithuanian SSR, 1957) p. 95.

[5] Chemist's Concise Handbook, 2 (in Russian) (Goskhimizdat, 1956).

[6] Yu. Yu. Lur'e, Calculation and Reference Tables for Chemists [in Russian] (Goskhimizdat, 1956).

[7] L. M. Mikheev, A. V. Novoselova, et al. J. Inorg. Chem. 1, 499 (1956).

[8] Yu. V. Karyakin and I. I. Angelov, Pure Chemical Reagents [in Russian] (Goskhimizdat, 1955).

[9] S. I. Orlova and D. S. Abramson, Control of Electrolytes and of Electrodeposit Quality [in Russian] (Mashgiz, 1950).

[10] W. F. Hillebrand and G. E. Lundell, Applied Inorganic Analysis (Goskhimizdat, 1937) [Russian translation].

[11] M. M. Sochevanova, Industrial Lab. 21, 530 (1955) [USSR].

[12] P. S. Titov, Coll. Sci. Trans. Moscow Inst. Nonferrous Metals and Gold 25, 361 (1955).

[13] V. I. Lainer and N. T. Kudryavtsev, Fundamentals of Electroplating [in Russian] (Metallurgy Press, 1953).

[14] A. A. Grinberg, Introduction to the Chemistry of Complex Compounds [in Russian] (Goskhimizdat, 1951).

[15] L. I. Antropov, J. Phys. Chem. 25, 1494 (1961) [USSR].


*Original Russian pagination. See C. B. translation.

[16] I. E. Gurevich, J. Appl. Chem. 28, 285 (1955) [USSR].*

[17] M. A. Loshkarev, V. I. Sotnikova and A. A. Kryukova, J. Phys. Chem. 21, 219 (1947). [USSR].

[18] V. N. Sotnikova and M. A. Loshkarev, J. Gen. Chem. 20, 755 (1950). [USSR].

[19] L. S. Zagainova and A. G. Stromberg, Proc. Acad. Sci. USSR 105, 747 (1955).

[20] B. V. Nekrasov, Course of General Chemistry [in Russian] (Goskhimzidat, 1952) p. 526.

[21] A. N. Frumkin and N. S. Polyanovskaya, J. Phys. Chem. 32, 157 (1958). [USSR].

[22] J. H. Mort, Iron and Steel, 30, 5, 183 (1957).

Received September 13, 1957.

* Original Russian pagination. See C.B. translation.

# ELECTRODEPOSITION OF CHROMIUM FROM A TETRACHROMATE BATH

A. Ya. Ryaboi and M. A. Shluger

The numerous investigations directed toward further improvement of the chromium-plating process have not yet yielded definite results which would make it possible to raise current efficiency, lower the temperature, and increase the throwing power of chromium electrolytes. Tetrachromate electrolyte must be regarded as one of the promising electrolytes for chromium depositon [1].

According to the literature, tetrachromate electrolytes yield almost nonporous, gray, easily polished deposits at room temperature, at a high current efficiency. In view of the fact that after being polished these coatings acquire a luster similar to that of chromium coatings from the usual electrolytes, and that the porosity of the coatings is low, tetrachromate electrolytes are of interest in relation to the production of protective and decorative coatings on steel without the use of under layers.

These electrolytes are especially worthy of attention for industrial use because of the low stresses in the coatings formed and of the high throwing power of the electrolytes. Studies of tetrachromate electrolytes are of great theoretical as well as practical importance. Investigation of the role of NaOH in the chromium-plating process may help to elucidate the mechanism of chromium deposition, which has not been studied sufficiently as yet.

The industrial adoption of this process is very difficult because data on chromium deposition from tetrachromate electrolytes are lacking in the literature.

The purpose of the present investigation was a study of the electrodeposition of chromium from tetrachromate electrolyte, and determination of certain properties of the deposits formed.

## EXPERIMENTAL

The electrolyte used for the experiments had the following composition (in g/liter): $CrO_3$ – 360-400, NaOH – 50 – 60, $H_2SO_4$ – 2 – 2.5, sugar 0.8–2. The current density was 50 amp/dm$^2$, temperature 20 ± 0.2°; electrolysis time 15 minutes.

The electrolyte was not subjected to preliminary electrolysis before the experiments.

The principal experiments were performed with steel specimens in the form of 2 cm square plates 1-1.5 mm thick. Perforated anodes 100 cm$^2$ in area were placed on each side of the specimen 7 cm from its surface. The electrolyte volume was 1.5 liters.

The specimens were ground and polished before application of the coatings. They were then degreased in gasoline and electrochemically (2 minutes at the cathode and 1 minute at the anode) in a solution of the usual composition. The specimens were pickled first in 10% sulfuric acid solution for 10 seconds, and then anodically in chromium electrolyte for 1 minute at current density of 40-50 amp/dm$^2$.

The specimens were held in special frames of organic glass, which shielded the edges, in order to ensure more uniform distribution of chromium over the surface.

Current efficiency was calculated from the weight changes of the specimens as the result of chrome-plating. Polarization curves were determined by means of the PPTV-1 potentiometer or the A4-M2 cathode voltmeter. A calomel half cell was used as the reference electrode.

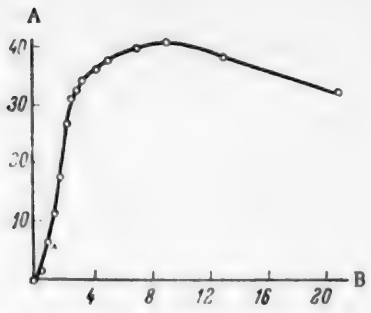


Fig. 1. Effect of sulfuric acid concentration on current efficiency: electrolyte composition (g/liter): $CrO_3$ 400, NaOH 60, sugar 1.5; current density 50 amp/dm$^2$, temperature 20°; A) current efficiency for chromium (%), B) $H_2SO_4$ concentration (g/liter).

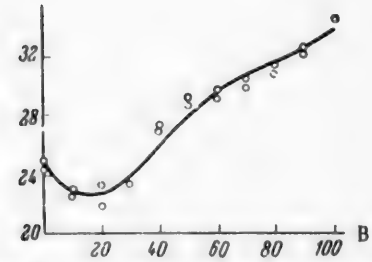


Fig. 2. Effect of caustic soda concentration on current efficiency: electrolyte composition (g/liter): $CrO_3$ 400, $H_2SO_4$ 2.5, sugar 1.5; current density 50 amp/dm$^2$, temperature 20°; A) current efficiency for chromium (%), B) NaOH concentration (g/liter)

Microhardness was determined by means of the PMT-3 apparatus, and internal stresses were investigated by the flexible-cathode method [2] with a special apparatus.

Porosity was determined by the usual method with the use of a solution of the following composition (in g/liter): potassium ferricyanide 10, ammonium chloride 30, sodium chloride 60.

Before the porosity determinations the chrome-plated objects were degreased and then kept in 3% NaCl solution of 45° for 10-15 minutes.

## Current Efficiency for Chromium

Effect of sulfuric acid. In experiments performed in order to study the influence of sulfuric acid concentration on current efficiency for chromium the sulfuric acid content of the electrolyte was varied in the range of 0.18-21.5 g/liter.

Fig. 1. shows that the relationship between current efficiency and sulfuric acid concentration is of the usual character for chromium electrolytes. The current efficiency has a maximum at a definite concentration.

However, good deposits are not obtained over the entire range of sulfuric acid concentration. In absence of sulfuric acid, or at low concentrations, the current efficiency is very low and only a black deposit is formed on the surface of the specimens. With increase of $H_2SO_4$ concentration the deposits become paler and velvety. The best deposits, easily polished, are obtained in the range of 1.5-2.5 g $H_2SO_4$ per liter. The optimum concentration is 2.0-2.5 g/liter, when good deposits are obtained at a current efficiency of 25-30%. At sulfuric acid concentrations of 7 g/liter, and over, bright stripes appear at the edges of the specimens, and the chromium becomes brittle and peels off. With a sulfuric acid content of 21.5 g/liter the deposit is dark.

Effect of alkali. Caustic soda is added to the electrolyte in order to form sodium tetrachromate, $Na_2O \cdot 4CrO_3$. The role of the tetrachromate ion in electrolysis is not sufficiently understood. It was therefore necessary to obtain the most detailed data possible on the influence of NaOH concentration on current efficiency and on a number of properties of the deposit and electrolyte. The caustic soda content of the electrolyte was varied in the range of 0-140 g/liter. At first, on addition of 10-20 g of caustic soda per liter, the current efficiency falls a little. (Fig. 2). The current efficiency then increases with increase of caustic soda concentration. Good chromium deposits are obtained with caustic soda contents of up to 60 g/liter, with current efficiencies of up to 30%. At 80-100 g/liter stripes of bright, brittle chromium deposits appear on the edges of the specimens; i.e., the external appearance is similar to that observed on excess increase of sulfuric acid concentration. With 140 g of caustic soda per liter chromium is not deposited. Thus for NaOH, as for $H_2SO_4$, there is a certain optimum concentration at which chromium is deposited at maximum current efficiency.

Polarization curves were plotted in order to determine the influence of caustic soda on the mechanism of chromium deposition.

Fig. 3 shows polarization curves for solutions of different caustic soda contents (0-150 g/liter) at 20-22°.

It is seen that at first addition of NaOH shifts the polarization curve in the direction of more positive cathodic potentials (Curves 2 and 3); this indicates that introduction of caustic soda facilitates the electrode

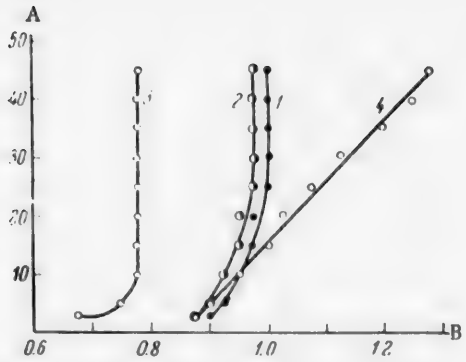


Fig. 3. Polarization curves for electrolyte containing (g/liter): $CrO_3$ 400, $H_2SO_4$ 2.5, sugar 1.5; A) current density (amp/$dm^2$), B) cathode potential (v); NaOH content (g/liter): 1) without NaOH, 2), 20, 3) 60, 4) 150.

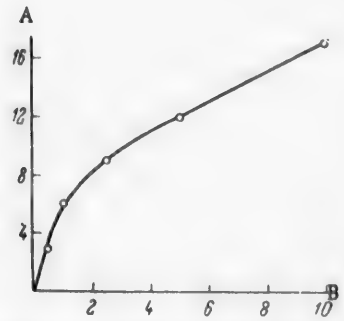


Fig. 4. Variation of the trivalent chromium content of the electrolyte with the amount of sugar added: A) $Cr_2O_3$ concentration (g/liter), B) amount of sugar added (g/liter); electrolyte composition (g/liter): $CrO_3$ 400, $H_2SO_4$ 2.5, NaOH 60.

process. Addition of a considerable amount of caustic soda (150 g/liter) when, as stated earlier, chromium is not deposited, shifts the polarization curve in the negative direction (Curve 4). This shows that excessive increase of the caustic soda concentration hinders the cathode reaction.

Effect of trivalent chromium. In the recipes given in various literature sources special reference is made to the necessary contents of trivalent chromium.

In our experiments the sugar concentration was varied from 0 to 10 g/liter, which corresponds to variations of trivalent chromium concentration from 0 to 17 g/liter (Fig. 4).

The experimental results show that trivalent chromium does not have any significant influence on current efficiency (Fig. 5). The small increase of current efficiency with increasing content of trivalent chromium is not of practical interest because brittle deposits which chip off are formed from electrolytes of this composition. The external appearance of the chromium coatings varies with the trivalent chromium content of the electrolyte. For example, at $Cr^{III}$ concentrations up to 10 g/liter the deposits are of good quality. When the $Cr^{III}$ concentration is 12 g/liter, brittle deposits which chip off form at the specimen edges. At 17 g of $Cr^{III}$ per liter, black chromium of unsatisfactory quality is deposited. The optimum sugar addition is 1.5-2 g/liter, when about 8-10 g/liter of trivalent chromium (calculated as $Cr_2O_3$) is formed in the electrolyte.

Effect of chromic anhydride. The experiments were performed with electrolytes containing from 100 to 500 g $CrO_3$ per liter.

The results (Fig. 6) showed that chromium is not deposited at a chromic anhydride concentration of 100 g/liter. On further increase of $CrO_3$ concentration to 260 g/liter chromium is deposited at high current efficience (45.4%). Subsequent increase of the chromic anhydride concentration reduces the current efficiency. Deposits of good quality are obtained at a concentration of 350-400 g of chromic anhydride per liter.

This dependence of current efficiency on the chromic anhydride concentration shows that in chromium plating it is very important to maintain the optimum ratio between $CrO_3$ and catalytic anions. The optimum ratio is obtained only at a strictly definite $CrO_3$ content.

Effect of temperature. To determine the effect of temperature on current efficiency the electrolyte temperature was varied in the 12-45° range.

It follows from Fig. 7 that the current efficiency changes little (by only 3%) with increase of temperature between 12 and 35°, but it drops sharply (by 11%) in the 35-45° range. The external appearance of the deposit also changes from a gray velvety color to pale gray, almost lustrous in the center of the specimen (at 35°). At 45° bright instead of gray chromium is deposited.

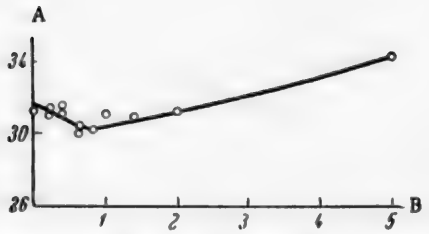


Fig. 5. Effect of trivalent chromium (addition of sugar to the electrolyte) on current efficiency:
electrolyte composition (g/liter): $CrO_3$ 400, $H_2SO_4$ 2.5, NaOH 60; current density 50 amp/dm$^2$, temperature 20°; A) current efficiency (%), B) sugar concentration (g/liter)

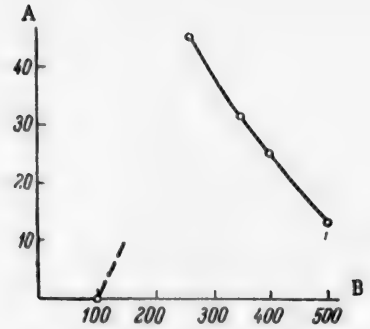


Fig. 6. Effect of chromic anhydride concentration on current efficiency: electrolyte composition (g/liter: $H_2SO_4$ 2.5, NaOH 60, sugar 1.5; current density 50 amp/dm$^2$, temperature 20°; A) current efficiency (%), B) $CrO_3$ concentration (g/liter).

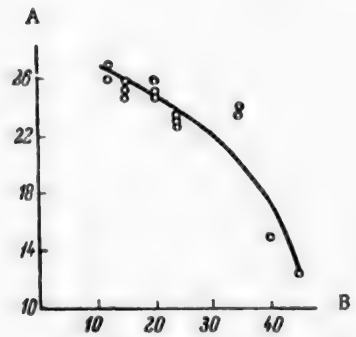


Fig. 7. Effect of electrolyte temperature on current efficiency:
electrolyte composition (g/liter): $CrO_3$ 400, $H_2SO_4$ 2.5, NaOH 60, sugar 1.5; curent density 50 amp/dm$^2$; A) current efficiency (%), B) temperature (°C).

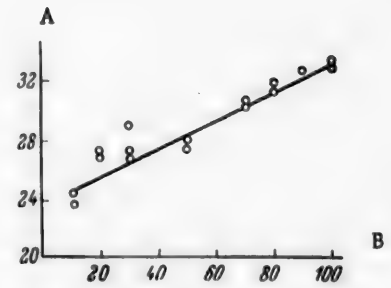


Fig. 8. Effect of current density on current efficiency:
electrolyte composition as shown in Fig. 7; temperature 20°; A) current efficiency (%), B) current density (amp/dm$^2$).

The effect of temperature on current efficiency and on the external appearance of the deposit may be attributed to the influence of temperature on tetrachromate. According to literature data [1], tetrachromate is stable up to 35°. Above 35° tetrachromate decomposes, with a sharp decrease of current efficiency and a change in the structure and external appearance of the deposit.

It should be pointed out, however, that the influence of temperature on the stability of tetrachromates has not been studied sufficiently. Therefore the observed changes cannot be ascribed to decomposition of tetrachromate only. Decomposition of tetrachromate is a reversible reaction. This is indicated by the following fact: after the electrolyte had been heated to 100° and then cooled to 20°, its initial properties were restored.

20° should be regarded as the optimum temperature.

Effect of current density. Current density was varied in the range of 10-100 amp/dm$^2$.

It follows from Fig. 8 that the current efficiency increases with increasing current density from 10 to 100 amp/dm$^2$. The external appearance of the deposit also varies with the current density. Good-quality deposits are those formed at current densities from 40 to 80 amp/dm$^2$. Increase of current density to 100 amp/dm$^2$ is permissible, but some faults at the specimen edges are observed at this current density.

## Some Properties of Coatings Formed from Tetrachromate Electrolyte

Microhardness. A distinctive characteristic of deposits formed from tetrachromate electrolytes is their low hardness. The chromium coatings have hardness of the order of 350-400 kg/mm$^2$ and can easily be polished to a luster usual in chromium coatings.

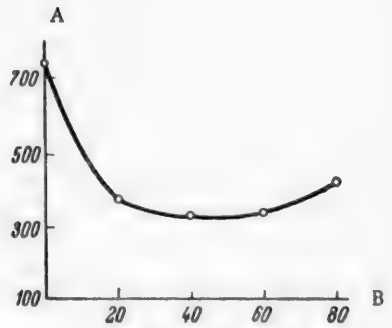


Fig. 9. Effect of caustic soda concentration on the microhardness of chromium coatings:
electrolyte composition as given in Fig. 7; current density 50 amp/dm$^2$, temperature 20°; A) microhardness (kg/mm$^2$), B) NaOH concentration (g/liter).

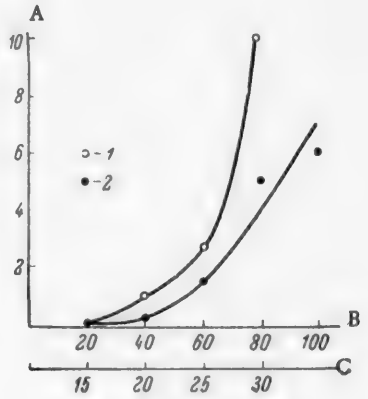


Fig. 10. Effects of electrolyte temperature and current density on porosity of chromium coatings:
electrolyte composition as given in Fig. 7; A) porosity (pores/cm$^2$) B) current density (amp/dm$^2$), C) temperature (°C): 1) f(t°), 2) f($D_c$).

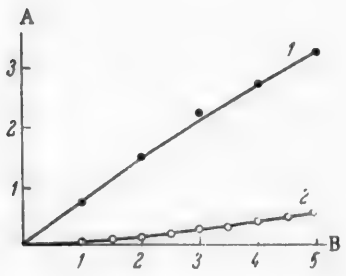


Fig. 11. Effect of thickness of chromium coatings on internal stresses:
A) displacement of cathode end (mm), B) coating thickness ($\mu$) 1) electrolyte containing (g/liter): 250 $CrO_3$ and 2.5 $H_2SO_4$, temperature 50°, current density 50 amp/dm$^2$; 2) tetrachromate electrolyte, temperature 22°, current density 40 amp/dm$^2$.

One of the most important factors determining hardness of the coatings is the caustic soda concentration. Hardness decreases with increase of NaOH concentration, and it is at a minimum at NaOH concentrations of 40-60 g/liter (Fig. 9).

Thus, it is possible to obtain chromium coatings from tetrachromate electrolyte which are twice or three times as soft as those formed from the usual electrolyte which are twice or three times as soft as those formed from the usual electrolytes.

Porosity. It is known that porosity of chromium coatings is the main cause of electrochemical corrosion of steel chromium-plated articles. To avoid corrosion, special chrome-plating procedures are used in order to obtain the so-called "milky" nonporous coatings.

Our experiments showed that coatings formed from tetrachromate electrolyte at 20-25° and current density 40-60 amp/dm$^2$ are of almost the same porosity as "milky" coatings [3]. The results of the experiments are plotted in Fig. 10.

It follows from Fig. 10 that porosity of the chromium deposits increases with increasing electrolysis temperature and current density.

The steel chromium-plated specimens were also tested for corrosion resistance by immersion in 3% sodium chloride solution for 500 hours at 20-25°. No traces of corrosion could be detected after these tests on specimens with coatings 30 and 60 $\mu$ thick.

Objects coated with triple Ni + Cu + Ni layers and objects coated in tetrachromate electrolyte were exposed on deck of the Diesel ship "Gruziya" [4]. The ship "Gruziya," which took our Olympic team to Melbourne, was at sea for 7 months and crossed the tropics twice. At the end of this time the objects coated with the triple layers were corroded, but no corrosion was found on objects chromium plated from the tetrachromate bath.

Internal stresses and structure of deposits. Internal stresses in electrolytic coatings have serious effects on their hardness, porosity [5], and other properties. It was therefore necessary to obtain comparative data on internal stresses in coatings formed from the usual and cold tetrachromate electrolytes.

In these experiments the coatings were deposited on plates 0.1 mm thick, 70 mm long, and 7 mm wide.

It follows from Fig. 11 that the internal stresses in coatings fromed from tetrachromate electrolytes are much lower than in those formed from the ordinary electrolyte.

It was shown by x-ray structural analysis that under the optimum conditions chromium of the hexagonal modification is deposited from tetrachromate electrolytes.

## SUMMARY

1. The optimum composition of cold tetrachromate electrolyte for chromium plating is (in g/ liter): chromic anhydride 350-400, sulfuric acid 2-2.5,caustic soda 40-60, sugar or glucose 1.5-2.

2. Plating from tetrachromate electrolytes should be carried out at 20± 3°, at current densities in the range of 40-80 amp/dm$^2$.

3. Chromium deposits formed from tetrachromate electrolytes have low hardness (350-400 kg/mm$^2$) and lower internal stresses and porosity than coatings deposited from the usual solution.

4. Tetrachromate electrolytes can be used for application of protective and decorative coatings without the use of copper or nickel underlayers. The thickness of the chromium coating must not be less than 20 $\mu$.

## LITERATURE CITED

[1] F. Taylor, Electroplating, 5, 4 (1952).

[2] M.,A. Shluger, Industrial Lab. 9 (1953) [USSR].

[3] V. I. Lainer and N. T. Kudryavtsev, Fundamentals of Electroplating, 1 [in Russian] (Metallurgy Press, 1953).

[4] S. L. Koltunov and N. A. Bogakovskii, News Letter on Exchange of Technological Experience of the Ukrainian Industrial Council, 37/109 (1957).

[5] A. T. Vagramyan and Z. A. Solov'eva, Methods of Investigation of Processes of Metal Electrodeposition [in Russian] (Izd. AN SSSR, 1955).

Received February 14, 1958.

# CATALYTIC REDUCTION OF FURFURAL TO SYLVAN

A. S. Sultanov and V. A. Maslennikova

Institute of Chemistry, Academy of Sciences Uzbek SSR

In connection with the extensive development of the wood hydrolysis industry, numerous investigations relating to syntheses based on furfural have been reported in the literature during the past few decades. Among the numerous chemical conversions of furfural, its reduction to sylvan is a reaction of independent interest.

Searches for a convenient method of effecting this reaction have been mainly concentrated on the conversion of furfural to piperylene by way of sylvan and tetrahydrosylvan. It is known that piperylene yields a rubber similar to butadiene rubber as the result of hot-sodium polymerization [1], and the rubber made by emulsion polymerization has satisfactory properties [2].

Recently Livshits and his co-workers have reported on their synthesis of rubberlike polymers of piperylene made by bulk polymerization and in aqueous emulsion They showed that rubber made from piperylene polymers is not inferior in its general properties to butadiene rubber [3]. Sylvan itself can be used as a solvent, and it can also be converted into a better solvent, tetrahydrosylvan [4], and into a number of other valuable products. However, the lack of convenient preparation methods is evidently an obstacle to wide utilization of sylvan derived from furfural.

Literature data show that the possible conversion of furfural to sylvan has been studied quite extensively [5-24]. Holdren [25] attempted to reduce furfural and furfuryl alcohol to sylvan by a flow method in presence of a known copper chromite catalyst [25]. He was able to show that if a mixture of furfural vapor and hydrogen in 1:5 molar ratio is passed through a layer of supported copper chromite catalyst heated to 200-225°, sylvan is formed in 95% yield, while furfuryl alcohol yields up to 70% of the theoretical yield of sylvan. The catalyst was used for 3 months with frequent reactivation. During this time 23 experiments and 22 reactivations were performed. The time of continuous operation of the catalyst in a single experiment is not given. On repeating these experiments we found that it is necessary to operate at a very low load on the catalyst; the catalyst rapidly became unserviceable and several days were required for reactivation. The yield was considerably lower than reported. Tsuda and co-workers [23] were also unable to obtain sylvan in yields over 44%. It was therefore necessary to find an effective catalyst for reduction of furfural to sylvan in a continuous process.

Metallic zinc was chosen as the basis for the catalyst, as it converts certain aldehydes to hydrocarbons by the Clemmensen reaction. In the Clemmensen reaction carbonyl compounds are reduced by hydrogen liberated by the action of hydrochloric acid on zinc. It is likely that the hydrogen at the instant of liberation covers the zinc surface to form a thin catalyst layer on which carbonyl groups are reduced to hydrocarbons.

Under conditions of heterogeneous catalysis, reduction of furfural with the aid of hydrochloric acid cannot, of course be expected to take place. It was therefore decided to use zinc alloyed with copper, which in its active state would convert molecular to atomic hydrogen and transfer it to the zinc.

To obtain zinc and copper in their active forms it was decided to use a ternary copper-zinc-aluminum alloy. The aluminum component of the alloy is readily removed by alkali, leaving zinc and copper in active form on the alloy surface. In order to avoid loss of zinc, 3% alkali solution was used.

TABLE 1

| Temperature (°C) | Catalyst | Feed: furfural (ml) | Feed: hydrogen (liters) | Time of catalyst operation (min) | Temperature (°C) | Sylvan yield: ml | Sylvan yield: % on furfural | Other products in catalyzate: furfural (ml) | Other products in catalyzate: furfuryl alcohol (ml) |
|---|---|---|---|---|---|---|---|---|---|
| 1 | Cu—Al (45 : 55) . . . . | 30 | 30 | 60 | 350 | 7 | 21.6 | 7 | — |
| 2 | Copper wire . . . . . | 15 | 10 | 30 | 280 | 1.5 | 9.3 | 10 | — |
| 3 | Devarda alloy: Zn—Cu—Al (5 : 45 : 50) | 20 | 15 | 60 | 300 | 9 | 41.6 | 4 | — |
| 4 | | 15 | 15 | 30 | 250 | 8.5 | 52.4 | — | — |
| 5 | | 15 | 10 | 15 | 250 | 6 | 37.0 | — | — |
| 6 | | 15 | 15 | 30 | 225 | 8.5 | 52.4 | — | — |
| 7 | | 15 | 10–12 | 30 | 450 | 8.0 | 50 | — | — |
| 8 | Zn—Cu—Al: (7.5 : 42 : 50) . . . . | 15 | 25 | 30 | 225 | 10.0 | 61.7 | — | — |
| 9 | (10 : 40 : 40) | 20 | 20 | 50 | 225 | 14 | 66.0 | — | — |
| 10 | | 15 | 20 | 35 | 225 | 10 | 61.7 | — | — |
| 11 | | 15 | 15 | 30 | 225 | 11 | 68 | — | — |
| 12 | Zn—Cu—Al: (12.5 : 37.5 : 50) . . . | 15 | 15 | 30 | 225 | 13 | 80 | — | — |
| 13 | (15 : 35 : 50) | 15 | 20 | 30 | 225 | 13 | 80 | — | — |
| 14 | | 25 | 35 | 60 | 250 | 21 | 80 | — | — |
| 15 | | 30 | 35 | 60 | 250 | 26 | 80 | — | — |
| 16 | | 35 | 50 | 90 | 250 | 31 | 82 | — | — |
| 17 | | 40 | 60 | 80 | 250 | 35 | 85 | — | — |
| 18 | | 50 | 90 | 120 | 250 | 43 | 80 | — | — |
| 19 | | 100 | 180 | 190 | 250 | 74 | 68.4 | — | 17 |
| 20 | Zn—Cu—Al (17 : 33 : 50) | 100 | 230 | 270 | 250 | 92 | 84.7 | — | 6 |
| 21 | | 160 | 434 | 395 | 250 | 144 | 83.2 | — | 14 |
| 22 | | 300 | 720 | 720 | 250 | 267 | 84.9 | — | 43 |
| 23 | | 500 | 1393 | 1380 | 250 | 400 | 74 | — | 55 |
| 24 | | 100 | 139 | 240 | 250 | 91 | 84 | — | 9 |
| 25 | | 300 | 445 | 720 | 250 | 287 | 88.6 | — | 20 |
| 26 | | 100 | 100 | 240 | 250 | 78 | 72.2 | — | 20 |
| 27 | | 100 | 81 | 240 | 250 | 78 | 72.2 | — | 20 |
| 28 | Zn—Cu—Al (20 : 30 : 50) | 100 | 180 | 240 | 250 | 84 | 77.8 | — | 20 |
| 29 | | 150 | 293 | 360 | 250 | 100 | 64.0 | — | 20 |
| 30 | Zn—Cu—Al (25.4 : 24.6 : 50) | 30 | 65 | 60 | 250 | 28 | 86 | — | 29 |
| 31 | | 180 | 400 | 360 | 250 | 137 | 70.4 | — | 29 |
| 32 | Zn—Al (50 : 50) | 15 | 20 | 30 | 250 | 1.5 | 9.2 | — | 5 |

This determined the qualitative composition of the proposed catalyst. It would have been dangerous to use more active metals such as nickel in place of copper, as they could have caused decomposition of the furfural molecule under the reduction conditions.

It was necessary to find the optimum quantitative proportions of the elements in the alloy. This, of course, had to be done experimentally. After tests on 8 samples of Zn–Cu–Al alloys in weight proportions ranging from 5:45: 50 to 45 : 5 :50 (with a constant aluminum content) we chose an original composition in proportions of 17: : 33 : 50.

This last zinc-copper-aluminum alloy composition proved to be the most effective catalyst for reduction of furfural to sylvan in a flow system, and gave 97% conversion of furfural (85% of sylvan and 12% of furfuryl alcohol) under atmospheric pressure at 225-250°. The catalyst was in continuous use for 12 hours without a decrease in the yields of the products.

This alloy was recommended by us as a catalyst for reduction of furfural to sylvan [26].

To determine the catalytic role of the alloy components, we performed separate experiments on reduction of furfural in presence of binary Cu – Al and Zn – Al alloys. As is clear from Table 1, low yields of sylvan were obtained. This confirmed our opinion that the ternary Zn – Cu –Al alloy must be used for this reaction.

## EXPERIMENTAL

Preparation of catalysts for tests. The metals were fused in a PT-6 type crucible furnace. The crucibles for the fusion were made from elutriated Kyshtym kaolin with addition of 10% (by weight) of asbestos fiber.

Weighed pieces of aluminum wire were put in the crucible. The furnace temperature was raised to 1000°. When this temperature had been reached, the required amount of metallic copper, also in the form of wire pieces, was put into the melted aluminum. The melt was stirred thoroughly with an Armco iron rod.

The temperature of the melt rose considerably owing to the vigorous chemical interaction between aluminum and copper. The crucible with the melt was then taken out of the furnace, and while the still liquid melt was cooling in the air a weighed quantity of arsenic-free metallic zinc was added. After thorough mixing, the melt was poured out by portions into cold water. The prepared alloy was then crushed into pieces 5-6 mm in size.

The percentage composition of the alloys was calculated from the weights of metals taken. Neither the finished alloys nor the surface layers which appeared after alkali activation were analyzed specially.

Activation of the catalyst. The catalyst was activated immediately before the experiments in the reactor. The stainless-steel reactor was placed vertically (length 650 mm, internal diameter 40 mm). The catalyst was charged in a 400 mm layer evenly in the middle of the reactor. This required 500 ml of the crushed catalyst (weight 800 g). It was then activated by 0.75 M caustic soda solution. The alkali solution passed upward from the bottom of the reactor through the catalyst layer at a rate of 30-35 ml/minute. The activation commenced with much evolution of heat and liberation of hydrogen; it was considered to be complete after 1.5 hours. This required 3 liters of solution. The catalyst was then washed with tap water until the wash water was weakly alkaline to phenolphthalein.

Reduction of furfural to sylvan. After the activated catalyst had been washed, the electric furnace was switched on to raise the temperature to 220°, and hydrogen was passed. When evolution of water vapor from the reactor ceased, the catalyst was considered to be ready for the experiments. The reactor temperature was automatically controlled by means of a thermoregulator.

Furfural was supplied through a buret under slight pressure. The furfural must be free from traces of acid; it was therefore treated with powdered calcium oxide before distillation. The furfural feed rate was regulated by means of the stopcock of the buret. Hydrogen was fed from a cylinder through a gas meter, washed in sulfuric acid and alkali and fed into the reactor. The gaseous reaction products passed through a condenser into the first receiver, cooled by ice mixture, and then into the second which was cooled strongly (by solid carbon dioxide). Excess hydrogen passed out into the air.

The results of the experiments are summarized in Table 1.

It follows from Table 1 that the optimum conditions for reduction of furfural to sylvan over copper-zinc-aluminum Raney-type alloy catalyst (33 : 17 : 50) are: furfural feed rate of 25 ml/hour through 500 ml of catalyst (or catalyst load rate 0.05 : 1 per hour), temperature range 225-250°, atmospheric pressure.

To determine the effective service life of the catalyst, samples were taken every hour. The samples were distilled from a flask fitted with a fractionating column. The yields of the products remained constant for 12 hours, after which there was an appreciable decrease (Experiment No. 23, Table 1). The experiment was then terminated and the catalyst was washed with alcohol or reactivated as described above. After reactivation the catalyst regained its initial activity and was again used for 12 hours, etc.

300 ml of furfural was fed into the reactor at a rate of 25 ml/hour, together with 445 liters of hydrogen at 37 liters/hour, for 12 hours. After separation of the aqueous layer the receivers contained 309 ml of colorless catalyzate; distillation of the catalyzate gave 287 ml (sylvan in 88.6% yield) of a liquid boiling at 60-65°, $n^{20}D$ = 1.4340, and 20 ml (furfuryl alcohol in approximately 6.2% yield) of a liquid boiling at 165-172°, $n^{20}D$ = = 1.4860. The residue contained 2 ml of high-boiling liquid products which were not investigated.

Determination of the optimum quantitative furfural-hydrogen ratio. To determine the molar ratio of furfural and hydrogen in the feed, special experiments were carried out; the results are given in Table 2.

TABLE 2

| Experiment No. | Furfural (ml) | Hydrogen (liters) | Molar ratio | Conversion (%) |
|---|---|---|---|---|
| 1 | 100 | 230 | 1 : 9 | 90 |
| 2 | 100 | 139 | 1 : 5 | 92 |
| 3 | 300 | 445 | 1 : 5 | 94 |
| 4 | 100 | 100 | 1 : 4 | below 90 |
| 5 | 100 | 81 | 1 : 3 | below 90 |

For economy in hydrogen consumption under the conditions of our experiments (in accordance with the results of Experiment No. 3, Table 2) a 1 : 5 ratio of furfural to hydrogen is recommended. The yield of sylvan in the catalyzate is then about 85%, and of furfuryl alcohol, 12%; total loss is 3% (Experiment No. 22, Table 1). However, the yield of sylvan can be increased considerably (to 88.6%) with 1 : 5.6 or 1 : 6 ratios (Experiment No. 25, Table 1). The total losses then reach 6%. The losses apparently increase owing to entrainment of sylvan vapor in the strong hydrogen stream. If suitable measures are taken, a 1 : 6 ratio can be used.

The total yields of furfural reduction products is lowered by polymerization of the furfuryl alcohol by-product, as it is known that it polymerizes readily even during distillation (especially in presence of traces of furfural).

## SUMMARY

1. It is shown that alloy catalysts can be used for reduction of furfural to sylvan, and a new copper-zinc-aluminum catalyst (33% Cu, 17% Zn, 50% Al in the initial mixture) is recommended for the reaction; this catalyst has an effective life of 12 hours. After loss of efficiency it is easily reactivated by washing with alcohol or weak alkali solution.

2. A method for reduction of furfural to sylvan in presence of this catalyst has been developed. This method gives 97% conversion of furfural with yields of 85% of sylvan and 12% of furfuryl alcohol.

## LITERATURE CITED

[1] H. Guinot, French Patent 811695 (1936); Zbl.* 2,1680 (1937).

[2] L. Burnette. Chem.Abs. 39, 631 (1945).

[3] L. A. Livshits, S. I. Il'ina, and V. N. Reikh, Chem. Ind. 6, 342 (1957)[ USSR].

[4] A. S. Sultanov and V. A. Maslennikova, Proc. Acad. Sci. Uzbek SSR 6, 58 (1953).

[5] M. Padoa, and U. Ponti, Zbl.*, I, 570, 1907; Atti R. Acc.,Lincei, 15 (2), 610 (1906).

[6] L. Wolf, Lieb. Ann., 384, 86 (1912).

[7] E. Richard, and H. Guinot, U.S.Patent 1739919 (1927); French Patent 639756; Zbl.* 2, 1322 (1928).

[8] N. Orlov and O. Radchenko, Proc. Acad. Sci, USSR 4, 286 (1934); J. Appl. Chem. 9, 249 (1936)[USSR].

[9] F. Peters, U. S. Patent 2082025; Chem. Abs. 31, 4991 (1937).

[10] H. Guinot, French Patent 811695 (1936); Zbl.* 2, 1680 (1937).

[11] H. Guinot, U. S. Patent 2456187; Chem. Abs. 43, 2218 (1948).

[12] C. Wilson, J. Chem. Soc., 61, (1945).

[13] R. Paul, Ch. A., 1588 (1942).

[14] L. Burnette, Ch. A., 39,631 (1945).

[15] L. Siepp, H. Geller and R. Korff., J. Am. Chem. Soc., 69, 672 (1947).

[16] J. Bremner and R. Keeys, J. Chem. Soc., 068 (1947).

[17] I. Mizuguchi, Ch. A., 42, 1802 (1948).

*Zbl. = Zentralblatt.

[18] L. Burnette, I. Johns, R. Holdren and R. Hixon, Ind. Eng. Ch., 40, 502 (1948).

[19] I. Johns and L. Burnette, U. S. Patent 2458857 (1949); Chem. Abs. 43, 3465 (1949).

[20] M. Katsuno, Ch. A., 43, 1718 (1949).

[21] Y. Hachihama, K. Kawata and M. Imoto, Ch. A., 44, 9722 (1950).

[22] J. Bremner, R. Keeys and D. Jones, British Patent 634709 (1950); Chem. Abs. 44, 6886 (1950).

[23] K. Tsuda, S. Yoshida, M. Yamada and Y. Maruya, Ch. A., 45, 6182 (1951).

[24] R. Lukes, C. Willson, J. Am. Chem. Soc. 73, 4790 (1954).

[25] R. Holdren, U. S. Patent 2445714 (1948); Chem. Abs. 42, 8214 (1948).

[26] A. S. Sultanov and V. A. Maslennikova, Soviet Authors' Certif. No. 107765 (July 6, 1957).

Received January 2, 1958.

# EFFECT OF THE GEOMETRICAL PARAMETERS OF THE SORBENT LAYER ON SORPTIONAL PURIFICATION OF MAIZE SUGAR

N. I. Gel'perin and A. I. Altykis

Despite the fairly extensive practical applications of adsorption from solutions under dynamic conditions, the calculation formulas published during the last few years are not general in character and are valid under limited conditions only. This is because it has not yet proved possible to represent fully the mechanism of dynamic sorption, the physicochemical properties of solutions and sorbents, hydrodynamic conditions, and geometrical parameters by means of theoretical equations. In particular, such a factor as the ratio of the height of the layer (l) to its diameter (d) for a constant amount of sorbent has not been evaluated quantitatively. The great significance of this factor, at least in certain instances, was demonstrated by us in a series of experiments the results of which form the subject of the present communication.

## EXPERIMENTAL AND DISCUSSION OF RESULTS

We studied the sorptional purification of maize sugar solutions in relation to the production of medical glucose. These solutions are known to contain particles of a colloidal nature which cause opalescence. However, pharmacopeia specifications require that solutions of medical glucose should be absolutely clear. We found experimentally that a very effective method for removal of opalescent particles from these solutions is by adsorption of neutral birchwood charcoal (OU) in columns operating in series.

The main purpose of the investigation was to study the influence of the ratio of the geometrical dimensions of the sorbent layer and of the solution feed rate on the course of the process.

The problem was investigated with the aid of a laboratory unit of five glass columns, the internal diameters of which were 17.4, 19.3, 22, 24.8 and 26 mm. The lower end of each column contained a grid which supported a layer of granular carbon. When the maize sugar solution was passed through, a column of liquid of the required height was maintained over the carbon layer. Equal weights (60 g) of carbon with 1.5-1 mm grains were put in the columns. The height of the sorbent ($l$) differed in each column in accordance with the different diameters (d). The characteristics of the sorbent layers in the experimental columns are given below.

| | | | | | |
|---|---|---|---|---|---|
| Diameter (mm) d . . . . . | 17.4 | 19.3 | 22 | 24.8 | 26 |
| Height of layer (mm) $l$ | 1180 | 940 | 715 | 560 | 536 |
| $\frac{l}{d}$ . . . . . | 67.9 | 48.7 | 32.5 | 22.55 | 20.4 |

It is seen that the $\frac{l}{d}$ ratio in the experimental columns varied between 20.4 and 67.9.

All the experiments were performed with 40% maize sugar solution at different flow rates, which were 2, 4, 6, 8, and 10 ml/minute. These rates corresponded to spray densities and volume velocities given in Table 1.

For regulation of the flow rate the solution level in the column was maintained at the required height. The times of protective action, referring to the instant at which opalescence appeared, are given in Table 2.

TABLE 1

Volume Velocities ($V_0$, ml/cc.minute) and Spray Densities ($V_1$, ml/cm$^2$· minute) in the Experimental Columns

| Flow rate V (ml/minute) | 2 | 4 | 6 | 8 | 10 |
|---|---|---|---|---|---|
| $V_0$ | 0.0074 | 0.0148 | 0.0222 | 0.0296 | 0.0370 |
| $V_1$ at d (in mm): | | | | | |
| 17.4 | 0.840 | 1.680 | 2.52 | 3.36 | 4.20 |
| 19.3 | 0.683 | 1.365 | 2.05 | 2.73 | 3.42 |
| 22 | 0.526 | 1.052 | 1.58 | 2.10 | 2.63 |
| 24.8 | 0.413 | 0.828 | 1.24 | 1.65 | 2.07 |
| 26 | 0.376 | 0.753 | 1.13 | 1.50 | 1.88 |

TABLE 2

Variation of the Time of Protective Action (θ Minutes) with the Flow Rate and Geometrical Dimensions of the Sorbent Layer for a Constant Weight of Carbon

| $\frac{l}{d}$ | Time of protective action at flow rate V (ml/minute) | | | | |
|---|---|---|---|---|---|
| | 2 | 4 | 6 | 8 | 10 |
| 67.9 | 112.5 | 45.3 | 19.2 | 11.6 | 8.1 |
| 48.7 | 80.5 | 35.3 | 15.3 | 9.76 | 6.5 |
| 32.5 | 53.5 | 23.2 | 11.48 | 6.88 | 4.5 |
| 22.55 | 37.5 | 16.18 | 8.00 | 5.0 | 3.2 |
| 20.4 | 33.0 | 14.50 | 7.32 | 4.5 | 3.0 |

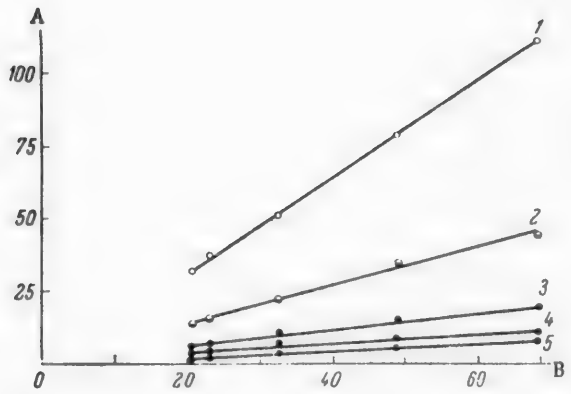


Fig. 1. Variation of the time of protective action (θ) with the geometrical dimensions $\frac{l}{d}$ of the sorbent layer at constant V:
A) time of protective action θ (minutes), B) $\frac{l}{d}$; flow rate V (ml/minute): 1) 2, 2) 4, 3) 6, 4) 8, 5) 10.

The data in Table 2 show that the time of protective action (θ) of the weight of carbon used greatly depends not only on the flow rate but also on the geometrical dimensions of the sorbent layer $\frac{l}{d}$.

Variations of θ at constant flow rate for different ratios of height to diameter of the sorbent layer are shown graphically in Fig. 1, where the ordinates represent experimental values of θ and the abscissa gives $\frac{l}{d}$ for our experimental columns.

Fig. 1 shows that the experimental points fit on a bundle of straight lines passing through the coordinate origin. Each line corresponds to a definite flow rate, and the slope of the lines relative to the abscissa axis decreases with increase of flow rate or, correspondingly, with decrease of the time of protective action of a given layer. This result suggests that, because of the large size of the adsorbed molecules, the decisive role in sorptional purification of maize sugar is played by internal diffusion. The linear increase of the time of protective action with increase of $\frac{l}{d}$ for a given weight of sorbent at V = constant

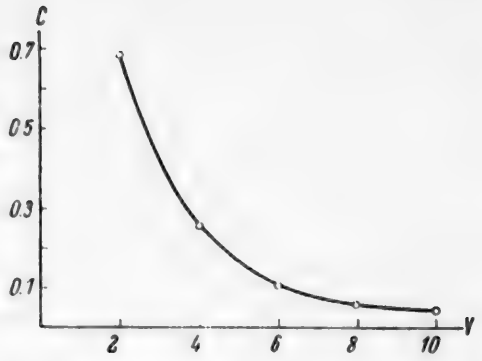


Fig. 2. Variation of the slope factor C in the equation $\theta = C \cdot \frac{l}{d}$ with the flow rate V.

is very significant. This relationship is especially pronounced at low flow rates, but persists, although to a lesser degree, at relatively high flow rates. The group of lines in Fig. 1 is represented by the general equation

$$\theta_{(V = \text{const})} = C \cdot \frac{l}{d} \qquad (1)$$

where C is the slope factor, constant for each flow rate.

The relationship between the slope factor C and the flow rate V is represented by the graph in Fig. 2, where V is taken along the abscissa axis, and values of C from Fig. 1 are taken along the ordinate axis.

Fig. 2 shows that the variation of C with V is represented by a hyperbola described by the equation

$$C = A \cdot V^{-m} \qquad (2)$$

where m = 1.785, and A = 8 for V > 2 ml/minute and A = 5.55 for V < 2 ml/minute.

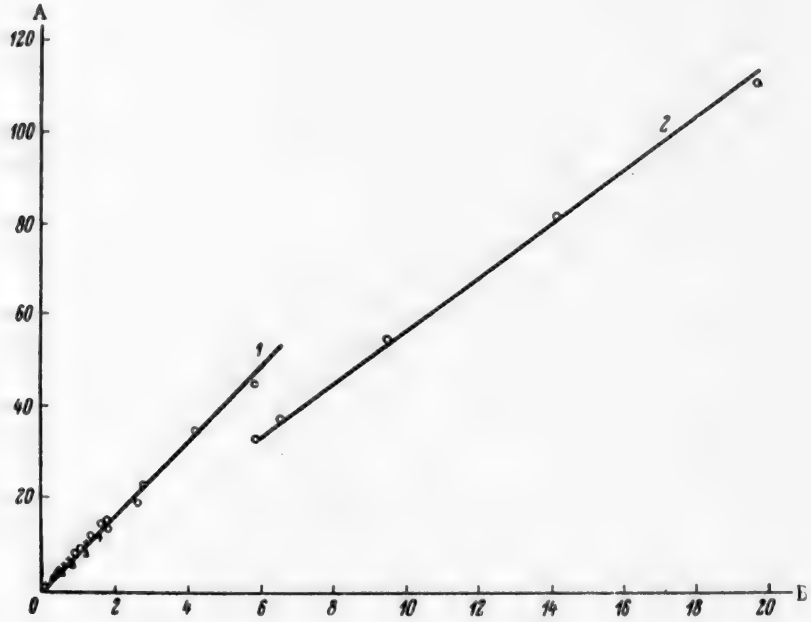


Fig. 3. Variation of the time of protective action with the volume velocity and the geometrical parameters of the sorbent layer:
A) time of protective action θ (minutes), B) values of $\frac{l}{d} \cdot \frac{1}{V^{1.785}}$

Lines: 1) Equation (3) and (4) at V < 2 ml/minute, 2) Equation (3) and (4) at > 2 ml/minute

Substitution of the values found for C into Equation (1) gives the following generalized relationships between the time of protective action, flow rate, and the geometrical ratio $\frac{l}{d}$ :

$$\left.\begin{aligned} &\text{for } V > 2 \text{ ml/min} \quad \theta = 8 \cdot V^{-1.785}\left(\frac{l}{d}\right), \\ &\text{for } V \leq 2 \text{ ml/min} \quad \theta = 5.55 \cdot V^{-1.785}\left(\frac{l}{d}\right), \end{aligned}\right\} \qquad (3)$$

where $\theta$ is in minutes and V is in milliliters per minute.

If we replace V (ml/minute) by the volume velocity ($V_0$), which represents the volume of solution flowing in 1 minute per 1 ml of sorbent, we have

$$\left.\begin{aligned} &\text{for } V > 2 \text{ ml/min} \quad \theta = 8\,(V_0 \cdot V_y)^{-1.785}\left(\frac{l}{d}\right), \\ &\text{for } V \leqslant 2 \text{ ml/min} \quad \theta = 5.55\,(V_0 \cdot V_y)^{-1.785}\left(\frac{l}{d}\right). \end{aligned}\right\} \qquad (4)$$

Equations (3) and (4) are shown graphically in Fig. 3; the values of $\theta$ are taken along the ordinate axis, and values of $V^{-1.785} \cdot \frac{l}{d}$ along the abscissa axis.

Points corresponding to experimental data are also shown in Fig. 3. It is seen that the experimental points fit satisfactorily on the straight lines corresponding to Equations (3) and (4), which therefore represent the process quite correctly.

## SUMMARY

1. For a given weight of carbon in the columns the time of protective action increases linearly with increase of the ratio $\frac{l}{d}$ at V = constant, and this relationship becomes more pronounced at decreased flow rates.

2. In sorption columns of the same dimensions, with $\frac{l}{d}$ = const, the time of protective action of the sorbent layer decreases rapidly with increase of flow rate.

Received July 17, 1957.

# A STUDY OF THE SEPARATION OF BUTYLENE-DIVINYL MIXTURE BY AN ABSORPTION METHOD

M. I. Bogdanov and E. P. Krushinskaya

Isolation of concentrated divinyl from butylene-divinyl mixtures inthe production of divinyl by catalytic dehydrogenation of n-butane is generally effected by absorption [1-3]. This method involves the formation of a water-soluble compound of divinyl with cuprous salts. Despite the large number of patents on the separation of divinyl from hydrocarbon mixtures by the absorption method [4-10], the chemical absorbent used industrially is ammoniacal copper acetate solution containing 3-3.5 g-atoms of cuprous copper per liter [1,11]. The use of solutions of higher cuprous copper contents proved unsuitable in practice.

Morrell and his associates [1] made a detailed study of the separation of butylene-divinyl mixtures by absorption in aqueous ammoniacal copper acetate solutions. They established the conditions for stability of the absorbent solution in relation to its composition, and determined the solubilities of divinyl, butylenes, acetylenic compounds with 3 and 4 carbon atoms in the molecules, and of other hydrocarbons at various temperatures, and studied certain other properties of the absorbent solution. Unfortunately, all the data in their paper on the solubility of hydrocarbons refer to an absorbent solution for which only the cuprous copper content is given (3 g-atoms /liter).

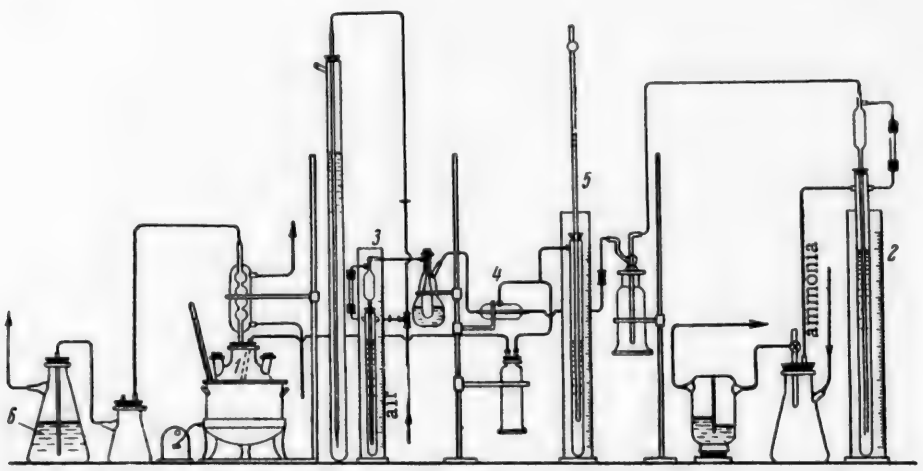


Fig. 1. Apparatus for preparation of the absorbent solution:
1) reactor, 2, 3) flow meters, 4) gas mixer, 5) manometer, 6) control flask.

In addition, the cited paper contains operational data on the experimental unit, and different technological variations of the process for separation of butylene-divinyl mixtures are discussed.

The object of the present investigation was a study of the influence of various factors (chemical composition of the solution, temperature, and divinyl content of the hydrocarbon mixture) on the absorption capacity of aqueous ammoniacal copper acetate solutions. The absorbent solution was analyzed for cuprous and cupric copper, acetic acid, and ammonia.

## EXPERIMENTAL

Preparation of the absorbent solution. Preparation of aqueous ammoniacal solutions of copper acetate by different methods is described in the literature [1].

In the present investigation the simplest method was used, in which metallic copper was allowed to react with an ammoniacal solution of ammonium acetate in a current of air and ammonia gas (Fig. 1). Two reactions take place simultaneously: a) dissolution of metallic copper in aqueous ammonia in presence of air, b) reduction of cupric to cuprous copper by means of metallic copper according to the equation

$$Cu^{++} + Cu \rightleftarrows 2Cu^{+}$$

The resultant aqueous solution was a multicomponent system which contained cuprous and cupric ammine acetates, ammonium acetate, and free ammonia.

The absorbent solution was analyzed for cuprous and cupric copper, acetic acid, and ammonia. The contents of excess acetate ions and free ammonia in the solution were also calculated. The excess acetate ion content (in g-ions/liter) was calculated from the acetic acid content of the absorbent solution after subtraction of acetic acid bound in the cuprous and cupric ammine complexes (1 mole of acid per 1 g-atom of cuprous copper, and 2 moles of acid per 2 g-atoms of cupric copper). The free ammonia was found from the total ammonia content after subtraction of the ammonia bound in complexes with cuprous and cupric copper (2 moles of ammonia per 1 g-atom of cuprous copper, and 4 moles of ammonia per 1 g-atom of cupric copper) and ammonia combined with excess acetic acid in the form of ammonium acetate.

Analysis of the absorbent solution. Cuprous copper, and the sum of cuprous and cupric copper, were determined by the dichromate and iodometric methods.

The content of cupric copper was found by difference. The ammonia and acetic acid contents were determined by steam distillation after decomposition of the absorbent solution by alkali and phosphoric acid solutions, respectively.

The starting materials were electrolytic copper in the form of wire 0.3-0.4 mm in diameter, technical glacial acetic acid (98.7%), aqueous ammonia containing 25% $NH_3$, and liquid ammonia.

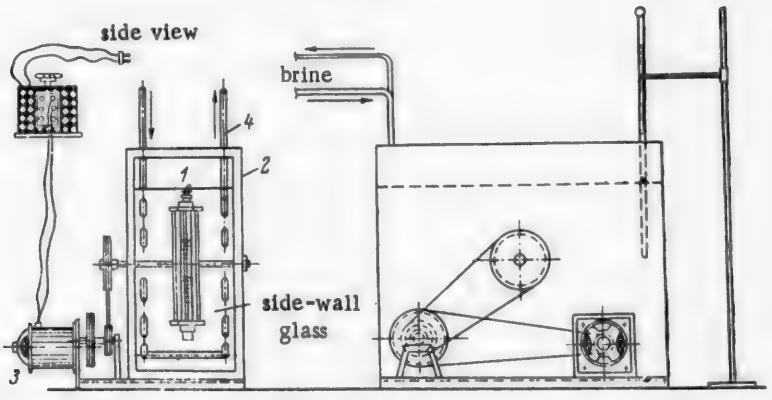


Fig. 2. Apparatus for determination of the solubility of divinyl in the absorbent solution:
1) mixer, 2) thermostat, 3) siphon tube, 4) motor.

## Determination of the Solubility of Divinyl in the Absorbent Solution

Equal volumes of the absorbent solution and divinyl, or of mixtures of divinyl with butylenes in the liquid state, were put into the mixer contained in a thermostat (Fig. 2). The divinyl content of concentrated divinyl was determined by absorption in maleic anhydride in Mal'tsev's apparatus [12], and in mixtures with butylenes by the bromination method [12]. The mixer was then rotated at 25-30 revolutions/minute for 4-8 hours. The solution was left to settle for 2 hours and 2 samples were then taken. The divinyl content of the hydrocarbon layer at equilibrium was generally found by calculation. Each of the samples was heated in a water bath to 90-95°. The hydrocarbons present in the solution were driven off and collected in a gas holder. The gas in the holder was diluted with an equal volume of air and analyzed for unsaturated hydrocarbons in the Orsat apparatus by absorption in 84% sulfuric acid, and for divinyl by the bromination method. As the solubility of butylenes in the absorbent solution is low, in some experiments the solubility of divinyl was found from the contents of unsaturated hydrocarbons (divinyl + butylenes).

## Influence of Various Factors in the Absorption Capacity of Aqueous Ammoniacal Copper Acetate Solutions

Effect of the chemical composition of the absorbent solution. The experiments were performed at 0° with a mixture containing 91% divinyl. The amount of dissolved divinyl was found from the total content of unsaturated hydrocarbons (divinyl + butylenes) in the solution (Table 1).

TABLE 1

Effect of the Chemical Composition of the Absorbent Solution on the Solubility of Divinyl at 0°

| Chemical composition of solution | | | | | | Solubility (wt.%) | |
|---|---|---|---|---|---|---|---|
| $Cu^+$ | $Cu^{++}$ | $NH_3$ | $CH_3COOH$ | excess | | | |
| in g-atoms/liter | | in moles/liter | | $NH_3$, moles/liter | $CH_3COO^-$ in m/l | $C_4H_6$ | $C_4H_8+C_4H_6$ |
| 2.64 | 0.54 | 11.0 | 4.2 | 3.08 | 0.48 | — | 3.7<br>3.8 |
| 3.28 | 0.34 | 11.5 | 4.35 | 3.2 | 0.39 | 4.4 | 4.7<br>4.7 |
| 3.22 | 0.24 | 11.6 | 4.35 | 3.55 | 0.65 | — | 4.6<br>4.6 |
| 3.17 | 0.34 | 11.7 | 4.78 | 3.07 | 0.93 | — | 4.5<br>4.6 |
| 3.21 | 0.44 | 10.7 | 4.60 | 2.01 | 0.51 | — | 4.7<br>4.6 |
| 3.30 | 0.40 | 9.4 | 4.37 | 0.93 | 0.27 | — | 4.6<br>4.6 |
| 4.0 | 0.40 | 12.5 | 5.37 | 2.5 | 0.57 | — | 4.8 |

It follows from Table 1 that the absorption capacity of the absorbent solution is determined mainly by the cuprous copper content of the solution. With ~ 3.3 g-atoms of cuprous copper per liter in the absorbent solution the solubility of divinyl is 4.4 wt. %. The solubility of butylenes under these conditions is ~0.3 wt.%. The solubility of divinyl decreases appreciably with decrease of cuprous copper concentration. On the other hand, increase of cuprous copper concentration causes little increase in the solubility of divinyl.

Variations of the concentration of excess acetate ions in the range of 0.3-0.9 g-ion/liter, and free ammonia in the range of 1-3 moles/liter, have no appreciable effects on the solubility of divinyl in the absorbent solution.

Effect of divinyl concentration. The effect of divinyl concentration was studied at 0° for divinyl concentrations in the hydrocarbon mixture from 4.6 to 91 molar % (Table 2).

TABLE 2

Effect of Divinyl Concentration in the Hydrocarbon Mixture on the Solubility of Divinyl at 0° in the Absorbent Solution

Composition of absorbent solution:

$Cu^{+}$ 3.18 g-atoms/liter,
$Cu^{++}$ 0.29 g-atom/liter,
$CH_3COOH$ 4.18 moles/liter,
$NH_3$ 11.2 moles/liter

| Divinyl concentration (molar %) | | Solubility (wt. %) | |
|---|---|---|---|
| in original mixture | at equilibrium | $C_4H_6$ | $C_4H_6+C_4H_8$ |
| 4.6 | 3.3 | 0.5 | 0.8 |
| 11.8 | 9.0 | 1.3 | 1.7 |
| 19.2 | 14.5 | 2.0 | – |
| 22.8 | 18.1 | 2.05 | – |
| 27.0 | 23.1 | 2.2 | – |
| 51.0 | 46.7 | 3.5 | 3.8 |
| 65.2 | 62.3 | 3.7 | 4.0 |
| 70.0 | 67.4 | 4.0 | 4.4 |
| 91.0 | 90.7 | 4.4 | 4.7 |

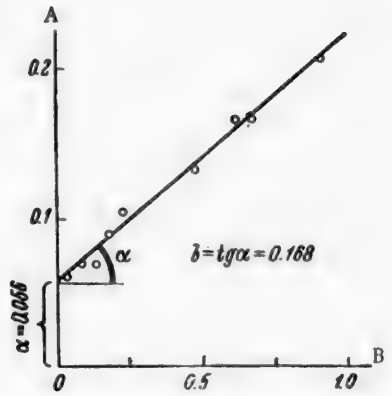


Fig. 3. Effect of divinyl concentration (wt. %) on its solubility in the absorbent solution at 0°:

A) $\frac{c}{s}$, B) divinyl concentration (mole fractions)

TABLE 3

Effect of Temperature on the Solubility of Divinyl in the Absorbent Solution

| Temperature (°C) | Divinyl concentration (molar %) | | Solubility (wt. %) | |
|---|---|---|---|---|
| | in original mixture | at equilibrium | $C_4H_6$ | $C_4H_6+C_4H_8$ |
| – 9 | 91 | 90.7 | 5.15 | 5.5 |
| 0 | | — | 4.4 | 4.7 |
| + 5 | | — | 3.9 | 4.1 |
| +10 | | — | 3.5 | 3.6 |
| +20 | | — | 2.4 | 2.4 |
| – 9 | 22.8 | 18.0 | 2.7 | — |
| 0 | | 18.1 | 2.05 | — |
| + 5 | | 20.1 | 1.6 | — |
| +10 | | 21.0 | 1.15 | — |
| +20 | | 21.5 | 0.8 | — |
| – 9 | 4.6 | 3.0 | 0.7 | 1.1 |
| 0 | | 3.3 | 0.5 | 0.8 |
| +20 | | 4.1 | 0.2 | 0.3 |

It is seen in Table 2 that the solubility of divinyl increases appreciably with its concentration.

The data of Table 2 were used to plot the relationship

$$\frac{c}{s} = \varphi(c),$$

where c is the divinyl concentration of the hydrocarbon mixture at equilibrium in mole fractions) and s is the solubility of divinyl in the absorbent solution (in wt.%). The experimental points fitted satisfactorily on a straight line (Fig. 3).

The line conforms to the following equation:

$$\frac{c}{s} = 0.056 + 0.168c.$$

Effect of temperature. The effect of temperature was studied between − 9 and + 20° for mixtures containing 91, 22.8 and 4.6 molar % of divinyl (Table 3).

It follows from Table 3 that the solubility of divinyl increases considerably with decrease of temperature.

For fuller characterization of the absorption process, equilibrium constants were calculated.

According to the literature [1], the reaction equation can be written

$$C_4H_6 + Cu_2^{++} \rightleftarrows C_4H_6 \cdot Cu_2^{++}.$$

Then the equilibrium constant for this reaction, expressed in concentrations, becomes

$$K_c = \frac{[C_4H_6 \cdot Cu_2^{++}]}{[Cu_2^{++}][C_4H_6]}. \quad (1)$$

Putting $[C_4H_6] = K \cdot N_{C_4H_6}$, where K is a proportionality factor and $N_{C_4H_6}$ is the divinyl concentration of the hydrocarbon mixture (in mole fractions) at equilibrium, we have

$$K_c' = K_c \cdot K = \frac{[C_4H_6 \cdot Cu_2^{++}]}{[Cu_2^{++}] \cdot N_{C_4H_6}}. \quad (2)$$

Equilibrium constants calculated from Equation (2) for different temperatures are given below:

| Temperature (°C) .... | − 9 | 0 | +5 | +10 | +20 |
|---|---|---|---|---|---|
| Equilibrium constant $K_c$ | 3.6 | 2.1 | 1.5 | 1.0 | 0.6 |

A plot of the logarithm of the equilibrium constant against the reciprocal absolute temperature is satisfactorily linear. The line is represented by the equation:

$$\log K = \frac{2033}{T} - 7.14.$$

The heat of absorption of divinyl, calculated from the slope of the straight line, was found to be 9.3 kcal/mole.

## SUMMARY

1. It is shown that the absorption capacity of the absorbent solution is mainly determined by its cuprous copper content. Variations of the contents of excess acetate ions in the range of 0.3-0.9 g-ion/liter and of free ammonia in the range of 1-3 moles/liter have no appreciable effect on the solubility of divinyl in the absorbent solution.

2. The experimental data were used to derive an expression for the relationship between the solubility of divinyl in the absorbent solution at 0° and the divinyl concentration in the hydrocarbon mixture, and to calculate the equilibrium constants for the absorption of divinyl by the absorbent solution between − 9 and + 20°.

## LITERATURE CITED

[1] C. E. Morrell, W. L. Paltz, I. W. Paskie, W. C. Asbury and C. L. Brown, Trans. Am. Inst. Chem. Eng., 42, 473 (1946).

[2] G. Egloff, Erdol Kohle., 7, 11, 710 (1954).

[3] P. W. Sherwood, Chim. et Ind., 73, 2, 290 (1955).

[4] British Patent 428106.

[5] British Patent 547730.

[6] British Patent 568818 (1945).

[7] British Patent 573046 (1954).

[8] British Patent 574839 (1946).

[9] U. S. Patent 238674 (1945).

[10] U. S. Patent 2386300 (1950).

[11] O. B. Litvin, Technology of Synthetic Rubbers [in Russian] (Goskhimizdat, 1950).

[12] A. I. Gulyaeva, V. F. Polikarpova and Z. K. Remiz, Analysis of the Products in the Production of Divinyl from Ethyl Alcohol by the Lebedev Process [in Russian] (Goskhimizdat, 1950).

Received October 19, 1957.

# THE BENZENOID STRUCTURE OF HYDROLYTIC LIGNIN

M. I. Chudakov, S. I. Sukhanovskii, and M. P. Akimova

The All-Union Scientific Research Institute of the Hydrolysis and Sulfite Alcohol Industry

Technical lignin, obtained by the treatment of wood by 0.5-1% sulfuric acid at 180° for 3-4 hours by the percolation hydrolysis process is a product which differs considerably from the protolignin present in unchanged plant tissues. In studies of its chemical nature [1] we found that the nucleus in the hydrolytic lignin molecule is extremely stable.

Numerous attempts have been made to obtain aromatic products form hydrolytic lignin by alkaline decomposition in aqueous solution or by alkaline fusion. In the former case lignin is activated with formation of alkali-soluble "lignin acids". Sodium salts of the latter are soluble in water, are of the phenolate type, and have ion-exchange properties [2], but subsequent alkaline fusion of "lignin acids" does not give any appreciable yields of aromatic compounds. In the second case, alkaline fusion of the original hydrolytic lignin yields not more than 10-12% of protocatechuic acid [3,4]. We advanced the hypothesis that hydrolytic lignin has only a low content (about 10-15%) of aromatic groups, apparently linked by ether bonds to the main heterocyclic lignin nucleus, in which carbon-carbon bonds predominate. Activation of hydrolytic lignin by aqueous alkalies destroys this aromatic grouping and is accompanied by demethylation and the appearance of a certain amount of phenolic hydroxyls which make the activated product soluble in alkalies.

The ability of protolignin in wood to react in the solid state similarly to the substance in solution indicates the presence of surface reactive groups [5]. In our opinion, alkaline activation of hydrolytic lignin consists of release of surface reactive groups, mainly as the result of demethylation, as was shown by our determination of the methoxyl balance [6]. However, alkaline activation causes considerable changes in and strengthening of the main lignin skeleton, as is shown by the behavior of "lignin acids" formed by such alkaline activation [1].

Hydrolytic lignins and products formed from them by alkaline activation cannot be regarded as substances of identical structure, as the conditions for their isolation are extremely diverse and difficult to take fully into account. However, all these products have a common structural component, quantitative determination of which is of undoubted theoretical and practical interest.

Kratzl [7] proposed as a criterion for lignin the formation of benzene polycarboxylic acids [8] from it on oxidation by alkaline permanganate.

The oxidation of lignin, peat, and coal by alkaline permanganate was studied in detail by Bone and his associates [9,10]. Oxidation yields mainly oxalic and benzene polycarboxylic acids, and also $CO_2$ and acetic acid. It was established by special experiments that, on further oxidation by permanganate, oxalic acid and benzene polycarboxylic acids are decomposed to a negligible extent. These workers also showed that oxidation of cellulose by alkaline permanganate yields oxalic acid, $CO_2$, and water only as the main products. Therefore the formation of benzene polycarboxylic acids by the oxidation of lignin, peat, brown coal, and anthracite is evidence of their benzenoid structure.

Randall et al. [11] studied the action of alkaline permanganate on six simple aromatic compounds. Their results showed that the oxidation products were never more complex than the original substances. It is also significant that benzene polycarboxylic acids are formed only from benzene nuclei not substituted with oxygen but with numerous substituent carbon atoms.

Compounds containing benzene nuclei directly substituted with oxygen atoms did not form benzene polycarboxylic acids, but were decomposed completely into $CO_2$, oxalic and acetic acids, and other products [8]. It follows that compounds containing phenolic hydroxyls, free or substituted, do not form polycarboxylic acids as the result of oxidation by alkaline permanganate.

Cabott and Purves[12] showed that oxidation of various lignin preparations mainly yields pentacarboxylic acid, with small amounts of tetracarboxylic acids [1,2,4,5]. Acids of this kind can be formed from aromatic units of Types I or II, substituted entirely with carbon atoms and not phenolic in character:

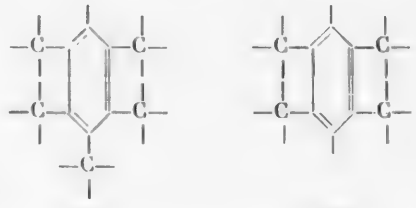

(I) (II)

If it is remembered that as the result of alkaline permanganate oxidation, according to Cabott's data [12], wood flour yields only 0.14% of polycarboxylic acids (calculated on the lignin). Willstatter's lignin yields 1%, Klason's lignin yields 2.4%, while periodate lignin which had been heated to 160° yields 5.7% at pH = 2.2, it is quite evident that the precursors of structures I and II must be formed by a definite kind of nuclear condensation during isolation of the lignin or during its thermochemical treatment. It must be emphasized that hexacarboxylic (mellitic) acid is obtained only from samples of alkali lignin in low yield (0.2%). Consideration of the original researches leads to the conclusion that the extent of nuclear condensation of the aromatic groups in lignin directly depends on the "harshness" of the methods used for its isolation. Harshness is taken to include a combination of the isolation conditions: chemical reagent, temperature, time.

The literature does not contain any data on the degree of cyclization of technical lignins. It was of definite interest to study the structural changes taking place in technical lignins during various additional chemical and thermal treatments.

It should be pointed out that oxidation by alkaline permanganate is not quantitative, and yields only a very low percentage of condensed benzene nuclei in lignin. However, in such cases it is important to obtain a comparison of the results which would serve as a criterion not only for evaluation of the original lignin but also for estimation of the harshness of the conditions used in its isolation and subsequent thermochemical treatment.

## EXPERIMENTAL

The following lignins were investigated.

1) Lignin from the Leningrad Hydrolysis Plant, washed free from acids, ground for 10 minutes in an M-10 vibratory mill, containing 2.7% ash, 0.3% reducing substances (by Bertrand's method), 15.0% difficultly hydrolyzable polysaccharides, and 10.4% methoxyls.

2) "Lignin acids" made by alkaline activation of original hydrolytic lignin at 180° (activation time 6 hours, caustic soda consumption 25% on the lignin, 7.5 liquor ratio). "Lignin acids" were isolated by acidification of the alkaline solutions by hydrochloric acid, filtered off, washed, and dried (the lignin contained 0.32% ash).

3) "Lignin acids" from the original hydrolytic lignin, obtained after alkaline fusion in petrolatum at 270° [4]. Ground hydrolytic lignin was granulated with caustic soda (100% on the lignin) and heated for 1.5 hours. The heat-treated granules were washed with benzene to remove petrolatum, dried, and dissolved in water. "Lignin acids" were isolated from the alkaline solution by addition of hydrochloric acid, filtered off, washed, and dried. The ash content was 2.2%.

Oxidation method. The oxidation was performed in an open enameled vessel 6 liters in capacity, placed in a water bath. In each oxidation experiment 30 g of lignin was taken and suspended in 4800 ml of 1% NaOH

solution. The oxidation was effected with continuous stirring by means of a stainless-steel stirrer. Permangate was added by portions in the following sequence: 115 g in the cold by small portions during 1 hour, 121 g on heating to 75-80°, by portions during 3 hours, and 54 g by portions during 4 hours at 75-80°. Oxidation was continued for a further 14 hours without addition of permanganate at 75-80° bath temperature. The whole oxidation process took 22 hours. Distilled water was added at intervals to the reaction mixture to replace losses due to evaporation. After the oxidation, residual $KMnO_4$ was decomposed by addition of a small amount of ethyl alcohol. The precipitated manganese dioxide was separated on a porcelain funnel, washed thoroughly, and discarded. The filtrate and wash waters were made up to a total volume of 7200 ml. After acidification with concentrated HCl to pH = 2-3 and complete removal of carbon dioxide, the solution was concentrated to one-sixth of its volume under vacuum at 30-40 mm residual pressure. Caustic soda was added to the concentrated solution to pH = 10.4. Addition of hot barium chloride solution (72 g $BaCl_2 \cdot 2H_2O$) to the hot alkaline concentrate caused the formation of a bulky precipitate of barium salts. The precipitate was heated in the mother liquor for 30 minutes, transferred to a No. 3 Schott filter, washed, and dried to constant weight at 105°. This precipitation quantitatively separated oxalic and benzene polycarboxylic acids in the form of snow-white barium salts. For determination of the oxalic acid content a weighed sample (0.1 g) of the dry barium salts was put in a measuring flask and covered with a 10-fold volume of 1 N HCl, and after it was dissolved the liquid was made up to the mark with distilled water. Oxalic acid was determined in an aliquot portion, after acidification with sulfuric acid, by titration with 0.1 N $KMnO_4$ (calculated as barium oxalate). The yield of barium salts of benzene polycarboxylic acids was found by difference, and calculated as benzene pentacarboxylic acid, because, according to Read and Purves [8], this is the acid predominantly formed by oxidation of lignins. The results of the analyses and calculations, as average values for series of duplicate determinations for each type of lignin, are given in the table.

Analytical Results

| Sample | Weight taken (g) | Yield of Ba salts (g) | | | Yield of benzene pentacarboxylic acid | |
|---|---|---|---|---|---|---|
| | | total acids | oxalic | poly-carboxylic acid | in g | % on lignin |
| Hydrolytic lignin | 29.19 | 50.0 | 48.5 | 1.5 | 0.7 | 2.4 |
| "Lignin acids" (activated at 180°) | 29.19 | 51.1 | 46.0 | 5.1 | 2.4 | 8.0 |
| "Lignin acids" (activated at 270°) | 29.3 | 63.0 | 47.3 | 15.7 | 7.76 | 25.2 |

## DISCUSSION OF RESULTS

The data in the table show that hydrolytic lignin yields not less than 2.4% of benzene polycarboxylic acids on oxidation. It follows that the nucleus of the hydrolytic-lignin complex has a benzenoid structure and can be schematically represented in the form of five benzene rings linked by –C–C– bonds:

Alkaline activation of hydrolytic lignin (in aqueous solution at 180°) yields "lignin acids" containing 8% of benzenoid structural groups.

Therefore two consecutive reactions take place in the course of alkaline activation: a) demethylation, leading to appearance of phenolic hydroxyls on the surface of the lignin complex, accompanied by removal of peripheral aromatic and carbohydrate groups; b) condensation, which results in considerable strengthening of the main skeleton and which forms additional points of benzenoid structure in the lignin. The tendency to an increase in the number of benzenoid groups as the result of alkaline and heat treatments is illustrated by the results of experiments on oxidation of "lignin acids" formed by alkaline fusion of hydrolytic lignin at a high temperature (270°). Oxidation of these "lignin acids" yields 25.2% of polycarboxylic acids, which probably include mellitic acid. It must be pointed out that condensation processes involving a sharp increase in the cyclization of the main lignin nucleus probably occur in parallel with a decrease of molecular weight and are accompanied by breakdown of the spatial structure of the original hydrolytic lignin. Whereas hydrolytic lignin, which contains only 2.4-2.5% of benzenoid structural groups, is insoluble in organic solvents or alkalies; "lignin acids" formed by alkaline heat treatment at 180 or 270° and containing 8-25% of benzenoid structural groups are completely soluble in alkalies and organic solvents (dimethylformamide), and soften on heating. This effect may be attributed to liberation of surface phenolic hydroxyls and splitting of the highly polymerized original hydrolytic lignin, accompanied by breakdown of carbohydrate residues, and removal of peripheral aromatic groups [1] and side chains carrying various functional groups.

Alkaline activation of hydrolytic lignin produces a definite state of "order" of the carbon compound, analogous to the molecular order noted by Kasatkin [13] in relation to coal metamorphism. This is characterized by "condensation of carbon into plane hexagonal networks at the expense of the disordered portion which consists of side chains peripherally bound to the networks, and mutual orientation of parallel atomic networks into layers."

Investigation of the degree of cyclization of lignins may be of value for evaluation of different technical lignins as raw materials for chemical conversion, and also as a basis for estimating the harshness of various technological processes of wood hydrolysis.

## SUMMARY

1. It is shown that hydrolytic lignin and its alkaline-activation products, "lignin acids," have a benzenoid structure.

2. Comparison of the yields of benzene polycarboxylic acids formed by oxidation of "lignin acid" samples by alkaline permanganate showed that the extent of nuclear condensation of the aromatic groups in lignin directly depends on the harshness of the methods used for the thermochemical treatment of lignin.

3. It is suggested that alkaline activation of hydrolytic lignin causes "ordering" of the carbon material, characterized by condensation of carbon into plane hexagonal networks.

## LITERATURE CITED

[1] A. P. Krasnova, S. I. Sukhanovskii, and M. I. Chudakov, J. Appl. Chem. 30, No. 12, 1827 (1957) [USSR].*

[2] I. V. Skrynnik, S. I. Sukhanovskii, and M. I. Chudakov, J. Appl. Chem. 31, No. 4, 655 (1958) [USSR].*

[3] K. Freudenberg, H. Harber and L. Markert, Ber., 61, 1760 (1928).

[4] M. I. Chudakov and S. I. Sukhanovskii, Trans. Kirov Academy of Wood Technology 7 (1956).

[5] F. E. Brauns, The Chemistry of Lignin, 206.

[6] S. I. Sukhanovskii and M. I. Chudakov, J. Appl. Chem. 28, 410 (1956) [USSR]*

[7] K. Kratzl, and G. Billek, Hozforsch., 10, 6 (1957).

[8] D. E. Read and C. B. Purves, J. Am. Chem. Soc. 74, 120 (1952).

[9] W. A. Bone, L. Horton and S. G. Ward, Proc. of Royal Soc. (London), A, 127, 480 (1930).

[10] W. A. Bone, L. G. B. Parsons, R. H. Sapiro and C. M. Groocock, ibid, A, 148, 492 (1935).

[11] R. B. Randall, M. Benger and C. M. Groocock, ibid. A, 165, 432 (1938).

* Original Russian pagination. See C. B. translation.

[12] J. M. Cabott and C. B. Purves, Pulp and Paper Mag. Canada, 57, 151 (1956).

[13] V. I. Kasatochkin, Bull. Acad. Sci. USSR, OTN, 9, 1321 (1951).

Received May 8, 1958.

# EFFECT OF WOOD PRETREATMENT ON THE YIELD AND PROPERTIES OF DIOXANE LIGNIN*

M. M. Chochieva and N. I. Nikitin

It was shown in the previous paper [1] that dioxane lignin isolated by a mild method from oak wood had a considerable content of hemicelluloses (up to 34.5%). It was desired to find conditions for obtaining the highest yield of dioxane lignin with the smallest possible content of accompanying hemicelluloses. In this connection a study was made of the effect of preliminary removal from oak wood of part of the hemicelluloses by alkaline extraction or by the action of microorganisms, and also of the influence of the degree of subdivision of the wood and certain other factors on the yield and chemical composition of dioxane lignin.

For alkaline extraction of the wood, sawdust (free from substances soluble in water and ether) was soaked in 4% NaOH for 24 hours at 20° and 1/15 liquor ratio. The alkaline extract was filtered, and the sawdust was washed free from alkali first with cold and then with hot water. For complete neutralization of the alkali the sawdust was then infused in 2.5% acetic acid, again washed with water to a neutral reaction, and dried under vacuum to an air-dry state.

This procedure gave the highest extraction of hemicelluloses (up to 43% of their total content) from oak wood.

The alkali-extracted air-dry sawdust was then extracted with dioxane in presence of a catalyst (0.1% HCl) for 28 hours by the method described previously [1].

Lignin was precipitated from dioxane solution by addition of dry ether or distilled water.

Preliminary alkaline extraction of part of the hemicelluloses from oak sawdust did not increase the yield of dioxane lignin. Thus, dry ether precipitated 14.7% of dioxane lignin on the weight of the original wood ** from dioxane solution, as compared with 16.7% obtained from nonextracted wood.

The results of chemical analyses of dioxane lignin and changes in its composition after it had been boiled in distilled water (5 hours, 1/30 liquor ratio) are given in Table 1.

As was to be expected, dioxane lignin obtained from oak wood extracted by 4% NaOH was the purer product, and contained only 21.0% of hemicelluloses as compared with the 34.5% found in lignin from non-extracted wood. The $OCH_3$ group content was considerably higher (19.2% as compared with 14.7% in lignin from nonextracted wood).

Alteration of the precipitation conditions, i.e., precipitation of dioxane lignin by water rather than ether, had a strong effect on the chemical composition of the product. Dioxane lignin precipitated by water contained 91.7% pure lignin with a high content of $OCH_3$ groups (22.3%). Its hemicellulose content was only 8.3% The uronic acid content was reduced threefold,,and the pentosan content was roughly halved (Table 1). Lignins precipitated from dioxane solution by ether and water,respectively,also differed considerably in their solubility in hot water. Dioxane lignin precipitated by ether had the higher solubility in water (28.3%). This is mainly due to its high hemicellulose content.

*Communication II.

**2.6% of lignin was also extracted by alkali.

TABLE 1

Composition of Dioxane Lignin from Oak Wood Previously Extracted with Alkali (% on Completely Dry Substance)

| Characteristics | Original lignin precipitated by | | Same lignins after hot- water treatment | |
|---|---|---|---|---|
| | ether, I | water, II | I | II |
| Elementary composition: | | | | |
| C | 57.00 | 57.88 | 60.08 | 61.92 |
| H | 6.14 | 5.56 | 5.63 | 5.81 |
| Methoxyl groups | 19.2 | 22.3 | 22.4 | 22.3 |
| Hydroxyl groups | 12.4 | 9.2 | 8.8 | 8.7 |
| Pentosans after correction for uronic acids | 14.3 | 6.5 | 5.2 | 4.0 |
| Uronic acids | 6.7 | 1.8 | 2.2 | 1.0 |
| Totak hemicelluloses | 21.0 | 8.3 | 7.4 | 5.0 |
| pure dioxane lignin | 79.0 | 91.7 | 92.6 | 95.0 |

TABLE 2

Comparison of the Chemical Composition of Healthy Oak Wood and Wood Damaged by P. sulphureus (% on the original wood)

| Oak wood | Kürschner cellulose, pentosan-free | Pentosans corrected for uronic acids | Uronic acids | Lignin obtained by means of 64% $H_2SO_4$ | $OCH_3$ groups | Substances soluble in hot water | Ether-soluble substances | Ash |
|---|---|---|---|---|---|---|---|---|
| Rotten | 21.4 | 11.6 | 8.1 | 34.3 | 9.0 | 26.5 | 0.6 | 0.7 |
| Healthy | 35.6 | 20.3 | 5.0 | 22.3 | 6.2 | 8.9 | 1.3 | 0.2 |

TABLE 3

Comparison of Yields of Dioxane Lignin Obtained from Oak Wood Under Different Conditions

| Oak wood | Yield (% on the original wood) |
|---|---|
| Rotten wood: | |
| sawdust without catalyst | 2.2 |
| wood flour without catalyst | 4.4 |
| sawdust with catalyst (0.1% HCl) | 15.2 |
| wood flour with catalyst (0.1% HCl) | 14.7 |
| Healthy wood: | |
| sawdust with catalyst (0.1% HCl) | 16.7 |
| wood flour with catalyst (0.1% HCl) | 16.4 |

It should be pointed out that dioxane lignin still contained 5-7.4% hemicelluloses after hot water treatment. It was more difficult to remove hemicelluloses by boiling water treatment from dioxane lignin precipitated by water than from dioxane lignin precipitated by ether. Thus, about 1/2 of the hemicelluloses from dioxane lignin precipitated by water and about 2/3 of the hemicelluloses from dioxane lignin precipitated by ether passed into the hot aqueous solutions.

The extraction of lignin by dioxane from oak wood destroyed by the fungus Polyporus sulphureus was next studied. Wood at the third stage of putrefaction, rotten and easily powdered, was taken for the investigation. Its chemical composition was greatly different from that of healthy oak wood (Table 2).

It follows from Table 2 that rotten oak wood had relatively high contents of lignin (34.3%), water- and ether-soluble substances, uronic acids, and ash. Its pentosan and cellulose contents were very low. It should be noted, however, that the increase of the lignin content in the rotten wood may have been due to resinification of decomposed carbohydrates by the action of 64% sulfuric acid (in lignin determination).

The method used previously was used in the extraction of dioxane lignin from rotten wood (after extraction of ether- and water-soluble substances) (Table 3). The lignin was precipitated by ether.

It follows from Table 3 that preliminary removal of a part of the carbohydrates from oak wood by the action of microorganisms likewise did not increase the yield of dioxane lignin (15.2%); this may have been caused by some modification of the native lignin by the action of the fungi, which influenced its solubility in dioxane.

It is interesting to note that the degree of subdivision of the wood (sawdust as compared with wood flour) had no appreciable influence on the yield of dioxane lignin in dioxane extraction, with 0.13% HCl, of either healthy oak wood (16.7 and 16.4%) or oak wood damaged by P. sulphureus (15.2 and 14.7%).

TABLE 4

Composition of Dioxane Lignin from Rotten Oak Wood (% on Completely Dry Substance)

| Characteristics | Original lignin extracted | | | Treated with hot water, extracted | |
|---|---|---|---|---|---|
| | without acid catalyst | | with acid catalyst | without acid catalyst | with acid catalyst |
| | from sawdust | from wood flour | | | |
| Elementary composition: | | | | | |
| C | 58.00 | 58.53 | 55.50 | 59.48 | 60.20 |
| H | 5.49 | 5.34 | 5.83 | 5.50 | 5.70 |
| Methoxyl groups | 17.3 | 16.4 | 16.4 | 17.1 | 18.9 |
| Hydroxyl groups | — | 11.0 | 10.1 | 8.5 | 10.1 |
| Pentosans after correction for uronic acids | Traces | 2.1 | 12.2 | 2.1 | 1.9 |
| Uronic acids | 3.0 | 2.0 | 4.4 | 1.1 | 3.8 |
| Total: | | | | | |
| hemicelluloses | 3.0 | 4.1 | 16.6 | 3.2 | 5.7 |
| pure dioxane lignin | 97.0 | 95.9 | 83.4 | 96.8 | 94.3 |
| Solubility in boiling water | — | 46.2 | 25.5 | — | — |

In extraction of rotten wood by dioxane without acid catalyst the degree of subdivision had a significant influence on the lignin yield. Thus, sawdust yielded 2.2% and wood flour 4.4% of dioxane lignin on the weight of the original wood.

The results of chemical analyses of dioxane lignin from rotten oak wood before and after treatment with boiling water are given in Table 4.

It is seen in Table 4 that dioxane lignin obtained by extraction of rotten wood without acid catalyst contained only 3.0-4.1% hemicelluloses, and the remaining 96-97% was pure lignin. Increased subdivision of the rotten wood increased the solubility of hemicelluloses in dioxane.

Another characteristic property of the same lignin is the high solubility in hot water (46.2%), and the somewhat lower content of methoxyl groups, which are probably split off from the lignin during destruction of the wood by the fungi [2].

Dioxane lignin isolated from rotten wood in presence of acid catalyst had a higher hemicellulose content

(16.6%). The amount of extracted pentosans in it was increased almost 6-fold, and of uronic acids 2.2-fold The content of $OCH_3$ groups was again low. The solubility in hot water fell to 25.5% (from 46.2%).

The contents of carbon and methoxyl groups in dioxane lignin from rotten oak wood increased somewhat after treatment with hot water.

## SUMMARY

1. Preliminary removal of part of the hemicelluloses from oak wood (by the action of 4% alkali or the wood-rotting fungus Polyporus sulphureus) did not increase the yield of dioxane lignin, but reduced its hemicellulose content. Dioxane lignin almost free from hemicelluloses (95.9%) was extracted (in 4.4% yield) in dioxane without acid catalyst from finely ground rotten oak wood. This lignin was half soluble in hot water.

2. The degree of subdivision of the wood (sawdust or wood flour) did not have any appreciable effect on the yield of dioxane lignin in the extraction of either healthy oak wood or oak wood damaged by P. sulphureus by dioxane with 0.1% HCl.

In extraction of wood (damaged by the same fungus) without acid catalyst the degree of subdivision had a considerable influence; the yield of dioxane lignin was twice as high from wood flour.

3. When dioxane lignin was treated with hot water, from 50 to 76% of the carbohydrates present was removed from the lignin-carbohydrate complex.

## LITERATURE CITED

[1] M. M. Chochieva and N. I. Nikitin, J. Appl. Chem. 30, No. 12, 1820 (1957) [USSR].*

[2] N. I. Nikitin, Chemistry of Wood [in Russian] (Izd. AN SSSR, 1951) p. 391.

Received December 16, 1957.

*Original Russian pagination. See C. B. translation.

# ACCELERATED POLYMERIZATION OF CAPROLACTAM

A. S. Shpital'nyi, M. A. Shpital'nyi, and N. S. Yablochnik

Accelerated or alkaline polymerization is the term usually applied to conversion of caprolactam into the polymer in presence of alkali metals or alkaline compounds [1-5].

In discussions of this process it was noted that in its initial stage reaction between the alkaline agent and the lactam yields the alkali salt of the lactam which really acts as the initiator causing the reaction to proceed at a high rate.

Reports of the formation of such salts can be found not only in description of processes activated by various alkali metals [2], but also in papers dealing with conversion of caprolactam into the polymer with the aid of alkaline reagents such as caustic soda, alkali carbonates, etc. [4].

Griel considers that the reaction between caustic soda and caprolactam under conditions of polymer formation (at 270-280°) proceeds according to the scheme

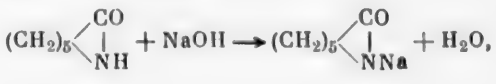

(1)

although proof of the possibility of this reaction is given only for the reaction of caprolactam with an alkali metal [6]. Further, like Hanford et al., Griel considers that the polymer formed in the interaction of caprolactam with alkaline compounds has the formula

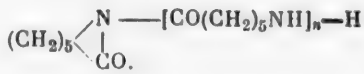

(2)

At the same time, he found carboxyl as well as amide groups in polymer washed free from alkali by water. He attributes the formation of carboxyl groups to hydrolysis of the lactam ring, for which, in his opinion, contact between the solid polymer and water is sufficient (for example, during extraction of crumbs or in band casting). Literature data indicate that the hydrolysis even of dissolved caprolactam is a lengthy process requiring high temperatures [7].

In contrast to Griel, Wichterle [5] adduces evidence in favor of an "intussusception-elimination" mechanism for the process of polymer formation, whereby the chain grows internally and not at the ends.

It follows from the foregoing that further information is required on the nature of the conversion of caprolactam in presence of alkali metals and alkaline compounds, especially in relation to polymerization schemes and the nature of the products formed by the reactions of caprolactam with various alkaline reagents.

In determination of the structure of the product formed by the reaction of caprolactam with alkaline compounds we found that if the reaction takes place at 280° and the alkaline reagent is caustic soda, the compound formed is not the sodium salt of the lactam but the sodium salt of aminocaproic acid.

The experiments were performed with considerable excess of caustic soda, to ensure conditions in which polymer formation is excluded, and which favor the formation of an easily analyzed compound of low molecular weight as the end product.

If the reaction mass contained, as reported [1], the sodium salt of caprolactam, the lactam could be extracted unchanged after neutralization.

In our experiments aminocaproic acid was extracted from the reaction mass.

When we replaced caustic soda by soda ash, also taken in considerable excess, the polymer was obtained.

Formation of aminocaproic acid by the interaction of caustic soda with caprolactam can be attributed to the reaction

$$(CH_2)_5\begin{matrix}CO\\|\\NH\end{matrix} + NaOH \rightleftarrows NaOOC(CH_2)_5NH_2. \qquad (3)$$

It was found in subsequent experiments that this salt can also initiate conversion of caprolactam into the polymer. It cannot be concluded from this that the caprolactam salt, especially its anion, takes no part in the process, as it would then be difficult to explain the rapid course of alkaline polymerization.

Therefore the scheme of polymer formation must be represented as follows in order to conform to experimental data and at the same time not to exclude participation of the sodium salt of the lactam in the reaction

$$H_2N(CH_2)_5COONa + (CH_2)_5\begin{matrix}CO\\|\\NH\end{matrix} \rightleftarrows H_2N(CH_2)_5COOH + (CH_2)_5\begin{matrix}CO\\|\\NNa\end{matrix} \rightarrow$$

$$\rightarrow H_2N(CH_2)_5CO \cdot NH(CH_2)_5COONa \text{ etc.,} \qquad (4)$$

$$H_2N(CH_2)_5COONa + \begin{matrix}CO-R-NH_2\\|\\NH-R_1-COOH\end{matrix} \rightarrow$$

$$\rightarrow H_2N(CH_2)_5CONHR_1COOH + H_2N \cdot RCOONa. \qquad (4a)$$

Reaction (4a), which causes depolymerization or transamidation of the polymer [8], differs from the corresponding Griel reaction [8] in that a salt of aminocaproic acid (or its derivatives) rather than a salt of caprolactam (or its derivatives is involved.

Confirmation of Reactions (3), (4), and (4a) is provided by the conversion of the polyamide into caprolactam by the action of caustic soda at 270-300°, which is one of the methods used for recovery of the lactam from polyamide wastes [9].

If sodium carbonate reacts with caprolactam similarly to NaOH, the reaction may be represented as follows:

$$2(CH_2)_5\begin{matrix}CO\\|\\NH\end{matrix} + Na_2CO_3 \rightarrow NaOOC(CH_2)_5NHCONH(CH_2)_5COONa. \qquad (5)$$

However, we did not succeed in isolating this last compound.

It was already stated earlier that when excess sodium carbonate reacted with caprolactam a water-soluble polymer and not a compound of low molecular weight was extracted from the reaction mass. The formation of the polymer was evidently caused by the low solubility of sodium carbonate in the caprolactam melt [4].

With regard to schemes representing the formation of polyamide polymers, it should be noted that most workers consider that conversion of caprolactam into the polymer in presence of alkaline compounds or alkali metals may be included among processes of the polymerization type. From the formal standpoint this interpretation is valid, because these processes are not accompanied by liberation of simpler molecules (water, alcohol, etc.) and the structural groups in the macromolecules of the polymer formed have the same composition as the monomer

There is no agreed opinion concerning the mechanism of this polymerization: some consider it to be ionic and assume that at least one end group is involved in the conversion (Griel); others believe that the participation of end groups is not essential, as the mechanism is of the "intussusception - elimination" type (Wichterle).

Therefore, without discussion of literature data on this question, we wish to show that the mechanism of the transamidation process studied by Porai-Koshits and his associates [10] can be used to explain any conversion of caprolactam into the polymer. Consider the following conversions:

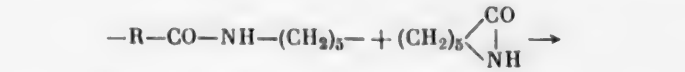

(6)

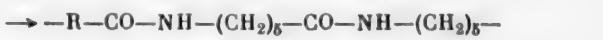

(7)

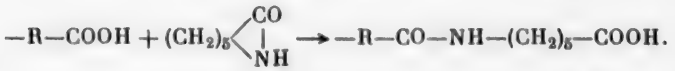

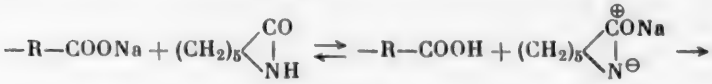

(8)

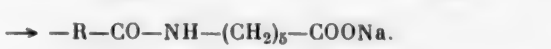

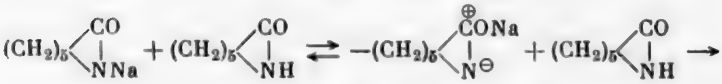

(9)

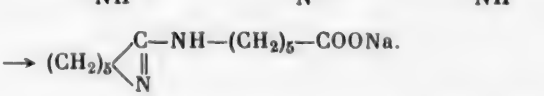

Here the reactions take place between complex functions consisting of CO, – NH, – OH, $>N^-$ and other groups, with different electron-donor and electron-acceptor activities.

Scheme (8) is applicable to the conversion of caprolactam into the polymer in presence of NaOH. It was already noted earlier that according to experimental data the reaction product of caprolactam and NaOH (with excess of alkali at 280°) is the sodium salt of aminocaproic acid. Intermediate compounds may be formed during this conversion:

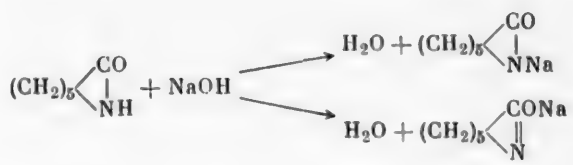

However, it was not possible to isolate them, probably because of hydrolysis of these cyclic compounds at high temperatures with conversion into the above-mentioned salt. The latter, as shown in Scheme (8), in its interaction with caprolactam should primarily assist in the formation of a compound with very active functional groups from caprolactam

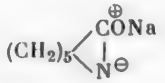

which can react vigorously both with carboxyl groups and with the lactam.

Scheme (9) represents the tautomeric transformation of the sodium salt of caprolactam to give the active form.

According to Porai-Koshits et al. [10], the transamidation mechanism in Schemes (7), (8), and (9) may be represented as follows:

Scheme (7)

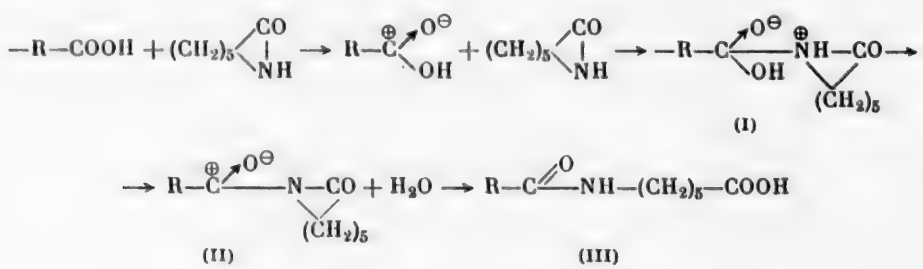

(10)

The principle of this scheme is maintained if addition of nitrogen from the amide group to carbon of the carboxyl group is accompanied by displacement of an $^-OH$ group. Then instead of Compound (I) we have Compound (IV) and hydroxyl:

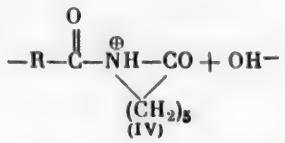

In both cases Compound (II) must next be formed, and at high temperatures this is hydrolyzed to Compound (III).

Scheme (8)

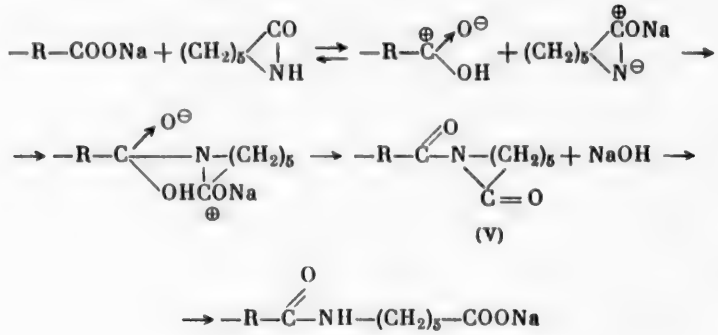

(11)

As stated earlier, the lactam ring in Compound (V) should break to form a sodium salt of the carboxylic acid.

Scheme (9)

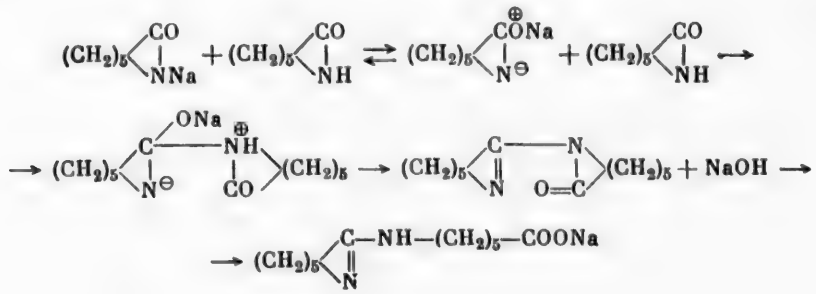

(12

This last scheme is not changed significantly if the caprolactam salt reacts by means of the $>N^-$ group

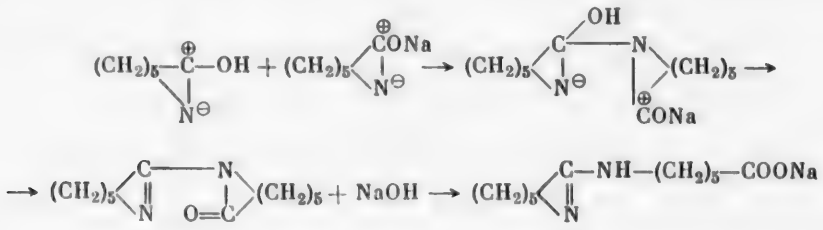

(13)

Thus, any method for conversion of caprolactam into the polymer may be explained in terms of the transamidation reaction studied by Porai-Koshits and his associates.

It is quite evident that Schemes (8) and (9), which involve the most active functional groups, should proceed at the highest rate.

According to Wichterle, the speed of the process in alkaline polymerization is also attributable to the activity of the lactam salt anion. However, he assumed that no end groups are present in the reaction mass, and considered that the active anion reacts only with the $-CO-NH^-$ group.

In the light of the foregoing, no special explanations are needed for inclusion of the interaction between functional $-COOH$ and $-NH_2$ groups, which takes place in the formation of nylon resin and which plays an important role in the formation of caprolactam resin [11], with the conversions, the mechanism of which can be represented in the form of the above-mentioned reactions:

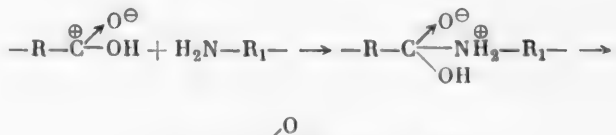

(14)

Thus, the classification of methods for production of polyamide polymers in relation to the nature of the starting materials and features of the processes themselves is somewhat arbitrary, as it is not associated with differences in the conversion mechanism. The fact that the classification is arbitrary in character follows not only from the above data but also from the technology of polyamide resin production. As an example, we may cite the well-known fact that the usual method for producing resin from caprolactam differs little from the process used in the production of nylon resin.

It was stated earlier that the initial products of the reactions of caprolactam with alkaline compounds and with metals are different: the former are alkali salts of aminocaproic acid (or their derivatives), while the latter are alkali salts of caprolactam.

At the same time, whatever the alkaline reagent used, the conditions exist for the formation of the alkali salt of the lactam in the reaction mass. Therefore, irrespective of the nature of the alkaline additive, alkaline polymerization always proceeds in a definite manner: the viscosity increases rapidly at the start of the process, and then falls slowly.

The foregoing considerations lead to the question of the manner in which the structure of the final product is influenced by differences in the nature of the initial products formed in the interaction of caprolactam with alkaline reagents.

The cited publications of Hanford and Griel indicate that the polymer structure should be identical in all cases, corresponding to the formula

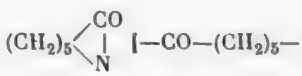

According to Griel, when metal is removed from the polymer the lactam ring is hydrolyzed and an end carboxyl group is formed. It is evident that an amino group is also liberated after removal of the metal. Therefore the polymer formed by alkaline polymerization, washed free from metal, does not differ in any way from the polymer made by the usual method.

Griel determined the end groups in polymers formed with the aid of alkaline compounds. We failed to find any data in the literature on the nature of the end groups in polyamides formed from caprolactam in presence of metallic sodium or other alkali metals. Hanford, who worked in this field, did not determine polymer end groups.

We found that, regardless of the nature of the alkaline reagent, all the polymers behave in analysis as if they have both amino and carboxyl end groups. It should be pointed out that if the structure of one end group in the macromolecule is of the form

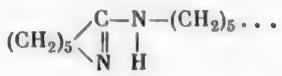

then one of the two nitrogens attached to the carbon must have basic properties and would be titrated like an amino group.

Therefore titration by standard alkaline and acid alcoholic solutions is not in itself proof that the macromolecule contains carboxyl and amino groups. We consider that, as follows from Schemes (6)-(12), certain polymers may have lactam rings as end groups.

In conclusion, we must note that we carried out experiments which confirmed Griel's view that the amount of added alkali regulates to a certain extent the size of the polymer macromolecule.

This stepwise character of the conversions brings alkaline polymerization closer to other reactions which lead to formation of polyamide polymers, and provides an experimental basis for the schemes given above.

## EXPERIMENTAL

Reaction of caprolactam with NaOH. A mixture of powdered caprolactam (2 g, 0.0 16 mole) and powdered NaOH (1.2 g, 0.03 mole) was heated in an ampoule for several hours under vacuum (p = 3 mm) on a water bath to remove traces of moisture. The ampoule was then sealed and kept for 2 hours at 280°. The melt was dissolved in water, and the solution was neutralized by 0.5 N sulfuric acid solution and then evaporated on the water bath. The dry residue was treated with ether. Caprolactam was not detected in the ether extracts. The residue was then treated with methyl alcohol. Ether was added to the methanol solution to precipitate crystals which had m.p. 202° after recrystallization from methanol. A mixed sample with ϵ -aminocaproic acid melted without depression. The yield of ϵ -aminocaproic acid was 75.75%

After ampoules containing caprolactam and small amounts of NaOH had been prepared as described above, they were held for 3 hours at 280°. They were then cooled, broken, the resin was crushed and washed for a long time with hot water until all traces of alkali had been removed. The washed resin was dried and analyzed [12]. The results of the analyses are given in Table 1.

Reaction of Na salt of aminocaproic acid with caprolactam. The Na salt of aminocaproic acid was made by addition of the calculated quantity of standard caustic soda solution to a solution of ϵ -aminocaproic acid and removal of water by evaporation of the solution on a water bath

A mixture of 0.0962 g (0.00062 mole) of this salt and 0.856 g (0.00076 mole) of caprolactam was put in an ampoule; air was displaced from the ampoule by means of nitrogen, and the ampoule was sealed and held at 280° for 2 hours. After treatment with ether and boiling water for 15 minutes the resin yield was 80%. The molecular weight (M) was found to be 7000 by titration of a solution of the resin in benzyl alcohol [12].

Reaction of caprolactam with sodium carbonate. A mixture of powdered caprolactam (3 g, 0.024 mole) and anhydrous sodium carbonate (3 g, 0.029 mole) was heated in a sealed ampoule for 2 hours at 280°. When the resultant melt was cooled and treated with hot water for 0.5 hour, most of it did not dissolve. The residue

was filtered off and washed with water to a neutral reaction. The resin yield was 65%; M = 1035.

After neutralization by sulfuric acid the combined filtrate and wash liquors were evaporated on a water bath. The dry residue was treated with ether. After evaporation of ether from the extract the residue consisted of crystals which did not depress the melting point of caprolactam in a mixed sample.

The amount of caprolactam extracted was 13.33%

Polymerization of caprolactam in presence of metallic sodium. Ampoules were charged with caprolactam and small amounts of metallic sodium, evacuated (p = 3 mm), sealed, and held for 1 hour.

Analytical data for the washed and dried resin are given in Table 2.

TABLE 1

Effect of the Amount of Caustic Soda Present During Polymerization on the Size of the Polyamide Macromolecules

| Amount of caprolactam | | Amount of NaOH | | Molecular ratio of caprolactam to NaOH | Molecular weight | |
|---|---|---|---|---|---|---|
| in g | in moles | in g | in moles | | found from carboxyl groups | found from amino groups |
| 2.26 | 0.02 | 0.16 | 0.004 | 5 : 1 | 1000 | 1000 |
| 2.26 | 0.02 | 0.08 | 0.002 | 10 : 1 | 1600 | 1400 |
| 3.39 | 0.03 | 0.07 | 0.00175 | 17 : 1 | 2000 | — |
| 2.26 | 0.02 | 0.016 | 0.0004 | 50 : 1 | 4350 | 4350 |

TABLE 2

Effect of the Amount of Metallic Sodium Present During Polymerization on the Size of the Polyamide Macromolecules

| Amount of caprolactam | | Amount of metallic sodium | | Molecular ratio of caprolactam to Na | Molecular weight | |
|---|---|---|---|---|---|---|
| in g | in moles | in g | in moles | | found from carboxyl groups | found from amino groups |
| 2 | 0.0176 | 0.07 | 0.003 | 5.8 : 1 | 1700 | 1250 |
| 4 | 0.0352 | 0.07 | 0.003 | 11.6 : 1 | 5000 | — |
| 5.65 | 0.05 | 0.02 | 0.00087 | 57 : 1 | 10000 | 8333 |

A mixture of 11.3 g (0.01 mole) of caprolactam and 1.15 g (0.05 mole) of metallic sodium was placed in a steel tube the lid of which was fitted with a Hofer valve. After evacuation of the tube (p = 5 mm) it was held for 2 hours at 270°. The mixture was dissolved in water (100 ml); the solution was neutralized with dilute sulfuric acid in presence of methyl orange. It was then evaporated in a porcelain basin on the water bath. The dry residue was divided into two portions: one portion was treated with ethyl and the other with methyl alcohol. Ether was added to the alcoholic extracts until they were strongly turbid. An oil separated out in the former case, and a sticky powder in the latter.

The molecular weight of both products, determined from the carboxyl group content, was found to be ~ 300.

## SUMMARY

1. It is shown that when caprolactam reacts with excess NaOH at 280° the sodium salt of aminocaproic acid is formed.

2. A scheme is put forward to represent the reaction of caprolactam with caustic soda.

3. The transamidation reaction postulated by B. A. Porai-Koshits is used as a basis of reaction schemes which show that the conversion mechanisms of caprolactam, diamines, and dicarboxylic acids into polyamide polymers do not differ from each other in principle.

4. Literature data concerning the stepwise nature of alkaline polymerization are confirmed; this brings this process closer to other reactions leading to the formation of polyamide polymers.

## LITERATURE CITED

[1] Swedish Patent 99037; Zbl. II, 2982 (1940); U. S. Patent 2251519.

[2] W. E. Hanford and R. M. Joyce, J. Polymer Sci. 3, 167 (1948).

[3] Hubert, German Patent Application 173389/39c; H. Klare, Chemistry and Technology of Polyamide Fibers (State Light Ind. Press, 1956) p. 96 [Russian translation].

[4] W. Griel, Report of Conference on Scientific and Technical Cooperation Between the USSR and the Peoples' Democracies in the Field of Synthetic Fiber Production [in Russian] (State Light Industry Press, 1956) p. 103; W. Grielu and H. Sieber, Faserforsch. u. Textiltechn., 6, 105 (1955); A. Garienko, W. Griel and H. Sieber, Faserforsch. u. Textiltechn., 6, 105 (1955)

[5] O. Wichterle, Faserforsch. u. Textiltechn., 6, 237 (1955); Report of Conference on Scientific and Technical Cooperation between the USSR and the Peoples' Democracies in the Field of Synthetic Fiber Production [in Russian] (State Light Industry Press, 1956) p. 217.

[6] L. Ruzicka, Helv. chim. Acta, 4, 472 (1921).

[7] R. Benson and T. Cairus, J. Am. Chem. Soc. 70, 2115 (1948).

[8] V. V. Korshak, Progr. Chem. 21, 121 (1952). [USSR].

[9] Z. A. Rogovin, Chemistry and Technology of Artificial Fibers [in Russian] (State Light Industry Press, 1952) p. 643.

[10] B. A. Porai-Koshits, O. F. Ginzburg, and L. S. Efros, J. Gen. Chem. 25, 530 (1956). [USSR].*

[11] A. S. Shpital'nyi, J. Gen. Chem. 26, 530 (1956). [USSR].*

[12] I. E. Waltz and G. W. Taylor, Anal. Chem. 19, 448 (1947).

Received February 19, 1958.

*Original Russian pagination. See C. B. translation.

# EFFECT OF AVERAGE MOLECULAR WEIGHT OF THE POLYMER ON THE RATE OF CAPROLACTAM FORMATION DURING THERMAL DEPOLYMERIZATION OF UNSTABILIZED POLYCAPROLACTAM•

N. D. Katorzhnov and A. A. Strepikheev

The All-Union Scientific Research Institute of Artificial Fibers

Synthetic fibers are being produced from polycaprolactam on a large scale both at home and abroad. However, a number of problems of polycaprolactam chemistry, including questions of depolymerization, require further clarification.

The fundamental relationships in the polymerization of ε-caprolactam have been determined by Soviet workers [1]. Strepikheev [2] a was the first to give an account of the thermodynamics of caprolactam polymerization. It was also shown in these investigations that the depolymerization of polycaprolactam is associated with dynamic equilibrium in the polymer-monomer system; this may be represented as follows:

$$H[-HN(CH_2)_5CO-]_nOH \rightleftarrows n(CH_2)_5\begin{matrix}NH\\|\\CO\end{matrix} + H_2O.$$

Under certain conditions equilibrium in the caprolactam-polymer system may be shifted completely in the direction of caprolactam formation, and as a result the depolymerization of the polymer may be taken almost to completion [2]. This fact is used industrially for decomposition of industrial wastes in polycaprolactam production and recovery of caprolactam [3].

In many instances the presence of caprolactam in the polymer and depolymerization of polycaprolactam are harmful or unnecessary, and special measures must be taken to limit or eliminate them. For example, presence of the monomer in technical polycaprolactam is undesirable, as the extrusion of capron fiber is thereby complicated considerably.

Apart from some general information [1], there is very little in the literature on the kinetics and mechanism of the reaction of polycaprolactam depolymerization. This paper contains the result of a study of the rate of thermal depolymerization of unstabilized polycaprolactam, i.e., polymer with free functional amino and carboxyl groups at the ends of the macromolecular chains.

## EXPERIMENTAL

For preparation of the original polycaprolactam, vacuum-distilled ε-caprolactam was polymerized at 260-300° for 10-20 hours in sealed ampoules in nitrogen, with additions of 0.2-3.0% of water on the weight of caprolactam. The molecular weights of the polymers were expressed in terms of specific viscosity of 0.5% solutions in cresol isomer mixture; the values found were 0.780, 0.612, 0.450, 0.400.

•Communication I in the series of investigations of the thermal depolymerization of polycaprolactam.

The polymer rods formed in the ampoules were shredded into fine shavings which were treated with boiling benzene until completely free from monomer and dried at 90° to constant weight. To provide constant initial conditions in many series of experiments, the shavings were mixed thoroughly and humidified in a thin layer in air (to 1.75% moisture content). The shavings, placed in 3-5 g lots in ampoules, were then dried under vacuum at 105-125°.

To determine the results of the drying, the water content of the resin in one of the ampoules was determined at definite intervals by means of the reaction with magnesium nitride. A series of polymers with moisture contents of 0.037, 0.118, 0.377, 0.74% was obtained in this manner. After the required moisture content had been reached the ampoules were carefully evacuated, filled with nitrogen, and sealed. Thermal depolymerization of caprolactam was continued for 0.5, 1, 3, and 5 hours at 230, 240, and 250°_ in a Hoepler ultrathermostat. The temperature was kept constant to within ±0.01°.

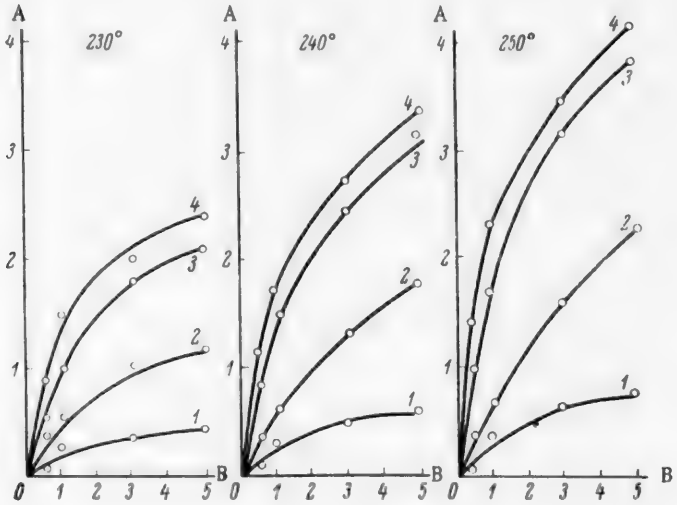


Fig. 1. Rate of monomer formation during thermal depolymerization of unstabilized polycaprolactam in presence of 0.037% of water: A) amount of caprolactam formed (%), B) duration of thermal depolymerization of polycaprolactam (hours); specific viscosity of original polymer: 1) 0.786, 2) 0.612, 3) 0.450, 4) 0.400.

At the end of the heating the resin was extracted from the ampoules, shredded, dried in a desiccator over phosphoric anhydride to constant weight, and analyzed for monomer content. The contents of low-molecular cyclic polymerization products (dimer and trimer) were not determined as, according to Strepikheev's data [2], their content is 4.5-5% and does not vary appreciably with temperature.

The amount of caprolactam formed during thermal depolymerization of polycaprolactam was determined by extraction in boiling benzene and drying at 100° to constant weight. In duplicate samples the monomer content did not differ by more than 0.3%

For molecular weight characterization, the specific viscosity of 0.5% solutions in cresol was determined for each sample after the extraction and drying.

The rate of caprolactam formation during thermal depolymerization of polycaprolactam in presence of 0.037 and 0.74% of water is shown graphically in Figs. 1 and 2.

The results obtained in a study of the influence of the original molecular weight of the polymer (specific viscosity of 0.5% polymer solution in cresol) on the rate of caprolactam formation in the thermal depolymerization of polycaprolactam, for an arbitrary reaction time (2 hours), are summarized in Fig. 3.

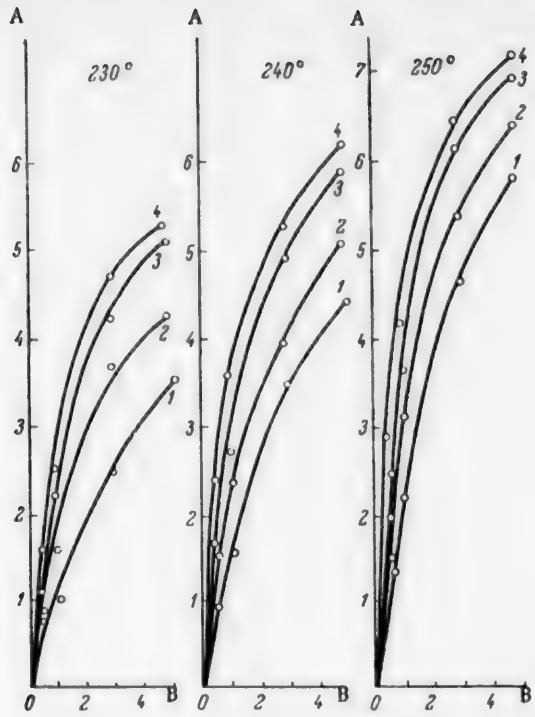


Fig. 2. Rate of monomer formation during thermal depolymerization of unstabilized polycaprolactam in presence of 0.74% of water: A) amount of caprolactam formed (%), B) duration of thermal depolycaprolactam (hours); specific viscosity of original polymer: 1) 0.786, 2) 0.612, 3) 0.450, 4) 0.400.

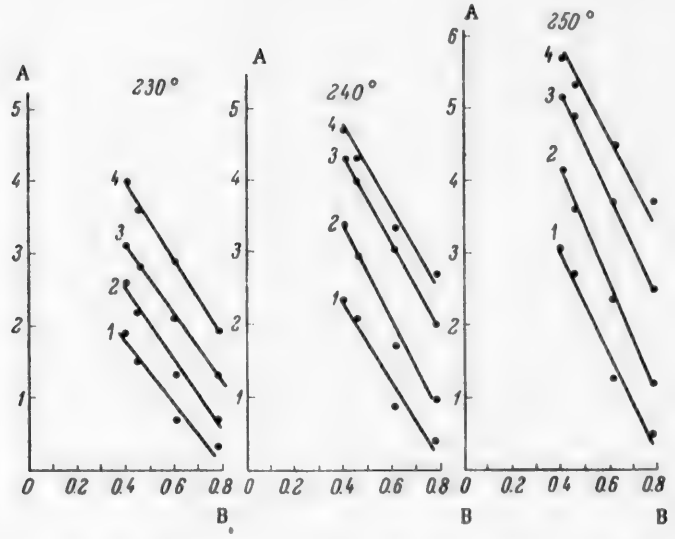


Fig. 3. Effect of average molecular weight of the polymer on the rate of caprolactam formation in the thermal depolymerization of polycaprolactam:
A) amount of caprolactam formed (%), B) specific viscosity of 0.5% polycaprolactam solution in cresol; moisture contents of polymers (%): 1) 0.037, 2) 0.118, 3) 0.377, 4) 0.74.

It is clear from these graphs that the highest rate of monomer formation is found for the polymer of the lowest average molecular weight.

It follows that the rate of thermal depolymerization is inversely proportional to the molecular weight of the polycaprolactam. Increase of the water content and rise of temperature accelerate the thermal depolymerization of polycaprolactam.

## SUMMARY

1. The rate of thermal depolymerization of unstabilized polycaprolactam (rate of monomer formation) depends on its average molecular weight: the lower the molecular weight, the higher is the rate of thermal depolymerization.

2. The rate of thermal depolymerization of polycaprolactam increases with increase of the amount of activator (water) present, and with increase of reaction temperature.

## LITERATURE CITED

[1] I. Knunyants, Z. Rogovin, E. Khait, and Yu. Rymashevskaya, J. Gen. Chem. 17, 987 (1947); 17, 1316 (1947) [USSR].*

[2] A. A. Strepikheev, Doctorate Dissertation [in Russian] (All-Union Scientific Research Institute for Artificial Fibers, 1949).

[3] A. A. Strepikheev and V. N. Topchibasheva, Authors' Certif. No. 10562 (September 13, 1949)

Received August 16, 1957.

*Original Russian pagination. See C. B. translation.

# DISSOLUTION OF COALS IN OILS DERIVED FROM COAL FOR PRODUCTION OF COAL-OIL PITCH

V. N. Novikov and B. S. Gurevich

The Eastern Scientific Research Institute of Coal Chemistry

There is an extensive literature on the action of organic solvents on coal. This type of coal treatment originated from attempts to separate the organic matter of coal into its components and thereby to investigate the nature of coal.

With the aid of high-boiling solvents some coals could be dispersed almost completely and others partially, with formation of colloidal solutions of coal [1-13]. The principal factor to influence the extent of the dissolution is the temperature of the process. Without the application of heat the coal only swells at best. The nature of the process is most correctly represented by the term "chemical dissolution".

The degree of metamorphism has a very significant influence on the solubility of coals. The highest yields of soluble fractions are obtained from gas coals and fat coals [8-10].

Studies of the petrographic components showed that the vitrainized portion and structural elements dissolved to an equal extent, and that the fusain group did not dissolve [8].

The yield of the soluble fraction is greatly lowered by oxidation of coals [7].

Mineral impurities settle out only partially together with the undissolved coal residues. The dissolved coal always contains some ash.

Treatment of coal with heavy solvents results in a number of interconnected complex processes: decomposition of the organic mass of the coal, accompanied by liberation of water vapor, tar, and gases; and dispersion of the chemically-changed coal substance.

As a result, a polydisperse system is formed in which the dispersion medium is the solvent and the disperse phase consists of coal breakdown products and mineral impurities. A certain proportion of the substances formed by the decomposition of coal becomes molecularly dissolved to some extent.

Our knowledge of the dissolution of coal in heavy solvents has now reached a level at which it is possible to apply the process on the industrial scale for various purposes: preparation of a product suitable for hydrogenation, and the production of ultrapure coal coke, which is used in the preparation of ultrapure aluminum [12].

Filippov and Gorovoi described a method in which coal is dissolved in oils [10] to give pitch which is a substitute for pitch made by distillation of coal tar. This type of pitch may be extensively used in industry as substitute for ordinary pitch in the production of roofing materials, for coal briquetting, and in road construction.

This paper contains the results of investigations performed in order to find suitable raw materials and optimum conditions for dissolution of coals in oils, for industrial trials of the Filippov and Gorovoi process for the production of coal-oil pitch.

## EXPERIMENTAL

Raw materials for production of coal-oil pitch. Coals from Eastern USSR were investigated for coal-oil pitch production (Table 1).

TABLE 1

Coal Analyses

| Pit | Coal grade | Ash content, % on dry substance | Volatile content, % on combustible mass |
|---|---|---|---|
| "Zhurinka" | D | 8.12 | 42.40 |
| "Polysaevskaya" | $G_{ener}$ | 8.12 | 41.5 |
| "Pionerka" | G2 | 5.33 | 42.25 |
| Kirov | G2 | 8.67 | 41.05 |
| "Komsomolets" | G1 | 7.12 | 41.88 |
| "Zyryanovskaya" | Zh2 | 9.17 | 38.90 |
| "Abashevskaya" | Zh2 | 7.48 | 37.60 |
| "Concentrate from Chertinskaya TsOF | Zh2 | 8.74 | 37.82 |
| "Baidaevskaya" | Zh2 | 9.68 | 34.80 |
| "Kapital'naya II" | Zh1 | 7.18 | 33.05 |
| "Kapital'naya I" | Zh1 | 7.70 | 29.82 |
| No.4 | Zh1 | 9.98 | 27.92 |
| Voroshilov | Kzh2 | 7.85 | 23.28 |
| Chul'man field, Southern Yakut Basin, seam $Jd^3$ | Zh | 7.25 | 33.95 |
| Volodarskii, Kizelovskii coalfield. | — | 21.21 | 41.70 |

TABLE 2

Analysis of Solvents

| Solvent | Specific gravity at 20° | Water content (%) | Contents of fractions (%) boiling at (°C) | | | |
|---|---|---|---|---|---|---|
| | | | 230 | 270 | 300 | 360 |
| Pitch tar | 1.226 | 1.5 | 0.06 | 0.23 | 0.38 | 3.37 |
| Pitch distillate | 1.151 | 1.0 | none | — | 13 | 29.0 |
| Chrysene fraction | 1.142 | 1.0 | 9%(235°) | — | 15 | 55.0 |
| 2nd anthracene fraction | 1.148 | — | none | 2.9 | 9 | 85.0 |
| Centrifuged anthracene | — | 1.0 | none | — | 26.32 | 61.0 |

The following solvents were investigated: soft pitch with a softening point of 48°, made from coal tar; pitch tar; pitch distillate (oil distillate formed by oxidation of pitch tar to high-melting pitch); chrysene fraction (distillates formed by oxidation of middle pitch to high-melting pitch); 2nd anthracene fraction; centrifuged anthracene (Table 2).

All the solvents were coking products of Kuznetsk coals.

Method of investigation. The coals were dissolved in a metal beaker 60 mm in diameter and 170 mm high, with stirring. The coal was ground to 3-0 mm particle size. The beaker with the solvent was placed in a crucible furnace where the solvent was heated to the required temperature. The total amount of coal and solvent, in 1 : 3 ratio, was 260 g. After the required temperature had been reached the coal was added by small portions during 7-10 minutes through a tube in the lid.

The dissolving time was counted from the instant when the temperature in the beaker reached the required level after the coal had been added. To determine when the pitch was ready during the dissolving, a sample was examined externally and smears were inspected under the microscope. The pitch was not left to settle for removal of mineral impurities. The finished pitch was poured into a tray and weighed when cool. The final concentrations of coal given in the tables are nominal values corresponding to the amounts of coal taken as percentages of the amounts of pitch obtained. The results of experiments on coal dissolution are given in Table 3.

TABLE 3

Characteristics of Coal-Oil Pitch from Different Coals

| Solvent | Dissolving temperature (°C) | Dissolving time (hr–min) | Total pitch yield (%) | Loss in dissolving (%) | Final coal concentration | Analysis of pitch | | | | Appearance of pitch in fracture |
|---|---|---|---|---|---|---|---|---|---|---|
| | | | | | | ash (%) | volatiles, % on dry substance | insoluble in toluene (%) | softening point, ring and rod method (°C) | |
| "Abashevskaya" pit (Zh2) | | | | | | | | | | |
| Soft pitch | 302 | 0—40 | 96.6 | 3.4 | 25.9 | 1.11 | 67.1 | 34.4 | 109 | Homogeneous, bright will dull grains |
| Pitch tar | 303 | 0—50 | 92.4 | 7.6 | 27.1 | 2.58 | 78.5 | 27.9 | 94 | Homogeneous, bright |
| Pitch distillate | 304 | 0—50 | 94.1 | 5.9 | 26.6 | 1.84 | 82.1 | 26.6 | 95 | Homogeneous, dull, elastic |
| "Kapital'naya II" pit (Zh1) | | | | | | | | | | |
| Soft pitch | 298 | 0—40 | 95.9 | 4.1 | 26.1 | 1.44 | 65.5 | 35.3 | 104 | Homogeneous, bright with dull grains |
| Pitch tar | 300 | 0—50 | 95.2 | 4.8 | 26.3 | 1.59 | 77.4 | 26.3 | 93 | Bright, uneven fracture |
| Pitch distillate | 301 | 0—40 | 94.1 | 5.9 | 26.6 | 1.67 | 85.0 | 23.5 | 62 | Homogeneous, dull, soft |
| Chrysene fraction | 298 | 0—50 | 92.2 | 7.8 | 27.2 | 1.62 | 81.6 | 25.4 | 70 | |
| 2nd anthracene fraction | 310 | 0—40 | 88.4 | 11.6 | 28.3 | 1.26 | 81.4 | 26.8 | 89 | Homogeneous, dull, elastic |
| Oil mixture 2 | 309 | 0—50 | 90.7 | 9.3 | 27.6 | 1.87 | 81.3 | 30.5 | 84 | Homogeneous, bright with dull grain |
| Oil mixture 1 | 300 | 0—30 | 69.3 | 30.7 | 36.1 | 1.70 | 70.6 | 34.1 | — | Homogeneous, bright, brittle |
| Crude anthracene | 309 | 0—50 | 86.1 | 13.9 | 29.0 | 1.65 | 78.6 | 27.4 | — | Dull, granular |

•Composition of mixture 2 (%): pitch distillate 45, chrysene fraction 35, crude anthracene 20.

••Composition of mixture 1 (%) : chrysene fraction 62, crude anthracene 38.

TABLE 3 (Cont'd.)

| Solvent | Dissolving temperature (°C) | Dissolving time (hr–min) | Total pitch yield (%) | Loss in dissolving (%) | Final coal concentration | Analysis of pitch | | | | Appearance of pitch in fracture |
|---|---|---|---|---|---|---|---|---|---|---|
| | | | | | | ash (%) | volatiles, % on dry substance | insoluble in toluene (%) | softening point, ring and rod method (°C) | |
| **"Zhurinka" pit (D)** | | | | | | | | | | |
| Soft pitch | 346 | 0—50 | 91.8 | 8.2 | 27.2 | 1.23 | 64.6 | 37.3 | 110 | Bright, uneven in fracture |
| Pitch tar | 347 | 1—00 | 86.1 | 13.9 | 29.1 | 0.96 | 77.0 | 29.3 | 110 | Bright, microporous |
| Pitch distillate . . . . . | 355 | 1—20 | 73.9 | 26.1 | 33.9 | 1.19 | 80.8 | 27.3 | 117 | Homogeneous, bright, uneven fracture with bright spots |
| Chrysene fraction . . . . . | 342 | 0—40 | 77.6 | 22.4 | 32.3 | 1.21 | 78.4 | 31.2 | — | Homogeneous, bright, uneven fracture with britht spots |
| **"Pionerka" pit (G)** | | | | | | | | | | |
| Soft pitch. . . . . | 351 | 0—40 | 95.5 | 4.5 | 26.2 | 0.82 | 63.90 | 38.9 | 112 | Homogeneous, bright with dull grains |
| Pitch tar . . . . . | 327 | 3—05 | 91.5 | 8.5 | 27.4 | 0.95 | 72.5 | 39.8 | 108 | Homogeneous, bright |
| Pitch distillate. . . . . | 350 | 0—40 | 89.6 | 10.4 | 27.9 | 1.00 | 84.1 | 26.3 | 101 | |
| Chrysene fraction . . . . . | 358 | 0—40 | 71.6 | 28.4 | 35.0 | 1.23 | 76.8 | 30.1 | 99 | |
| 2nd anthracene fraction. . . . . | 341 | 0—30 | 80.0 | 20.0 | 31.3 | 1.20 | 79.4 | 29.6 | 88 | |
| Oil mixture 2* | 347 | 0—40 | 85.0 | 15.0 | 29.4 | 1.20 | 79.3 | 27.7 | 95 | |
| Oil mixture 1** | 350 | 0—30 | 69.3 | 30.7 | 36.1 | 1.70 | 70.6 | 34.1 | 118 | Homogeneous, bright brittle |

## Effects of Various Factors on Dissolution of Coals.

Investigation of the solubility of a series of coals of the Donets and Kuznetsk field, from long-flame to lean, showed that gas and fat coals dissolve the most easily and with highest yields (up to 92%) of soluble fractions [8,9]. These observations were confirmed by the present investigation. Long-flame coal from the "Zhurinka" pit in all cases gave lower yields of pitch than gas coal from the "Pionerka" pit, despite the equal volatile contents of these coals. This is because of the lower thermal stability of the organic matter in long-flame coal. Unexpectedly, Kizelovskii coal from the Volodarskii pit proved more difficult to dissolve than gas and fat coals from the Kuznetsk field.

In a production process it is necessary to ensure the most complete dissolution of the coal, avoiding high temperatures, to give a homogeneous product with the maximum yield. On these considerations the use of long-flame, coking, and other highly metamorphosed coals for the production of coal-oil pitch is not promising. We therefore present data on the characteristic representatives of gas coals (from the "Pionerka" pit) and fat coals (from the "Abashevskaya" and "Kapital'naya II" pits of the Kuznetsk fields) (Table 3).

TABLE 4

Yield of Volatile Products and Soluble Fractions from Solid Residues of Heated Coal in Relation to the Heating Temperature (% on Combustible Matter)

| Heating temperature (°C) | Yaroslavskii pit | | | | | No.10 pit, Osinovskii coalfield | | | | |
|---|---|---|---|---|---|---|---|---|---|---|
| | gas phase | | soluble fraction of solid residue | soluble fraction of solid residue | solid insoluble residue | gas phase | | soluble fraction of solid residue | total yield of gas phase and soluble fraction | solid insoluble residue |
| | total yield | including tar | | | | total yield | including tar | | | |
| 350 | 2.47 | 1.69 | 86.15 | 88.7 | 11.3 | 1.62 | 1.01 | 91.55 | 93.2 | 6.8 |
| 370 | 3.25 | 2.05 | 86.60 | 89.9 | 10.1 | 2.33 | 1.66 | 89.90 | 92.2 | 7.8 |
| 390 | 5.32 | 3.80 | 84.25 | 89.6 | 10.4 | 2.74 | 2.01 | 89.90 | 92.6 | 7.4 |
| 410 | 8.29 | 5.60 | 78.60 | 86.9 | 13.1 | 5.84 | 3.64 | 85.90 | 91.7 | 8.3 |
| 430 | 16.68 | 11.81 | 40.05 | 56.3 | 43.7 | 11.68 | 7.29 | 77.40 | 89.1 | 10.9 |
| 450 | 20.78 | 14.40 | 12.10 | 32.9 | 67.1 | 14.62 | 9.96 | 31.80 | 46.4 | 53.6 |
| 470 | 21.66 | 14.83 | 0.58 | 22.2 | 77.8 | 15.50 | 10.11 | 1.16 | 16.7 | 83.3 |

Solvents. The nature of the solvent has a significant influence on the quality of the coal-oil pitch formed. The products can be divided by a number of characteristics into two groups in relation to the solvent used: those obtained 1) with the use of soft pitch and pitch tar, and 2) with the use of lighter solvents.

Coal-oil pitches of the first group differ little from coal-tar pitch. They are homogeneous, hard, lustrous, and brittle, and have lower volatile contents and higher softening temperatures than pitches of the second group.

Coal dissolves more easily in heavier solvents – soft pitch and pitch tar. In addition to the greater amount of dispersion medium available at the final stage of dissolving, because of lower distillate losses, the higher molecular weights of the solvents are also significant in this case.

Pitches of the second group are softer, elastic, and in some cases rubberlike. Pitches of this group usually exhibit a dull fracture, and their softening temperatures are lower. The distillate yields during the dissolving are increased 4 to 5-fold, and the coal concentration in the pitch is therefore higher than in pitches of the first group.

Crude anthracene by itself is unsuitable as a solvent; the product has a granular structure. Certain amounts of crude anthracene may be utilized in mixtures with other oils.

Dissolving temperature. The dispersion of coal must be carried out at temperatures which ensure fairly extensive decomposition of the organic matter of the coal. When gas and fat coals are heated, appreciable decomposition occurs even at 300°.

TABLE 5

Yields and Quality of Coal-Oil Pitch in Relation to the Dissolving Temperature

| Pit | Coal grade | Solvent | Dissolving temperature (°C) | Dissolving time (hr–min) | Pitch yield (%) | Final coal concentration (%) | Analysis of pitch: volatiles, % on dry substance | Analysis of pitch: insoluble in toluene | Analysis of pitch: softening temperature, ring and rod method (°C) | Appearance of pitch in fracture |
|---|---|---|---|---|---|---|---|---|---|---|
| "Pionerka" | G-2 | Pitch tar | 302 | 1—00 | 92.8 | 26.9 | 79.35 | 28.00 | — | Coal not dissolved completely |
| | | The same | 327 | 3—05 | 91.5 | 27.3 | 72.47 | 33.9 | 108 | Bright, homogeneous |
| | | Pitch distillate | 303 | 2—10 | 90.0 | 27.8 | 82.68 | 26.31 | — | Dull, homogeneous |
| | | The same | 350 | 0—40 | 89.6 | 27.9 | 84.08 | 26.25 | 101 | Bright, homogeneous |
| Kirov | G | Pitch tar | 300 | 1—10 | 91.5 | 27.3 | 73.46 | 28.5 | — | Coal not dissolved completely |
| | | The same | 352 | 0—40 | 94.2 | 26.6 | 76.98 | 34.15 | 94 | Bright, homogeneous |
| "Zyryanovskaya" | Zh2 | Pitch tar | 298 | 1—10 | 96.1 | 26.0 | 78.18 | 27.35 | 92 | |
| | | The same | 352 | 1—00 | 90.6 | 27.6 | 77.94 | — | 94 | |

Investigation of the dissolution of coal with determination of the gas-phase yield (tar, pyrolysis water, and gas) showed that the maximum yields of soluble fractions from the solid residue of heated coal are obtained at 350-390° with different coals [9]. On further increase of temperature, irreversible condensation processes commence and intensify, with formation of increasing amounts of insoluble residue and gas phase (Table 4). In view of this, the dissolving should be performed without excessive increase of temperature in order to obtain higher yields of coal-oil pitch.

It was found that gas coal does not dissolve completely at 300° under the experimental conditions used (Table 5). The product after settling had a granular structure, with a dull fracture. When the temperature was raised to 327° (average over the experiment), bright and homogeneous pitch was obtained, but only after heating for 3 hours. A homogeneous product with a bright fracture could be obtained only when the temperature was raised to 350°; the melt was ready 40 min after this.

A temperature of 300° proved sufficient for the formation of a homogeneous melt from fat coal. At 350° fat coal dissolved very rapidly, but the amounts of distillate increased substantially and the pitch yield fell. It was seen quite clearly that fat coal dissolves more easily than gas coal. Accordingly, in the subsequent experiments gas coals were dissolved at 350° and fat coals at 300°.

Dissolving time. Visual observations of the dissolving process at temperatures of the order of 350° showed that the dispersion of gas and fat coals from the Kuznetsk coalfield proceeds very rapidly.

A macroscopically homogeneous lump of gas coal from the Kirov pit, 60 × 35 mm in size, was placed in pitch distillate heated to 350°. It was found that the coal did not dissolve on the surface. By the combined action of heat and the solvent the monolithic lump rapidly disintegrated into small grains; after three minutes the largest grains were only 3-5 mm in diameter, and in less than one hour a homogeneous melt was formed.

The softening temperature falls with increase of the dissolving time but after 40 minutes it remains unchanged; this shows that the properties of the system become stabilized.

Microscopical examination of pitch samples taken consecutively during the dissolving of coal ground down to 3-0 mm particle size showed that under the experimental conditions the melt becomes homogeneous about 40 minutes after the last portion

of coal has been added. Accordingly, in laboratory experiments on gas and fat coals from the Kuznetsk coalfield the dissolving time after the end of the coal addition was fixed at 40 minutes.

Coal concentration. To determine the influence of coal concentration on the quality of coal-oil pitch, gas coal from the "Pionerka" pit and fat coal from the "Kapital'naya I" pit were dissolved in pitch distillate (Table 6).

Increase of the coal concentration has a regular and appreciable influence on pitch quality: the softening temperature and toluene-insoluble residue increase sharply, the ash content rises, and the volatile yield falls. The yield of toluene-insoluble residue (disperse phase) corresponds to the given coal concentration.

TABLE 6

Effect of Coal Concentration on the Quality of Coal-Oil Pitch. Dissolving time 40 minutes

| Amount of coal (%) | Actual dissolving temperature (°C) | Ash calculated on dry substance (%) | Volatiles calculated on dry substance (%) | Insoluble in toluene (%) | Softening temperature by ring and rod method (°C) | Pitch |
|---|---|---|---|---|---|---|
| | | | "Pionerka" pit | | | |
| 25 | 347 | 0.81 | 81.6 | 24.9 | 93.3 | |
| 30 | 340 | 1.63 | 78.5 | 30.3 | 110.5 | Brittle |
| 40 | 344 | 1.99 | 72.0 | 40.8 | 118 | |
| 50 | | Coal not dissolved | | | | |
| | | | "Kapital' naya II" pit | | | |
| 25 | 302 | 1.23 | 81.80 | 24.3 | 88.3 | Soft, homogeneous |
| 30 | 304 | 1.46 | 77.5 | 29.3 | 106 3 | Brittle " |
| 40 | 290 | 2.83 | 67.0 | 42.6 | 152.3 | Brittle, not quite homogeneous, porous in top layer |
| 50 | 306 | 3.53 | 62.3 | 49.8 | 158.5 | Brittle, heterogeneous |

With 40% of gas coal the pitch was very viscous at 344°. With 50% of coal the dissolution was not complete, a heterogeneous mass of softened and deformed coal grains being formed. The amount of solvent proved insufficient in this case.

It was possible to raise the concentration of fat coal to 50%. A viscous melt was obtained.

These observations are very important in relation to the technology of coal dissolving. It is evident that under production conditions, if the pitch has to be pumped through pipes, more than 40% of coal cannot be used for dissolving.

At high coal concentrations strong frothing occurred in all cases; this was due to the high viscosity of the melt, which prevented free liberation of vapors.

## SUMMARY

1. Coals of a low degree of metamorphism can be used for the production of coal-oil pitch. The best results are obtained by the dissolving of gas and fat coals, which dissolve easily and completely at relatively low temperatures.

A wide range of products can be used as solvents, from soft pitch to the 2nd athracene fraction.

2. The optimum dissolving temperature for gas and fat coals is 350°. Increase of temperature leads to excessive losses of solvent owing to distillation of low-boiling fractions.

3. The coal grain size has virtually no effect on the dissolution rate.

4. Pitches of a great variety of properties can be made by the use of different coal mixtures and different solvents. Increase of the amount of coal results in increase of the peat softening temperature, increase of ash content, and decrease of the volatile content.

5. Coal-oil pitch made from fat or gas coal and soft pitch or pitch tar is similar in appearance to ordinary coal-tar pitch: it is hard, brittle, and has a conchoidal fracture. Pitch made with the use of oils is less hard, elastic, and in some cases rubberlike.

6. Increase of the coal concentration above 35-40% is undesirable under production conditions.

## LITERATURE CITED

[1] A. Gillet et al., Bl. Soc. chim. Belg. 41, 511 (1932); Brennstoff Chemie, 17, 22, 421 (1936); Fuel,15, 5,124 (1936).

[2] A. Pott and H. Broche, Gluckauf, 39, 903 (1933).

[3] J. M. Pertierra, Fuel, 12, 1, 23 (1934).

[4] R. S. Asbury, Ind. Eng. Ch. 20, 6, 687 (1936).

[5] G. Agde and R. Hubertus, Braunkohlenarchiv, 46 (1936).

[6] M. K. D'yakova et al., Proc. Acad. Sci. USSR 20, No. 9, 679 (1938); J. Appl. Chem. 13, 1189 (1940); 15, 173 (1942) [USSR].*

[7] L. L. Nestorenko, Doctorate Dissertation [in Russian] (Khar'kov Polytech. Inst. 1952).

[8] V. I. Zabavin, Bull. Acad. Sci. USSR, OTN, 4, 27 (1941); Trans. Inst. Combustible Minerals, Acad. Sci. USSR 5, 36 (1955); Doctorate Dissertation [in Russian] (Inst. Combustible Minerals, Acad. Sci. USSR, Moscow, 1954).

[9] V. N. Novikov, J. Appl. Chem. 24, No. 3, 314 (1951) [USSR].*

[10] B. S. Filippov and G. P. Gorovoi, Coke and Chemistry 8, 46 (1957).

[11] M. A. Stepanenko and T. Ya. Gogoleva, Bull. Sci.- Tech. Information, Khar'kov Scientific Research Institute of Coal Chemistry 1, 33 (1956).

[12] Coke and Gas, 95, 105-107 (1947).

[13] M. A. Stepanenko, N. I. Matusyak, and T. Ya. Gogoleva, Coke and Chemistry 1, 32 (1957).

Received August 13, 1957.

*Original Russian pagination. See C. B. translation.

# PRODUCTION OF QUINALDINIC ACID FROM COAL-TAR BASES

M. M. Potashnikov and B. E. Kogan

Quinaldinic acid is now extensively used as a reagent for macro- and microgravimetric determination of zinc, copper, cadmium, and uranium, for their separation from other metals, and for colorimetric determination of ferrous iron.

Quinaldinic acid 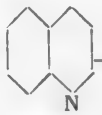 is a crystalline yellowish or white powder, which dissolves with difficulty in cold and easily in hot water, is easily soluble in hot chloroform and benzene, and crystallizes from the latter in the anhydrous state. Quinaldinic acid crystallizes readily from water, with two molecules of water which are lost at 100°. When heated above its melting point (to 160°) quinaldinic acid is decarboxylated and converted into quinoline.

Quinaldinic acid is made by bromination of quinaldine and hydrolysis of quinaldine tribromide by dilute sulfuric acid [1].

Quinaldinic acid can also be prepared by oxidation of quinaldine by a solution of chromic acid in dilute sulfuric acid [2, 3]. Methylol derivatives of quinaldine are easily oxidized by nitric acid to give quinaldinic acid [4].

The greatest difficulties in the preparation of quinaldinic acid are associated with the synthesis of quinaldine rather than with its oxidation. The literature contains descriptions of several methods for preparation of quinaldine [5-8], most of which are modifications of the aldehyde method of Debner and Miller [9].

The complexity of the synthesis and the high cost of the starting materials restrict the wide utilization of quinaldine and quinaldinic acid.

Coal-tar bases form an important source of quinaldine and quinaldinic acid. The quinaldine content of bases isolated from coal-tar fractions boiling up to 300° is about 5% [10,11]. Bases isolated from the heavy (absorption) fraction of coal tar contain 8-10% of quinaldine.

The relatively low concentration of quinaldine in coal-tar bases and the similarity in the properties of quinaldine and other quinoline and isoquinoline compounds present in these bases cause great difficulties in the isolation of quinaldine. Attempts have been made to isolate quinaldine from coal-tar bases by repeated fractionation followed by repeated recrystallization of sulfates isolated from enriched quinaldine fractions [12]. However, satisfactory results were not achieved as the quinaldine yield was low [12].

Quinaldinic acid may be prepared from the quinaldine present in coal-tar bases without isolation of quinaldine. It is known that quinaldine, in contrast to its nearest accompanying substances – quinoline and isoquinoline – reacts with formaldehyde on heating to form a mixture of methylol derivatives [4] which are easily oxidized by nitric acid (even if dilute) to quinaldinic acid. Quinoline and isoquinoline are not oxidized by nitric acid under the usual conditions, and it is therefore unnecessary to isolate methylol derivatives of quinaldine from their mixtures with quinoline and isoquinoline. By the use of these properties of quinaldine and the products of its reaction with formaldehyde, quinaldinic acid can be prepared from coal-tar bases by the following procedure.

1) Preparation of methylol derivatives of quinaldine

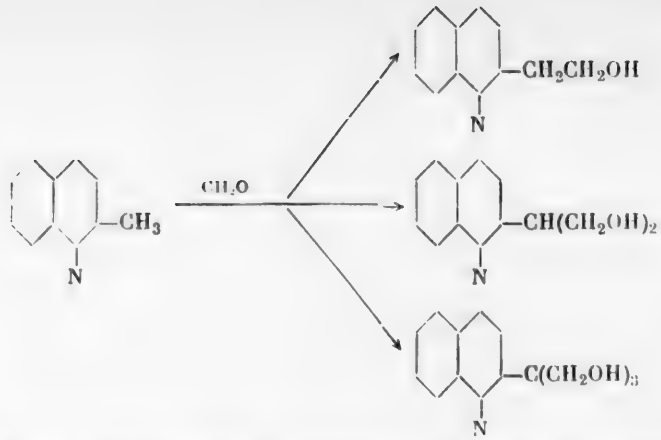


2) The interaction of quinaldine with formaldehyde can also yield vinylquinaldine by a reaction analogous to the formation of vinylpyridine from α-methylpyridine and formaldehyde [13].

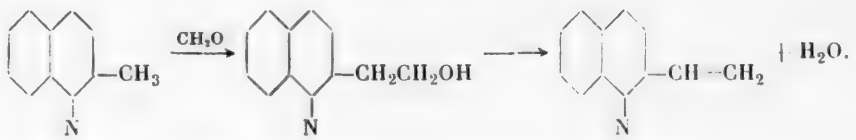


3) Oxidation of the reaction products of quinaldine and formaldehyde with formation of quinaldinic acid nitrate

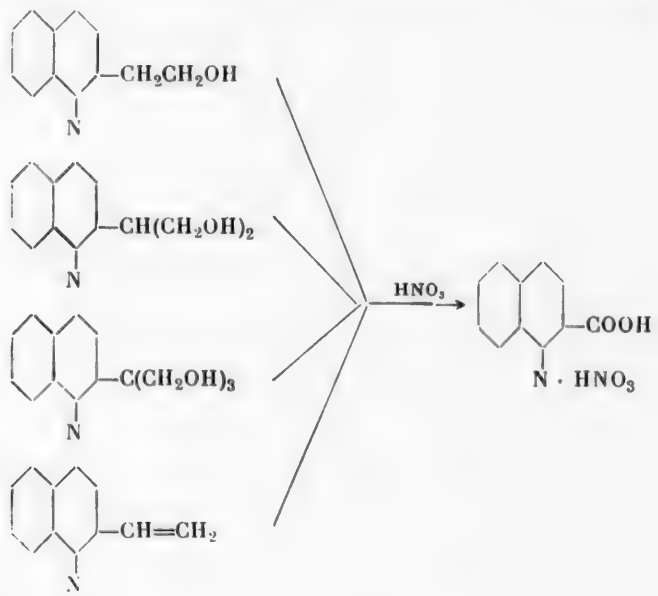


4) Conversion of quinaldinic acid nitrate into the sodium salt and decomposition of this salt by hydrochloric acid

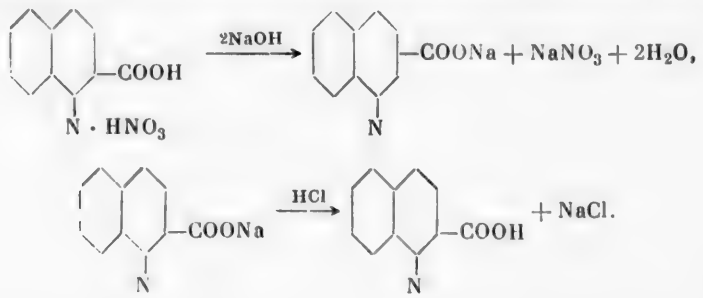

## EXPERIMENTAL

The starting material for preparation of quinaldinic acid was the mixture of bases isolated from the heavy (absorption) fraction of coal tar. These bases had the following characteristics: $d_4^{20}$ 1.089, boiling range (90%) 234-295°, water content 9%, bases 82.2%

The bases were distilled to remove water and to separate the high-boiling tarry fraction and other non-volatile impurities. The distillate had the following characteristics: $d_4^{20}$ 1.078, boiling range (90%) 240-260°, content of bases 91.4%, traces of water.

For isolation of a quinaldine-rich fraction the distilled bases were fractionated (on the pilot scale) in a 6-meter column packed with single-turn spirals 10 mm in internal diameter, made from iron wire 1 mm thick. The head fraction, consisting mainly of quinoline and isoquinoline, and the quinaldine fraction were collected. The fractions were collected at a reflux ratio of 8-10. The yields were: head fraction 55.2%, quinaldine fraction 18.4%

The 243-246° fraction, containing 29% quinaldine, was taken for preparation of quinaldinic acid. In addition to quinaldine, this fraction contained 26% quinoline and 45% isoquinoline.

Two parts by weight of this fraction and one part by weight of 40% formaldehyde (corresponding to a quinaldine-formaldehyde molar ratio of about 1:3) were put in a round-bottomed flask fitted with a stirrer and reflux condenser. The mixture was boiled with stirring for 4 hours, after which water and unchanged formaldehyde were distilled off. Preliminary experiments showed that under these conditions almost all the quinaldine present in the fraction reacts with the formaldehyde. The amount of unchanged quinaldine remaining is less than 1%

TABLE 1

Preparation of Quinaldinic Acid Nitrate

| Data | Experiment No. | | | | |
|---|---|---|---|---|---|
| | 1 | 2 | 3 | 4 | 5 |
| Weight ratio of quinaldine fraction to 40% formaldehyde | 2.00 | 1.91 | 1.98 | 1.95 | 1.44 |
| Yield of reaction products of quinaldine fraction and formaldehyde (wt.% on quinaldine fraction) | 117.3 | 117.3 | 117.3 | 114.5 | 111.0 |
| Weight ratio of 50% nitric acid to reaction products of quinaldine fraction and formaldehyde | 3.98 | 3.86 | 4.22 | 4.11 | 4.05 |
| Yield of quinaldinic acid nitrate (wt. %): | | | | | |
| on the reaction products of quinaldine fraction and formaldehyde | 30.7 | 36.7 | 33.1 | 28.9 | 31.5 |
| on the quinaldine fraction | 36.1 | 43.2 | 39.0 | 33.1 | 34.9 |
| on quinaldine present in the quinaldine fraction | 124.5 | 149.0 | 134.5 | 114.1 | 120.0 |

The reaction products consisted on a viscous dark- brown liquid. The total yield of reaction products after removal of water and residual formaldehyde was 111-117% on the original fraction.

The reaction products were oxidized in a round-bottomed flask fitted with a reflux condenser. Nitric acid of about 50% concentration was put into the flask which was placed on a water bath heated to 80-85°, and the mixture for oxidation was added in small portions.

The amount of nitric acid by weight was 4 times the weight of the mixture for oxidation. After all the

mixture had been added the reaction mass was kept in the water bath at 80-85° for two hours until evolution of brown nitrous fumes ceased; it was then transferred to a crystallizer and kept at room temperature for 20 hours. The precipitated crystals of quinaldinic acid nitrate were filtered off and washed with a little cold water. The results of the experiments are given in Table 1.

The filtrate after separation of the quinaldinic acid nitrate crystals contained quinoline and isoquinoline nitrates. After decomposition of the filtrate by alkali a fraction enriched with quinoline and isoquinoline was isolated.

Quinaldinic acid nitrate was converted into its sodium salt by treatment with 20% caustic soda solution on warming, to an alkaline reaction.

The solution of the sodium salt of quinaldinic acid was cooled at room temperature. The deposited crystals were filtered off and washed on the filter with a small amount of cold water. The salt was removed from the filter and dissolved in water with warming; concentrated hydrochloric acid was added in small portions to the hot solution to a neutral reaction. The crystals of quinaldinic acid which formed in the cooled solution were filtered off, washed with a little cold water, and dried at 100°. When dried, the quinaldinic acid melted at 156-157° and contained 99.1% of the pure substance (the content was determined by titration of a weighed sample of the quinaldinic acid with 0.1 N NaOH solution).

A single recrystallization from water yielded quinaldinic acid melting at 155.5-156.5°, containing 99.6-99.9% of the pure substance. The results of the experiments are given in Table 2.

TABLE 2

Preparation of Quinaldinic Acid

| Yields of quinaldinic acid (%) | | | | Characteristics of quinaldinic acid | | Notes |
|---|---|---|---|---|---|---|
| on the nitrate | on the fraction | on quinaldine | of the-oretical yield | melting point (°C) | purity (%) | |
| 45.6 | 16.5 | 56.8 | 47.0 | 156.0—156.5 | 99.8 | After recrystallization from water |
| 30.8 | 13.3 | 45.8 | 37.9 | 156.0—157.0 | 99.1 | Without recrystallization |
| 39.0 | 15.2 | 52.5 | 43.4 | 155.5—156.5 | 99.9 | After recrystallization from water |
| 27.5 | 9.1 | 31.4 | 25.9 | 155.5—156.5 | 99.6 | |
| 38.6 | 13.5 | 46.3 | 38.2 | 155.0—156.0 | 99.7 | |

## SUMMARY

1. A method has been developed for preparation of quinaldinic acid from quinaldine present in coal-tar bases without isolation of quinaldine in the pure form; it is based on the reaction of quinaldine with formaldehyde followed by oxidation of the methylol derivatives formed with nitric acid [14].

2. The quinaldinic acid so prepared melts within 1° and contains 99.6-99.9% of the pure substance after a single recrystallization from water.

3. The base fraction after removal of quinaldine is enriched with quinoline and isoquinoline, and can be used as raw material for their isolation.

## LITERATURE CITED

[1] L. M. Kul'berg, Syntheses of Organic Reagents [in Russian] (Goskhimizdat, 1947

[2] O. Debner, W. Miller, Ber. 16, 2472 (1883).

[3] J. Houben, Methods of Organic Chemistry, IV, 1 Book 2 (1949) p. 905 [Russian Translation].

[4] V. Meyer and P. Jacobson. Lehrbuch der Organischen Chemie (1923).

[5] N. S. Kozlov and P. N. Fedoseev, J. Gen. Chem. 6, 250 (1936)[USSR].

[6] I. F. Kryuk, J. Gen. Chem. 19, 1507 (1940) [USSR].

[7] B. I. Ardashev, J. Gen. Chem. 19, 550 (1949) [USSR].*

[8] G. I. Mikhailov, J. All-Union Sci. Res. Inst. Chem. Reagents 20, 269 (1951) [USSR].

[9] O. Debner, and W. Miller, Ber., 16, 2465 (1883).

[10] P. P. Karpukhin, Proc. Conf. on Cyclic Raw Materials [in Russian] (1936) p. 53.

[11] V. N. Novikov, Coke and Chemistry 8, 36 (1956).

[12] M. M. Krasovitskaya and A. S. Nepomnyashchaya, Trans. Khar'kov Sci. Res. Inst. Coal Chemistry 12-13, 195 (1938).

[13] L. A. Shmidt, Org. Chem. Ind. 5, 339 (1938).

[14] M. M. Potashnikov and B. E. Kogan, Authors' Certif. No. 108369 (1957).

Received 8 July, 1957.

*Original Russian pagination. See C. B. translation.

# LIQUID-PHASE OXIDATION OF HIGH-MOLECULAR PETROLEUM HYDROCARBONS

S. R. Sergienko, R. Ya. Semyachko, and P. N. Galich

The influence of the chemical nature of the original hydrocarbons on the direction and rate of oxidation was demonstrated in our earlier publications [1-3] for individual $C_{11}$-$C_{13}$ hydrocarbons and different hydrocarbon groups isolated from Diesel fuels. Special attention was devoted to elucidation of the hydrocarbon structures primarily responsible for tar formation during liquid-phase oxidation of hydrocarbons. However, the literature is still virtually devoid of data on the direction and rates of liquid-phase oxidation of higher hydrocarbons ($C_{15} - C_{30}$) present in heavier petroleum fractions. Nevertheless hydrocarbons of this type are of outstanding interest for two reasons: first, because they are present in lubricating oils and heavy motor fuels, the role of which is increasing continuously, and second, because these hydrocarbons have complex and in most instances, hybrid structures, with molecules simultaneously containing structural elements of several main hydrocarbon types (paraffinic, cycloparaffinic, and aromatic). Both the great scientific interest of compounds of this type and the fundamental difficulties in experimental investigations of their behavior in various reactions stem from this fact. Whereas in the case of lighter petroleum motor fuels it was necessary to take into consideration the mutual influence of different hydrocarbon groups present in the mixture on the course of the reaction, in the case of high-molecular petroleum hydrocarbons it becomes necessary to consider the mutual influence of different structural elements present in complex hybrid or mixed molecules.

The great practical significance of liquid-phase oxidation reactions of high-molecular petroleum hydrocarbons of hybrid structure prompted us to undertake a series of experimental investigations in this new, very important, and extremely difficult field.

## EXPERIMENTAL

In view of the fact that the presence of considerable amounts of sulfur compounds makes the course of the oxidation processes extremely complicated, low-sulfur petroleum of Gyurgyan origin was chosen for the investigation. In order to exclude chemical changes in the structure of the high-molecular petroleum hydrocarbons during their isolation, the following procedure was adopted. The gasoline-gas oil fraction of the petroleum (up to 325°) was distilled off under vacuum at bath temperature not exceeding 250°. It was shown earlier [4] that under these conditions Gyurgyan petroleum does not undergo chemical changes. The petroleum residue was then separated chromatographically on coarse-pored activated silica gel (ASG) into tarry and hydrocarbon fractions, and the latter was again separated chromatographically into three main groups: paraffin-cycloparaffinic (PCP), monocyclic aromatic (MCA), and condensed bicyclic aromatic (CBCA) hydrocarbons [5, 6]. The unseparated high-molecular hydrocarbons and the individual groups, the properties of which are given in Table 1, were studied in the present investigation. The oxidation was effected by atmospheric oxygen at atmospheric pressure (air feed rate 5-6 liters/hour) in the liquid phase at two different temperatures (150 and 175°) during 100 hours, samples being taken for investigation after 10, 25, 50, and 75 hours. The method and apparatus used were described in an earlier paper [2].

The course of the oxidation process was indicated by the variations in the contents of peroxide compounds, saponifiable, acid, and hydroxylic substances, determined potentiometrically [7-10] in the reaction products (Figs 1-3). At the end of the oxidation (after 100 hours) the reaction products were separated in accordance with the following scheme:

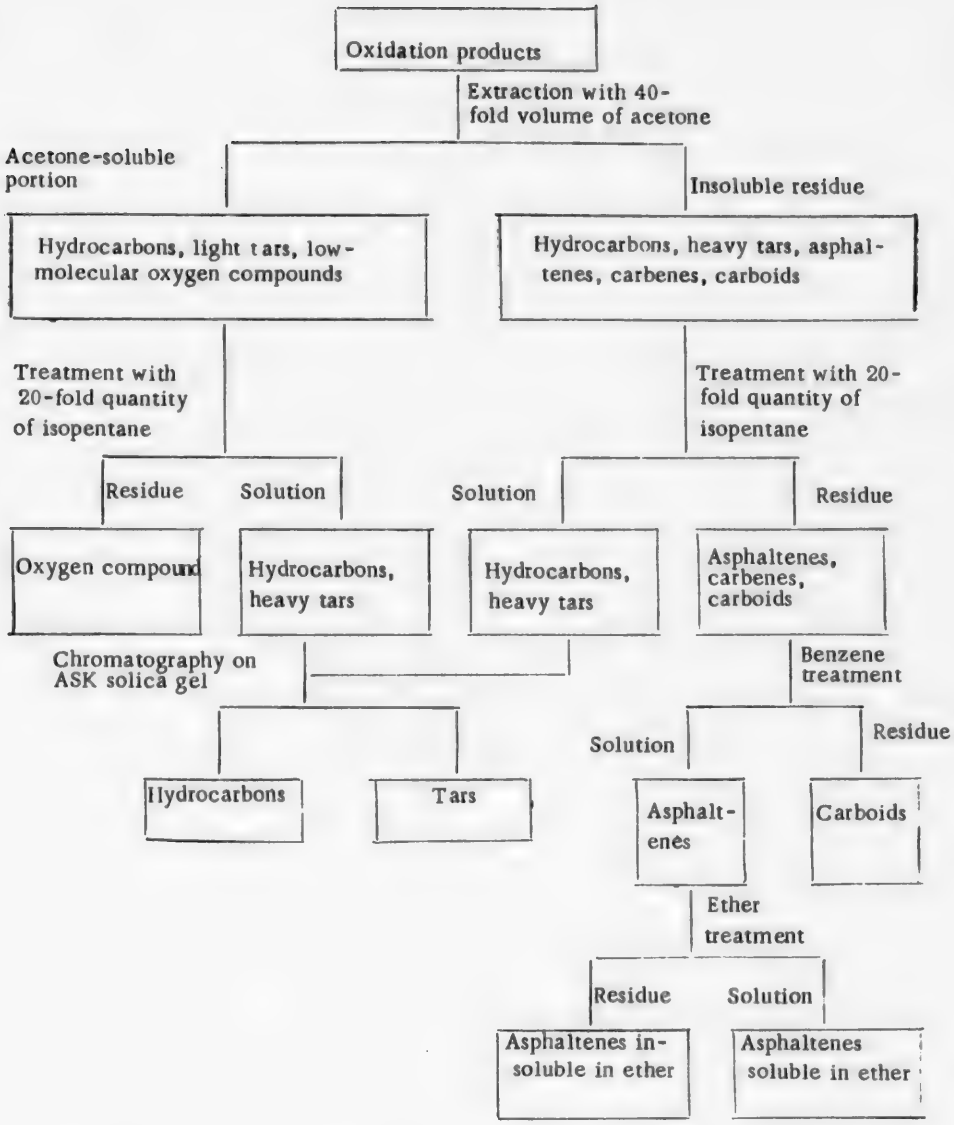


The main constituents of the reaction mixture were then investigated.

## Oxidation Characteristics of High-Molecular Hydrocarbons from Gyurgyan Petroleum

The variations of the contents of functional groups with oxidation time show that there are some common characteristics between the oxidation of unseparated high-molecular hydrocarbons and hydrocarbon groups isolated from them (PCP, MCA, and CBCA), as well as some features specific for individual hydrocarbon groups. As the paraffin-cycloparaffinic hydrocarbons form the main part of unseparated high-molecular hydrocarbons and, moreover, structural elements of this hydrocarbon class also play an important part in molecules of aromatic hydrocarbons (MCA and CBCA), it is quite natural that the general character of the oxidation of unseparated hydrocarbons is quite closely reminiscent of the oxidation of paraffin-cycloparaffinic hydrocarbons. It is also evident that the structural similarity of the two groups of aromatic hydrocarbons MCA and CBCA) determines both some degree of analogy in the course of their oxidation, and a sharper distinction between this and the oxidation of unseparated and paraffin-cycloparaffinic hydrocarbons. Common features of the oxidation of all the studied groups of high-molecular hydrocarbons at both temperatures (150 and 175°) are: 1) peroxide compounds are the first oxygen compounds to appear in the reaction mixture; 2) acidic compounds and hydroxylic compounds

TABLE 1

Composition and Properties of High-Molecular Petroleum Hydrocarbon Groups

| Hydrocarbon groups | Molecular weight | $d_4^{20}$ | $n_D^{20}$ | Group composition (wt. %) | | | Elementary composition (%) | | | | | C/H | Empirical formula | Homologous series |
|---|---|---|---|---|---|---|---|---|---|---|---|---|---|---|
| | | | | ПШП | МЦА | БЦА | C | H | S | N | | | | |
| Paraffin–cycloparaffinic | 292 | 0.8735 | 1.4790 | 91.2 | 6.8 | — | 86.57 | 13.49 | — | — | | 6.4 | $C_{21.0}H_{39.5}$ | $C_nH_{2n-2.5}$ |
| Monocyclic aromatic . . . . . | 329 | 0.9306 | 1.5179 | 1.8 | 93.8 | 3.0 | 87.83 | 11.95 | 0.39 | — | | 7.3 | $C_{24.0}H_{39.1}S_{0.04}$ | $C_nH_{2n-5.8}$ |
| Condensed bicyclic aromatic . . . . . | 420 | 1.0142 | 1.5920 | — | 99 | — | 88.88 | 0.91 | 0.83 | 0.51 | | 8.9 | $C_{31.0}H_{41.6}S_{0.1}N_{0.08}$ | $C_nH_{2n-20.6}$ |
| Not separated . . . . . | 315 | 0.9170 | 1.5093 | 49.3 | 21.1 | 23.2 | 86.96 | 12.57 | 0.37 | 0.22 | | 6.9 | $C_{22.8}H_{39.7}S_{0.05}N_{0.05}$ | $C_nH_{2n-5.9}$ |




Fig. 1. Variation of peroxide numbers with oxidation time at 150 and 175°:
A) peroxide number, B) oxidation time (hours);
1) high-molecular paraffin-cycloparaffinic hydrocarbons, 2) high-molecular unseparated hydrocarbons.

appear after a definite peroxide concentration in the reaction products has been reached, and are therefore formed by decomposition of peroxides; 3) neutral (saponifiable) oxygen compounds are formed in appreciable amounts only after a definite concentration of acidic products has been reached in the reaction mixture; they represent the final conversion stage so far as low-molecular oxidation products are concerned, and serve as the starting material for oxidative condensation processes which lead to formation of tarry substances of higher molecular weight. The amounts and, to some extent, the nature of the latter depend on the chemical nature of the oxidized hydrocarbons.

Paraffin-cycloparaffinic hydrocarbons (PCP) have a well defined induction period of oxidation at 150°; this is shown by the fact that after 10 hours of oxidation only small amounts of peroxides were formed, with total absence of any other oxygen compounds. At 175° there is almost no induction period, and during the first 10 hours of oxidation peroxide formation passes through its maximum, with consequent appearance of acidic and saponifiable substances in the reaction products. Hydroxylic compounds were not detected at any stage of the oxidation process at either temperature; this indicates that they must be the substances which determine the reaction of ester formation in the process.

TABLE 2

Composition of Oxidation Products from Different Hydrocarbon Groups of Gyurgyan Petroleum

| Original hydrocarbons | Composition of oxidation products (%) | | | | | | | | | | | |
|---|---|---|---|---|---|---|---|---|---|---|---|---|
| | 150° | | | | | | 175° | | | | | |
| | hydrocarbons | low-molecular oxygen compounds | tars | asphaltenes | carboids and carbenes | total oxygen compounds | hydrocarbons | low-molecular oxygen compounds | tars | asphaltenes | carboids and carbenes | total oxygen compounds |
| Paraffin-cycloparaffinic | 83.4 | 0.6 | 15.3 | 0.4 | 0.3 | 16.6 | 76.1 | 1.5 | 19.4 | 1.7 | 1.3 | 23.9 |
| Monocyclic aromatic | 89.1 | 5.2 | 5.7 | Следы | Следы | 10.9 | 66.6 | 7.3 | 18.5 | 7.6 | Следы | 33.4 |
| Condensed bicyclic aromatic | 55.9 | 3.4 | 28.8 | 11.9 | Следы | 44.1 | 46.8 | 12.3 | 16.9 | 20.8 | 3.2 | 53.2 |
| Unseparated high-molecular | 87.8 | 1.5 | 4.7 | 5.0 | 1.0 | 12.2 | 70.9 | 1.1 | 10.2 | 6.3 | 11.5 | 29.1 |




Fig. 2. Variation of acid numbers with oxidation time at 150 and 175°:
A) acid number, B) oxidation time (hours); 1) high-molecular paraffin-cycloparaffinic hydrocarbons, 2) high-molecular monocyclic aromatic hydrocarbons, 3) high-molecular condensed bicyclic aromatic hydrocarbons, 4) high-molecular unseparated hydrocarbons.

At 150° the process was less extensive both with regard to the amount of hydrocarbons oxidized (17%) (Table 2) and with regard to the conversion of oxygen-containing products, whereas at 175° the process went quite far — about 25% of the original hydrocarbons was oxidized, and a considerable proportion on the oxidized products consisted of such products of deep condensation and carbonization as asphaltenes, carbenes, and carboids, and also low-molecular oxygen-containing breakdown products. The oxidation process also had a great influence on the hydrocarbon fraction isolated from the oxidation products (Table 3). In this fraction the content of benzene homologs was more than doubled, which shows that in prolonged oxidation at 175° dehydrogenation of hexamethylene to benzene rings becomes appreciable.

Monocyclic aromatic hydrocarbons (MCA) at 150° also have an induction period, and the process as a whole results in a lower degree of oxidation than

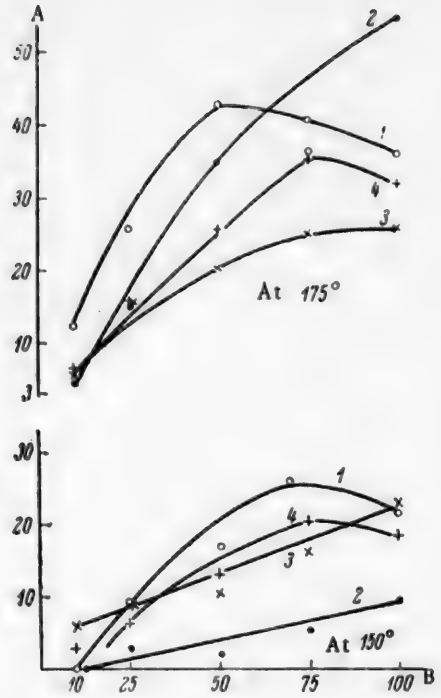


Fig. 3. Variation of saponification numbers with oxidation time at 150 and 175°: A) saponification number, B) oxidation time (hours); 1) high-molecular paraffin-cycloparaffinic hydrocarbons, 2) high-molecular monocyclic aromatic hydrocarbons 3) high-molecular condensed bicyclic aromatic hydrocarbons, 4) high-molecular unseparated hydrocarbons.

in the case of PCP, so that after 100 hours of oxidation only 11% of the original hydrocarbons was oxidized, whereas at 175° 33% was oxidized. The contents of peroxide compounds were low throughout the process both at 150 and at 175°, and did not pass through any appreciable maximum at the initial stage, as was the case in the oxidation of PCP hydrocarbons. This is quite consistent with the results obtained by us earlier [3] in the oxidation of aromatic hydrocarbons in Diesel fuel.

Increase of the oxidation temperature by 25° (from 150 to 175°) had an even more pronounced effect on the MCA than on the PCP high-molecular hydrocarbons. In this case, in contrast to the former, condensed bicyclic aromatic systems were formed from benzene rings; this may be attributed to two reactions: dehydrogenation of systems of the tetralin type, or condensation of benzene rings, the former being the more probable.

Condensed bicyclic aromatic hydrocarbons (CBCA) exhibited smaller differences in oxidation behavior at two different temperatures (150 and 175°) than the two hydrocarbon groups discussed above (PCP and MCA). The fact that the amounts of peroxide compounds present at the initial stage of the process were very small is without doubt the main reason why the increase in the contents of acidic and neutral (saponifiable) oxygen compounds in the reaction products is extremely slow (especially at 150°). Toward the end of the oxidation process (after 100 hours) the reaction products contained 44% of oxygen compounds at 150°, and 53% at 175°; they were predominantly high-molecular tarry asphaltenic substances. As in the oxidation of MCA hydrocarbons, larger amounts of asphaltenes and low-molecular oxidation products are formed at the higher temperature (175°). Formation of polycyclic condensed aromatic structures in the remaining unoxidized hydrocarbons is appreciable, especially at 175°.

TABLE 3

Changes in the Group Composition of High-Molecular Hydrocarbons of Gyurgyan Petroleum in Liquid-Phase Oxidation

| High-molecular hydrocarbons | Group composition of hydrocarbons (wt.%) | | | | | | | | | | |
|---|---|---|---|---|---|---|---|---|---|---|---|
| | original | | | isolated after oxidation | | | | | | | |
| | | | | 150° | | | | 175° | | | |
| | PCP | MCA | CBCA | PCP | MCA | CBCA | PCA | PCP | MCA | CBCA | PCA |
| Paraffin–cycloparaffinic | 91.2 | 6.8 | — | 92.5 | 6.3 | — | — | 81.7 | 15.0 | — | — |
| Monocyclic aromatic | 1.8 | 93.8 | 3.0 | 5.3 | 80.3 | 7.9 | — | 6.5 | 87.9 | 2.1 | — |
| Condensed bicyclic aromatic | — | — | 99 | — | 3.8 | 5.1 | 38.6 | — | — | 63.6 | 35 |
| Unseparated high-molecular | 49.3 | 21.1 | 23.2 | 46.1 | 34.2 | 12.3 | — | 51.1 | 37.6 | 9.8 | — |

Unseparated high-molecular hydrocarbons presented a very complex picture on oxidation, and increase of the oxidation temperature had a strong influence both on the degree of oxidation of the hydrocarbons (12% at 150° and 29% at 175°) and on the depth of conversion of the oxidized products. The unoxidized portion of the hydrocarbons differed sharply in composition from the hydrocarbon mixture taken for oxidation: the greatest degree of conversion was found for the condensed aromatic portion, which is the main source of tarry asphaltenic substances forming the major part of the oxygen-containing reaction products.

Analysis of the results obtained in oxidation of high-molecular hydrocarbons of complex hybrid molecular structure leads to a series of general conclusions which are of great scientific and practical importance both for an understanding of the nature and the reactions of hydrocarbons of this complex chemical composition, and for elucidation of the nature of the genetic relationships between the hydrocarbon and heteroorganic high-molecular components of petroleum.

## SUMMARY

1. It is shown that the oxidation reaction in conjunction with chromatographic separation provides a route to a deeper insight into the chemical nature of high-molecular petroleum hydrocarbons with a predominant hybrid (mixed) type of molecular structure.

2. It is shown that in the oxidation of high-molecular petroleum hydrocarbons,compounds containing condensed aromatic structures in their molecules are the chief source of tarry asphaltenic substances; this is very strong evidence in favor of a direct genetic relationship between condensed aromatic high-molecular hydrocarbons and tarry asphaltenic substances in petroleum. On the basis of these results the general genetic relationship between the hydrocarbon and tarry portions of petroleums (oils → tars → asphaltenes) may be clarified considerably in the form of the following genetic system:

condensed bicyclic aromatic compounds
↓
condensed polycyclic aromatic compounds
↓
tars
↓
asphaltenes

3. Owing to the presence of considerable amounts of monocyclic paraffinic and aliphatic structural elements in hybrid monocyclic aromatic (MCA) and condensed bicyclic aromatic (CBCA) high-molecular petroleum hydrocarbons, liquid-phase oxidation of the latter generally yields a certain amount of paraffin-cycloparaffinic and paraffin-cycloparaffin-monocyclic aromatic hybrid structures; this process is more pronounced at moderate temperatures and is greatly masked under more harsh temperature conditions owing to complications caused by secondary reactions.

4. When the oxidation temperature is increased by 25°, from 150 to 175°, asphaltenes begin to predominate among the oxidation products of high-molecular condensed aromatic hydrocarbons, while tars (in the scheme: condensed aromatic hydrocarbons → tars → asphaltenes) merely provide an intermediate stage in the hydrocarbon conversion.

5. It is shown that high-molecular paraffin-cycloparaffinic hybrid hydrocarbons oxidized in the liquid phase at 150- and 175° pass through a maximum peroxide content within the first 10 hours; this maximum precedes the start of formation of acidic, saponifiable, and hydroxylic oxygen compounds. This pronounced maximum of peroxide formation is not observed in the oxidations of high-molecular aromatic hydrocarbons.

6. When high-molecular paraffin-cycloparaffinic hydrocarbons are oxidized at 175° benzene rings are formed, while in the case of benzene homologs,condensed aromatic systems are produced; this indicates that under these conditions oxygen causes dehydrogenation of hexamethylene to benzene rings, and of tetrahydronaphthalene to naphthalene rings.

7. It is shown that bicyclic aromatic condensed hydrocarbons are the most easily condensed both at 150 and at 175°, followed by monocyclic aromatic and unseparated high-molecular hydrocarbons, which are

similar in their tendency to oxidation. Paraffin-cycloparaffinic hydrocarbons are oxidized more easily at 150° than the other hydrocarbons, yielding low-molecular oxidation products, but at 175°, when oxidative condensation of the oxidation products becomes more pronounced, they are converted to a lesser extent than the others.

## LITERATURE CITED


[1] S. R. Sergienko and P. N. Galich, J. Appl. Chem. 28, 735 (1955) [USSR].*

[2] S. R. Sergienko and P. N. Galich, Proc. Conf. on Catalytic Hydrogenation [in Russian] (Alma-Ata, 1956) p. 255.

[3] S R. Sergienko and P. N. Galich, J. Appl. Chem. 29, 1568 (1956) [USSR].*

[4] S. R. Sergienko, Bull. Acad. Sci. Azerbaidzhan SSR 9, 3 (1953).

[5] S. R. Sergienko, I. O. Delone, B. E. Davydov, and M. P. Teterina, Trans. Inst. Petroleum Acad. Sci. USSR 4, 18 (1954).

[6] S. R. Sergienko, R. Ya. Semyachko, and B. E. Davydov, Trans. Inst. Petroleum Acad. Sci. USSR 12, 65 (1958).

[7] S R. Sergienko, N. A. Izmailov, L. L. Spivak, and P. N. Galich, J. Analyt. Chem. 10, 315 (1955) [USSR].*

[8] S. R. Sergienko, P. N. Galich, N. A. Izmailov, and L. L. Spivak, J. Analyt. Chem. 11, 731 (1956) [USSR].*

[9] S. R. Sergienko, P. N. Galich, and L. L. Spivak, J. Analyt. Chem. 12, 139 (1957) [USSR].

[10] M. N. Sokolova, Trans. Inst. Petroleum Acad. Sci. USSR 1, 277 (1950).



Received May 16, 1957.


*Original Russian pagination. See C. B. translation.

# THE USE OF HYDROCARBON FUEL IN CELLS WITH SOLID ELECTROLYTES

V. S. Daniel'-Bek, M. Z. Mints, V. V. Sysoeva, and M. V. Tikhonova

During recent year there has been a considerable number of investigations of fuel cells with solid electrolytes, intended for high-temperature operation; these include the work of Baur et al. [1-4], Davtyan [5-7], Gorin [8-10], and Bischoff [11,12]. It should be noted, however, that neither these investigations nor researches on fuel cells in general have as yet led to the development of devices suitable for technical use.

The efficiency of these sources of current can be expressed in two ways: as the ratio of the amount of electrical energy produced at a given operating temperature to the heat of combustion of the consumed fuel at the same temperature, or as the ratio of the same amount of electrical energy to the heat of combustion or calorific power of the consumed fuel determined under standard conditions, i.e., at room temperature, We shall use the second method for expressing efficiency, as it is of greater technical significance.

A number of workers, including Davtyan [7], have performed thermodynamic calculations of the theoretical maximum values for the efficiency and e.m.f. of high-temperature fuel cells using different types of fuel: carbon, carbon monoxide, hydrogen. We have recalculated these values with the aid of more recent data [13, 14]. The results are presented graphically in Fig. 1 and Fig. 2.

In some instances the efficiency exceeds 100% Such values are to some extent conventional, as they indicate that in such a case the electrochemical process is accompanied by absorption of heat from the surroundings, and to prevent cooling and to maintain the system at the required operating temperature an additional consumption of the corresponding amount of fuel is needed. Thus, the maximum efficiency from the technical standpoint does not exceed 100% in such cases.

The e.m.f. values given in Fig. 2 are calculated on the assumption that the oxidizing agent in the cell is pure oxygen at atmospheric pressure. If air is used, the e.m.f. is less by 0.01 to 0.05 v, according to the temperature.

In considerations of the possible utilization of fuel cells as sources of electricity for communications and broadcasting equipment in nonelectrified regions it is very important that the cells should require little or no attention. The use of gas producers is undesirable for this reason, and the possibility of using liquid fuel, and in particular gasoline, is of great interest. The literature contains no information on the operation of fuel cells with the use of hydrocarbon fuel, and it was necessary to investigate the matter experimentally. The investigation was preceded by thermodynamic calculations of the theoretical values of e.m.f. and efficiency in the electrochemical oxidation of various hydrocarbons.

The most detailed data for the first two members of the paraffin series, methane and ethane, and also for octane, are given below. Octane was chosen because it occupies a middle position in the gasoline fraction and may be regarded as a typical constituent of gasoline. Cyclohexane was chosen as a typical naphthenic hydrocarbon. The free energy ($A_T$), efficiency ($\eta_2 = \frac{A_T}{Q_{298}} \cdot 100$) and e.m.f. (E) of electrochemical oxidation at temperatures of 298, 500, 1000, and 1500° on the absolute scale were calculated for these four substances (Table 1). In addition, these values were calculated for a number of other hydrocarbons of the methane series up to dodecane (b.p. 216°) and for certain unsaturated and cyclic hydrocarbons at one temperature, namely

TABLE 1

Maximum Values of the Efficiency and e.m.f. in Electrochemical Oxidation of Certain Hydrocarbons at Different Temperatures

| Temperature | | Methane $CH_4 + 2O_2 \rightarrow CO_2 + 2H_2O$ $Q_{298} = 212798$ cal/mole | | | Ethane $C_2H_6 + 3\frac{1}{2}O_2 \rightarrow 2CO_2 + 3H_2O$ $Q_{298} = 372820$ cal/mole | | | Octane $C_8H_{18} + 12\frac{1}{2}O_2 \rightarrow 8CO_2 + 9H_2O$ $Q_{298} = 1307530$ cal/mole | | | Cyclohexane $C_6H_{12} + 9O_2 \rightarrow 6CO_2 + 6H_2O$ $Q_{298} = 936980$ cal/mole | | |
|---|---|---|---|---|---|---|---|---|---|---|---|---|---|
| in °K | in °C | $A_T$ (cal/mole) | $\eta_2$ (%) | E (v) | $A_T$ (cal/mole) | $\eta_2$ (%) | E (v) | $A_T$ (cal/mole) | $\eta_2$ (%) | E (v) | $A_T$ (cal/mole) | $\eta_2$ (%) | E (v) |
| 298 | 25 | 195240 | 91.75 | 1.058 | 350340 | 93.97 | 1.084 | 1267260 | 96.92 | 1.098 | 912510 | 97.40 | 1.098 |
| 500 | 227 | 193267 | 90.82 | 1.047 | 350159 | 93.97 | 1.084 | 1278609 | 97.79 | 1.108 | 921368 | 98.35 | 1.109 |
| 1000 | 727 | 191664 | 90.07 | 1.038 | 354222 | 95.01 | 1.096 | 1317110 | 100.73 | 1.141 | 950528 | 101.46 | 1.144 |
| 1500 | 1227 | 191929 | 90.09 | 1.039 | 361343 | 96.95 | 1.118 | 1363547 | 104.29 | 1.181 | 984204 | 105.05 | 1.184 |

1000 K (727°C)(Table 2). Our calculations of free-energy and enthalpy changes in the formation of hydrocarbons and in combustion of carbon and hydrogen were based mainly on data of Korobov and Frost, Esin and Gel'd, and others [13-15].*

Consideration of the results of thermodynamic calculations leads to the conclusion that when hydrocarbon mixtures in the proportions found in various gasolines are used in fuel cells in the 500-1000° range they can theoretically give efficiencies of up to 95-100% with e.m.f. up to 1.10-1.15 v.

The device used for experimental investigation of cells working on vapors of gasoline and other liquid fuels is shown schematically in Fig. 3. Gasoline vapor is fed into the central chamber 1 of the apparatus from chamber 2 by means of a wick contained in a vertical tube 3. To test that the chamber is completely filled, gasoline vapor is lit at the orifice 4 of the exit tube 5. The two wide sidewalls of the chamber have openings in the form of rectangular (or round) windows in which the cells are inserted. Thus, two cells are fitted and tested in each apparatus, heated in the furnace 6. Each cell consists of solid electrolyte 7 and two electrodes: hydrocarbon 8 and air 9. The solid electrolyte was in the form of a rectangular or round plate fixed in a steel frame: the latter was attached to the body of the cell. To form the electrode, a perforated metal plate (usually Nichrome) was pressed against the surface of the solid electrolyte and coated with a thin layer of the appropriate electrode material. A current lead was welded to the perforated plate. Other electrode designs with thickened layers of electrode materials were tested, including the design described by Davtyan [6,7]. A considerable number of tests was performed with the solid electrolyte composition recommended by Davtyan, but instead of calcined monazite, reactive cerium dioxide was used (Electrolyte XVII/1). Similar results were obtained with a modification of this composition, with a lower content of cerium dioxide (Electrolyte XVII/6). The compositions for these two solid electrolytes are given below, and the variations of their specific resistance with temperature are plotted in Fig. 4.

| | XVII/1 | XVII/6 |
|---|---|---|
| $Na_2CO_3$ | 43 | 53 |
| Technical sodium silicate (modulus 2.8) | 10 | 12 |
| $CeO_2$ | 27 | 10 |
| $WO_3$ | 20 | 25 |

*Recently newer data have been published by Maslov, e.g. [16-18]. However, our values for efficiency and e.m.f. would be changed very little if these data were used for calculations.

TABLE 2

Maximum Values of the Efficiency and e.m.f. in Electrochemical Oxidation of Hydrocarbons at T = 1000°K (t = 727°C)

| Hydrocarbon class | Hydrocarbon | $A_{1000}$ (cal/mole) | $Q_{298}$ (cal/mole) | $\eta_2$ (%) | E (v) |
|---|---|---|---|---|---|
| Saturated (paraffins) of normal structure | Methane | 191664 | 212798 | 90.07 | 1.038 |
| | Ethane | 354222 | 372820 | 95.01 | 1.096 |
| | Propane | 514810 | 530605 | 97.02 | 1.115 |
| | Butane | 674878 | 687982 | 98.10 | 1.125 |
| | Pentane | 835306 | 838800 | 99.58 | 1.131 |
| | Hexane | 995884 | 995010 | 100.09 | 1.136 |
| | Heptane | 1156502 | 1151270 | 100.45 | 1.139 |
| | Octane | 1317110 | 1307530 | 100.73 | 1.141 |
| | Nonane | 1477728 | 1463800 | 100.98 | 1.144 |
| | Decane | 1638346 | 1620060 | 101.13 | 1.145 |
| | Undecane | 1798964 | 1776320 | 101.27 | 1.146 |
| | Dodecane | 1959582 | 1932590 | 101.40 | 1.147 |
| Unsaturated (olefins) | Ethylene | 310325 | 337234 | 92.02 | 1.120 |
| | Propylene | 466544 | 491987 | 94.83 | 1.123 |
| | Octene | 1268304 | 1279130 | 99.15 | 1.145 |
| | Decene | 1589580 | 1594020 | 99.72 | 1.148 |
| Cyclic (naphthenes, and benzene series) | Cyclopentane | 788470 | 78654 | 100.25 | 1.114 |
| | Methylcyclopentane | 944688 | 941140 | 100.38 | 1.137 |
| | Cyclohexane | 950528 | 936880 | 101.46 | 1.144 |
| | Benzene | 770450 | 780510 | 98.71 | 1.112 |
| | Toluene | 925538 | 933750 | 99.12 | 1.114 |
| | m-Xylene | 1083566 | 1086950 | 99.69 | 1.118 |

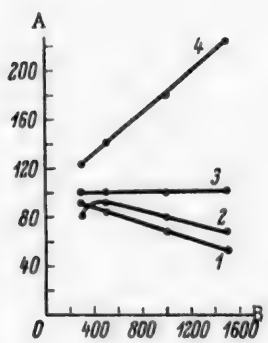


Fig. 1. Maximum efficiency as a function of temperature: A) efficiency (%), B) temperature (deg K); maximum efficiencies for the reactions: 1) $CO + 0.5O_2 = CO_2$, 2) $H_2 + 0.5O_2 = H_2O$; 3) $C + O_2 = CO_2$; 4) $C + 0.5O_2 = CO$.

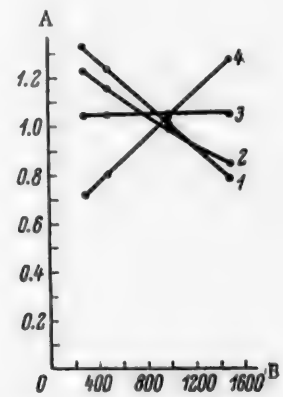


Fig. 2. Maximum e.m.f. as a function of temperature: A) electromotive force (v), B) temperature (deg K); maximum e.m.f. for the reactions: 1) $CO + 0.5O_2 = CO_2$, 2) $H_2 + 0.5O_2 = H_2O$, 3) $C + O_2 = CO_2$, 4) $C + 0.5O_2 = CO$.

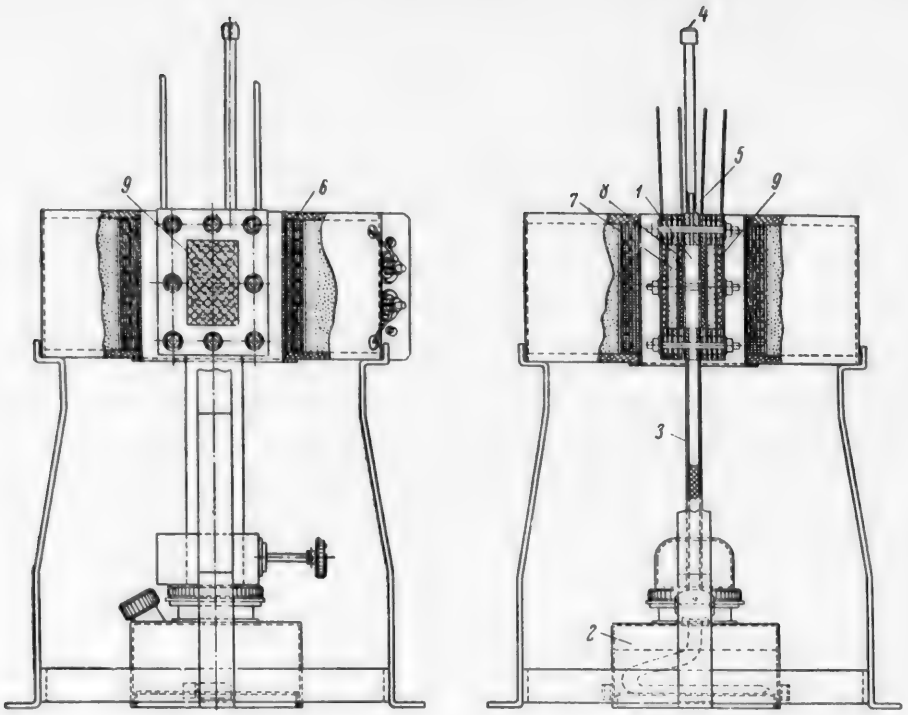


Fig. 3. Apparatus for tests of fuel cells with liquid fuel.

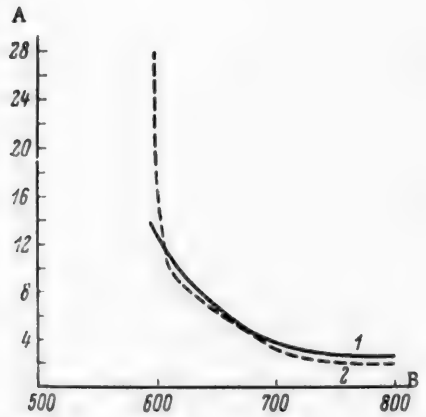


Fig. 4. Effect of temperature on specific resistance of solid electrolytes XVII/1 (1) and XVII/6 (2):
A) specific resistance $\rho$ (ohm·cm), B) temperature (°C).

For preparation of the electrolyte the components were melted together and the melt was kept at 900-1000° until $CO_2$ evolution ceased. This gas evolution was the result of interaction of $Na_2CO_3$ with acidic oxides ($SiO_2$ and $WO_3$) to form the corresponding salts, sodium metasilicate and tungstate. The following substances were tested as active masses for the hydrocarbon electrodes: disperse (carbonyl) iron, Davtyan's mixture ($Fe_2O_3$ + Fe + Clay), ferric oxide, and copper and magnesium chromites. Various oxides: $Fe_2O_3$, $Fe_3O_4$, CuO, NiO, $CeO_2$, CdO were tested as materials for the air electrode. They all gave approximately equivalent results, and therefore most of the subsequent experiments were performed with Davtyan's mixture for the hydrocarbon electrode and magnetite for the air electrode. The cells were tested not only with gasoline, but also with fuel gases – carbon monoxide and hydrogen.

It was found in tests of the cells with gasoline that the cells develop an electromotive force and when in circuit with an external resistance can produce an electric current, thus producing electrical energy by the reaction of gasoline combustion conducted electrochemically. The cell characteristics (e.m.f., current density, potential, specific power) were approximately the same as with hydrogen or carbon monoxide. This confirmed experimentally that it is possible in principle to operate fuel cells with gasoline. The e.m.f. was somewhat below the theoretical value found by thermodynamic calculation; this may be attributed to the existence of some electronic conductance (in addition to ionic) in the solid electrolyte used. In fact, $CeO_2$ and $WO_3$ have the properties of semiconductors, and it would be natural to expect that an electrolyte containing these oxides would have some electronic conductance, and this must lower the cell e.m.f.

In illustration of the results obtained, variations of temperature, e.m.f. and internal resistance of the cell in one of the experiments are plotted in Fig. 5. It is seen from these results that the cells become efficient at temperatures above 600°. The best results were usually obtained at 700-750°, and further increase of temperature did not improve the results. The cells had e.m.f. of 0.8-0.9 v and internal resistance of about 0.1-0.2 ohm per $dm^2$ of effective area (with solid electrolyte 2-3 mm thick). The cells could be put in circuit with an external resistance and operated at current densities of 1.0-1.5 amp/$dm^2$ at a fairly stable voltage of 0.5-0.7 v. After several hours of operation the electrical characteristics of the cell gradually deteriorated. In repeated tests the cells usually operated at lower voltages than initially. The current-voltage characteristics of one of the cells, determined during brief application of load (at 750°), are plotted in Fig. 6.

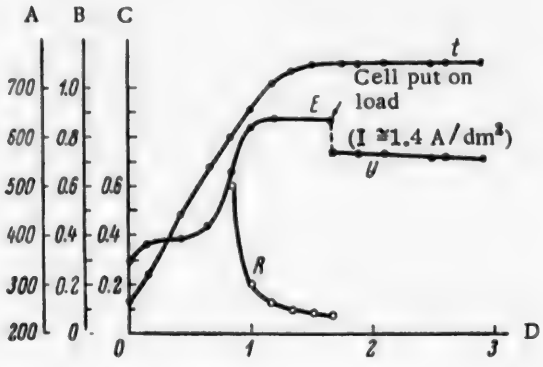


Fig. 5. Graph showing typical results of fuel cell tests with the use of gasoline:
A) temperature (°C), B) e.m.f. (E) and voltage (in v), C) internal resistance R (ohm/$dm^2$), D) time (hours). 1) Cell put on load (I ≈ 1.4 amp/$dm^2$)

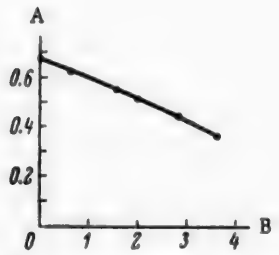


Fig. 6. Current-voltage characteristics of fuel cell at t = 750°:
A) voltage (v), B) current density (amp/$dm^2$).

Most of the test were carried out with B-70 gasoline. In addition, comparative tests were performed on different grades of gasoline, and approximately the same results were obtained. The greatest defect of the cells, which as yet prevents their technical use, is inadequate stability in operation. This instability was found both with gasoline and with gaseous fuels – carbon monoxide or hydrogen. The instability may be due to the following causes: 1) the existence of cationic conductance in the solid electrolyte, which would lead to changes in the electrolyte composition during operation of the cell; 2) reduction of some of the electrolyte components (in particular, $Na_2WO_4$) by the fuel, with an increase in the electronic component of the conductance and a consequent decrease of cell e.m.f.; 3) increasing permeability of the solid electrolyte to gases.

The last of these factors is the most pronounced, and its existence was established experimentally. Various technological procedures were tried for preparation of the solid electrolyte plates: casting, molding of the half-melted viscous mass, cold pressing followed by sintering, etc. The specimens so made differed in gas permeability, but no regular distinctions between the characteristics of the cells made with them could be detected. Thus, within certain limits some degree of gas permeability in the solid electrolyte does not have any significant influence on the cell performance. However, the gas permeability subsequently increases both by formation of micro- and macrocracks, and by increase of porosity owing to structural changes in the solid electrolyte. It was found experimentally that considerable gas permeability, such that gasoline vapor penetrates to the air electrode, results in a sharp drop of the cell e.m.f. These facts are important in relation both to cells run on gasoline, and to cells run on carbon monoxide or hydrogen. However, in the case of benzene there is another important factor: incomplete combustion of the gasoline takes place in the pores and cracks of the solid electrolyte, with formation of carbon which gradually builds conducting bridges which short-circuit the cell electrode.

Thus, to increase the service life of the fuel cells described in this paper it is necessary to eliminate the above-mentioned defects of the solid electrolyte, and primarily to ensure fairly stable impermeability to gases.

## SUMMARY

1. Thermodynamic calculations and experimental results show that fuel cells with solid electrolytes can

be operated with the use of hydrocarbon fuel, including gasoline, giving fairly high values of electromotive force (0.8-0.9 v).

2. In tests of experimental cells it was found that the best characteristics are obtained at 700-750°. It was shown that the cells can operate at current densities up to 1.0-1.5 amp/dm$^2$ at 0.5-0.7 v. However, after several hours the electrical characteristics deteriorate because of inadequate chemical and mechanical stability of the solid electrolytes used.

## LITERATURE CITED


[1] E. Baur and R. Brunner, Z. Elektroch. 43, 9, 725 (1937).

[2] E. Baur and H. Preis, Z. Elektroch. 43, 9, 727 (1937).

[3] E. Baur, Bull. Schweiz. Elektrotechn. Ver. 17, 478 (1939).

[4] E. Baur, Brennst. Chem. 20, 385 (1939).

[5] O. K. Davtyan, Bull. Acad. Sci. USSR, OTN, 1, 107 (1946).

[6] O. K. Davtyan, Bull. Acad. Sci. USSR, OTN, 2, 215 (1946).

[7] O. K. Davtyan, The Problem of Direct Conversion of Chemical Energy of Fuel into Electrical Energy [in Russian] (Izd. AN SSSR, 1947).

[8] E. Gorin and Pittsburgh Consolidation Coal Co. U.S. Patent 2570543 (1951).

[9] E. Gorin and Pittsburgh Consolidation Coal Co. U.S. Patent 2581650 (1952).

[10] E. Gorin and Pittsburgh Consolidation Coal Co. U.S. Patent 2581651 (1952).

[11] K. Bischoff, Brennst. Warmekr. 3, 154 (1951).

[12] Watson, Research 7, 34 (1954).

[13] O. A. Esin and P. V. Gel'd, Physical Chemistry of Pyrometallurgical Processes, 1 [in Russian] (Metallurgy Press, 1950).

[14] Selected Values of Chemical Thermodynamic Properties, Nat. Bur. Standards Circular No. 500 (1952).

[15] M. D. Tilicheev (editor), Physicochemical Properties of Individual Hydrocarbons, 3 [in Russian] (State Fuel Tech. Press, 1951).

[16] P. G. Maslov, Proc. Acad. Sci. USSR 86, No. 5 (1952).*

[17] P. G. Maslov, J. Appl. Chem. 26, No. 4 (1953) [USSR].*

[18] P. G. Maslov, J. Appl. Chem. 26, No. 5 (1953) [USSR].*


Received June 25, 1957.

*Original Russian pagination. See C. B. translation.

# EFFECT OF THIO DERIVATIVES OF UNSATURATED PHOSPHONIC ACIDS ON THE ANTIOXIDANT PROPERTIES OF MINERAL OIL*

K. K. Papok, K. N. Anisimov, B. S. Zuseva, and N. E. Kolobova

In an earlier paper we considered the effects of diesters, tetraalkyl diamides, and dipiperidides of unsaturated phosphonic acids on the antioxidant properties of MS-20 oil [1].

In extension of our studies of the effects of derivatives of unsaturated phosphonic acids, we investigated the effects of dithioethyl esters of unsaturated phosphonic and thiophosphonic acids, and of esters on alkylthiovinylphosphonic acids on the antioxidant properties of MS-20 oil (Table 1).

Compounds of the following type were prepared for the investigation:

$$ROCH = CHPO(SR)_2,$$

$$RCH = CHPO(SR)_2,$$

$$ROCH = CHPS(SR)_2,$$

$$RSCH = CHPO(OR)_2,$$

where R is $C_2H_5$, $C_4H_9$, $CH_3-O-CH_2CH_2$, $C_2H_5-O-CH_2-OH_2$, $C_4H_9-O-CH_2-CH_2$, $C_6H_5$ and $C_6H_{13}$.

All these thio compounds were prepared by reactions of the corresponding acid dichlorides with mercaptans in diethyl ether [2].

The dithioethyl esters of β-alkoxy(phenoxy) vinylphosphonic, vinylphosphonic, and vinylthiophosphonic acids and the esters of alkyl thiovinylphosphonic acids are all liquids which are readily soluble in organic solvents and mineral oils. All the compounds are stable on keeping.

The constants of the synthesized substances: boiling point, refractive index, and density, are given in Table 2.

The effects of the thio compounds on the antioxidant properties of mineral oils, in terms of thermooxidative stability, volatility, and lacquer formation, are given in the same tables.

For tests of the effect of various thio compounds on the antioxidant properties of MS-20 oils the dithioethyl ethers of β-alkoxy ethoxyvinylphosphonic (AP-8, AP-10), β-phenoxyvinylphosphonic (AP-5), and phenylvinylphosphonic (AP-7, AP-9) and β-phenoxyvinylthiophosphonic (AP-4) acids were synthesized and investigated (Table 1).

In addition, the diesters of alkyl thiovinylphosphonic acids (AP-38, AP-39, AP-40; Table 2) were studied.

It follows from Table 1 that on addition of 2% of thio compounds of unsaturated phosphonic acids to MS-20 oil the most effective antioxidant is the diethyl ester of β-ethoxyethoxyvinylphosphonic acid; in its presence the thermooxidative stability reaches 100, while lacquer formation is zero (AP-8).

Replacement of the ethoxy group in AP-8 by the butoxy group lowers the antioxidant properties by 25% (AP-10).

*Communication III.

TABLE 1

Effect of Dithioethyl Esters of Unsaturated Phosphonic and Thiophosphonic Acids on the Antioxidant Properties of MS-20 Oil

| Code mark | Formula of compound | Name of compound | Boiling point (°C) | $n^{20}_D$ | $d^{20}_4$ | Properties of MS-20 oil + 2% of compound (%) | | | Thermo-oxidative stability (min) |
|---|---|---|---|---|---|---|---|---|---|
| | | | | | | volatility | working fraction | lacquer formation | |
| MS-20 | — | Oil | — | — | — | 61 | 19 | 20 | 23 |
| AP-8 | $C_2H_5—O—CH_2—CH_2—O—CH=CHPO(SC_2H_5)_2$ | Dithioethyl ester of β-ethoxyethoxyvinylphosphonic acid | 169 (2 mm) | 1.5403 | 1.1197 | 55 | 45 | 0 | 100 |
| AP-10 | $n\text{-}C_4H_9—O—CH_2—CH_2—O—CH=CHPO(SC_2H_5)_2$ | Dithioethyl ester of β-butoxyethoxyvinylphosphonic acid | 186 (2 mm) | 1.5365 | 1.1180 | 54 | 46 | 0 | 75 |
| AP-5 | $C_6H_5—O—CH=CHPO(SC_2H_5)_2$ | Dithioethyl ester of β β-phenoxyvinylphosphonic acid | 162 (1) | 1.5860 | 1.1535 | 56 | 40 | 4 | 67 |
| AP-3 | $C_6H_5—CH=CHPO(SC_2H_5)_2$ | Dithioethyl ester of β-phenylvinylphosphonic acid | 168 (1) | 1.6248 | 1.1469 | 57 | 41 | 2 | 58 |
| AP-7 | $CH_3—O—CH_2—CH_2—O—CH=CHPS(SC_2H_5)_2$ | Dithioethyl ester of β-methoxyethoxyvinylthiophosphonic acid | 157 (2) | 1.5890 | 1.1579 | 55 | 45 | 0 | 81 |
| AP-9 | $C_2H_5—O—CH_2—CH_2—O—CH=CHPS(SC_2H_5)_2$ | Dithioethyl ester of β-ethoxythoxyvinylthiophosphonic acid | 176 (2) | 1.5745 | 1.1417 | 50 | 50 | 0 | 83 |
| AP-4 | $C_6H_5—O—CH=CHPS(SC_2H_5)_2$ | Dithioethyl ester of β-phenoxyvinylthiophosphonic acid | 155 (1) | 1.6336 | 1.3142 | 58 | 38 | 4 | 68 |

TABLE 2

Effects of Sulfur Introduced into the Ester Group and the Radical on the Antioxidant Properties of Compounds

| Code mark | Formula of compound | Name of compound | Boiling point (°C) | $n_D^{20}$ | $d_4^{20}$ | Properties of MS-20 oil + 2% of compound (%) | | | Thermo-oxidative stability at 250° (min) |
|---|---|---|---|---|---|---|---|---|---|
| | | | | | | volatility | working fraction | lacquer formation | |
| MS-20 | — | Oil | — | — | — | 61 | 19 | 20 | 23 |
| AP-43 | $C_2H_5-O-CH_2-CH_2-O-CH=CHPO(OC_2H_5)_2$ | Diethyl ester of β-ethoxyethoxyvinylphosphonic acid | 153 (2mm Hg) | 1.4512 | 1.0812 | 64 | 24 | 12 | 24 |
| AP-3 | $C_2H_5-O-CH_2-CH_2-O-CH=CHPO(SC_2H_5)_2$ | Dithioethyl ester of β-ethoxyvinylphosphonic acid | 169 (2) | 1.5403 | 1.1197 | 55 | 45 | 0 | 100 |
| AP-53 | $C_6H_5-CH=CHPO(OC_2H_5)_2$ | Diethyl ester of β-phenylvinylphosphonic acid | 138 (2) | 1.5325 | 1.1082 | 58 | 34 | 8 | 31 |
| AP-3 | $C_6H_5-CH=CHPO(SC_2H_5)_2$ | Dithioethyl ester of β-phenylvinylphosphonic acid | 168 (1) | 1.6248 | 1.1469 | 57 | 41 | 2 | 58 |
| AP-46 | $C_2H_5-O-CH=CHPO(OC_4H_9\text{-н.})_2$ | Dibutyl ester of β-ethoxyvinylphosphonic acid | 144 (5) | 1.4492 | 1.0069 | 60 | 25 | 15 | 30 |
| AP-38 | $C_2H_5-S-CH=CHPO(OC_4H_9\text{-н.})_2$ | Dibutyl ester of ethylthiovinylphosphonic acid | 168 (3) | 1.4890 | 1.0317 | 63 | 23 | 14 | 28 |
| AP-48 | $н.\text{-}C_4H_9-O-CH=CHPO(OC_4H_9\text{-н.})_2$ | Dibutyl ester of β-butoxyvinylphosphonic acid | 144 (1) | 1.4491 | 0.9879 | 58 | 29 | 13 | 31 |
| AP-40 | $н.\text{-}C_4H_9-S-CH=CHPO(OC_4H_9\text{-н.})_2$ | Dibutyl ester of butylthiovinylphosphonic acid | 153—154 (2) | 1.4848 | 1.0235 | 62 | 29 | 9 | 34 |
| AP-55 | $C_2H_5-O-CH=CHPO(OC_6H_{13}\text{-н.})_2$ | Dihexyl ester of β-ethoxyvinylphosphonic acid | 157—158 (2) | 1.4511 | 0.9710 | 59 | 37 | 4 | 44 |
| AP-39 | $C_2H_5-S-CH=CHPO(OC_6H_{13}\text{-н.})_2$ | Dihexyl ester of β-ethoxyvinylphosphonic acid | 165 (1) | 1.4808 | 1.0059 | 62 | 29 | 9 | 30 |

The antioxidant properties of dithioethyl esters of β-alkoxy ethoxyvinylthiophosphonic acids are not changed if the radical on the left is changed from $C_1$ to $C_2$ (AP-7, AP-9).

Thioesters of β-phenoxyvinylphosphonic, phenylvinylphosphonic, and phenoxyvinylthiophosphonic acids (AP-5, AP-3, AP-4) are less effective antioxidants than thioesters of β-alkoxy vinylphosphonic and β-alkoxy vinylthiophosphonic acids (AP-7, AP-8, AP-9, AP-10).

Comparison of the thioesters of β-ethoxyethoxyvinylphosphonic and β-ethoxyethoxyvinylthiophosphonic acids showed that both are most effective antioxidants, but in the case of the dithioethyl ester of β-ethoxyethoxy-vinylthiophosphinic acid the thermooxidative stability is lowered somewhat, from 100 to 83 minutes (AP-8, Ap-9).

The thio group in the thioester of β-phenoxyvinylthiophosphonic acid had no influence on the antioxidant properties (AP-4, AP-5).

The results obtained with all these thioesters of unsaturated phosphonic and thiophosphonic acids clearly demonstrate the favorable effect of sulfur on the antioxidant properties of the compounds. It was found that the most effective antioxidants are the compounds AP-8, AP-9, AP-7, and AP-10, which confer a thermooxidative stability of 75 to 100 minutes to MS-20 oil, with zero lacquer formation.

Comparison of diesters with thioesters of unsaturated phospnonic and thiophosphonic acids showed that the latter have considerably better antioxidant properties, and decrease lacquer formation to zero (AP-43, AP-8; AP-53, AP-3 Table 2).

Investigation of the diesters of alkyl thiovinylphosphonic acids showed that all the compounds of this type are devoid of antioxidant properties (AP-38, AP-39, AP-40; Table 2).

## SUMMARY

1. The effects of thioesters of unsaturated phosphonic and thiophosphonic acids, and of diesters of alkyl-thiovinylphosphonic acids, on the antioxidant properties of mineral oil have been studied; it was found that thioesters of β-alkoxy (phenoxy) vinylphosphonic and β-alkoxy (phenoxy) vinylthiophosphonic acids are effective antioxidants; the most powerful of these is the dithioethyl ester of β-ethoxyethoxyvinylphosphonic acid.

2. The antioxidant properties of esters of unsaturated phosphonic acids are greatly improved by introduction of sulfur.

3. Esters of alkyl thiovinylphosphonic acids do not increase thermooxidative stability or diminish lacquer formation.

## LITERATURE CITED

[1] K. K. Papok, K. N. Anisimov, B. S. Zuseva and N. E. Kolobova, J. Appl. Chem. 32, No. 2, 358 (1959).

[2] K. N. Anisimov, N. E. Kolobova, and A. N. Nesemyanov, Bull. Acad. Sci. USSR, Div. Chem. Sci. 5, 823 (1955); 6, 999 (1955).

Received December 17, 1957.

# THE POSSIBILITY OF GAS-PHASE CATALYTIC SYNTHESIS OF VINYL ACETATE WITH THE REACTION COMPONENTS IN STOICHIOMETRIC PROPORTIONS

R. M. Flid and A. V. Chirikova

In the usual industrial process [1] for production of vinyl acetate, a mixture of acetylene and acetic acid vapor is passed over zinc acetate on activated carbon in the 170-180° temperature range at a space velocity of 150-300 liters / liter of catalyst.hour. As the catalyst activity diminishes, the temperature is gradually raised to 220-240°. A characteristic feature of the process is that acetylene must be taken in 8 to 15-fold excess over the stoichiometric ratio. Decrease of this ratio results in formation of ethylidene diacetate, the addition product of two acetic acid molecules and acetylene.

We have shown [2] that the synthesis of vinyl acetate involves two parallel reactions, which depend on the presence of acetic acid monomer and dimer in the reaction mixture

$$C_2H_2 + CH_3COOH_{(g)} \longrightarrow CH_2{=}CHOCOCH_3 \qquad (1)$$

$$C_2H_2 + (CH_3COOH)_{2(g)} \longrightarrow CH_3CH(OCOCH_3)_2 \qquad (2)$$

The equilibrium proportions of the monomeric and dimeric forms of acetic acid are determined by the temperature and degree of dilution. When vinyl acetate is synthesized as indicated above, an 8 to 15-fold excess of acetylene lowers the partial pressure of acetic acid and thus favors almost complete dissociation of the dimer even at relatively low temperatures (170-180°).

Thermodynamic analysis [3] shows that for synthesis of vinyl acetate with the stoichiometric proportions of acetylene to acetic acid the temperature of the process must be raised to 240-260°.

It is evident that if the synthesis is performed with the components in the stoichiometric ratio the productivity of the catalytic unit should be increased and isolation of vinyl acetate should be easier.

Tests of an industrial catalyst sample (zinc acetate on activated carbon) at 250-290° with the components in stoichiometric ratio showed that the catalyst loses selectivity and is rapidly deactivated, while the catalyzate has a considerable polymer content.

Our search for catalysts for the high-temperature synthesis was based on the theory, developed by one of us [4], that the catalyst should be capable of complex formation with acetylene and acetic acid.

The search was conducted in two directions: a) replacement of acetate by other zinc salts in which the zinc would be bound more stably by the anion; b) replacement of activated carbon by other supports for zinc acetate or oxide.

In either case weakening of the catalytic properties at the lower temperatures (180-220°) should ensure adequate activity with increase of temperature (260-290°). This effect would be obtained if only because the polarizing effect of the zinc ion increases. The weakening of the properties should not be extensive, as the temperature increase is relatively small.

## EXPERIMENTAL

The methods used for the experiments and analyses were described previously [2]. All the experiments were performed at 270°, with the stoichiometric ratio of $C_2H_2$: $CH_3COOH$ and at over-all space velocity of 200-300 liters/liter of catalyst · hour. Each experiment was started at 210-220°, and the temperature was gradually raised to 260-270° over a period of 3-4 hours. The readings were started 1.5-2 hours after the required temperature had been reached.

In tests of catalysts prepared by different methods (coprecipitation, impregnation of granules with solutions of zinc salts, or mixing of fine powders with subsequent peptization, drying, and calcination) the initial activity, changes of activity and selectivity with time, mechanical strength, and the possibility of loss of zinc acetate from the surface were all taken into account.

Of the large number of catalysts tested only samples supported on activated alumina and zinc oxide retained sufficiently high activity and selectivity during prolonged operation, had adequate mechanical strength, and did not lose zinc acetate from the surface.

The support used was granulated $\gamma$-$Al_2O_3$ grade A-2.

For preparation of the catalyst the granules were heated to 400-450° and then impregnated with aqueous ammonium chloride solution containing dissolved zinc oxide. The granules were dried and heated in a muffle furnace at 400-450° for 1.5-2 hours to remove $NH_4Cl$; the $ZnO/Al_2O_3$ granules were then impregnated with aqueous NaOH solution, calcined, and impregnated with acetic acid.

The amount of alkali added was $10^{-3}$ mole per mole of $Al_2O_3$. The catalyst was dried for 1.5-2 hours at 100-120° and then placed in the catalytic reactor and heated in a current of nitrogen for 2-4 hours at 300-350°.

The method used for preparation of the active-alumina granules also has a significant effect on the activity and selectivity of the catalyst.

Sample No. 1. The commercial granules were ground and mixed thoroughly with active aluminum hydroxide and graphite in 100:20:20 proportions by weight, peptized by means of 50% $HNO_3$ solution, molded, dried for 1.5 hours at 70° and 4.5 hours at 150°, and calcined in a muffle furnace until the graphite was completely burned away. The granules had bulk density 0.55 and porosity 68.2%

TABLE 1

Effect of Temperature on Yield of Vinyl Acetate

| Temperature (° C) | Conversion of acetic acid (%) | Yield of vinyl acetate on acetic acid (molar %) | | Notes |
|---|---|---|---|---|
| | | passed | converted | |
| 250 | 25.4 | 23 | 91 | 3% of ethylidene diacetate found in condensate |
| 270 | 49.0 | 45 | 92 | |
| 290 | 51.3 | 36 | 70.4 | Condensate strongly colored. Resinification observed, increasing with time. |

Sample No. 2. This was prepared in the same manner, but the powders were mixed without graphite. The weight ratio was: $\gamma$-$Al_2O_3$ : $Al(OH)_3$ = 100 : 20.

Sample No. 3. Grade A-2 $\gamma$-$Al_2O_3$ was used without previous grinding.

The following yields of vinyl acetate were obtained after 3 hours at 270°, space velocity ~ 250 liters/liter

of catalyst-hour at the stoichiometric ratio $C_2H_2$ : $CH_3COOH$ = 1 : 1.

| Yield | Sample 1 | Sample 2 | Sample 2 |
|---|---|---|---|
| On acid passed . . . . . | 48.5 | 45 | 17.9 |
| On acid converted . . . . . | 87 | 92 | 65 |

TABLE 2

Effect of $C_2H_2$ : $CH_3COOH$ Ratio on Yield of Vinyl Acetate

| Molar ratio | Yield of vinyl acetate on acetic acid (molar %) | | Productivity (g vinyl acetate per liter of catalyst per hour) |
|---|---|---|---|
| | passed | converted | |
| 1 : 1 | 45.45 | 92.0 | 216 |
| 1 : 1.2 | 38.2 | 94.3 | 198 |
| 1 : 1.5 | 31.0 | 96.2 | 184 |
| 1 : 2.0 | 28.0 | 98.0 | 179 |
| 1 : 3.9 | 7.0 | 100 | 59.5 |

TABLE 3

Effect of Catalyst Operating Time on Activity

| Catalyst and molar $C_2H_2$ : $CH_3COOOH$ ratio | Yield of vinyl acetate (molar %) and catalyst operating time (hours) | | | | | | | | |
|---|---|---|---|---|---|---|---|---|---|
| | 3 | 5 | 10 | 20 | 40 | 60 | 80 | 100 | 120 |
| | | | | On acetic acid * | | | | | |
| Sample No. 2 | 29 | 38.2 | 45.0 | 43.2 | 40.6 | 29.1 | 9.4 | — | — |
| | 78 | 97.0 | 92.0 | 93.1 | 89.4 | 74.1 | 58.2 | — | — |
| $C_2H_2$ : $CH_3COOH$=1 : 1 | | | | On acetylene | | | | | |
| | 29.3 | 37.8 | 43.8 | 43.6 | 40.9 | 26.8 | 8.6 | — | — |
| | 65 | 91.6 | 94.3 | 90.1 | 83.7 | 71.4 | 51.2 | — | — |
| | | | | On acetic acid | | | | | |
| Sample No.1 | 34.8 | 46.4 | 45.3 | 43.8 | 43.2 | 39.2 | 29.2 | 17.4 | 8.5 |
| | 82.1 | 89.3 | 94.2 | 97.4 | 92.3 | 89.3 | 87.3 | 80.0 | 64.7 |
| $C_2H_2$ : $CH_3COOH$=1 : 1 | | | | Sample No. 1 | | | | | |
| | 35.2 | 46.9 | 48.2 | 41.8 | 45.4 | 40.4 | 20.4 | 17.6 | 9.2 |
| | 71.3 | 91.2 | 90.7 | 92.3 | 91.8 | 86.5 | 81.2 | 63.5 | 48.3 |
| | | | | On acetylene | | | | | |
| | 28.3 | 29.5 | 29.5 | 28.8 | 29.6 | 29.3 | 29.1 | 28.7 | 28.4 |
| Sample No.1 | 97.2 | 98.8 | 100 | 97.4 | 99.2 | 96.8 | 97.4 | 97.3 | 95.1 |
| $C_2H_2$ : $CH_3COOH$=1 : 2 | | | | On acetylene | | | | | |
| | 55.2 | 58.4 | 59.3 | 57.1 | 58.4 | 58.2 | 58.3 | 60.4 | 59.2 |
| | 93.4 | 97.2 | 100 | 98.3 | 97.3 | 98.4 | 98.1 | 97.1 | 90.1 |

*The first row in each case represents the yields calculated on the acetic acid (or acetylene) passed, and the second, on the amounts converted.

It was also found that the optimum ratio of $\gamma$-$Al_2O_3$ : ZnO = 2 : 1 (molar).

To find the optimum process conditions, the influence of temperature and $C_2H_2$ : $CH_3COOH$ ratio were studied.

Effect of temperature. The experiments were performed with Sample No. 2 in the 250-290° range at molar ratio $C_2H_2$ : $CH_3COOH$ = 1 : 1 and space velocity 250 liters/liter of catalyst-hour. The duration of the experiments was 1-1.5 hours. It is clear from the data in Table 1 that the maximum yields of vinyl acetate, calculated on the acid passed or converted, are obtained at 270°. Increase of temperature, especially at the start of the synthesis, is undesirable because of the secondary reactions of condensation and polymerization, which in their turn lower the catalyst activity.

Effect of $C_2H_2$ : $CH_3COOH$ ratio. The experiments were performed at 270° at over-all space velocity 250 liters/liter of catalyst-hour. The duration of the experiments was 1-1.5 hours. It is clear from the data in Table 2 that although increase of the molar ratio of acetic acid to acetylene to 1.5-2.0 lowers the productivity somewhat, it makes the process more selective. The productivity attained under these conditions is 6 to 7 times as high as the present industrial value. Isolation of vinyl acetate is almost complete as the result of cooling to + 6 to + 7° instead of − 45 to − 50°.

To test variations of catalyst activity with time, a series of lengthy experiments was performed at 270° and over-all space velocity of 250-280 liters/liter of catalyst-hour. Catalyst samples Nos. 1 and 2 were tested. The molar $C_2H_2$ : $CH_3COOH$ ratio was varied from 1 : 1 to 1 : 2.

It follows from the data in Table 3 that despite a fairly high initial activity the best and most constant results were obtained at the molar ratio $C_2H_2$ : $CH_3COOH$ = 1 : 2. It is likely that the observed decrease of activity at 1 : 1 ratio is due to polymerization of acetylene, with blocking of the catalyst surface.

The fact that zinc acetate is not lost from the surface of catalysts No. 1 and No. 2, in contrast to all the other catalysts tested may perhaps be attributed to the formation of surface zinc aluminates by the reaction between zinc and aluminum oxides. The results of x-ray structural analysis support this hypothesis.

The x-ray patterns of Samples No. 1 and No. 2 contain new lines which are not due either to $\gamma$-$Al_2O_3$ or to ZnO.

## SUMMARY

1. It is shown that vinyl acetate can be made by a catalytic process in the gas phase at molar ratios of $C_2H_2$ : $CH_3COOH$ = 1 : 1 and 1 : 2.

2. The optimum process conditions are: temperature 270-275°, over all space velocity 250-300 liters / liter of catalyst per hour. This results in 30% conversion of acetic acid and 60% conversion of acetylene, with selectivity reaching 96-98%. The output per liter of catalyst per hour is 6 to 7 times as high as at present.

3. A method for preparation of a catalyst for this process is described.

## LITERATURE CITED

[1] J. Copenhaver and M. Bigelow, Acetylene Chemistry (12, 1954) p. 166 [Russian translation]; P. Faram, Monomers, 1 (1951) p. 51 [Russian translation]; S. N. Ushakov et al., J. Appl. Chem. 22, 1005, 1013 (1947); 13, 1629 (1940) [USSR].

[2] R. M. Flid and A. V. Chirikova, J. Gen. Chem. 27, 5 (1957) [USSR].

[3] W. Weltner, J. Am. Chem. Soc. 77, 3041 (1955).

[4] R. M. Flid, J. Phys. Chem. 32, 2339 (1958) [USSR].

Received July 5, 1957

# DIRECT DISAZO DYES – DERIVATIVES OF OXADIAZOLE AND THIODIAZOLE

N.S. Dokunikhin, B.M. Krasovitskii, R.M. Matskevich, V.A. Blinov, and Z. Ya. Vitokhina

Numerous studies of the relationship between the structure and substantivity of various dyes have demonstrated the favorable effect of long chains of conjugated double bonds on the ability of dyes to become attached to cotton fibers [1,2]. For example, benzidine dyes (I) with chains of such type in the molecule,

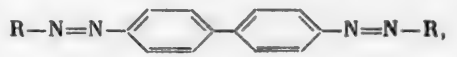

(I)

where R is the azoic coupling component, are substantive for cotton.

It is also known that many dyes with heterocyclic nuclei in their molecules have the properties of direct dyes. They include dyes derived from benzimidazole [3-5], and quinophthalone dyes the molecules of which are based on quinoline nuclei [6,7]; many dyes containing the benzothiazole group (such as Primuline Yellow [8] and monoazo dyes obtained from p-dehydrothiotoluidine [9]) have the properties of direct dyes; dyes based on the triazine nucleus [10] are also found to be substantive.

It follows that direct azo dyes containing heterocyclic nuclei contained in long chains of conjugated double bonds should be of considerable interest. An example is provided by the disazo dyes described by Modena, furan derivatives (II), with good substantivity for cotton [11]:

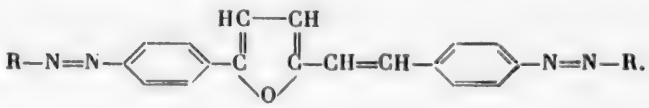

(II)

We prepared the disazo dyes (III) and (IV) in which, as in dyes (I) and (II), the auxochromes are linked by a chain of conjugated double bonds, with an oxadiazole or thiodiazole ring included in the chain:

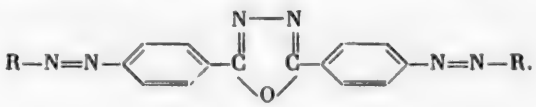

(III)

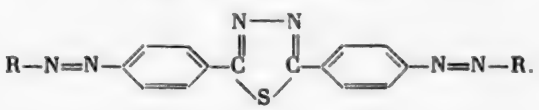

(IV)

The diazo components of these dyes – 2,5-bis-(4-aminophenyl)-1,3,4-oxadiazole and 2,5-bis-(4-aminophenyl)-1,3,4-thiodiazole – were prepared by reduction of the corresponding nitro compounds. The latter, in their turn, are formed from N, N'-bis-(4-nitrobenzoyl)-hydrazine, which reacts with thionyl chloride to give 2,5-bis-(4-nitrophenyl)-1,3,4-oxadiazole, and with phosphorus pentasulfide to give 2,5-bis-(4-nitrophenyl)-1,3,4-thiodiazole.

The structure of the resultant diamines is confirmed by deamination, which yields the previously-described 2,5-diphenyl-1,3,4-oxadiazole and 2,5-diphenyl-1,3,4-thiodiazole.

Dyes (III) and (IV) (azoic coupling components 1,8-aminonaphthol-3,6-disulfonic acid and 1,8-aminonaphthol-2,4-disulfonic acid) have the properties of direct dyes: they are taken up satisfactorily by cotton fabrics giving violet dyeings of various shades.

Investigation of fastness of the dyeings to water, soap solution, and perspiration showed that after treatment with the preparation DTsU (condensation product of dicyanodiimide with formaldehyde) or DTsM (DTsU with added copper acetate) fastness of dyes (III) and (IV) to these treatments is considerably increased.

## EXPERIMENTAL

2,5-Bis-(4-nitrophenyl)-1,3,4-oxadiazole. The literature contains only a brief reference to the formation of 2,5-bis-(4-nitrophenyl)-1,3,4-oxadiazole by the reaction of N,N'-bis-(4-nitrobenzoyl)-hydrazine with thionyl chloride [12]. We determined the preparation conditions more precisely, and synthesized the compound as follows: 8.3 g (0.025 mole) of N,N'-bis-(4-nitrobenzoyl)-hydrazine was dissolved on heating under reflux in 50 ml of nitrobenzene, 15 ml of thionyl chloride was added, and the solution was boiled for 1 hour. On the following day the precipitate was separated from the nitrobenzene and washed with benzene. The yield was 4.3 g (55%).

2,5-Bis-(4-nitrophenyl)-1,3,4-oxadiazole is a flesh-colored crystalline powder, m.p. 302° (literature data, 302° [12]).

2,5-Bis-(4-aminophenyl)-1,3,4-oxadiazole. 3.12 g (0.01 mole) of 2,5-bis-(4-nitrophenyl)-1,3,4-oxadiazole was dissolved in 25 ml of pyridine on heating under reflux, and 180 ml of 1 N solution of sodium disulfide in pyridine was then added dropwise to the boiling solution during one hour. The color of the solution changed from yellow to dirty green. The solution was cooled and poured into water (1 liter); the pale yellow precipitate was filtered off, washed several times with water, and dried. The yield was 2.4 g (95%).

Found %: *$NH_2$ 12.32, 12.34. $C_{14}H_8ON_2(NH_2)_2$. Calculated %: N $H_2$ 12.70.

The product was a pale yellow powder, m.p. 254-255°, readily soluble on heating in alcohol, nitrobenzene, glacial acetic acid, and pyridine, sparingly soluble in benzene and ether.

Deamination of 2,5-bis-(4-aminophenyl)-1,3,4-oxadiazole. 0.1 g of 2,5-bis-(4-aminophenyl)-1,3,4-oxadiazole was dissolved in a mixture of 20 ml of water and 1 ml of concentrated hydrochloric acid, and the calculated quantity of sodium nitrite was added to the solution cooled to 0°. To the resultant diazo solution 1 g of potassium hypophosphite ($KH_2PO_2$) was added with thorough stirring, the solution was filtered, and left overnight. The precipitate was filtered off, washed with water, and recrystallized from alcohol; m.p. 135-136°C (literature data, 135-136°) [14].

2,5-Bis-(4-nitrophenyl)-1,3,4-thiodiazole. 3.3 g (0.1 mole) of N,N'-bis-(4-nitrobenzoyl)-hydrazine was dissolved in dry nitrobenzene (20 ml) on heating under reflux, and 6 g of freshly-prepared phosphorus pentasulfide [15] was added to the boiling solution. The solution boiled up and darkened. The mixture was boiled for 15 minutes more. The precipitate which formed on cooling was filtered off, washed with soda solution and with water, and recrystallized from pyridine. The yield was 0.72 g (22%).

Found %: N 16.74. $C_{14}H_8O_4N_4S$. Calculated %: N 17.07.

The product was a yellow powder, m.p. 331° (in a copper block heated to 320°), readily soluble in hot pyridine and nitrobenzene, insoluble in alcohol and benzene.

2,5-Bis-(4-aminophenyl)-1,3,4-thiodiazole. This amine was prepared by reduction of 2,5-bis-(4-nitrophenyl)-1,3,4-thiodiazole. The reduction was performed as in the preparation of the corresponding oxadiazole derivative; 0.55 g of the nitro compound gave 0.42 g of amine (93%).

Found %: $NH_2$ 11.90, 11.77; S 11.99. $C_{14}H_8N_2S(NH_2)_2$. Calculated %: $NH_2$ 11.94, S 11.94.

The product is a yellow powder, m.p. 247-248°, soluble in alcohol, insoluble in water, benzene, and ether.

*Analyzed by potentiometric titration with 0.01 N sodium nitrite solution [13].

Deamination of 2,5-bis-(4-aminophenyl)-1,3,4-thiodiazole was performed similarly to deamination of 2,5-bis-(4-aminophenyl)-1,3,4-oxadiazole. The deamination product was purified by the Stolle method [16]: the dried precipitate was dissolved in alcohol and an alcoholic solution of silver nitrate was added; a small amount of dark precipitate was formed, which was filtered off, and the filtrate was diluted with water; 2,5-diphenyl-1,3,4-thiodiazole was precipitated. After this operation had been performed 3 times the purified product had m.p. 141° (literature data, 141-142° [16]).

Dyes from 2,5-bis-(4-aminophenyl) derivatives of 1,3,4-oxa- and 1,3,4-thiodiazole. Both amines were diazotized by the usual method: addition of the calculated quantity of sodium nitrite to a solution of the amine in hydrochloric acid. Coupling with 1,8-aminonaphthol-3,6-disulfonic acid and 1,8-aminonaphthol-2,4-disulfonic acid was effected in an alkaline medium, maintained alkaline by addition of soda. The dyes were freed of mineral impurities by the acetate method and then separated chromatographically on aluminum oxide.

Fastness of the dyes to water, soap solution, and perspiration. 2% dyeings produced by dyes derived from oxadiazole (III) and thiodiazole (IV) were tested for fastness to water, soap solution, and perspiration. Dyeings previously treated with DTsU and DTsM were also tested. The test results for dyes type (III) and (IV) are given in the table. Dyes in which the azoic coupling component was 1,8-aminonaphthol-3,6-disulfonic acid are indicated by "a" and those with 1,8-aminonaphthol-2,4-disulfonic acid by "b." The fastness is assessed on a five-point scale; the numerator indicates change of shade, and the denominator represents staining of white material.

| Test | Dye fastness (points) | | | | | | | | | | | |
|---|---|---|---|---|---|---|---|---|---|---|---|---|
| | IIIa | | | IIIb | | | IVa | | | IVb | | |
| | no treatment | DTsU | DTsM | no treatment | DTsU | DTsM | no treatment | DTsU | DTsM | no treatment | DTsU | DTsM |
| Water | 4/2 | 4—5/5 | 5/5 | 5/2 | 5/5 | 5/5 | 4/1 | 5/5 | 5/5 | 4/2 | 5/5 | 5/5 |
| Soap solution | 4/2 | 5/4 | 5/3 | 4,2 | 5/4 | 5/3 | 4/1 | 5/4 | 5/4 | 4/1 | 5/4 | 5/4 |
| Perspiration | 4/1 | 4/5 | 5/4 | 4/2 | 4/5 | 4/5 | 4/1 | 4/5 | 5/5 | 4/2 | 4/5 | 5/5 |

## SUMMARY

1. New direct disazo dyes — derivatives of oxadiazole and thiodiazole have been prepared; they are attached satisfactorily to cotton fibers.

2. The dyes derived from oxadiazole and thiodiazole produce dyeings on cotton which are fairly fast to water, soap solution, and perspiration after treatment with DTsU and DTsM.

## LITERATURE CITED

[1] E. Schirm, J. prakt. Ch., 144, 69 (1935).

[2] S. F. Filippychev, Some Aspects of the Synthesis and Use of Dyes [in Russian] (Goskhimizdat, Leningrad, 1956) p. 21.

[3] E. Lellmann u. R. Hailer, Ber., 26, 2795 (1893).

[4] A. E. Porai-Koshits, Selected Works [in Russian] (izd. AN SSSR, Moscow—Leningrad, 1949) p. 143.

[5] B. A. Porai-Koshits and Ch. Frankovskii, Abstracts of Papers at the Scientific and Technical Conference on Synthesis and Use of Organic Dyes [in Russian] (Ivanovo, 1956) p. 24; J. Gen. Chem. 28, 934 (1958).

[6] A. E. Porai-Koshits and A. I. Kulikov, J. Gen. Chem. 8, 124 (1938). [USSR].

[7] B. I. Ardashev and Z. V. Malina, J. Gen. Chem. 21, 1349 (1951). [USSR].*

[8] P. Ruggli, J. Soc. Dyers and Colorists (Jubilee issue) 77 (1934).

*Original Russian pagination. See C. B. translation.

[9] I. M. Kogan, Chemistry of Dyes [in Russian] (State Sci. Tech. Press Chem. Lit., Moscow, 1956) p. 145.

[10] German Patent 436, 179, Frdl. 15, 531; K. Venkataraman, Chemistry of Synthetic Dyes (Goskhimizdat, Leningrad, 1956) p. 657 [Russian translation].

[11] G. Modena, Ricerca scient. 25, 589 (1955) Ref. Zhur. Khim. 51912 (1955).

[12] R. Stolle u. A. Bombach, J. prakt. Ch. [2], 74, 22 (1906).

[13] L. M. Litvinenko and A. P. Grekov, J. Analyt. Chem. [USSR] 10, 164 (1955).*

[14] E. Gunther, Ann., 252, 61 (1889).

[15] G. Bornemann, Inorganic Preparations [in Russian] (State Chem. Tech. Press, 1933) p. 76.

[16] R. Stolle, J. prakt. Ch. [2], 69, 158 (1904).

[17] C. Robinson and H. Mills, Proc. Roy. Soc., 131A, 576 (1931).

Received July 26, 1957.

*Original Russian pagination. See C. B. translation.

# SYNTHESIS OF MONOALKYL MALEATES

S. N. Ushakov, A. F. Nikolaev, A. M. Toroptseva, and

M. S. Trizno

Research workers are taking increasing interest in various derivatives of unsaturated dibasic acids (maleic, fumaric, itaconic). Compounds of considerable interest are acid esters of maleic acid, which can undergo copolymerization with various mono- and divinyl compounds with formation of polymers having a variety of properties and capable of further modification. This creates wide potentialities for the technical utilization of maleic acid esters. Despite the publication of a considerable number of patents and several papers describing monoesters of maleic acid and copolymers of alkyl maleates with vinyl compounds, no systematized data are as yet available on the synthesis and properties of various monoesters of maleic acid.

In one paper [1] it is reported that monoethyl maleate can be prepared by brief heating of maleic anhydride with excess of absolute ethyl alcohol on a water bath; a mixture of monoethyl and diethyl maleate and maleic acid is obtained. Monoethyl maleate was obtained pure by multistage treatment of the mixture with potassium carbonate, ether, alcohol, dilute hydrochloric acid, and ether again. It is stated in another paper [2] that monoethyl maleate can be prepared by rapid addition of the necessary amount of absolute ethyl alcohol to maleic anhydride at 110-120°.

Analysis of the reaction product showed the presence of 95% monoethyl maleate and some unchanged maleic anhydride. The monoethyl maleate was not purified. Vacuum distillation caused internal rearrangement with formation of a mixture of monoethyl maleate, diethyl maleate, and maleic acid.

One of the present authors [3] prepared monomethyl maleate by the action of heat on a mixture of pure maleic anhydride with a small excess of absolute methyl alcohol at 65°.

Monomethyl maleate [4] has been prepared by the action of heat on methallyl alcohol with maleic anhydride at 40-45° for one hour, and acid esters of the hydroxyalkylamides of palmitic, stearic, and oleic acid were made by the heating of the corresponding alcohols with equimolecular amounts of maleic anhydride for 3 hours at 95-100° [5] or 90-120° [6].

A monoester was prepared from maleic anhydride and secondary isohexanol [7] by the action of heat at 80° to a constant acid number.

Consideration of the foregoing literature data on the preparation of monoalkyl maleates discloses that they have been synthesized by different workers over a wide range of temperatures and with different reaction times.

In the present investigation monoesters of maleic acid were prepared by the reactions of maleic anhydride with equimolecular amounts of the corresponding alcohols. Aliphatic primary, secondary, and tertiary alcohols of normal and iso structure, and cyclic and aromatic dihydric and trihydric alcohols were used in the syntheses.

The reactions between maleic anhydride and alcohols can be represented by the scheme

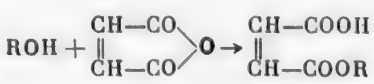

Prolonged heating, especially at high temperatures, and lengthy keeping of the monoesters formed results in internal regrouping with formation of diesters and maleic acid:

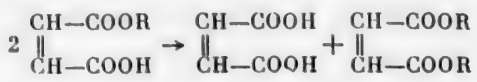

## EXPERIMENTAL

Anhydrous alcohols were used for the syntheses of monoalkyl maleates. Methanol was first dried by calcined copper sulfate, and then distilled through a 1-meter rectifying column packed with single-coil glass spirals. Ethyl alcohol was treated with a small amount of KOH, dehydrated by boiling for 3 days over calcined quicklime, and then distilled through the column. The remaining aliphatic alcohols (up to and including amyl) were dried by calcined copper sulfate and then distilled through the rectifying column in presence of a small amount of metallic sodium The other alcohols were dehydrated by distillation from a flask fitted with a fractionating column.

The alcohols used for synthesis of acid maleate esters are listed in Table 1.

TABLE 1

Properties of Alcohols

| Alcohol | Structural formula | Molecular weight | Boiling point (in °C, at 760 mm) | $n_D^{20}$ |
|---|---|---|---|---|
| Methyl | $CH_3OH$ | 32.04 | 64.7 | 1.3312(15°) |
| Ethyl | $C_2H_5OH$ | 46.07 | 78.3 | 1.3614 |
| Propyl | $C_2H_5—CH_2OH$ | 60.09 | 97.2 | 1.3850 |
| Isopropyl | $(CH_3)_2CHOH$ | 60.09 | 82.2 | 1.3776 |
| Butyl | $CH_3(CH_2)_2CH_2OH$ | 74.12 | 117.7 | 1.3993 |
| Isobutyl | $(CH_3)_2CH—CH_2OH$ | 74.12 | 108 | 1.3977(15°) |
| Tertiary butyl | $(CH_3)_3—COH$ | 74.12 | 82.8 | 1.3878 |
| Isoamyl(optically active) | $CH_3—CH_2—CH(CH_3)—CH_2OH$ | 88.16 | 128 | 1.4109 |
| Benzyl | 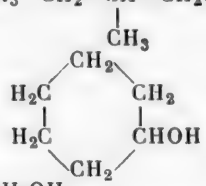 | 100.17 | 160—161 | 1.468 |
| Phenol | $C_6H_5OH$ | 94.12 | 181.2 | 1.5403(45°) |
| Benzyl | $C_6H_5CH_2OH$ | 108.14 | 205 | 1.5396 |
| Methylisohexyl | $CH_3—CHOH—(iso\ C_6H_{11})$ | 130.22 | 174 | — |
| Ethylene glycol | $HOCH_2—CH_2OH$ | 62.07 | 197.2 | 1.4318 |
| Glycerol | $CHOH(CH_2OH)_2$ | 92.09 | 290 | 1.4729 |

Maleic anhydride was purified by vacuum distillation. The melting point of the maleic anhydride used in the syntheses was 53-53.5°.

Maleic anhydride and the alcohol were put in a three-necked flask fitted swith a reflux condenser, stirrer, and thermometer, and warmed on a water of glycerol bath. For determination of the reaction rate and the time required to complete the synthesis, after the maleic anhydride had dissolved, samples were taken from the flask at definite intervals and titrated with 0.1 N NaOH solution in presence of phenolphthalein to determine the carboxyl group contents, from which the monoester contents were calculated. Heat is evolved when maleic anhydride reacts with alcohols.

TABLE 2

Effect of Temperature on the Synthesis Times of Monoalkyl Maleates

| Monoester | Synthesis time (min) | | | |
|---|---|---|---|---|
| | 60° | 80° | 100° | 120° |
| Monomethyl maleate | 120 | 45 | 45 | — |
| Monoethyl maleate | 180 | 60—75 | 60—75 | — |
| Monopropyl maleate | — | 60—75 | 60—75 | — |
| Monoisopropyl maleate | — | 150—180 | 135—180 | — |
| Monobutyl maleate | — | 75—90 | 75—90 | 60 |
| Monoisobutyl maleate | — | 75—90 | 75—90 | — |
| Monoisoamyl maleate | — | 30 | 30 | — |
| Monocyclohexyl maleate | — | 45— 60 | 30 | — |
| Monobenzyl maleate | — | 90—105 | 90—105 | — |
| Monoglycol maleate | — | 45— 60 | 45— 60 | — |
| Monoglyceryl maleate | — | 60 | 15 | — |

The syntheses were performed at different temperatures in order to determine the effect of temperature on the reaction rate.

Effect of temperature on the reaction rate. The results of experiments performed in order to determine the effect of temperature on the synthesis time with the above-named alcohols are presented in Table 2.

The synthesis time is the time required to complete the reaction of monoester formation from the instant at which the reaction temperature is reached in the bath. The experiments showed that the optimum temperature for preparation of most of the acid esters of maleic acid is about 80°. Decrease of temperature to 60° greatly lowers the reaction rate while increase of reaction temperature to 100° and over, does not, as a rule, lead to any appreciable increase in the reaction rate but causes partial decomposition of monoesters with formation of diesters and maleic acid, which is precipitated from the reaction mixture in the form of crystals. Prolonged heating of the monoesters at 60 and 80° also leads to formation of diesters and maleic acid. Primary alcohols react very readily with maleic anhydride, and the greater proportion of the reagents in such cases interacts within the first 30-45 minutes. The rate of monoester formation is considerably lower with secondary alcohols.

Comparison of the reaction times with propyl and isopropyl alcohols shows that in the former case the reaction rate is more than double the reaction rate in the latter. In the case of methylisohexyl carbinol the rate of monoester formation is even lower. When this reaction was carried out at 80°, after three hours the monoester content was only 62%; at 120° it was 79% after the same time. The cyclic secondary alcohol (cyclohexanol) reacts similarly to primary alcohols.

The reaction with phenol does not proceed to any significant extent. After the mixture had been heated at 80 or 100° for 3 hours the carboxyl group content fell by only 3%. It also proved impossible to obtain a monoester by the reaction of maleic anhydride with tertiary butyl alcohol.

The reaction proceeds readily with benzyl alcohol, ethylene glycol, and especially with glycerol.

Properties of monoalkyl maleates. The first 7 monoesters of maleic acid listed in Table 3 are colorless, transparent, fairly viscous liquids with a characteristic odor. Monoglycol maleate is a viscous, and monoglyceryl maleate a very viscous liquid. The viscosity of monoalkyl maleates increases with the molecular weight of the alcohol used for preparation of the ester. Monobenzyl and monocyclohexyl maleates are white crystalline substances.

Monobenzyl maleate crystallizes in the form of transparent rectangular plates melting at 51-53°. Monocyclohexyl maleate forms acicular crystals with m.p. 60-62°.

The liquid monoesters of maleic acid prepared as described above are fairly stable on keeping and can be stored unchanged for several months. Monomethyl maleate is particularly stable on keeping. When kept under

laboratory conditions for one year, its monoester content, density, and refractive index remained unchanged. The exception is monoethyl maleate, in which crystals of maleic acid appear after a few days.

It must be pointed out, however, that only monoesters which are at least 99% pure after synthesis are stable at room temperature. In cases in which, as the result of continued heating of the reaction mixture after completion of the synthesis, there was even a slight decrease of monoester content (as the result of formation of maleic acid and diester) the regrouping continued on standing and the maleic acid content progressively increased.

Monoalkyl maleates are unstable when heated. Heating results first in a change of color (the monoesters become yellow and later brown), and at temperatures close to the boiling points decomposition begins with liberation of crystalline and gaseous products. Vacuum distillation is also accompanied by decomposition.

The densities, refractive indices, and acid numbers of the monoesters were determined. The molecular weights (from the acid numbers) and molecular refractions were calculated from the results.

The densities, acid numbers, and refractive indices given in Table 3 are average values for several determinations; the purity of the monoesters taken for these determinations was 96.5-100%.

It follows from the data in Table 3 that the densities of monoesters decrease in the homologous series with increase of the molecular weight of the alcohol.

TABLE 3

Properties of Monoesters of Maleic Acid

| Monoester | Appearance | Density | | $n_D^{20}$ | Molecular refraction | | Acid number | Molecular wt. | | Purity (wt. %) |
|---|---|---|---|---|---|---|---|---|---|---|
| | | $d_{20}^{20}$ | $d_4^{20}$ | | calculated | found | | calculated | found | |
| Monomethyl maleate | Viscous liquid | 1.2651 | 1.2614 | 1.4640 | 28.013 | 28.536 | 432 | 130 | 130 | 98—100 |
| Monoethyl maleate | | 1.1791 | 1.1753 | 1.4571 | 32.631 | 33.360 | 393 | 144 | 142.8 | 98.5—100 |
| Monopropyl maleate | | 1.1364 | 1.1325 | 1.4583 | 37.249 | 38.070 | 358 | 158 | 156.8 | 99—100 |
| Monoisopropyl maleate | | 1.1268 | 1.1236 | 1.4521 | 37.249 | 37.930 | 356 | 158 | 157.6 | 99—100 |
| Monobutyl maleate | | 1.1037 | 1.1002 | 1.4570 | 42.580 | 41.867 | 327 | 172 | 171.5 | 99.7—100 |
| Monoisobutyl maleate | | 1.0946 | 1.0911 | 1.4546 | 42.750 | 41.867 | 326 | 172 | 172 | 99.6—100 |
| Monoisoamyl maleate | | 1.0675 | 1.0642 | 1.4572 | 47.600 | 46.485 | 303.5 | 186 | 185 | 98—100 |
| Monoglycol maleate | | 1.3182 | 1.3135 | 1.4859 | 34.970 | 34.156 | 347 | 160 | 161.5 | 97—99 |
| Monoglyceryl maleate | Very viscous liquid | 1.3739 | 1.3691 | 1.5024 | 40.970 | 40.299 | 298 | 190 | 188 | 97—100 |
| Monobenzyl maleate | White crystals | 1.3002 | 1.2960 | -- | — | — | 280 | 206 | 200 | 96.5—100 |
| Monocyclo hexyl maleate | | 1.2568 | 1.2530 | — | — | — | 282 | 198 | 198.8 | 97—100 |

Comparison of the molecular refractions calculated from the experimental densities and refractive indices with the molecular refractions calculated from the atomic refractions of the elements in the monoalkyl maleate molecules shows that experimental MR is always somewhat higher than the MR calculated from atomic refractions. The discrepancy varies between 0.5 and 1, and is least for monomethyl maleate.

Molecular weights found from the acid numbers are very close to the values calculated from the chemical

composition. The solubilities of the monoesters in water and organic solvents (methanol, ethanol, acetone, dioxane, ethyl acetate, diethyl ether, pyridine, dichloroethane, methylene chloride, chloroform, ligroine, n-hexane, benzene, and xylene) were also determined.

Monoalkyl maleates are soluble in all organic solvents with the exception of aliphatic hydrocarbons, in which they are insoluble. The first five monoesters listed in Table 3 dissolve readily in water; monoisobutyl maleate dissolves with more difficulty,and monoesters No. 7 to 11 dissolve on gentle heating. Monoglyceryl maleate is considerably less soluble than the other monoesters in all solvents except dioxane and ethyl acetate.

## SUMMARY

1. Monoesters of maleic acid were prepared from maleic anhydride and alcohols (monohydric primary, secondary, and tertiary aliphatic alcohols of normal and iso structure, cyclic and aromatic alcohols, polyhydric alcohols); it was found that the reaction proceeds readily with primary aliphatic alcohols and is complete within 45-90 minutes. The reaction proceeds with much more difficulty with secondary aliphatic alcohols, and acid esters were not obtained with tertiary alcohols. The reaction proceeds readily with cyclic secondary alcohols, with primary aromatic alcohols, and with dihydric and trihydric alcohols.

2. The optimum synthesis temperature for most of the esters is 80°; decrease of temperature for most of the esters is 80°; decrease of temperature to 60° lowers the rate on monoalkyl maleate formation, and increase to 100° and over results in decomposition of monoesters with formation of dialkyl maleates and maleic acid.

## LITERATURE CITED

[1] J. Shields, J. Chem. Soc. 59, 740 (1891).

[2] R. Heiligmann, and E. McSweeney, Ind. Eng. Ch. 44, 113 (1952).

[3] S. N. Ushakov, S. P. Mitsengendler and B. M. Polyatskina, J. Appl. Chem. 23, No. 5, 512 (1950) [USSR].*

[4] U. S. Patent 2254382 (1941); Chem. Abs. 35, 7975 (1941).

[5] British Patent 615665 (1949); Chem. Abs. 43, 4500 (1949); Swiss Patent 248209 (1948); Chem. Abs. 8712 (1949).

[6] Swiss Patent 256764 (1948); Chem. Abs. 43, 8713 (1949); Swiss Patent 256765 (1948); Chem. Abs. 43, 8713 (1949).

[7] U. S. Patent 2537017 (1951); Chem. Abs. 45, 3170 (1951).

Received January 7, 1958.

*Original Russian pagination. See C. B. translation.

# MECHANISM OF JOINT POLYCONDENSATION PROCESSES

G. A. Shtraikhman

Institute of High-Molecular Compounds, Academy of Sciences USSR

Despite the great technical and biological significance of joint polycondensation processes, there is no theory of such processes at the present time. This paper is an attempt to elucidate certain relationships associated with the formation mechanism and composition of polycondensation products.

The condensation reaction involves interaction of two functional groups so that certain parts of these groups are split off, the fragments combine, and a new bond is formed between the residues of the reacting molecules.

The polycondensation process, i.e., condensation leading to the formation of macromolecules of varying degrees of complexity (linear, branched, or three-dimensional), occurs as a series of consecutive elementary condensation reactions, in which the reacting molecules must be bifunctional at least.

The first work in the field of the kinetics of condensation reactions consisted of the classic researches of Menshutkin [1,2] who showed, in particular, that the esterification rate constant is independent of the length of the fatty acid or alcohol chain, but depends on the molar concentrations of hydroxyl and carboxyl groups. Most of the studies of polycondensation processes which have since been reported by various authors relate to the formation of polyesters and polyamides.

Korshak and his associates have shown [3-5] that the reaction of adipic acid with decamethylene glycol conforms to a bimolecular mechanism, at least up to degree of polymerization 28.6 (molecular weight 4200), and the rate constants calculated from a second-order reaction equation for different temperatures have constant values. Similar results were obtained for the reactions of adipic acid with ethylene glycol and sebacic acid with hexamethylenediamine. Kogan [6,7] showed that the polyesterification of phthalic anhydride with ethylene glycol proceeds by a bimolecular mechanism. Al'tman and Kedrinskii [8] reached a similar conclusion in a study of the reactions of ethylene and propylene glycols with phthalic anhydride. Flory [9-11] showed by means of numerous examples that polycondensation of glycols with dibasic acids in presence of acid catalysts (such as p-toluenesulfonic acid) conforms to a second-order reaction law, at least up to degree of polymerization 90, which corresponds to a molecular weight of about 10000. Despite the manifold increase of molecular size and more than a 2000-fold increase of viscosity, there are no indications of a decrease in the reaction rate constant.

On the basis of available experimental data Flory formulated the principle that the activity of each type of functional groups remain the same at all stages of polycondensation. The principle of equal activity greatly simplifies kinetic analysis of polycondensation reactions, since it makes it possible to disregard entirely the complex structure of the molecules involved in the polycondensation. Instead, the process can be regarded merely as a reaction between functional groups without differentiation by size of the molecules to which they are attached. Thus, the rate constant generally does not vary with the degree of complexity of the molecules involved at different stages of a given process.

If a bifunctional compound can undergo polycondensation with itself, we have the case

$$x—A—y + x—A—y \xrightarrow{k} x—A—A—y + x—y, \qquad (1)$$

where x −A and y − A are the functional groups as a whole, and x and y are the portions of these groups which are split off.

In two-component joint polycondensation of bifunctional compounds two cases must be distinguished, dependent on whether each of the two types of reacting molecules contains similar or different functional groups.

In the first case we have

$$x—A—x + y—B—y \xrightarrow{k} x—A—B—y + x—y. \quad (2)$$

The whole process consists of a series of elementary reactions of Type (2), representing interaction between two kinds of functional groups, x −A and y −B, present in the reaction zone. Thus, there is no difference in principle from homopolycondensation processes which consist of elementary Type(1) reactions between x − A and y − A functional groups, in the sense that each mechanism is based on one elementary process only.

The mechanism of Reaction (2) predetermines a regular alternation of − A − and − B − units in the polymer.

In the second case of two-component polycondensation of bifunctional compounds the components may contain different functional groups, such as x − A −y and x − B − y Then the reaction zone contains four types of functional groups (x − A, y − A, x − B, y− B), and the over-all mechanism of the polycondensation process may be represented by a scheme consisting of four elementary reactions of macromolecular chain formation:

$$x—A—y + x—B—y \xrightarrow{k_1} x—A—B—y + x—y, \quad (3)$$

$$x—B—y + x—A—y \xrightarrow{k_2} x—B—A—y + x—y, \quad (4)$$

$$x—A—y + x—A—y \xrightarrow{k_3} x—A—A—y + x—y, \quad (5)$$

$$x—B—y + x—B—y \xrightarrow{k_4} x—B—B—y + x—y. \quad (6)$$

The polymer chain then contains four different types of linkage (− A − B −, − B − A−, −A − A − and −B − − B −), the relative proportions of which, under given conditions, must depend on the relative magnitudes of the rate constants $k_1$, $k_2$, $k_3$, and $k_4$. •

Regular alternation of − A − and − B − units in the polymer would then be an exception rather than the rule.

In three-component joint polycondensation of bifunctional compounds we can consider three possible cases of polymer formation:

| I | II | III |
|---|---|---|
| x—A—y | x—A—x | x—A—x |
| x—B—y | x—B—y | x—B—x |
| x—C—y | y—C—y | y—C—y |

Let us consider more fully Case III, which is of great interest in relation to the synthesis of condensation copolymers.

Here the reaction zone contains two monomer types, x − A− x and x − B − x, which do not react with each other, but each can react with the third type y−C−y.

Therefore the entire process is based on interaction between two pairs of functional groups: (x − A) and (y − C) on the one hand, and (x − B) and (y − C) on the other.

$$R—A—x + y—C—R' \xrightarrow{k_1} R—A—C—R' + x—y, \quad (7)$$

$$R—B—x + y—C—R' \xrightarrow{k_2} R—B—C—R' + x—y. \quad (8)$$

• − A − B − and − B − A − units are, of course, the same, but they must be considered separately as they are formed by two different elementary processes of chain formation.

This type of joint polycondensation includes the formation of polyesters from two dicarboxylic acids and a glycol or two glycols and a dicarboxylic acid, formation of polyamides from two dicarboxylic acids and a diamine or two diamines and a dicarboxylic acid, formation of polysulfide polymers from two dihalides and an alkali polysulfide, formation of phenol-aldehyde resins from two phenols and an aldehyde, etc.

If we assume a second-order reaction mechanism then the rate of binding of (A − x) and (B − x) functional groups, respectively, in Equation (7) can be represented as follows:

$$-\frac{d[A-x]}{dt} = k_1[A-x][C-y], \tag{9}$$

$$-\frac{d[B-x]}{dt} = k_2[B-x][C-y], \tag{10}$$

where [A − x], [B − x] and [C − y] are the existing concentrations of the functional groups (in moles/liter). Division of Equation (9) by (10) gives

$$\frac{d[A-x]}{d[B-x]} = \frac{k_1}{k_2} \cdot \frac{[A-x]}{[B-x]}. \tag{11}$$

The ratio of the rate constants of the elementary reactions under isothermal conditions is a constant quantity which we denote by $\alpha$.

The left-hand side of the differential Equation (11) represents the composition of a polymer fragment formed at a given time instant, in the form of the molar ratio of monomer A and B residues, which we can denote by a' and b'. The right-hand side contains $\alpha$, the constant for the system, and the ratio of the initial functional-group concentrations [A − x] and [B − x], which can be denoted by a and b.

Then Equation (11) can be written

$$\frac{a'}{b'} = \alpha \cdot \frac{a}{b}. \tag{12}$$

Equation (12), which is an expression of the Rayleigh law, shows that in the general case, if $\alpha \neq 1$, the composition of the polymer formed differs from the composition of reaction mixture. Therefore the concentrations of components A and B in the reaction mixture must vary during the conversion.

It therefore becomes necessary to use the integral form of the composition equation.

Integration of Equation (12) gives

$$a/a_0 = (b/b_0)^{\alpha}, \tag{13}$$

where $a_0$ and $b_0$ are the initial concentrations of the functional groups [A − x] and [B − x] in the reaction mixture, and a and b are their existing concentrations.

The constant $\alpha$ for the system can be determined experimentally by measurements of the existing concentrations a and b of the functional groups at a certain stage in the process. Since direct determination is difficult, these concentrations may be found indirectly from analytical data for the composition of the isolated polymer and its yield. The initial concentrations $a_0$ and $b_0$ must be known. The calculation is performed with the aid of Equation (13), which can be written in a more convenient logarithmic form:

$$\alpha = \lg \frac{a}{a_0} / \lg \frac{b}{b_0}. \tag{14}$$

The constant $\alpha$ can also be found from separate kinetic investigations of polycondensation in two binary systems, composed of monomers A and C and B and C, by means of the equation

$$\alpha = k_1/k_2. \tag{15}$$

## SUMMARY

An equation for copolymer composition is derived for the case of three-component polycondensation; it is shown that the copolymer composition is connected with the constant $\alpha$ for the system and with the concentrations of functional groups in the mixture.

## LITERATURE CITED

[1] N. A. Menshutkin, J. Russ. Phys. - Chem. Soc. 9, 316 (1877).

[2] N. A. Menshutkin, J. Russ. Phys. - Chem. Soc. 13, 523 (18881).

[3] S. R. Rafikov and V. V. Korshak, Proc. Acad. Sci. USSR 64, 211 (1949).

[4] G. N. Chelnokova, S. R. Rafikov, and V. V. Korshak, Proc. Acad. Sci. USSR 64, 353 (1949).

[5] V. V. Korshak, Methods of High-Polymer Organic Chemistyr, 1 [in Russian] (Izd. AN SSSR, Moscow, 1953) p. 510.

[6] A. I. Kogan, J. Appl. Chem. 9, 1070 (1936)[USSR].

[7] A. I. Kogan, J. Appl. Chem. 10, 900 (1937)[USSR].

[8] S. S. Al'tman and V. V. Kedrinskii, Data on Cracking and on Chemical Conversion of Cracking Products [in Russian] (Moscow, 1936) p. 364.

[9] P. J. Flory, J. Am. Chem. Soc., 61, 3334 (1939).

[10] P. J. Flory. J. Am. Chem. Soc,, 62, 2261 (1940).

[11] P. J. Flory. Principles of Polymer Chemistry. Cornell Univ. Press, Ithaca, N. Y. (1953).

Received January 14, 1958.

# DEPENDENCE OF THE POLYMERIZATION RATE OF ACRYLONITRILE ON THE HYDRODYNAMIC PROCESS CONDITIONS •

E. S. Roskin

The S. M. Kirov Textile Institute, Leningrad

It has been shown in a series of earlier publications and papers on acrylonitrile [1-8] that stirring of the reaction medium sharply lowers the polymerization rate, lengthens the induction period, and has an adverse effect on the technological properties of the polymer. At a certain stirring rate, which we term the critical rate, polymerization does not occur at all, and can commence only some time after the stirring has been stopped.

Quite recently Thomas, Gleason, and Mino [9] confirmed that, in the polymerization of acrylonitrile in aqueous solution in presence of an oxidation-reduction system consisting of a mixture of sodium chlorate and sulfite, stirring of the medium also lowers the reaction rate.

On the basis of these observations, we, jointly with the staff of the "Rulon" works of the Gor'kii Council of National Economy, have developed and put into operation [11] an industrial process for static polymerization of acrylonitrile, effected without stirring or special heating.

It was originally believed that atmospheric oxygen which may be trapped by the stirrer blades has an inhibiting effect on the polymerization kinetics [3, 11-13].

Detailed investigations have shown that although atmospheric oxygen has an inhibiting effect on acrylonitrile polymerization, this effect is not nearly as strong as is generally thought. In fact, Stoy [14] showed that oxygen is a powerful inhibitor only in the polymerization of acrylonitrile made by direct synthesis from acetylene and hydrogen cyanide. This product always contains a certain amount of vinyl derivatives of acetylene as an impurity. These are easily oxidized by atmospheric oxygen to the corresponding peroxides, which are the actual polymerization inhibitors. Since in all our investigations we were concerned with acrylonitrile made by dehydration of ethylene cyanohydrin, the influence of atmospheric oxygen was not sufficiently strong to inhibit polymerization completely. We confirmed by numerous careful experiments in oxygen-free argon with oxygen-free components that intensive stirring had an inhibiting effect on acrylonitrile polymerization even under conditions such that contact of oxygen with the reaction medium was certainly excluded. However, further investigations showed that not every type of stirring has this effect. It was found experimentally that, on the whole, only stirring which causes turbulent motion of the reaction mixture has an inhibiting effect on acrylonitrile polymerization. After the shaking or stirring had stopped, polymerization started again after a certain induction period, proportional to the shaking or stirring time.

The Reynolds number, modified for stirring processes, can be used as a quantitative measure of the influence of stirring in heterophase polymerization in general.

$$Re_s = \frac{\rho n d^2}{\eta}, \qquad (1)$$

where $Re_s$ is the Reynolds number for stirring, $\rho$ is the density of the liquid (in g/cc), n is the stirrer speed

• Communication III in the present series [1, 2].

($sec^{-1}$), d is the stirrer diameter (in cm), and $\eta$ is the absolute viscosity of the reaction medium (in $g \cdot cm^{-1} \cdot sec^{-1}$).

The diameter of a normal stirrer is taken to be

$$d = \frac{D}{3}, \tag{2}$$

where D is the diameter of the vessel (in cm).

Substitution of Equation (2) into Equation (1) gives

$$Re_s = \frac{\rho n D^2}{9\eta}. \tag{3}$$

When acrylonitrile is polymerized in aqueous solution, a polyacrylonitrile suspension is formed, the viscosity of which can be calculated from the Einstein-Batschinski equation

$$\eta = \eta_0 (1 + 4.5\varphi), \tag{4}$$

where $\eta_0$ is the viscosity of the dispersion medium and $\varphi$ is the volume concentration of the solid phase in the liquid.

Since

$$\varphi = \frac{CK}{\gamma}, \tag{5}$$

where C is the initial monomer concentration in the reaction medium (in g/cc), K is the percentage conversion of monomer to polymer, and $\gamma$ is the density of the polymer (in g/cc; 1.17 for polyacrylonitrile), we have from Equations (3), (4), and (5)

$$Re_{pol} = \frac{\rho n D^2}{9\eta_0 \left(1 + 0.045 \frac{CK}{\gamma}\right)}, \tag{6}$$

where $Re_{pol}$ is the modified Reynolds number in polymerization.

When K = 0, i.e., for the induction period or the very earliest polymerization stage, Equation (6) is analogous to Equation (3), which is the one to be used in practice for solution of the problem of the initial stirring conditions.

However, as polymerization proceeds, K tends to 100%, and for the greatest value of C (approximately 0.10 g/cc in the case of acrylonitrile) this leads to a decrease of about 20% in $Re_{pol}$. It is therefore permissible to raise the stirrer speed subsequently by 20%. Decrease of $Re_{pol}$ satisfactorily explains the known poor reproducibility of heterophase polymerization. It is evident that $Re_{pol}$ will have different values which depend on the shape of the reaction vessel and the stirrer design. For example, with cylindrical reactors with smooth walls and with the use of propeller two-blade stirrers set at an angle of 22.5°, the stirrer diameter being 1/3 of the vessel diameter, $Re_{pol}$ is of the order of $3 \cdot 10^4$. If under these conditions the stirrer rotates at a speed corresponding to $Re_{pol} > 3 \cdot 10^4$, the reaction of acrylonitrile polymerization stops completely.

It has been found experimentally that in a reactor 60 cm in diameter polymerization stops at 45-47 revolutions/minute. In a reactor 100 cm in diameter, polymerization did not proceed even at 16-18 revolutions/minute.

Calculations based on Equation (3) show that when reactors 2 meters in diameter are used, polymerization of acrylonitrile should cease when the stirrer speed exceeds 4 revolutions/minute.

When beakers about 10 cm in diameter were used as polymerization vessels, polymerization still took place at stirrer speeds in excess of 1000 revolutions/minute.

However, when ordinary flasks were used instead of cylindrical vessels, polymerization of acrylonitrile ceased at stirrer speeds considerably lower than speeds corresponding to $Re_{pol} = 3 \cdot 10^4$. This is due to conditions in which the shape of the flask favors turbulence at considerably lower stirrer speeds. For example, polymerization in a flask 12 cm in diameter ceased at a stirrer speed of 300 revolutions/minute, which corresponds to $Re_{pol} = 8 \cdot 10^3$. Correspondingly higher stirrer speeds were needed to arrest acrylonitrile polymerization in flask of lower capacity.

Shaking of the reaction mixture in a vertical or horizontal direction has a particularly pronounced effect in stopping polymerization. Polymerization is stopped when the horizontal shaking rate is 70-80 oscillations per minute, irrespective of the type of vessel in which the reaction mixture is contained.

The necessary steps were taken in all the experiments to exclude the influence of atmospheric oxygen.

## DISCUSSION OF RESULTS

The polymerization rate of acrylonitrile in aqueous solution and the duration of the induction period depend on the stirring conditions. To account for this, only a hypothetical mechanism can be postulated at the present time, based on the fact that the macroprocess (stirring) has a decisive influence on the microprocess (polymerization). It follows that the polymerization reaction must commence in some kind of supermolecular formations.

Our preliminary experiments demonstrate the influence of the laminar velocity gradient on the polymerization rate, qualitatively analogous to the influence of stirring.

It may be postulated that the initial reaction stage proceeds by an emulsoid mechanism in fairly large molecular "swarms" with an acrylonitrile concentration much higher than the average value. It can be shown that the stability of these swarms is determined by a certain critical radius •

$$R = 0.8 \frac{\gamma}{\eta g}, \tag{7}$$

where R is the critical radius of a swarm ("droplet"), $\gamma$ is the interfacial tension (at the boundary between the "droplet" and the homogeneous solution), $\eta$ is the macroscopic viscosity of the solution, and g is the velocity gradient.

The numerical coefficient 0.8 corresponds to the c.g.s. system.

These "droplets" or swarms may arise as the result of heterophase fluctuations [15], the probability of which is high because of the limited solubility of acrylonitrile in water. The formed "droplets" should be considerably stabilized after formation of polymerization centers within them, with subsequent growth of the polymer chain into the "droplet."

The forming chain thus plays a "cementing" role, freezing the heterophase fluctuation.

It follows from Equation (7) that stirring (i.e., the velocity gradient g) has the directly opposite effect, tending to shorten the life of the fluctuation, i.e., to bring the swarm or "droplet" back into solution.

The suggested mechanism explains, at least qualitatively, the inhibiting effect of stirring on the polymerization of acrylonitrile in aqueous solution.

A similar effect is apparently produced by ultrasonic vibrations at 500 and 200 kc, which, according to Aybar, Senvar, and Akin [16] inhibit polymerization of acrylonitrile in aqueous solutions in presence of hydrogen peroxide and ferric salts.

The influence of stirring, demonstrated by us in the case of acrylonitrile polymerization, is probably of more general significance. It is probable that the stirring regime has a serious influence not only on heterophase polymerization reactions but also on other analogous interactions. The inhibiting effect of intensive stirring on the rate of heterophase polymerization of methyl methacrylate was demonstrated by Rutkovskii and Goncharov [17]. Ac-

•The appropriate calculations were performed by us jointly with V. M. Aslanyan.

cording to their results, methyl methacrylate polymerization stops completely at stirrer speeds of 1000 revolutions/minute and over.

The fact that the stirring conditions have not received due attention from research scientists and industrial workers accounts for the well-known apparent "insensitivity" which results from the use of relatively small reactors and low stirrer speeds, common in laboratory and industrial practice.

## SUMMARY

1. The polymerization rate of acrylonitrile in aqueous solution is an inverse function of $Re_{pol}$ and the laminar velocity gradient.

2. The view is put forward that the stirring regime has a significant influence on the course of heterophase reactions.

## LITERATURE CITED

[1] E. S. Roskin, J. Appl. Chem. 30, 124 (1957)[USSR].*

[2] E. S. Roskin, J. Appl. Chem. 30, 1030 (1957) [USSR].

[3] E. S. Roskin, Trans. S. M. Kirov Textile Inst. Leningrad 6, 77 (1955).

[4] E. S. Roskin, Summaries of Papers at the Sci. Tech. Conference of the S. M. Kirov Textile Inst. Leningrad, 1952-1953 [in Russian].

[5] E. S. Roskin, ibid (1955).

[6] E. S. Roskin, ibid (1957).

[7] E. S. Roskin, Textile Ind. No. 11 (1956).

[8] E. S. Roskin, IXth Conference on General Problems of the Chemistry and Physics of High Polymers [in Russian] (1957).

[9] W. M. Thomas, E. H. Gleason, G. Mino, J. Polym. Sci., XXIV (1957).

[10] K. A. Lisichenko, E. A. Kulev, A. I. Konkhin, and E. S. Roskin, Summaries of Papers at the Sci.-Tech. Conference on High Polymers [in Russian] (Dzerzhinsk, 1958).

[11] Z. A. Rogovin, Principles of the Chemistry and Technology of Artificial Fiber Production [in Russian] (State Light Industry Press, 1957) p. 675.

[12] Z. A. Rogovin, Z. A. Zazulina, et al. J. Chem. Ind. No. 5 (1958) [USSR].

[13] A. Hunyar, H. Reichert, Faserforsch. u. Textiltechn., 5, 1 (1954).

[14] A. Stoy, Chemicky prum., 9 (1956).

[15] Ya. N. Frenkel', Kinetic Theory of Liquids [in Russian] (Izd. AN SSSR, 1955).

[16] S. Aybar, C. B. Senvar u. C. Akin, Comuns. fac. Sci. Univ. Ankara, 413 (1952); Ch. A., 48, 7928(1954).

[17] B. N. Rutkovskii and G. S. Goncharov, J. Appl. Chem. 26, 434 (1953)[USSR]*

Received October 15, 1958.

*Original Russian pagination. See C. B. translation.

# ESTERIFICATION OF WEAKLY HYDROXYETHYLATED CELLULOSE

N. I. Klenkova and O. M. Kulakova

In a number of papers by different investigators the interesting fact is noted that introduction of a small number of hydrophobic groups in the cellulose structure increases its hydrophilic properties. This effect has been observed in methylation, ethylation, hydroxyethylation, and other processes [1-4].

This effect is explained on the hypothesis that the introduced bulky radicals, substituting individual hydroxyl groups in cellulose, at the same time break hydrogen bonds between neighboring hydroxyls and prevents intermolecular hydrogen bonding between all the free hydroxyls even after washing and drying of the product. Investigations of the infrared spectra of partially esterified celluloses [5] show that esterification releases hydroxyl groups from hydrogen bonds and loosens the fiber structure. While the degree of substitution is still low, there is apparently a large number of accessible chain regions in the system, and the reagents act as those regions.

Weakly hydroxyethylated fibers may be especially valuable, as they can be easily formed by treatment of alkali cellulose with ethylene oxide vapor at room temperature.

The properties of low-substituted hydroxyethyl celluloses have been studied by Shorygin and Rymashevskaya [6], Nikitin, Rudneva, Klenkova [4,7,8] and others. These investigations [4,8] have shown that weakly hydroxyethylated fibers, in addition to their pronounced hydrophilic porperties, have very high reactivity in formylation, acetylation, and hydrolysis.

Certain attempts to utilize the properties of hydroxyethylated celluloses have been made by Shorygin and Rymashevskaya [6], who suggested the use of low-substituted hydroxyethylcelluloses for the production of artificial fibers. These investigations were continued by Kargin and Kuril'chikov, but the fibers obtained had low strength.

Fournier [10] performed extensive work on the production of various mixed derivatives of cellulose from low-substituted hydroxyethylation products.

The production of cellulose ester by the action of alkyl halides of low reactivity on cellulose activated by ethylene oxide may be of considerable interest.

Cellulose esters are usually prepared under very harsh conditions, with extensive degradation of the cellulose chains and poor mechanical properties of the products. Such derivatives as propylcellulose, butylcellulose, and hexylcellulose are not used because of their poor mechanical properties, although in other properties (resistance to alkalies, acids, and water, water repellency) they are superior to ethylcellulose which is used industrially.

Nowakowski prepared butylcellulose by the action of normal butyl bromide on alkali cellulose at 100° with vigorous stirring. He succeeded in obtaining di- and trisubstituted ester- after 30-33 hours by multistage esterification with subsequent addition of solid alkali. Ushakov and Kon'kova prepared butylcellulose of degree of substitution 1.6-2.3, not less than 12 hours being needed for the esterification in an autoclave at 120-125°. Even harsher conditions are required for preparation of amyl- and hexylcellulose [11].

The purpose of the present investigation was to study the possibility of using milder conditions and accelerating the preparation of cellulose esters by pretreatment of alkali cellulose with ethylene oxide, which in practice is a very easy method for loosening the fiber structure.

## EXPERIMENTAL

Purified cotton wool and wood viscose pulp were used for the investigations. The alkylation agents were butyl chloride and bromide, isobutyl bromide, amyl iodide, and isoamyl bromide.

For preparation of weakly hydroxyethylated cellulose, the original cellulose material was mercerized by the action of caustic soda solution, pressed, loosened, and then treated with ethylene oxide vapor in closed jars at room temperature. Part of each sample treated with ethylene oxide was used for determination of hydroxyethyl groups, and the rest was treated with the appropriate alkyl halide in a sealed tube.

The contents of hydroxyethyl groups and of alkyl groups after esterification were determined by the Viebock and Schwappach method, and by elementary analysis.

Parallel experiments were performed on the esterification of alkali cellulose treated with ethylene oxide and untreated.

The first series of experiments was carried out under the following conditions.

The original cellulose was treated with 17.5% caustic soda solution for 45 minutes, and then with 50% caustic soda solution; after the swelling treatment the alkali cellulose was pressed out to press ratio 4 and loosened. The ethylene oxide treatment was continued for 2-2.5 hours at 20°. Esterification of alkali cellulose, after treatment with ethylene oxide and untreated, was carried out in sealed tubes at 100° for 6 hours in a glycerol bath. The reaction products were washed for a long time with hot water and treated with steam to remove residual alkyl halides.

The activating effect of pretreatment of alkali cellulose with ethylene oxide on the formation of butyl- and amylcellulose is shown by the data below.

| Cellulose product | Contents (%) | |
|---|---|---|
| | hydroxyethyl groups in sample after treatment with ethylene oxide | alkyl groups (apart from hydroxyethyl in final product |
| Butylcellulose from alkali cellulose: | | |
| treated with ethylene oxide | 10.6 | 36.2 |
| not treated with ethylene oxide | 0 | 8.8 |
| Butylcellulose from alkali cellulose: | | |
| treated with ethylene oxide | 6.8 | 36.1 |
| not treated with ethylene oxide | 0 | 17.6 |
| Isobutylcellulose from alkali cellulose: | | |
| treated with ethylene oxide | 13.2 | 16.2 |
| not treated with ethylene oxide | 0 | 4.5 |
| Amylcellulose from alkali cellulose: | | |
| treated with ethylene oxide | 10.6 | 24.3 |
| not treated with ethylene oxide | 0 | 3.2 |
| Isoamylcellulose from alkali cellulose: | | |
| treated with ethylene oxide | 6.2 | 13.6 |
| not treated with ethylene oxide | 0 | 5.2 |

It follows from the above data that weakly hydroxyethylated fibers give products with considerably higher alkyl group contents after esterification by alkyl halides at 100° for 6 hours than do cellulose fibers not subjected to such pretreatment. This fact also confirms the earlier hypothesis that hydroxyethyl groups entering the structure of the cellulose fiber loosen it and make it more accessible to reagents.

A series of experiments was performed under somewhat modified conditions. In view of the observed fact that ethylene oxide penetrates more easily and uniformly into cellulose swollen in 17.5% caustic soda solution than into cellulose swollen in 50% alkali, in these experiments the cellulose, after mercerization in 17.5%

caustic soda solution, pressing, and loosening, was immediately treated with ethylene oxide and only after that treated with 50% caustic soda and then subjected to esterification by means of alkyl halides.

The results of a series of experiments on the preparation of butylcellulose by the action of butyl bromide on alkali cellulose treated and not treated with ethylene oxide are given below (temperature 100°).

| | Butoxyl group content (%) in final product after butylation | | |
|---|---|---|---|
| Butylation time (hours) | 1 | 3 | 6 |
| After treatment with ethylene oxide (hydroxyethyl group content 7.7%) | 13.9 | 35.7 | 49.0 |
| Without ethylene oxide pretreatment | 7.8 | – | 14.2 |

The above data also demonstrate the strong influence of ethylene oxide treatment, i.e., introduction of a small number of hydroxyethyl groups into the cellulose fiber structure, on subsequent butylation of cellulose by means of butyl bromide.

A series of experiments was performed on butylation of cellulose with dry alkali introduced into the tubes. In all cases the final products had much lower butoxyl group contents, while their ash contents were very much higher (up to 35%).

In butylation of alkali cellulose by means of butyl chloride under the conditions described above the cellulose was etherified with very great difficulty and very low degrees of substitution were attained even with the weakly hydroxyethylated samples; this may be attributed to predominance of side processes. The etherification conditions were not specially chosen so as to prevent these processes.

For comparison of the properties of butylcellulose with those of weakly hydroxyethylated butylcellulose, conditions were chosen for etherification of alkali cellulose, with an without pretreatment by ethylene oxide, by means of butyl bromide, such that butylcellulose and weakly hydroxyethylated butylcellulose with similar contents of butoxyl groups were obtained. This was achieved by butylation of alkali cellulose at 140° for 2 hours. The mercerization and hydroxyethylation conditions were as before (as in the second series of experiments).

Numerous experiments showed that the butoxyl group content of butylcellulose prepared without pretreatment of the alkali cellulose by ethylene oxide was from 40 to 47%, whereas samples obtained after pretreatment contained from 50 to 57% (and the latter also contained from 7 to 12% hydroxyethyl groups).

The yields of butylcellulose after esterification and washing reached 120% on the weight of the original cellulose; the yields of weakly hydroxyethylated butylcellulose reached 150%.

For investigation of the properties of butylcellulose and weakly hydroxyethylated butylcellulose, films were prepared by slow evaporation of 6% solutions of these ethers in alcoholic benzene (the solutions were previously centrifuged to remove the insoluble fractions). The films so obtained had the following alkyl group contents.

| | Butoxyl group contents (%) | Hydroxyethyl group contents (%) |
|---|---|---|
| Butylcellulose from cotton cellulose | 47 | 0 |
| Butylcellulose from wood viscose pulp | 45.5 | 0 |
| Weakly hydroxyethylated butylcellulose from cotton cellulose | 54.5 | 7.4 |
| Weakly hydroxyethylated butylcellulose from wood viscose pulp | 51.0 | 5.8 |

It was found that weakly hydroxyethylated butylcellulose has somewhat higher intrinsic viscosity (1.2) in alcohol–benzene solution than butylcellulose (0.8).

Certain mechanical properties of these films, their melting (softening) temperatures, decomposition (discoloration) temperatures, hygroscopicity, and acid resistance were determined.

The mechanical properties and melting and decomposition temperatures of butylcellulose and weakly hydroxyethylated butylcellulose films are given below.

| | Hydroxyethylated butylcellulose from | | Butylcellulose from | |
|---|---|---|---|---|
| | cotton cellulose | wood viscose pulp | cotton cellulose | wood viscose pulp |
| Breaking load (kg): | | | | |
| maximum | 9.3 | 9.5 | 1.1 | 1.8 |
| minimum | 6.2 | 6.5 | 0.2 | 1.4 |
| Elongation (mm): | | | | |
| maximum | 30 | 40 | 9 | 8 |
| minimum | 15 | 20 | 1 | 5.5 |
| Elongation (%): | | | | |
| maximum | 20 | 22 | 5 | 4.4 |
| minimum | 8 | 10 | 3 | 2.8 |
| Breaking length (m): | | | | |
| maximum | 3200 | 3200 | 1600 | 1500 |
| minimum | 2500 | 2300 | 300 | |
| Tensile strength (mean) of film ($kg/mm^2$) | 4.4 | 4.8 | 2.1 | 2.6 |
| Melting or softening temperature (°C) | 170–180 | 185–195 | 160–180 | 175 |
| Decomposition or discoloration temperature (°C) | 190 | 170 | 160 | 160 |

The foregoing data show that the tensile strength of hydroxyethylated butylcellulose films is double that of butylcellulose films prepared under the same conditions; the elongation at break is also several times as great. The melting and decomposition temperatures differ little, but are somewhat higher for the hydroxyethylated samples.

Some literature data [12] on the properties of cellulose ethers are given below.

| Sample | Softening temperature (°C) | Water absorption (% on ester weight) | Tensile strength of film ($kg/mm^2$) | Elongation at break (%) |
|---|---|---|---|---|
| Ethylcellulose | 165–185 | 3–6 | 5.5–7 | 20–38 |
| Propylcellulose | 160–170 | 0.5 | 3.5 | 15–20 |
| Butylcellulose | 140–170 | 0.3 | 2–2.4 | 7–10 |
| Hexylcellulose | 55–65 | 0.16 | 0.4 | 3–4 |

Our data on the hygroscopicity and acid resistance of butylcellulose and weakly hydroxyethylated butylcellulose films are given on the following page.

For hygroscopicity determinations the samples were kept in desiccators over water. The acid resistance was determined from the weight losses of samples kept in sulfuric acid of 35° Bé for 6 days and then washed with water.

Our investigations show that by introduction of a small quantity of hydroxyethyl groups into cellulose it is possible to obtain, relatively easily, weakly hydroxyethylated butylcellulose which is close to ethylcellulose in

its mechanical properties and melting point, and which has low hygroscopicity and high resistance to acids. Films made from this weakly hydroxyethylated butylcellulose are colorless, transparent, very elastic, and retain these properties after prolonged exposure at a low temperature ( − 50°). According to our results and to literature data, butylcellulose films have only half the tensile strength of these films, and very low extensibility.

It seems likely that the poor mechanical properties of ordinary butylcellulose are due not so much to peculiarities of their intermolecular structure [12] as to the harsh conditions used in its preparation, causing degradation of the cellulose. The structure of alkali cellulose is apparently less permeable to the alkylation agent at high temperatures, and side reactions occur more easily under these conditions. In weakly alkylated alkali cellulose the hydroxyethyl groups create steric obstacles to linking of hydroxyl groups at high temperatures, and the alkylation agent diffuses into the fiber and reacts with the free hydroxyl groups more easily.

| Sample | Hygroscopicity (% water absorbed on sample weight) | | Acid resistance (% weight loss of sample) |
|---|---|---|---|
| | after 24 hours | after 15 days | |
| Hydroxyethylated butylcellulose: | | | |
| from cotton wool . . . . . | 1.6 | 2.2 | 0.5 |
| from viscose wood pulp . . . . . | 2.4 | 2.8 | 0.6 |
| Butylcellulose: | | | |
| from cotton wool . . . . . | 9.2 | 9.2 | 5.6 |
| from viscose wood pulp. . . . . | 8.8 | 21.0 | 3.0 |

## SUMMARY

1. Treatment of alkali cellulose with ethylene oxide has a peculiar activating effect on the structure of cellulose fibers. The hydroxyethyl groups introduced into the cellulose structure form a steric obstacle to mutual approach of the cellulose chains; the reagent has freer access to the hydroxyl groups within the cellulose fiber.

2. Alkyl halides react much more easily with weakly hydroxyethylated alkali cellulose than with ordinary alkali cellulose, and the final products are more highly substituted.

3. It is shown that it is possible in principle to prepare highly substituted butylcellulose with good mechanical properties, low hygroscopicity, and high resistance to acids from weakly hydroxyethylated cellulose.

## LITERATURE CITED

[1] G. Jayme and A. Froundjian, Cellulosechemie, 18, 9 (1940).

[2] J. C. Bletzinger, Ind. Eng. Ch., 35, 474 (1943); L. W. Aiken, Ind. Eng. Ch. 35, 1206 (1943).

[3] N. I. Nikitin, A. M. Plekhanova, and T. I. Rudneva, J. Appl. Chem. 20, 1185 (1947); N. I Nikitin, T. I. Rudneva, J. Appl. Chem. 13, 9 (1940); Proc. Acad. Sci. USSR 23, 240 (1940); N. I Nikitin and T. I. Rudneva, Org. Chem. Ind. 7, 398 (1939) [USSR].

[4] N. I. Klenkova, Dissertation [in Russian] (S. M. Kirov Academy of Wood Technology, 1949); N. I. Nikitin and N. I. Klenkova, J. Appl. Chem. 24, 296 (1951) [USSR].*

[5] V. N. Nikitin, J. Phys. Chem. 23, 775, 786 (1949) [USSR].

[6] P. P. Shorygin and Yu. A. Rymashevskaya, Artif. Fiber 6 (1933); J Gen. Chem. 6, 1632 (1932). [USSR].

[7] N. I. Nikitin and T. I. Rudneva, Org. Chem. Ind. 7, 398 (1939) [USSR].

[8] N. I Klenkova, J. Appl. Chem. 28, 393 (1956) [USSR]. *

[9] V. A. Kargin and E A. Kuril'chikov, Trans. All-Union Sci. Res. Inst. Artificial Fibers 144 (1937); E. A. Kuril'chikov, Dissertation [in Russian] (Ivanovo Technological Inst. 1952).

[10] P. E. Fournier, Ann. Chim., 7, 75 (1952).

*Original Russian pagination. See C. B. translation.

[11] S. N. Ushakov, Cellulose Esters [in Russian] (1941).

[12] Z. A. Rogovin and N. N. Shorygina, Chemistry of Cellulose and Associated Substances [in Russian] (1953) p. 466.

Received February 15, 1958.

# OZONATION OF LIGNIN

D. V. Tishchenko

Ozonolysis of unsaturated and aromatic compounds is a generally accepted method for determination of their structure. A number of workers attempted to apply this method for determination of the structure of native and isolated lignins, but without any appreciable success. Some of them subjected aqueous suspensions of lignin or lignified tissues to the action of unspecified quantities of ozone for various times, investigated the aqueous solutions formed [1], and found them to contain carbonic, acetic, formic, and oxalic acids. Others ozonated isolated lignins in the form of solutions or suspensions in aqueous or anhydrous organic solvents until faintly colored solutions were obtained or until the suspensions were dissolved almost completely, treated the solutions with water, and looked for the individual products of ozonolysis [2]. They found the same acids and, in the case of maize lignin, small amounts of anisic acid. In all cases ozonolysis of lignin also yielded amorphous products of high molecular weight.

In our opinion, the lack of success in the use of ozonolysis can be ascribed to a number of causes. Let us consider some of them. It is unreasonable to expect that the primary ozonolysis products would be retained in ozonolysis of lignins in aqueous suspensions: water immediately decomposes ozonides with formation of substances containing aldehyde, ketone, and acid groups, and of hydrogen peroxide. Hydrogen peroxide and ozone oxidize these aldehydic, ketonic, and hydroxy acids to the simplest acids named above. Richtzenhain ozonized sprucewood lignin, isolated by the hydrochloric acid method, in really anhydrous ethyl acetate, but only to incomplete dissolution (80-90%) of the lignin, decomposed the ozonide solution by water, and found only the above-named acids among the individual compounds; he also obtained amorphous oxidized products of high molecular weight.

It is now known that the molecular weight (M) of native lignin is not less than 10,000 [3], and that it is composed of hydroxyphenylpropane units linked both by carbon–carbon and ether (aryl–alkyl and alkyl–alkyl) bonds [4]. The parent substance is coniferyl alcohol, and the intermediate compounds are dehydrodiconiferyl alcohol, D- and L-pinoresinol, and guaiacylglycerol-β-coniferyl ether. In the first two of these compounds the structural units are linked both by carbon–carbon and by ether bonds, and in the third, by an ether bond only. The manner of linking of these dimeric units in the biosynthesis of the lignin macromolecule is not yet known, but it is highly probable that the new bonds are mainly of the ether type and also carbon–carbon. If this is so, ozonolysis of lignin with complete saturation of benzene rings with ozone should give oxalic-acid derivatives (from the benzene rings; about 2 moles per mole of the nominal structural unit of lignin with M = 180) and aliphatic compounds containing 5-8 carbon atoms and aldehyde, ketone, alcohol, and acid groups. The extent of condensation of the lignin should complicate this result appreciably but not decisively [5]. If not all the benzene rings are saturated with ozone, ozonolysis would yield a considerably more complex mixture of high molecular weight. It seems that none of the workers on this problem carried ozonation of any lignin to the end. It is therefore not surprising that their results did not provide any information on the structure of lignin. Moreover, even the products of total ozonolysis of lignin ($C_5 - C_8$ compounds with the above-mentioned functional groups) can hardly be separated by the "classic" methods (crystallization, distillation).

It follows from the foregoing that in renewed researches on the ozonolysis of lignin it is important to take into account the conditions of application of this method, and to define immediate and ultimate aims.

In our opinion, the immediate problems are: 1) determination of quantitative yields of ozonides from various lignins; 2) investigations of their optical activity; 3) determination of the presence or absence of

chemical bonds between lignin and carbohydrates in wood; 4) determination of the yield of oxalic acid in decomposition of lignin ozonide by water with subsequent careful additional oxidation.

Determinations of quantitative ozonide yields from different lignins are important for solving the problems of the "quantitative aromaticity" both of native and of isolated lignins. The periodical literature still contains statements in support of the views of Hilpert and Schutz, who favored the theory that native lignin is "non-aromatic." For example, K. Kurschner [6] states that "the proportion of aromatic lignin in wood is low," while K. Kurschner and Yu. Gostomskii [7] consider that spruce wood contains not 27-28% but 13-16% of "aromatic" lignin. At the same time, there is no experimental proof of the "100% aromaticity" of native and isolated lignins (apart from the biosynthesis of lignin from coniferyl alcohol, effected by Freudenberg). To the best of our knowledge the highest yield of aromatic oxidation products obtained from any lignin does not exceed 60% on the lignin taken [8]. It is now generally accepted that the lignin macromolecule contains very few aliphatic double bonds, not more than one per 40-60 methoxyl groups [9]. In this case when the addition of ozone to lignin is considered these double bonds may be disregarded, and only the double bonds in the benzene rings of lignin need to be taken into account. If it is assumed that native conifer lignin consists entirely of aromatic structural units of M = 180 containing one benzene ring each, then, in complete ozonation of such lignin three ozone molecules must be added to each unit with formation of an ozonide of M = 180 + 144 = 324. The yield must be 180% on the weight of lignin.

If such a triozonide, completely soluble in a nonhydroxylic solvent, can be obtained by ozonation of wood, it would become possible to solve the question of the possible to solve the question of the possible optical activity of native lignin not subjected to the racemizing effects of acids, alkalies, or prolonged colloidal milling. It is known that all the lignin solutions investigated up to now have been found to be optically inactive, but the above-named racemizing influences were not excluded in the preparation of these solutions. Freudenberg's synthetic biolignin is also inactive, but it was synthesized from inactive coniferyl alcohol, although with the aid of optically active enzymes. If it is assumed that native conifer lignin is built from the same dimeric structural units (dehydrodiconiferyl alcohol, D- and L-pinoresinol, and guaiacylglycerol-β-coniferyl ether) as Freudenberg's synthetic lignin, primarily with formation of ether bonds between these dimeric units, then ozonolysis of such lignin with careful subsequent oxidation of the ozonolysis products by alkaline permanganate should yield about two molecules of oxalic acid for each benzene ring in the lignin.

The formation of this quantity of oxalic acid would be additional experimental confirmation that lignin is built entirely from phenylpropane units.

Scholler's lignin (from conifer wood, hydrolytic), free from carbohydrates and dried to constant weight at 100° and 0.01 mm (containing 96.3% Klason's lignin, 2.3% ash, 12% $OCH_3$), which is generally taken to be the most highly "condensed," was ozonized in acetic anhydride or anhydrous ethyl acetate with stirring, without access of atmospheric oxygen ($P_2O_5$ at the entry and exit to the system). The ozone concentration was about 4% by weight. The absorption of ozone was far from complete right from the start. In both cases ozonation was continued until the brown lignin suspension was completely dissolved to give a pale yellow solution and a white suspension of ash. In both cases the solution was filtered under suction through a glass filter into a weighed Wurtz flask, and the ash was washed with the same solvent, dried, and weighed. The amount agreed with the analytical value. The filtrates were evaporated under vacuum (10-15 mm, bath temperature not over 40°, $P_2O_5$ tube at the capillary end) and then taken to constant weight at 0.01 mm and bath temperature not over 30°.

Ozonation in acetic anhydride yielded 124% "ozonide" on the weight of ashless lignin, and in ethyl acetate, 182%. Each ozonide was dissolved in its respective solvent; the same amount of ozone as in the first experiment was passed through the solution, and the solvent was then removed; in the case of acetic anhydride the weight of ozonide remained unchanged (124% on the lignin), and in the case of ethyl acetate the yield was 179% on the lignin. The ultraviolet absorption spectrum of the first ozonide has a prominent absorption band at about ~280 mμ, characteristic of the benzene ring, but this is not found in the spectrum of the second ozonide. It must be assumed that acetylation of Scholler's lignin creates steric hindrances to ozonation of the benzene rings, so that triozonide in about 180% yield on the lignin cannot be obtained. This triozonide is formed by ozonation in anhydrous ethyl acetate. Moreover, it should be noted that partial or even complete solution of any lignin in ozonation in a nonaqeuous solvent does not guarantee triozonide formation: ozonation must be continued until the dissolution is complete and the ozonide yield must be checked. Both solutions were optically inactive. The same yield (176%) was obtained by ozonation of sprucewood acetic-acid lignin in anhydrous ethyl acetate [10]. As stated above, this proves the "100% aromatic" nature of conifer lignin and shows that it is built completely from phenylpropane units.

After removal of ethyl acetate the triozonide was a pale yellow, very viscous liquid. When heated above 55-60° it decomposed with slight deflagration and charring. When stirred with cold water for 18 hours and then warmed on the water bath (90° for 2 hours) it dissolved almost completely. When this solution was oxidized in the cold by alkaline permanganate to a pink color persistent for 12 hours, it yielded 98% oxalic acid calculated on the lignin taken, i.e., almost exactly 2 molecules per structural lignin unit of M = 180; this once again confirms that Scholler's lignin is "100% aromatic." When these results had been obtained it became possible to carry out ozonationof lignin in wood. Sprucewood flour, extracted by dichloroethane, acetone, and hot water, was dried to constant weight at 100° and 10 mm (the product contained 28.0% Klason's lignin). 30.25 g of wood flour and 200 ml of anhydrous ethyl acetate was taken for the ozonation. The ozonation was effected as described above. 420 liters of ozonized oxygen (26.9 g of ozone) was passed, after which the wood was separated from the solution by suction, washed with ethyl acetate, covered with 200 ml of ethyl acetate, and ozonized again. The solvent was removed from the filtrates under vacuum (final pressure 0.01 mm) at bath temperature not higher than 40°. The residue (7.05 g) was a very viscous, almost colorless liquid which decomposed above 60° with slight deflagration. The second ozonation (420 liters passed) yielded 8.2 g of residue, and the third ozonation (140 liters passed) of the same wood sample yielded 3.1 g; the total weight of residue was 18.35 g. If this residue is assumed to be lignin triozonide of M = 180 + 144 = 324, then its lignin content should be 10.2 g. The wood flour sample contained 30.25 × 0.28 = 8.47 g of lignin. After threefold ozonation of the wood flour dried under vacuum at 40°, 20.0 g remained (10.25 g dissolved), containing 6.7% Klason's lignin with 11.3% methoxyl content. Since Klason's sprucewood lignin contained 15-16% methoxyl, it may be assumed that the "lignin" of the residual wood flour contained 70% Klason's lignin, i.e., the residual wood flour contained 0.7 × × 20.0 g × 0.067 = 0.94 g of Klason's lignin. Together with 10.2 g of "lignin" in the ozonide this gives 11.14 g, whereas the original wood sample contained 8.47 g. It follows that when the sprucewood flour was ozonized, not only lignin triozonide but also carbohydrates went into solution. If the triozonide of M = 324 contains one methoxyl group, then the methoxyl content should be 9.7%. Direct determinations (by the Viebock and Schwappach method) of methoxyl groups in ozonides I, II, and III gave: .I) 10.1 and 10.3%, II) 6.1 and 6.1%, III) 5.8 and 5.9%. The ozonized sprucewood flour contained 1.7 and 1.7% $OCH_3$, and the original wood contained 5.5% $OCH_3$.

The methoxyl balance is:

| | | | |
|---|---|---|---|
| 7.05 g | ozonide I | gave | 0.7120 g methoxyl |
| 8.20 g | " II | " | 0.5002 g " |
| 3.16 g | " III | " | 0.1833 g " |
| 20.0 g | ozonized wood flour | " | 0.3400 g " |
| | | Total | 1.7355 g |
| 30.25 g original wood gave | | | 1.6638 g methoxyl |
| | | Difference | 0.0717 g |

Therefore by its methoxyl content ozonide I is the almost pure triozonide of native sprucewood lignin. Ozonides II and III are respectively 68 and 60% triozonide containing 32 and 40% respectively of methoxyl-free substances (probably carbohydrates). Thus, not less than 43% of the lignin in sprucewood dissolves as the triozonide in neutral anhydrous ethyl acetate in the first instance. The residual lignin then goes into solution accompanied by carbohydrates, in the proportions of 60-68% lignin triozonide to 40-32% carbohydrates. It follows that sprucewood contains both lignin bound chemically with carbohydrates, and lignin not so bound (not less than 43%). The molecular weight of the carbohydrates bound with the lignin cannot be high: M of native sprucewood lignin (according to Bjorkman) is about 11,000. If ozonides II and III contain about 60% lignin triozonide and about 40% carbohydrates, then these products, after subtraction of ozone, should contain lignin and carbohydrates in the ratio of 46:54, i.e., if one lignin macromolecule (M =11,000) is chemically combined with one carbohydrate molecule, the molecular wieght of the carbohydrate should be 12,000-13,000 (hemicelluloses).

The lignin not combined with carbohydrates dissolves first during ozonation in ethyl acetate, and is the

more accessible. Probably this is lignin of the middle lamella. Lange [11] found that the middle lamella contains over 70% lignin. When this lignin has been dissolved, the cell-wall lignin, which is apparently bound chemically with carbohydrates, also begins to dissolve.

## SUMMARY

1. It was found that dissolution of any given lignin during ozonation in an organic solvent is not proof that ozonation is complete.

2. Exhaustive ozonation of sprucewood lignin (Scholler's and acetic-acid lignin) in ethyl acetate yields an ozonide in a yield of about 180% on the weight of lignin taken, which corresponds to the triozonide of a structural unit with M = 180, containing one benzene ring. The ultraviolet spectrum of the triozonide does not contain an absorption band at about 2800 A. The triozonide solution is optically inactive. Decomposition of the triozonide by water with careful subsequent oxidation by permanganate gave about two molecules of oxalic acid per structural unit of M = 180. This, and the fact that the calculated yield of ozonide was obtained, is proof that the investigated sprucewood lignins are "100% aromatic."

3. Stepwise ozonation of sprucewood (flour) yielded not less than 43% of pure lignin triozonide which passed into solution in ethyl acetate, in the first instance, followed by triozonide containing methoxyl-free substances (carbohydrates) in approximately 1:1 ratio. If these substances are carbohydrates, their molecular weight cannot exceed 12,000-15,000. The triozonide of native sprucewood lignin, not subjected to any racemizing influences, was optically inactive.

## LITERATURE CITED

[1] F. Brauns. The Chemistry of Lignin. N. Y., 536 (1952); F. Konig, Cellulosechemie, 2, 93 (1921); C. Doree, J. Ch. Soc., 101, 497 (1912); 103, 677 (1913); K. Freudenberg, Lieb. Ann., 518, 62 (1935).

[2] H. Hibbert, J. Am. Chem. Soc., 61, 2698 (1939); M. Phillips, Chem. Soc.,55, 3469 (1933); H. Richtzenhain, Ber., 75, 269 (1942).

[3] A. Bjorkman, Svensk Papperstidning, 59, 477 (1956).

[4] K. Freudenberg, Naturwiss., 41, 231 (1954); Ber., 88, 617 (1955).

[5] D. Tishchenko,J. Appl. Chem. 32, No. 1, 157 (1959) [USSR].*

[6] K. Kurschner, Faserforschung undTextiltechnik, 7, 461 (1953).

[7] K. Kurschner and Yu. Gostomskii, J. Appl. Chem. 29, 1529 (1956) [USSR].

[8] J. Pearl, J. Am. Chem. Soc., 71, 2196 (1949).

[9] E. Adler et al. Acta Chem. Scand.,2,93,839 (1948).

[10] F. Brauns, J. Am. Chem. Soc., 67, 648 (1945).

[11] P. Lange, Svensk Papperstidning, 47, 262 (1944); 48, 241 (1945).

Received December 16, 1958.

*Original Russian pagination. See C. B. translation.

# DULCITOL FROM LARCH ARABOGALACTAN

A. F. Zaitseva, A. Z. Karpov, S. Z. Levin, and S. D. Antonovskii

Institute of Forestry of the Academy of Sciences USSR, the Leningrad Scientific Research Institute of Petroleum Processing and Production of Liquid Synthetic Fuel, and the S. M. Kirov Academy of Wood Technology.

The discovery of 10-12% of the water-soluble polysaccharide arabogalactan in the wood of the Daur larch, which is one of the commonest trees of Eastern Siberia, the Far East, and Yakutiya, but which is unfortunately utilized little as yet, has focused considerable attention on the utilization of this substance, which is easily extracted from the wood.

Without touching upon the work carried out by the Laboratory of the Institute of Forestry jointly with the Academy of Wood Technology on the use of Daur larch as a source of cellulose [1], in this paper we report only the results of experiments on hydrogenation of arabogalactan extracted from the wood after additional hydrolysis.

Arabogalactan is a mixed polysaccharide which contains, on the average, 1 anhydroarabinose residue to 6 anhydrogalactose residues $[(C_6H_{10}O_5)_6(C_5H_8O_4)]_n$. It follows from this formula that hydrolysis of this polysaccharide yields 6 galactose molecules to 1 arabinose molecule. As the result of hydrogenation we expected to obtain polyhydric alcohols, mainly dulcitol with a small amount of arabitol.

There have been indications in the recent literature that the production of polyhydric alcohols is of great practical importance [2]. The presence of a large number of hydroxyl groups in hexitols and pentitols determines their reactivity, which leads to the formation of a variety of products. Because of a number of their properties, pentitols and hexitols are widely used instead of glycerol in the chemical, paper, textile, and other industries. For example, sorbitol is used as a starting material for the synthesis of various organic substances [3]: alkyl resins, ascorbic acid, anticorrosion coatings. It is also used as an emulsifier and humidity stabilizer in tobacco production, confectionery, perfumery, and the production of other consumer goods. Mention should also be made of the production of xylitol from agricultural wastes [4].

We did not find any data in the literature on the industrial production and utilization of dulcitol. However, because of its properties dulcitol may be as valuable a product of polysaccharide conversion as other polyhydric alcohols. The production of dulcitol from water-soluble components of larch is of interest also because the raw material is not a source of foodstuffs. Moreover, in view of the enormous amounts of larch available in forests and of the new pulp mills being planned for its conversion, there is every reason to believe that arabogalactan may become a cheap raw material not only for the hydrolysis industry but also for hydrogenation.

## EXPERIMENTAL

Extracted larch gum (ELG) from the production plant of the Nyandoma station of the Arkhangel'sk province was used for hydrogenation.* The dry gum residue contained 94.5% arabogalactan and 1.5% ash. After hydrolysis of 20% arabogalactan solutions (by 0.15% $H_2SO_4$ at 170° for 20 minutes) and neutralization to pH = 7.3, the dry residue from the neutralized product contained 89.5% reducing substances, 3.8% ash, and

*We thank E. M. Berkman and M. Ya. Zhivotovskii for help in obtaining the extracted larch gum.

6.7% unhydrolyzed arabogalactan. The reducing substances were 89.2% galactose (determined as mucic acid) and 10.8% arabinose (by difference). Qualitative chromatography confirmed that the neutralized product contained only two sugars – galactose and a small amount of arabinose. Hydrogenation experiments with neutralized hydrolyzed arabogalactan were carried out in a continuous unit in presence of a stationary granulated catalyst consisting of Ni on kieselguhr (made industrially). The mixture of solution and hydrogen was fed downward through the catalyst. The catalyst was activated directly in the reactor before the experiments by reduction with hydrogen at a high temperature (400°). The degree of hydrogenation was estimated both from the contents of residual sugars (RS) and from the dulcitol yield.

For quantitative determination of dulcitol the hydrogenation products were first filtered warm in order to dissolve dulcitol and to remove suspended catalyst particles. The filtered liquid was then cooled, an aliquot portion was evaporated down to a small volume, and after a precipitate was deposited the latter was separated from the mother liquor by suction through a weighed filter. A separate portion was used to determine the moisture content of the precipitate, and the yield of unpurified product was calculated. Analyses showed that the unpurified product contained traces of reducing substances and about 0.5% ash. The melting point of the unpurified product was found to be 169-171°. After recrystallization from hot water the product was entirely free from reducing substances and melted at 183-184°. The melting point indicated that the hydrogenation product mostly consisted of dulcitol with only a small admixture of arabitol (the melting point of arabitol is 103°, and of dulcitol 189°). The hydrogenation product before recrystallization was therefore called "crude dulcitol."

Several series of hydrogenation experiments were performed in order to determine the dulcitol yield in relation to the pressure and time of catalyst operation. The results of experiments at different pressures (sugar concentration in the original raw material 15%, pH = 7.3, hydrogenation temperature 120°) are given below.

| Pressure (atmos) | RS (% of solution weight) | pH | Yield of crude dulcitol (% on original RS) |
|---|---|---|---|
| 30 | 0.2 | 5.9 | 76.1 |
| 75 | 0.3 | 5.9 | 85.2 |
| 150 | 0.03 | 5.9 | 97.8 |

It was found that with increase of pressure from 30 to 150 atmos the dulcitol yield increases from 76 to 97.8% (on the weight of the original RS).

The results of hydrogenation experiments with different times of operation of Ni catalyst on kieselguhr are given below (sugar concentration in the original raw material 15%, pH = 7.3, hydrogenation temperature 120°, pressure 150 atmos).

| Time of continuous operation of catalyst (hours) | RS (% of solution weight) | pH | Yield of crude dulcitol (% on original RS) |
|---|---|---|---|
| 12 | 0.03 | 5.9 | 97.8 |
| 24 | 0.02 | 5.9 | 97.0 |
| 36 | 0.06 | 5.9 | 96.9 |
| 150 | 0.6 | 5.9 | 93.2 |
| 166 | 1.3 | 5.9 | 87.9 |

The results of these experiments showed that during the first 36 hours of catalyst operation (under otherwise constant conditions) high yields of dulcitol were obtained (98-97%).

During subsequent operation the dulcitol yield fell somewhat, and after 166 hours the yield was ~ 88 %.

Experiments for more precise determination of conditions for hydrogenation and hydrolysis of a larch arabogalactan are continuing.

## SUMMARY

1. Hydrogenation of aqueous solutions of hydrolyzed larch gum (ELG) in a continuous unit in presence of stationary Raney Ni catalyst on kieselguhr (of industrial manufacture) proceeds quite effectively.

2. At a hydrogenation temperature of 120° and 150 atmos pressure the yield of crude dulcitol during the first 36 hours of continuous catalyst operation was over 97% (calculated on the weight of the original reducing substances).

We take this opportunity to thank N. I. Nikitin for valuable advice in the course of this work.

## LITERATURE CITED

[1] A. F. Zaitseva, I. P. Fedorishcheva, S. D. Antonovskii, and N. I. Nikitin, Paper Ind. 2, 9 (1955); A. F. Zaitseva and I. P. Fedorishcheva, Paper Ind. 8,9 (1955); A. F. Zaitseva, I. P. Fedorishcheva, and N. I. Nikitin, Hydrolysis and Wood Chem. Ind. 2, 3 (1957) [USSR].

[2] H. F. J. Wenzl, Holzforschung 10, 5, 129 (1956); S. V. Chepigo, A. A. Balandin, N. A. Vasyunina, and A. P. Sergeev, Chem. Sci. and Ind. 2, 4 (1957) [USSR].

[3] H. B. Hass and O. H. Lamborn, Ind. Eng. Chem. 47, 1396 (1955); V. I Maksimov, V. V. Nikonova, A. F. Lazarev, and L. A. Zvereva, J. Gen. Chem. 9, 936 (1939); E. M. Adaskin, N. I. Ziminova, B. L. Lebedev, and S. V. Pavlov, J. Appl. Chem. 31, 595 (1958) [USSR].

[4] S. V. Chepigo and N. A. Vasyunina, Hydrolysis and Wood Chem. Ind. 6, 3 (1956); S. V. Chepigo, Chem. Sci. and Ind. 2, 1 (1957). [USSR].

Received July 12, 1958.

# BOOK REVIEW

DATA BOOK ON LIQUID – VAPOR EQUILIBRIA. Compiled by V. B. Kogan and V. M. Fridman, Edited by Prof. Dr. Tech. Sci. V. V. Kafarov (Goskhimizdat, 1957).

Enormous amounts of factual data have now been accumulated in many branches of chemical science and technology, but the greater proportion of the experimental data is scattered among numerous periodical publications, often not readily available to many engineers and chemists.

The production rate of publications of the review and reference type undoubtedly lags far behind the rate at which data are accumulated. Therefore the recent publications by Goskhimizdat of a number of large reference works, such as the two-volume "Data Book on Solubilities in Salt Systems," the three-volume "Chemist's Handbook," and the "Data Book on Liquid–Vapor Equilibria" reviewed here, must be regarded as most useful and timely.

This book is the first complete collection of systematized experimental data on liquid–vapor phase equilibria published up to 1955 in the Russian and foreign literature. The only similar publication was the handbook compiled by Ju Chin Chu and his co-workers and published in 1950 in the United States. However, that handbook, which contains only 167 tables of equilibrium data, is very incomplete and contains hardly any references to the numerous publications of Russian workers.

The data book under review may prove very useful to scientific workers, students in universities and technical colleges, planners and technologists in a number of industries, such as the chemical, petroleum, hydrolytic and others, who are concerned in their work with studies of the properties of solutions, distillation processes and equipment design, and other technological processes.

The book consists of four principal sections of unequal size. The first, introductory section contains an introduction to thermodynamics and the principles of methods for verification of experimental data on liquid–vapor equilibria in binary and ternary systems. This is undoubtedly a useful section, as methods for verification and analysis of data, which are very important, are inadequately covered in the literature, and there have been no review publications on this question or critical evaluations of different methods.

In this section the first pages are the least successful. It is very difficult to present the most general and fundamental principles of thermodynamics in a few pages, and this proved to be so in this instance. In our opinion, this section contains a number of badly edited and inaccurate expressions. Very likely these general questions might have been omitted, on the assumption that they are known in the elementary form to the reader. In the following pages more attention should have been devoted to presentation of Konovalov's laws and Vrevskii's rules. There is hardly any discussion of the influence of pressure and temperature variations on the nature of liquid–vapor equilibria and changes in azeotrope compositions; and yet these questions are of great practical significance and, moreover, are abundantly illustrated by the factual data contained in the book.

We consider that the next edition of the book should include a section devoted to a review of methods for experimental investigation of liquid–vapor equilibria, with a brief account of the principles and applicability conditions of different methods, and a detailed bibliography.

Among the errors in the first section, the omission of the differential of $y_2$ and a minus sign in Equation (94 must be noted.

The second and largest section contains equilibrium data for binary systems (768 tables). This is a very full summary, although data for some systems have been omitted; for example, the system nitrogen–sulfur dioxide (D. S. Tsiklis, Zh. Fiz. Khim. 21, 349, 1947), water–glycerol (D. F. Stedman, Trans. Farad. Soc., 24,289

1928), water–nicotine (D. F. Kelly et al., J. Chem. Soc.L.511, 1942)chloroform–toluene (M.A. Rosanoff et al., J. Am. Chem. Soc. 36, 1803, 1914), and certain others. Tables 81-84 contain equilibrium data for the system water–formic acid, but in Table 84 the order of the components is inconsistent with Tables 81-83. There are errors in Tables 133 and 638. In the case of some systems there are discrepancies between the names used for the components in the tables and in the indexes.

The third section contains equilibrium data for 94 three-component systems and for 8 systems of more than three-component.

This section is also a very full and valuable summary of data on ternary systems. It should be noted, however, that boiling point data for the solutions are not given for a number of ternary systems (for example, the system acetone–chloroform–benzene, Table 833, and others), and it is stated that such data are lacking. In reality the boiling points for these systems have been determined, but the results were obtained in experiments unconnected with determinations of equilibrium phase compositions, and are sometimes given in other papers. These data should have been included in the book, or appropriate reservations should have been made in the text or the preface.

The data book ends with carefully compiled formula and alphabetical indexes and a list of the literature. The book is easy and convenient to use. It might have been even better if the component with the smallest number of carbon atoms in the formula was given first in each table. The book is well produced, the graphical material is neatly presented, and there are very few misprints.

The defects listed above do not detract from the value of the book, the publication of which is to be welcomed.

In view of the fact that many new papers on liquid–vapor equilibrium studies are published every year, the data book should be published again with appropriate additions in the near future. This is especially justified in view of the directions of the Plenum of the Central Committee of the CPSU concerning acceleration of the development of the chemical industry, as liquid–vapor equilibrium data are necessary for improvement of existing and development of new methods for separation of volatile substances, and for searches for methods of the most rational utilization of many kinds of raw materials in the chemical industry.

A. V. Storonkin, A. G. Morachevskii, and M.P. Susarev.

W. Schumb, C. N. Satterfield, and R. L. Wentworth, HYDROGEN PEROXIDE. Translated from English (Foreign Literature Press, Moscow, 1958) 576 pp.

Hydrogen peroxide has become an important chemical product and is now being manufactured on a large scale. Whereas by the end of the Second World War the production of 85% hydrogen peroxide was the best that chemical technology could achieve, 90% solutions are now being produced. Continuous manufacture of an almost anhydrous product is described in certain patents. Hydrogen peroxide (especially its highly concentrated solutions) is now extensively used in many branches of industry.

According to the American journal,Chemical Engineering Progress,(52, No. 11, 54, 1956), the consumption of hydrogen peroxide in the United States in 1955 was 40,000,000 lb (18,000 long tons). The uses of hydrogen peroxide are spreading into new fields, such as the production of polyethylene.

Therefore the publication of a new and valuable book on hydrogen peroxide is very timely; this book has been produced fairly promptly in Russian translation by the Foreign Literature Press. This publication is to be welcomed, as there are few books on the chemistry and technology of hydrogen peroxide.

"Hydrogen Peroxide" by Schumb, Satterfield, and Wentworth is a detailed monograph which consists of a scientific review of the present status of the theory and practice of hydrogen peroxide production, its physical and chemical properties, analytical methods, and technical uses. The book contains a full and extensive review of available literature data, which can be a valuable source of information for users of hydrogen peroxide in the textile, pulp, and paper industries.

All three authors were engaged in research on hydrogen peroxide at the Massachusetts Institute of Technology from 1945, and also in training of technology students specializing in the field of production of hydrogen peroxide and its derivatives.

They quote experimental research results not published previously. The extensive German industrial experience of the production and uses of hydrogen peroxide, gained during the Second World War, has been utilized in the book.

The monograph consists of 12 chapters. Literature up to the middle of 1954 is cited at the end of each chapter. The bibliography contains about 2800 references, including many to publications in Russian. The book has a detailed subject index and is well illustrated (with drawings, graphs, and photographs). The text contains 89 tables.

The first chapter deals with the discovery of hydrogen peroxide, technological development of processes for its production, and the nomenclature of peroxy compounds.

The second and third chapters, entitled "Formation and Manufacture," are concerned with the production of hydrogen peroxide from water or from its elements (Chapter 2), and from peroxy compounds (Chapter 3).

Chapter 2 contains details of the mechanism of the reaction of oxygen with hydrogen, formation of hydrogen peroxide in the electric discharge, autooxidation, and reduction of oxygen on a cathode. A good account is given of the photochemical reaction between hydrogen and oxygen (pp. 55-60).

The third chapter contains a description of the preparation of hydrogen peroxide from inorganic peroxides (of barium and sodium), and an account of the theoretical principles of the production of hydrogen peroxide by electrolysis. The industrial electrolytic process for manufacture of hydrogen peroxide is described in detail.

An important chapter is Chapter 4: "Concentration, Purification, Structural Materials, Handling." It is clear from the title that this chapter deals with a whole range of important problems in the technology of hydrogen peroxide: production of concentrated hydrogen peroxide and purification of the solutions, structural materials used for process equipment, storage and transportation, physiological action of hydrogen peroxide, and explosive characteristics of its solutions. There is much useful material here for chemical engineers.

The fifth chapter, "Physical Properties," contains the thermodynamical, electrical, and spectroscopic properties of hydrogen peroxide and data on the principal physical properties of its solutions (specific gravity, viscosity, dielectric constant, surface tension).

Data on the physical properties of deuterium peroxide are of special interest. Table 61 on p. 253 is noteworthy; this contains data on the liquidus temperatures for the system deuterium peroxide – heavy water. Other tables in this section also contain useful data. Table 60 (p. 253) contains certain physical constants of deuterium peroxide solutions: density, refractive index, and viscosity. Table 62 (p. 254) gives the heat capacities of deuterium peroxide solutions in heavy water.

The sixth chapter "Structure," deals with the theoretical aspects of the structure of hydrogen peroxide.

The seventh chaper, "Chemical Properties," presents a classification, thermodynamics, and mechanism of the reactions of hydrogen peroxide, isotope exchange in these reactions, reactions of hydrogen peroxide with inorganic substances in organic chemistry, and the role of hydrogen peroxide in biological processes.

The eighth chapter, "Decomposition Processes," contains information on the decomposition of hydrogen peroxide vapor, decomposition under the influence of radiations, electrolytic decomposition of $H_2O_2$, and decomposition in the liquid phase by inorganic catalysts.

The ninth chapter, "Stabilization," is concerned with stabilization of hydrogen peroxide solutions. It deals with determinations of the stability of hydrogen peroxide solutions and the influence of pH and temperature on

stability. The chapter concludes with a section on stabilizers for hydrogen peroxide (general principles of stabilization, stannate, oxine, phosphates, stabilization mechanism).

In the tenth chapter, "Analytical procedures," details are given on qualitative detection of $H_2O_2$, quantitative analysis of hydrogen peroxide solutions by volumetric permanganate titration, iodometric methods, titration by cerium compounds), gasometric and colorimetric methods, and analysis of mixtures. There is a very brief section (15 lines) on polarographic analysis of hydrogen peroxide solutions.

A very interesting chapter is the eleventh, "Uses of Hydrogen Peroxide," which contains an account of various fields of application of this compound: bleaching, use of $H_2O_2$ as an oxidizing agent (rayon production, dyeing, removal of iron from salt solutions), as a depolarizer, in chemical analysis (Table 86 on p. 498 contains 33 examples of the use of hydrogen peroxide in chemical analysis), in chemical synthesis, and in medicine.

During the Second World War Germany developed the use of pure stable 85% hydrogen peroxide as an energy source of submarines, torpedoes, rockets, and shells.

The twelfth and final chapter, "Inorganic Peroxy Compounds," seems to be rather sketchy and hastily written; this chapter contains a brief account of peroxides of various elements, in particular of the metals of groups I-VIII of Mendeleev's periodic system, and peroxy acids and their salts. Three pages are allotted to peroxy compounds of elements of group I, and the same number to peroxides of group II metals. Very little space (only two pages) is given to a description of the properties and production technology of such an industrially important peroxy compound as sodium peroxide. More detail should have been given here. The text of the book indicates that the authors had sufficient data at their disposal to be able to write suitably, without signs of haste, a chapter on metal peroxides. Technical information from the German and Japanese chemical industries was available to them, to say nothing of the considerable experience of the American factories.

On the whole, the book is a valuable contribution to the chemistry of hydrogen peroxide. The Russian edition will find a place in every technical library.

The book can be used as a manual by chemists, technologists, and planners working on research problems and applications of hydrogen peroxide and its derivatives, and as a textbook by students of chemical engineering colleges and chemical faculties of the universities.

I. Ya. Volkind.

PLASTICS AND THEIR FIRE HAZARDS by V. V. Bokshitskii, Ministry of Public Economy RSFSR Press, Moscow, 1958.

In 1958 the Ministry of Public Economy RSFSR Press published V. V. Bokshitskii's book "Plastics and their Fire Hazards." This is perhaps the first and only monograph dealing with fire prevention in the production and use of plastics, which are the most modern and advanced materials of our time.

The book contains general information on the technology and properties of plastics, and much attention is devoted to safety from fire in the production, storage, and use of plastics. Different types of raw materials used in plastics production are considered separately, because (as the author correctly points out on p. 29) they are often more inflammable than plastics themselves. As is pointed out in the summary of the book, it is intended for fire-protection workers and can be used by engineers and technologists of planning and construction organizations and by the administrative bodies of the appropriate undertakings and institutions. It is also of undoubted interest to technologists in plastics factories.

The book consists of 10 chapters (140 pages) and an appendix containing 6 pages of tables.

The first six chapters deal with the production technology of different types of plastics and questions of fire safety relating to them. The remaining four chapters contain various information on fire-prevention measures in the construction, maintenance, and utilization of production and storage buildings in undertakings engaged in the production and processing of plastics.

Chapter I, "General Information on Plastics and Their Properties," contains definitions of the terms "plastics" and "high polymers" as the basis of plastics, and also of other components (fillers, plasticizers, solvents, dyes, etc.).

The fire hazards of solvents used in plastics production are discussed; a classification of solvents and a table of fire-hazard data are given; the chapter contains data on the physical properties of plastics, their classification (by the effects of heat and also by the method used for production of the principal binding material), and general information on their fire hazards and methods for distinguishing plastics by their behavior in a naked flame.

It should be pointed out that the list of chemically-resistant plastics (p 22) does not include Teflon (polytetrafluoroethylene), a very valuable material which, as is well known, is the most chemically-resistant material available at the present time. It is very surprising that this unique product, which is being increasingly used in technology, is entirely ignored in the whole book.

Page 25 contains a gross error, aluminum being described as an alkali metal

Attention must also be drawn to the lack of clarity in the section "Thermosetting Plastics," as in this section (and in the whole book) there is no explanation of the essential difference between thermoplastics, in which the process of reversible fusion is merely a change of state, and thermosetting plastics, in which irreversible hardening is associated with chemical reactions (polymerization or polycondensation).

Chapter II, "Plastics Based on Condensation Resins," deals with technological production processes for phenolic and amino resins, laminated plastics, and various molding materials. The different kinds of raw materials used in these processes, their fire hazards, methods of fire extinction for different inflammable materials, and various fire-protection measures taken in the factories are considered separately.

There are certain defects requiring correction in this chapter. On page 30 formalin is for some reason taken to be identical with formaldehyde (whereas in reality the former is an aqueous solution of the latter, as the author himself states on p. 32).

It is difficult to determine from the text on p. 42 whether urotropine is supposed to be an organic filler or a hardening agent. This material is included in both groups on the same page, and that without any qualification.

In Chapter III, "Plastics Based on Polymerization Resins," out of all the extensive range of this group the author gives information on the production technology, raw materials, and fire hazards of only four: polystyrene, polyvinyl chloride, polyvinyl acetate, and polymethyl methacrylate.

For some reason the corresponding data on polyethylene are not considered, although this material is mentioned at the begining of the chapter (p. 63). However, it would have been of definite use to present such data, as polyethylene production is of certain interest with regard to fire hazards in relation to individual stages in the technological processes where there are risks of explosion (for example, as the result of incorrect metering of oxygen fed into the polymerization reactor).

On p. 45 the formula of urotropine is wrong. On p. 70 a double bond is omitted from the chemical formula of vinyl acetate, making the formula incomplete and incorrect.

On pages 15, 64, and 75 obviously incorrect melting points are given for acetone, hydrogen peroxide, and acetylene. On page 75 "bivalent metals" should be put rather than "diatomic metals." On page 67 hydrofluoric acid is wrongly described at one point as fluoric acid

It is also incorrect to state (page 67) that polystyrene is the best material for storage of hydrofluoric acid. Polytetrafluoroethylene is, of course, superior to polystyrene in this respect.

Chapter IV, "Plastics Based on Proteins," deals with the production and fire hazards of only one type of protein plastics, galalith, which is no longer of any special importance, although it is of some limited interest in relation to the explosive hazards of galalith dust.

Chapter V, "Plastics Based on Cellulose Esters," contains a description of one type of plastics made from nitrocellulose, known as celluloid.

It contains a detailed account of the whole technological process of the production of celluloid and articles made from it (mixing of nitrocellulose with alcoholic camphor solution, filtration of the celluloid mixture, rolling and pressing, cutting of blocks and drying of sheets, straightening and polishing of celluloid plates); there is a separate description of processes for recovery of celluloid and scrap motion-picture film, whith a detailed discussion of the fire hazards at all stages of the technological process, inflammability of the raw materials, and methods of fire extinction.

In Chapter VI, "Plastics Based on Acetylcellulose and Their Fire Hazards," which consists of only 3 pages, the production, uses, and fire hazards of cellulose acetate are discussed.

Chapter VII, "General Measures for Fire Prevention in the Construction, Maintenance, and Use of Industrial and Storage Buildings," contains general information on measures of fire prevention which should be taken to ensure safety from fire prevention which should be taken to ensure safety from fire in undertakings producing or converting plastics.

Special attention must be paid to proper storage of raw materials and finished products, technically correct electrification of buildings, and fire-fighting water supplies in various sections and storehouses in plastics factories, and therefore the last three chapters (VIII-X) in the book and an extensive appendix in the form of large tables are quite justifiably devoted to these questions.

It must be noted that it would have been desirable to include relevant data on polyamide, polyester, and epoxy resins, polyethylene, etc. in the book.

The book contains a considerable number of inaccuracies and misprints, and a number of faults not mentioned in this review, which must be eliminated.

It should be stated in conclusion that despite these numerous errors and faults and the not very careful scientific editing at some points, which lower the value of the monograph, the book may on the whole be used for its intended purpose, although in a new edition considerable augmentation and revision is necessary, together with absolute elimination of all the faults noted.

I. G. Filatov

## SIGNIFICANCE OF ABBREVIATIONS MOST FREQUENTLY ENCOUNTERED IN SOVIET PERIODICALS

| | |
|---|---|
| FIAN | Phys. Inst. Acad. Sci. USSR. |
| GDI | Water Power Inst. |
| GITI | State Sci.-Tech. Press |
| GITTL | State Tech. and Theor. Lit. Press |
| GONTI | State United Sci.-Tech. Press |
| Gosenergoizdat | State Power Press |
| Goskhimizdat | State Chem. Press |
| GOST | All-Union State Standard |
| GTTI | State Tech. and Theor. Lit. Press |
| IL | Foreign Lit. Press |
| ISN (Izd. Sov. Nauk) | Soviet Science Press |
| Izd. AN SSSR | Acad. Sci. USSR Press |
| Izd. MGU | Moscow State Univ. Press |
| LEIIZhT | Leningrad Power Inst. of Railroad Engineering |
| LET | Leningrad Elec. Engr. School |
| LETI | Leningrad Electrotechnical Inst. |
| LETIIZhT | Leningrad Electrical Engineering Research Inst. of Railroad Engr. |
| Mashgiz | State Sci.-Tech. Press for Machine Construction Lit. |
| MEP | Ministry of Electrical Industry |
| MES | Ministry of Electrical Power Plants |
| MESEP | Ministry of Electrical Power Plants and the Electrical Industry |
| MGU | Moscow State Univ. |
| MKhTI | Moscow Inst. Chem. Tech. |
| MOPI | Moscow Regional Pedagogical Inst. |
| MSP | Ministry of Industrial Construction |
| NII ZVUKSZAPIOI | Scientific Research Inst. of Sound Recording |
| NIKFI | Sci. Inst. of Modern Motion Picture Photography |
| ONTI | United Sci.-Tech. Press |
| OTI | Division of Technical Information |
| OTN | Div. Tech. Sci. |
| Stroiizdat | Construction Press |
| TOE | Association of Power Engineers |
| TsKTI | Central Research Inst. for Boilers and Turbines |
| TsNIEL | Central Scientific Research Elec. Engr. Lab. |
| TsNIEL-MES | Central Scientific Research Elec. Engr. Lab.—Ministry of Electric Power Plants |
| TsVTI | Central Office of Economic Information |
| UF | Ural Branch |
| VIESKh | All-Union Inst. of Rural Elec. Power Stations |
| VNIIM | All-Union Scientific Research Inst. of Meteorology |
| VNIIZhDT | All-Union Scientific Research Inst. of Railroad Engineering |
| VTI | All-Union Thermotech. Inst. |
| VZEI | All-Union Power Correspondence Inst. |

Note: Abbreviations not on this list and not explained in the translation have been transliterated, no further information about their significance being available to us. — Publisher.

# Chemistry Collections

# IN ENGLISH TRANSLATION

Consultants Bureau's chemistry collections, a unique venture in the translation-publishing field, consist of articles on specialized subjects, selected by specialists in each field, from Soviet chemical journals published in translation by CB. These collections are then presented in symposium form.

Periodically we shall issue new collections taken from the latest volumes of our journals, not only on subjects already covered but also on those which prove most valuable to current scientific research. The following is one of the most recent additions to our list of collections (information on forthcoming titles available on request).

## SOVIET RESEARCH IN FUSED SALTS (1956)

42 papers taken from the following Soviet chemistry journals, 1956: Soviet Journal of Atomic Energy; Journal of General Chemistry; Journal of Applied Chemistry; Bulletin of the Academy of Sciences, USSR, Division of Chemical Sciences; Proceedings of the Academy of Sciences, USSR, Chemistry Section. The entire collection consists of one volume, in two sections.

| | | |
|---|---|---|
| I | Systems (23 papers) | $ 30.00 |
| II | Electrochemistry: Aluminum and Magnesium, Corrosion, Theoretical; Thermodynamics; Slags, Mattes (19 papers) | 20.00 |
| THE COMPLETE COLLECTION | | $ 40.00 |

also available in translation . . .

## SOVIET RESEARCH IN FUSED SALTS (1949-55)

125 papers taken from the following Soviet chemistry journals, 1949-55: Journal of General Chemistry; Journal of Applied Chemistry; Bulletin of Academy of Sciences, USSR, Div. Chemical Sciences; Journal of Analytical Chemistry. Sections of this collection may be purchased separately as follows:

| | |
|---|---|
| Structure and Properties (100 papers) | $110.00 |
| Electrochemistry (8 papers) | 20.00 |
| Thermodynamics (6 papers) | 15.00 |
| Slags and Mattes (6 papers) | 15.00 |
| General (5 papers) | 12.50 |
| THE COMPLETE COLLECTION | $150.00 |

*NOTE: Individual papers from each collection are available at $7.50 each. Tables of contents sent upon request.*

CB collections are translated by bilingual scientists, and include all photographic, diagrammatic and tabular material integral with the text. Reproduction is by multilith process from "cold" type; books are staple bound in durable paper covers.

## CONSULTANTS BUREAU, INC.

227 WEST 17TH STREET, NEW YORK 11, N. Y.

# PROCEEDINGS OF THE FIRST ALL-UNION CONFERENCE ON RADIATION CHEMISTRY, MOSCOW, 1957

THIS UNPRECEDENTED RUSSIAN CONFERENCE on Radiation Chemistry, held under the auspices of the *Division of Chemical Sciences, Academy of Sciences, USSR* and the *Ministry of Chemical Industry* , aroused the interest of scientists the world over. More than 700 of the Soviet Union's foremost authorities in the field participated and, in all, fifty-six reports were read covering the categories indicated by the titles of the individual volumes listed below. Special attention was also given to *radiation sources used in radiation-chemical investigations.*

Each report was followed by a general discussion which reflected various points of view in the actual problems of radiation chemistry: in particular, on the *mechanism of the action of radiation on concentrated aqueous solutions,* on the *practical value of radiation galvanic phenomena,* on the *mechanisms of the action of radiation on polymers, etc.*

The entire "Proceedings" may be purchased as a set, or individual volumes may be obtained separately as follows:

**Primary Acts in Radiation Chemical Processes**
*(heavy paper covers; 5 reports, approx. 38 pp., illus., $25.00)*
**Radiation Chemistry of Aqueous Solutions**
*(heavy paper covers, 15 reports, approx. 83 pp., illus., $50.00)*
**Radiation Electrochemical Processes**
*(heavy paper covers, 9 reports, approx. 50 pp., illus., $15.00)*
**Effect of Radiation on Materials Involved in Biochemical Processes**
*(heavy paper covers, 6 reports, approx. 34 pp., illus., $12.00)*
**Radiation Chemistry of Simple Organic Systems**
*(heavy paper covers, 9 reports, approx. 50 pp., illus., $30.00)*
**Effect of Radiation on Polymers**
*(heavy paper covers, 9 reports, approx. 40 pp., illus., $25.00)*
**Radiation Sources**
*(heavy paper covers, 3 reports, approx. 20 pp., illus., $10.00)*

**PRICE FOR THE 7-VOLUME SET**
: $125.00

NOTE: *Individual reports from each volume available at $12.50 each. Tables of Contents sent upon request.*

*CB translations by bilingual scientists include all photographic, diagrammatic, and tabular material integral with the text.*

CONSULTANTS BUREAU, INC.
227 WEST 17TH STREET, NEW YORK 11, N. Y